

UNIVERSITY OF OKLAHOMA  
GRADUATE COLLEGE

NADH-DEPENDENT, FERREDOXIN-INDEPENDENT HYDROGEN PRODUCTION IN  
TWO MODEL SYNTROPHIC BACTERIA

A DISSERTATION  
SUBMITTED TO THE GRADUATE FACULTY  
in partial fulfillment of the requirements for the  
Degree of  
DOCTOR OF PHILOSOPHY

By  
NATHANIEL ANDREW LOSEY  
Norman, Oklahoma  
2019

NADH-DEPENDENT, FERREDOXIN-INDEPENDENT HYDROGEN PRODUCTION IN  
TWO MODEL SYNTROPHIC BACTERIA

A DISSERTATION APPROVED FOR THE  
DEPARTMENT OF MICROBIOLOGY AND PLANT BIOLOGY

BY

Dr. Michael J. McInerney, Chair

Dr. Amy V. Callaghan

Dr. Anne K. Dunn

Dr. Lee R. Krumholz

Dr. Michael R. Markham

© Copyright by NATHANIEL ANDREW LOSEY 2019  
All Rights Reserved.

## Acknowledgements

I would like to start by thanking my doctoral advisor, Dr. McInerney, who has been a patient and inspirational mentor. I also thank Neil Wofford for his invaluable instruction and help with performing enzymatic assays, operating analytical equipment and anaerobic cultivation. Dr. Florence Mus from Dr. John Peters lab constructed the plasmid used in Chapter 2 encoding the genes for the *Syntrophomonas wolfei* [FeFe]-hydrogenase. Hunyh Le generated the experimental data for methane and hydrogen measurements from *Syntrophomonas* cultures described in Chapter 2. I would also like to thank my previous colleagues in the McInerney lab, Dr. Kim Thomas, Dr. Johannes Kung, Dr. Bryan Crable, Hunyh Le, and Ebony Martin for their help performing experimental science and navigating graduate school. I am grateful to my committee members, Dr. Callaghan, Dr. Krumholz, Dr. Dunn, and Dr. Markham for their time, effort and critiques of my doctoral research. I would also like to thank my family for their continued support and encouragement. In addition, my peers during graduate school, Dr. Chris Marks, Dr. Blake Stamps, Dr. Joshua Cooper, and Brian Bill for their helpful scientific discussions.

## TABLE OF CONTENTS

Acknowledgements.....	iv
Table of Contents.....	v
List of Tables.....	vii
List of Figures.....	viii
Abstract.....	xi
CHAPTER 1: Hydrogen Production During Syntrophic Fatty Acid and Aromatic Acid Oxidation .....	1
Importance of Anaerobic Syntrophy in Global Carbon Cycling.....	2
The Unique Challenge of Syntrophy: Re-Oxidizing the High Redox Potential Electron Carriers NADH and Electron Transfer Flavoprotein.....	3
Flavin-Based Electron-Bifurcating Enzymes and the Rnf Complex.....	9
Re-Oxidation of Reduced Cofactor Pools, NADH and Electron Transfer Flavoprotein in <i>S.</i> <i>wolfei</i> and <i>S. aciditrophicus</i> .....	15
References.....	28
CHAPTER 2. <i>Syntrophomonas wolfei</i> Uses a NADH-Dependent, Ferredoxin-Independent, [FeFe]-Hydrogenase to Reoxidize NADH.....	42
Abstract.....	43
Importance.....	44
Introduction.....	45
Results.....	48
Discussion.....	57
Methods.....	67

References.....	75
Supplemental Figures and Tables .....	83
CHAPTER 3. A NADH-Dependent, Ferredoxin-Independent [FeFe]-Hydrogenase from	
<i>Syntrophus aciditrophicus</i> .....	93
Abstract.....	94
Introduction.....	95
Results.....	97
Discussion.....	121
Methods.....	149
References.....	155
Supplemental Figures and Tables .....	164
CHAPTER 4: NADH-Dependent, Ferredoxin-Independent Hydrogen Production as a Detailed	
Example of Syntrophic Metabolism .....	175
Characteristics of Proposed NADH-Dependent, Ferredoxin-Independent Hydrogen and	
Formate Production by <i>S. wolfei</i> and <i>S. aciditrophicus</i> .....	176
Unanswered Questions: Acyl-CoA Oxidation Mechanisms in <i>S. wolfei</i> and <i>S. aciditrophicus</i> :	
and Intracellular NADH/NAD <sup>+</sup> Ratios .....	188
Summary: NADH-Dependent, Ferredoxin-Independent Hydrogen Production, Exemplifies	
the Intimate Nature of Syntrophic Metabolism in Co-Culture Between Syntrophic	
Metabolizers and Methanogenic Partners.....	192
References.....	196
Supplemental Figures.....	202

## List of Tables

Table 1. Purification of NADH-dependent [FeFe]-hydrogenase, Hyd1ABC.....	48
Table 2. Specific Activities of the Purified, NADH-Dependent [FeFe]-Hydrogenase, Hyd1ABC. .....	51
Table 3. Equilibrium Hydrogen Partial Pressures Produced by NADH-Dependent [FeFe]- Hydrogenase, Hyd1ABC at Different pH and NADH to NAD <sup>+</sup> ratios. ....	56
Table 4. List of Primers Used for Construction of pETDuet-1 SwHydABC, pCDFDuet-1 SwHydEFG and pCDFDuet-1 SwFd. ....	67
Table 5. Purification of NADH-Dependent [FeFe]-Hydrogenase, HydAB. ....	98
Table 6. Peptides Detected by HPLC MS-MS Analysis of the Purified Recombinant HydAB Fraction. ....	102
Table 7. HPLC MS-MS Identification Results of Partially Purified <i>S. aciditrophicus</i> Ferredoxin Fraction. ....	105
Table 8. Specific Activities of Purified Recombinant HydAB.....	113
Table 9. Equilibrium Hydrogen Concentrations Produced by NADH-Dependent [FeFe]- Hydrogenase, HydAB with Varied NADH/NAD <sup>+</sup> ratios. ....	117
Table 10. List of Plasmids Used for the Expression of the <i>S. aciditrophicus</i> HydAB and Ferredoxin. ....	150

## List of Figures

Figure 1. Competing Proposals for Electron Flow in Electron-Bifurcating [FeFe]-Hydrogenases. .....	14
Figure 2. Reduced Cofactor Generation during Syntrophic Butyrate Oxidation in <i>S. wolfei</i> .....	15
Figure 3. Reduced Cofactors from Syntrophic Benzoate Oxidation in <i>S. aciditrophicus</i> ..	17
Figure 4. Alternative Explanations for NADH Re-Oxidation in <i>S. wolfei</i> and <i>S. aciditrophicus</i> .	20
Figure 5. Alignment <i>S. wolfei</i> and <i>S. aciditrophicus</i> of EtfB Subunits. ....	24
Figure 6. Proposed Mechanism of Etf Re-Oxidation in <i>S. wolfei</i> and <i>S. aciditrophicus</i> .....	24
Figure 7. SDS-PAGE of NADH-Dependent [FeFe]-Hydrogenase, Hyd1ABC. ....	49
Figure 8. Native PAGE of the NADH-Dependent [FeFe]-hydrogenase, Hyd1ABC. ....	50
Figure 9. Reduction of NAD <sup>+</sup> by the Purified, NADH-Dependent [FeFe]-Hydrogenase, Hyd1ABC with Hydrogen as the Electron Donor. ....	52
Figure 10. The Effect of NADH and Reduced Ferredoxin on Hydrogen Production by Hyd1ABC. ....	54
Figure 11. Comparison of Predicted Conserved Domains Present in Characterized Multimeric [FeFe]-Hydrogenases and Multimeric Formate Dehydrogenases. ....	61
Figure 12. SDS PAGE of Recombinant <i>S. aciditrophicus</i> HydAB Purified from <i>E. coli</i> by Nickel Affinity Chromatography.....	99
Figure 13. Native PAGE Analysis of Recombinant <i>S. aciditrophicus</i> HydAB Purified from <i>E.</i> <i>coli</i> by Nickel Affinity Chromatography.....	101
Figure 14. SDS-PAGE of Recombinantly Produced <i>S. aciditrophicus</i> Ferredoxin from <i>E. coli</i> and Ferredoxin Partially Purified from <i>S. aciditrophicus</i> .....	110
Figure 15. The Reduction of NAD <sup>+</sup> by HydAB is not Ferredoxin Dependent. ....	112



Figure 16. Production of Hydrogen from NADH by HydAB in the Presence of Reduced Ferredoxin Generating System. ....	114
Figure 17. Production of Hydrogen from NADH by HydAB Independent of Reduced Ferredoxin. ....	116
Figure 18. Hydrogen Partial Pressures During the Metabolism of Crotonate, Cyclohex-1-ene-1-carboxylate, and Benzoate by Pure cultures of <i>S. aciditrophicus</i> and Co-cultures of <i>S. aciditrophicus</i> with <i>Methanospirillum hungatei</i> .....	120
Figure 19. Differences in Cofactor Binding Sites between Electron-Bifurcating, NADH-Dependent and Ferredoxin-Dependent Enzymes and NADH-Dependent, Ferredoxin-Independent Enzymes. ....	129
	135
Figure 21. Summary of Differences Between the Electron-Bifurcating [FeFe]-Hydrogenases and Formate Dehydrogenases and NADH-Dependent, Ferredoxin-Independent Enzymes .	141
Figure 22. Proposed Electron Flow in NADH-Dependent, Ferredoxin-Independent [FeFe]-Hydrogenases. Electron flow depicted for <i>T. thermophilus</i> Nqo1-Nqo and, <i>C. eutropha</i> formate dehydrogenase as illustrated by Hille et al. 2014. Blue arrows indicate electron flow. ....	146
Figure 23. Conserved Domains in Predicted Cytoplasmic <i>S. wolfei</i> and <i>S. aciditrophicus</i> Formate Dehydrogenases Suggest Function as NADH-Dependent, Ferredoxin-Independent. ....	177
Figure 24. Butyrate Oxidation by <i>S. wolfei</i> with NADH-Dependent, Ferredoxin-Independent Hydrogen Production. ....	180
Figure 25. Butyrate Oxidation by <i>S. wolfei</i> with NADH-Dependent, Ferredoxin-Dependent, Electron-Confurcating Hydrogen Production. ....	181

Figure 26. Features of *S. wolfei* and *S. aciditrophicus* [FeFe]-Hydrogenases and Formate Dehydrogenases Match Proposed Physiological Role, Hydrogen Production from NADH. .... 184

Figure 27. Redox Reactions in Cytochrome-Free Hydrogenotrophic Methanogens such as *Methanosprillum hungatei*. .... 190

Figure 28. Syntroph NADH/NAD<sup>+</sup> Ratio Compared to Methanogen F<sub>420</sub>H<sub>2</sub>/F<sub>420</sub> Ratio. .... 191

Figure 29. Narrow Hydrogen Partial Pressure Overlap Between Syntrophic Metabolizers and Methanogenic Partner. .... 194

## Abstract

The relationship between a fatty acid-oxidizing, hydrogen-producing bacterium and a hydrogen consuming methanogenic partner has long served as a model system for anaerobic syntrophic metabolism. This process is dependent on low hydrogen and formate concentrations maintained by the methanogenic partner to allow the fatty acid-oxidizing bacterium to continually re-oxidize cofactors such as NADH that are generated by fatty acid oxidation. Two multimeric [FeFe]-hydrogenases from two different syntrophic model organisms, *Syntrophomonas wolfei* and *Syntrophus aciditrophicus* were produced by heterologously expressing the genes encoding for two [FeFe]-hydrogenase and genes for [FeFe]-hydrogenase maturation in *Escherichia coli*. The *S. wolfei* recombinant Hyd1ABC was found to consist of three subunits Hyd1A, Hyd1B, and Hyd1C with molecular weights of 63.0 kDa, 43.0 kDa and 13.0 kDa. *S. wolfei* Hyd1ABC was observed as a heterotrimer with an  $\alpha\beta\gamma$  configuration and a molecular mass of 115 kDa. The *S. aciditrophicus* purified recombinant HydAB consisted of two subunits HydA and HydB with molecular weights 68.5 kDa and 66.0 kDa and suggested to consist of a  $\alpha_2\beta_2$  configuration. Both the *S. wolfei* Hyd1ABC and *S. aciditrophicus* HydAB were found to re-oxidize the cofactor NADH in a ferredoxin-independent manner. These NADH-dependent, ferredoxin-independent hydrogen production mechanisms provide *S. wolfei* and *S. aciditrophicus* with an energetic advantage under syntrophic conditions compared to the alternative which is NADH-dependent, ferredoxin-dependent electron confurcating hydrogen production. It is proposed that several differences in conserved residues within the HydB subunits are responsible for the observed ferredoxin-independent nature of these enzymes. These results demonstrate that NADH-dependent, ferredoxin-independent hydrogen production occurs in two phylogenetically distant organisms, *S. wolfei* a member of the phylum Firmicutes and *S.*

*aciditrophicus* a Deltaproteobacteria. This suggests a unifying theme for syntrophic fatty acid-oxidizing bacteria, in the form of NADH-dependent, ferredoxin-independent hydrogen production.

Hydrogen partial pressures determined during pure culture and co-culture growth suggest that both *S. wolfei* and *S. aciditrophicus* must maintain high NADH/NAD<sup>+</sup> ratios for NADH-dependent, ferredoxin-independent hydrogen production. NADH-dependent, ferredoxin-independent hydrogen production completes the pathway for how high redox potential electrons generated from 3-hydroxyacyl-CoA oxidation are used to produce hydrogen. It could be suggested that the observed dependence of syntrophic metabolizers on a hydrogen consuming partner is the result of a dependence on cofactor re-oxidation methods that utilize specifically high redox potential electrons. Other syntrophic metabolisms may be predicted to rely on mechanisms for re-oxidizing cofactors that also specifically utilize high redox potential electrons for hydrogen and formate production or direct interspecies electron transfer.

**CHAPTER 1: Hydrogen Production During Syntrophic Fatty Acid and Aromatic Acid  
Oxidation**

## **Importance of Anaerobic Syntrophy in Global Carbon Cycling**

Methane is of interest currently because it is a potent greenhouse gas and because of its potential as a renewable energy source (Stams and Plugge, 2009; Angelidaki et al., 2011). Methane-producing microorganisms, called methanogens, are obligately anaerobic Archaea that produce methane from a variety of substrates including hydrogen, formate, methyl-containing compounds and acetate. Methanogenesis plays a key role in the global carbon cycle due to the production of methane in anaerobic environments where it is estimated that approximately one gigaton of methane is produced each year (Thauer et al., 2008). Methanogenesis becomes the only process for anaerobic decomposition of organic matter when all other terminal electron acceptors (such as nitrate, sulfate, oxygen) are depleted (Stams and Plugge, 2009). The process of methanogenesis in anaerobic environments involves multiple steps. The first step is hydrolysis of polymeric substrates such as polysaccharides, lipids, and proteins followed by primary fermentation to produce various organic compounds including alcohols, organic acids (acetate, propionate, lactate, butyrate), hydrogen, formate and CO<sub>2</sub> (McInerney et al., 2009). Some of these primary fermentation products (hydrogen, formate, acetate, and certain methyl-containing compounds) can be utilized directly by methanogens. Other primary fermentation products such as primary alcohols, propionate, longer chain fatty acids, and lactate cannot be utilized directly by methanogens. The conversion of these remaining primary fermentation products to substrates suitable to methanogenesis (hydrogen, formate or acetate) is performed by a group of metabolic specialists in a process termed syntrophy (McInerney et al., 2009). There are a number of types of microbial associations that have been referred to as syntrophy such as amino acid cross feeding (Nelson, 1951), the sharing of other metabolites required for biosynthesis (Pacheco et al., 2018), and other mutualistic interactions (Morris et al., 2013). However, for the remainder of this

document, I use the term syntrophy to refer to a specific interaction that occurs under anaerobic conditions between a bacterium oxidizing an organic compound (a primary fermentation product) that is dependent on having low hydrogen/formate levels maintained by a hydrogen/formate-consuming microorganism such as a methanogen or sulfate reducer (McInerney et al., 2009). Syntrophy involving the oxidation of these primary fermentation products and the transfer of the resulting high redox potential electrons to methanogens is the rate-limiting step in anaerobic decomposition of carbon (McInerney et al., 2009).

Microorganisms that grow on these primary fermentation products deal with the difficult task of producing hydrogen and formate from high redox potential electrons while also conserving energy for growth (Schink, 1997; McInerney et al., 2009). Syntrophic metabolizers perform a critical role in global carbon cycling but face unique thermodynamic challenges related to the production of hydrogen or formate and energy conservation.

### **The Unique Challenge of Syntrophy: Re-Oxidizing the High Redox Potential Electron Carriers NADH and Electron Transfer Flavoprotein**

Understanding the unique metabolic machinery and physiology of syntrophic metabolizers, particularly related to their ability to produce hydrogen or formate from high redox potential electrons, is crucial to fully understanding the key steps that control global anaerobic carbon decomposition. During syntrophy, the oxidation of the primary fermentation products results in electrons of high redox potentials, which are carried by the reduced cofactors NADH and electron-transferring flavoprotein (Etf). Using electrons of such high redox potentials to produce formate and hydrogen presents a thermodynamic challenge. The oxidation-reduction potential of hydrogen under standard conditions (partial pressure of 1 atm) is ( $E_0' = -414 \text{ mV}$ ).

Similarly, the oxidation-reduction potential of formate under standard conditions (1 M) is ( $E_0' = -432$  mV). However, the electron donors used to produce hydrogen or formate are estimated to be much higher in potential, NADH ( $E_0' = -320$  mV (Thauer et al., 1977)) and  $E_{\text{red}}$  ( $E' = -10$  mV to  $E' = -126$  mV depending on butyryl-CoA/crotonyl-CoA redox potential). Estimates of the butyryl-CoA/crotonyl-CoA pair have varied from as low as  $E_0' = -126$  mV (Gustafson et al., 1986),  $E_0' = -79$  mV (Fink et al., 1986), to as high as  $E_0' = -10$  mV (Sato et al., 1999). The process of oxidizing a high redox potential donor and transferring electrons to a lower redox potential donor is energetically unfavorable. However, in syntrophic co-cultures the hydrogenotrophic methanogen partner can maintain hydrogen concentrations as low as 1 Pascal which corresponds to a higher redox potential for hydrogen ( $E' = -260$  mV) (Sieber et al., 2012). This is also true for the redox potential of formate, which is  $E' = -290$  mV at 10  $\mu\text{M}$  formate (Sieber et al., 2012). Thus, as long as hydrogen or formate are maintained at low concentrations, which raises their predicted redox potentials, it is thermodynamically favorable to produce hydrogen from electrons with a high redox potential. The maintenance of the low levels of hydrogen and formate in natural environments is likely the function of hydrogenotrophic methanogens. Producing large amounts of biomass from syntrophic metabolizers can prove challenging and as a result there have been a limited number of biochemical investigations. In many cases, the enzymatic machinery used by syntrophic metabolizers to convert high redox potential electrons to hydrogen or formate has been inferred from studies on primary fermenters. As primary fermenters produce reduced cofactors pools with electrons at much lower redox potentials such as reduced ferredoxin and typically produce much higher hydrogen concentrations than syntrophic metabolizers do, it is possible that these inferences about syntrophic metabolism may ultimately prove to be incorrect.



*Syntrophomonas wolfei* is a Gram-positive rod-shaped bacterium and is phylogenetically a member of the phylum Firmicutes (McInerney et al., 1981; Sieber et al., 2010). *S. wolfei* serves as a model for the syntrophic metabolism of the short-chain fatty acids such as butyrate to the methanogenic substrates: hydrogen, formate and acetate. The sequencing of the *S. wolfei* genome identified key enzymes required for syntrophic metabolism (Sieber et al., 2010) but did not detect genes needed to grow by primary fermentation or by respiration, suggesting *S. wolfei* may be an obligate syntrophic metabolizer. Physiological studies of *S. wolfei* have supported this conclusion as *S. wolfei* specializes in growing under syntrophic conditions with the notable exception of its ability to grow in pure culture on unsaturated fatty acids, such as crotonate (McInerney et al., 1981; Beaty and McInerney, 1987). It is unclear as to how available unsaturated fatty acids, such as crotonate are in the environment (Wilson et al., 2017), but it seems unlikely that crotonate metabolism is *S. wolfei*'s ecological function. Additional proteomic studies further support many of the earlier genomic predictions (Sieber et al., 2015).

Recently, experiments have suggested that members of the genus *Syntrophomonas* grow faster syntrophically when electroconductive materials are added (such as activated charcoal or magnetite) as evidenced by increased methane production rates (Salvador et al., 2017; Fu et al., 2018; Zhao et al., 2018). The stimulation of methanogenesis in the presence of conductive materials has suggested that syntrophic metabolizers such as *S. wolfei* may possess the ability to directly transfer electrons to the methanogenic partner, in a process called direct interspecies electron transfer, as opposed to the production of hydrogen or formate. Little is known about the components required for direct electron transfer. In addition, key details of the enzymatic machinery responsible for the production of hydrogen and formate are lacking, in particular, the physiological electron carriers that are used for hydrogen and formate production. Understanding

the mechanisms by which *S. wolfei* transfers electrons to its methanogenic partner is the key to understanding the nature of syntrophic metabolism.

*S. aciditrophicus* serves as a model for the syntrophic metabolism of benzoate to hydrogen, formate and acetate. *S. aciditrophicus* is a Gram-negative, deltaproteobacterium isolated from sewage sludge (Jackson et al, 1999). *S. aciditrophicus* has been studied due to its ability to metabolize benzoate, cyclohexane carboxylate and crotonate in syntrophic co-culture (Elshahed et al., 2001). Detailed studies have also investigated metabolism of crotonate and benzoate in pure culture (Elshahed and McInerney, 2001; Mouttaki et al., 2007). Evidence was presented that the synthesis of cyclohexane carboxylate and benzoate from acetate occurs during pure culture metabolism (Mouttaki et al., 2007). The study of syntrophic benzoate degradation is crucial to understanding anaerobic decomposition as benzoate and the metabolite benzoyl-CoA are often key intermediates in anaerobic decomposition of aromatic compounds (Harwood et al., 1998; McInerney et al., 2008; McInerney et al., 2009). The *S. aciditrophicus* genome was the first sequenced genome from a syntrophic specialist and served as a blueprint for interpretation of genomes for many syntrophic specialists (McInerney et al., 2007; Sieber et al., 2010). In addition, *S. aciditrophicus* has an unusual mechanism for ATP synthesis involving the use of pyrophosphate and AMP to make ATP during acetyl-CoA metabolism (James et al., 2016; James et al., 2019, in preparation). Recently, it has been reported that *S. aciditrophicus* possesses electrically conductive pili and can grow by direct interspecies electron transfer with *Geobacter sulfurreducens* (Walker et al., 2018). *S. aciditrophicus* possesses many unique traits; however, key details are unclear about the redox carriers and enzymes used to produce hydrogen and formate, or to transfer electrons by direct interspecies electron transfer.

Re-oxidation of NADH and Etf<sub>red</sub> to produce hydrogen and formate occurs by enzymes known as either hydrogenases or formate dehydrogenases. Evidence for the importance of hydrogen and formate in syntrophic interactions is based on the requirement for the presence of the partner organism such as a hydrogenotrophic methanogen, which are limited to consuming hydrogen and formate (McInerney et al., 1981; Beaty and McInerney, 1987; Jackson et al., 1999; McInerney et al., 2009). In addition, the detection of low levels of hydrogen in syntrophic co-cultures and the inhibition of syntrophic metabolism by the addition of hydrogen support this conclusion (Boone et al., 1989; Stams and Dong, 1995). Genes predicted to encode for hydrogenases and formate dehydrogenase have also been identified in the genomes of syntrophic organisms (McInerney et al., 2007; Sieber et al., 2010; Plugge et al., 2012) as well as the partner hydrogen consuming organisms (Gunsalus et al., 2016).

Hydrogenases catalyze the reversible reduction of protons with electrons to produce molecular hydrogen. There are three types of known hydrogenases distinguished by the composition of metals in the active site: [FeFe], [NiFe] and [Fe] (Volbeda et al., 1995; Peters et al., 1998; Peters et al., 2015; Søndergaard et al., 2016). [Fe]-hydrogenases lack [Fe-S] centers, only reduce the cofactor methenyltetrahydromethanopterin, and are only found in methanogenic Archaea (Shima et al., 2008). [NiFe]-hydrogenases are present in Bacteria, Archaea and Eukaryotes and contain a nickel atom and an iron atom in the active site, which coordinate with a CN- group (Peters et al., 2015). [FeFe]-hydrogenases have been found in bacterial and eukaryote genomes and contain two iron atoms in the active site, which coordinates a cysteine thiolate group (Peters et al., 2015). [FeFe]-hydrogenases are irreversibly inactivated by exposure to oxygen while [NiFe]-hydrogenases can often be reactivated using reductants (Vignais and Billoud, 2007). [FeFe]-hydrogenases and [NiFe]-hydrogenases have been identified in the

genomes of syntrophic organisms and are proposed to catalyze hydrogen production from NADH and reduced flavin cofactors (McInerney et al., 2007; Sieber et al., 2010; Plugge et al., 2012; Sieber et al., 2012; Sedano-Núñez et al., 2018). It has been suggested that [FeFe]-hydrogenases catalyze hydrogen production at faster rates than [NiFe]-hydrogenases (Vignais and Billoud, 2007).

Formate dehydrogenase have also been identified in the genomes of syntrophic organisms and likely utilize the same electron donors as those used by hydrogenases. These enzymes catalyze the reversible reduction of CO<sub>2</sub> and an electron pair to produce formate. These enzymes contain [Fe-S] clusters and either a molybdenum or tungsten containing metallopterin cofactor (Niks and Hille, 2019). They are separate from another class of formate dehydrogenases, the cofactor-less NADH-dependent formate dehydrogenases, which are typically found in eukaryotes and which have not been suggested to be present in syntrophic metabolizers (Niks and Hille, 2019). Formate dehydrogenases are also used to re-oxidize reduced cofactors generated during syntrophic metabolism and can be used by a methanogenic partner to oxidize formate to produce methane. The difference between formate and hydrogen as the primary means of transferring electrons has been debated. Diffusion modeling of syntrophic co-culture conditions has suggested that formate can account for 95% of the total number of electrons transferred compared to hydrogen (Boone et al., 1989; Stams and Dong, 1995). However, the addition of hydrogenase inhibitors had a far more pronounced effect than formate dehydrogenase inhibitors on inhibiting syntrophic butyrate oxidation in a co-culture of *S. wolfei* and *Methanosprillum hungatei*, suggesting a crucial role for hydrogen (Sieber et al., 2014). It has been also proposed that both hydrogen and formate act simultaneously as electron transfer carriers between syntrophic metabolizers and methanogenic partners (Schink et al., 2017). At

least one study has suggested that small differences in redox potential exist between the two metabolites in anaerobic environments where syntrophic metabolism occurs (Montag and Schink, 2018).

### **Flavin-Based Electron-Bifurcating Enzymes and the Rnf Complex**

Recently, the roles of a number of electron-bifurcating enzymes have been elucidated in anaerobic microorganisms. The discovery of electron-bifurcating enzymes has changed our concepts on how cellular electron carriers are re-oxidized in anaerobic microorganisms.

Electron-bifurcation allows two electrons of the same potential to be split so that one electron becomes more reduced (and thus is thermodynamically more favorable in additional reduction reactions) while the other electron becomes more oxidized (and thus less thermodynamically favored as a reductant) (Buckel and Thauer, 2018b; Buckel and Thauer, 2018a; Schuchmann et al., 2018). In the reverse direction, electron confurcation, such reactions facilitate the two-electron reduction of a quinone or flavin cofactor by coupling the thermodynamically unfavorable oxidation of a high redox potential donor with the thermodynamically favorable oxidation of a low potential donor in a process that involves the formation of a semiquinone reactive intermediate (Buckel and Thauer, 2018a). Such electron-bifurcation reactions can link different electron carrier pools inside of an anaerobic organism and allow the reduction of the low potential carrier ferredoxin. It has been suggested that in many aspects reduced ferredoxin represents a form of energy currency as ferredoxin's low reduction potential can be used to conserve energy by generating a chemiosmotic gradient. This gradient can in turn be used to generate ATP by the Rnf Complex, which is explained later (Buckel and Thauer, 2018b; Buckel and Thauer, 2018a; Schuchmann et al., 2018). Detailed summaries of

these electron-bifurcating enzymes can be found in a number of recent reviews on the topic (Baymann et al., 2018; Buckel and Thauer, 2018b; Buckel and Thauer, 2018a). The flavin-based, electron-bifurcating enzymes have been proposed to belong to one of four groups: 1. EtfAB containing, 2. NADH-dependent, ferredoxin-NADP<sup>+</sup> oxidoreductase (NfnAB)-homolog containing, 3. NADH:ubiquinone oxidoreductase (NuoF)-homolog containing and 4. heterodisulfide reductase (HdrABC)-homolog containing (Buckel and Thauer, 2018b). Examples of EtfAB-containing, electron-bifurcating enzymes include the electron-bifurcating butyryl-CoA dehydrogenase from *Clostridium kluyveri* (Li et al., 2008), the electron-bifurcating caffeyl-CoA reductase from *Acetobacium woodii* (Bertsch et al., 2013), the electron-bifurcating lactate dehydrogenase from *A. woodii* (Weghoff et al., 2015), and an electron-bifurcating FixABCX complex from *Azotobacter vinelandii* (Ledbetter et al., 2017). NfnAB-containing electron-bifurcating complexes that have been studied include the electron-bifurcating transhydrogenase from *C. kluyveri* (Wang et al., 2010) and the electron-bifurcating transhydrogenase from *Pyrococcus furiosus* (Lubner et al., 2017). Electron-bifurcating enzymes that contain a NuoF-homolog include the electron-bifurcating [FeFe]-hydrogenases from *Thermotoga maritima* (Schut and Adams, 2009), *A. woodii* (Schuchmann and Muller, 2012), *Moorella thermoacetica* (Wang et al., 2013c), *Ruminococcus albus* (Zheng et al., 2014), *Caldanaerobacter tencongensis* (Soboh et al., 2004; Kelly et al., 2015) and *Desulfovibrio fructosovorans* (Kpebe et al., 2018). Other electron-bifurcating enzymes containing a NuoF-homolog include an electron-bifurcating, formate-dependent dehydrogenase from *Clostridium acidurici* (Wang et al., 2013b) and an electron-bifurcating [FeFe]-hydrogenase in a functional complex with a formate dehydrogenase from *Clostridium autoethanogenum* (Wang et al., 2013a). The first well characterized example of an electron-bifurcating HdrABC containing

complex was the MvhADG/HdrABC complex from *Methanothermobacter marburgensis* (Kaster et al., 2011) which bifurcates electrons from hydrogen to a higher redox potential to reduce a disulfide bond (CoM-S-S-CoB, the oxidized form of coenzyme M and coenzyme B) and to a lower redox potential to reduce ferredoxin. Another example of an HdrABC-containing, electron-bifurcating complex is the heterodisulfide reductase from *Methanosarcina acetivorans* (Yan et al., 2017) which bifurcates electrons from coenzyme 420 (F<sub>420</sub>) to a higher redox potential to reduce the CoM-S-S-CoB bond and to a lower redox potential to reduce ferredoxin.

There are only three detailed mechanisms of electron flow in electron-bifurcating enzymes: the NADH-dependent, ferredoxin-NADP<sup>+</sup> oxidoreductase from *Pyrococcus furiosus* (Nfn1) (Lubner et al., 2017), the electron-bifurcating butyryl-CoA dehydrogenase from *Acidaminococcus fermentans* (Bcd) (Chowdhury et al., 2014), and the cytochrome *bc-1* complex of the respiratory chain (Mitchell, 1975; Buckel and Thauer, 2018b). Only the Nfn1 and *A. fermentans* Bcd systems are flavin-based as the cytochrome *bc-1* complex involves quinone-based electron bifurcation. Common characteristics of flavin-based, electron-bifurcating enzymes include: the low potential electron carrier ferredoxin, multiple flavin cofactors per enzyme complex, iron-sulfur centers, and separate electron flow paths for the high redox potential electron donor and the low potential electron donor to the site of electron bifurcation.

Ferredoxins are small acidic proteins that contain one to three [Fe-S] centers of varying conformation ([2Fe-2S], [4Fe-4S], [3Fe-4S]) and are viewed as only being able to accommodate a single electron (Sticht and Rosch, 1998; Buckel and Thauer, 2018b). Reported redox potentials for ferredoxins vary from  $E' = -340$  mV in *A. fermentans* (Thamer et al., 2003) to  $E' = -500$  mV in *Hydrogenobacter thermophilus* (Li and Elliott, 2016), although  $E_0' = -410$  mV is most often used in models of electron-bifurcating enzymes. It has long been considered that ferredoxins

from different organisms are interchangeable when used with enzymatic assays (Buckel and Thauer, 2018b). Ferredoxin from *Clostridium pasteranium* is often used when assaying ferredoxin-dependent enzymes as the use of this organism allows the convenient purification of large amounts of ferredoxin (Buckel and Thauer, 2018b). Ferredoxin has been identified as one of the electron donors in all currently known flavin-based electron-bifurcating enzymes (Baymann et al., 2018; Buckel and Thauer, 2018b; Buckel and Thauer, 2018a). Electron-bifurcating enzymes have been proven crucial to understanding anaerobic metabolisms in methanogens, homoacetogens, and primary fermenting organisms. However, no electron-bifurcating enzymes have been purified and characterized from syntrophic metabolizers and their potential roles are mostly inferred from genomic evidence.

The Rnf complex (named for *Rhodobacter* nitrogen fixation) is a six-subunit complex first discovered in *Rhodobacter capsulatus* that was suggested to play a crucial role in nitrogen fixation (Schmehl et al., 1993). Detailed study and experimentation with the Rnf complex in *A. woodii* (Biegel and Müller, 2010) showed that it is a membrane-bound, Na<sup>+</sup>-translocating ferredoxin:NAD<sup>+</sup> oxidoreductase. The Rnf complex has been suggested to be important in many anaerobic organisms for conserving energy by generating a chemiosmotic gradient coupled to the oxidation of ferredoxin and reduction of NAD<sup>+</sup>. It has been now suggested that reduced ferredoxin should be viewed as an energy-rich compound as it can be used by a Rnf complex to generate an ion gradient which in turn can be used to produce ATP using an ATP synthase (Buckel and Thauer, 2018b; Muller et al., 2018). The Rnf complex can also function to make reduced ferredoxin from NADH using the ion gradient in order to provide reduced ferredoxin for biosynthesis and benzoyl-CoA reduction in *S. aciditrophicus* (McInerney et al., 2007).



The electron-bifurcating [FeFe]-hydrogenases are part of the NuoF-homolog containing flavin-based electron-bifurcating enzymes. At least six enzymes of this type have been purified and enzymatically characterized; however, the electron flow within these multimeric enzymes is still a mystery. Putative electron-bifurcating [FeFe]-hydrogenases have been identified in the genomes of several syntrophic metabolizers and two such enzymes are the focus of this dissertation.

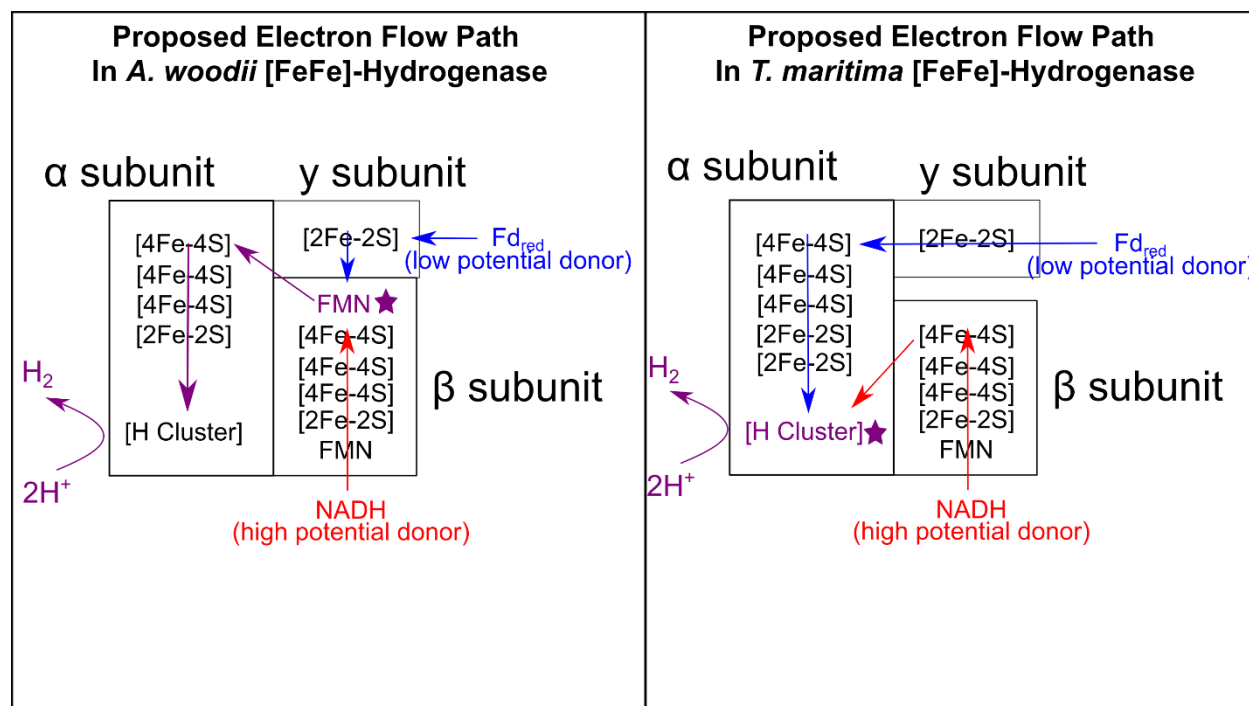
It has been observed that there are similarities between the beta subunit of the electron-bifurcating hydrogenases and the NuoF subunit of the NADH:ubiquinone oxidoreductase that is involved in NADH oxidation (Buckel and Thauer, 2018a). In particular they share predicted NADH- and FMN-binding sites. However, the only FMN predicted to be bound in the beta subunit of the electron-bifurcating hydrogenases is considered unsuitable as the site of electron bifurcation. This is due to the close proximity of FMN to the NADH-binding site, suggesting that the proposed role of this FMN is limited to facilitating the two-electron oxidation from NADH (Buckel and Thauer, 2013; Baymann et al., 2018; Buckel and Thauer, 2018a). In current proposed mechanisms for electron-bifurcation, the initial electron transfer involves a thermodynamically unfavorable transfer to FMN. The transfer of electrons from NADH to this FMN is thermodynamically favorable and does not match the proposed mechanism in other electron-bifurcating enzymes (Buckel and Thauer, 2018a). Instead, another cofactor must serve as the site of electron bifurcation. At least two different explanations have been proposed for electron bifurcation in NADH-dependent, ferredoxin-dependent [FeFe]-hydrogenases.

The first explanation derived from the study of the *A. woodii* electron-bifurcating [FeFe]-hydrogenase suggests that a second bound but, as yet, unidentified flavin cofactor (see Figure 1) is present in the beta subunit and serves as the site of electron bifurcation (Buckel and Thauer,

2018a). A slight modification of this scheme (Schuchmann et al., 2018) has also been suggested that includes two additional bound flavins. The necessity for two additional flavins is due to the limitation of iron sulfur centers to accommodate only a single electron at a time.

**Figure 1. Competing Proposals for Electron Flow in Electron-Bifurcating [FeFe]-**

**Hydrogenases.** The left panel represents electron flow similar to that proposed by (Buckel and Thauer, 2018a) where electron-bifurcation occurs at a second flavin present in the beta subunit. The right panel represents electron flow similar to that proposed by (Peters et al., 2018) where electron bifurcation occurs at the H-cluster. Arrows indicate electron flow. Purple stars indicate cofactors acting as the site of electron-bifurcation.



The second explanation suggests that the active site of the *T. maritima* [FeFe]-hydrogenase, the [H]-cluster (Figure 1), serves as the site of electron bifurcation (Peters et al., 2018). The explanation argues that the [H]-cluster, the catalytic site of proton reduction, is

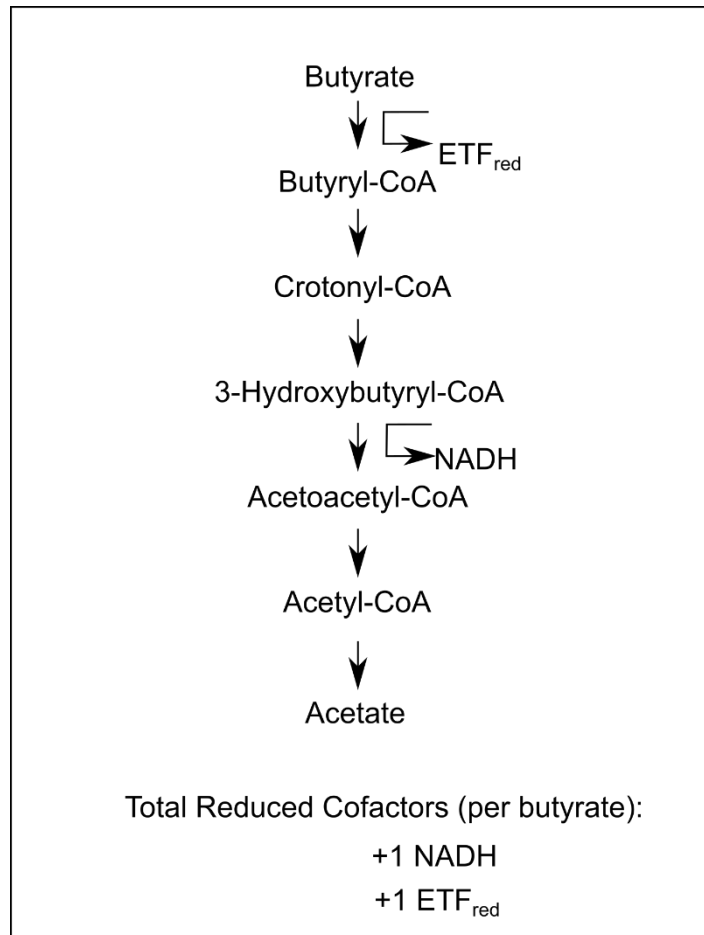
capable of accommodating two electrons of different redox potential simultaneously. The metallopterin cofactor at the catalytic site of the electron-bifurcating formate dehydrogenases is also proposed to have the ability to accommodate two electrons of different redox potentials. Therefore, this electron flow scheme could also operate in electron-bifurcating formate dehydrogenases.

### **Re-Oxidation of Reduced Cofactor Pools, NADH and Electron Transfer Flavoprotein in *S. wolfei* and *S. aciditrophicus***

During the oxidation of butyrate by *S. wolfei*, there are two oxidation-reduction steps that generate reduced cofactors. The first step, the oxidation of butyryl-CoA to crotonyl-CoA, is believed to produce reduced electron transfer flavoprotein (ETF<sub>red</sub>) with a high redox potential ( $E' = -125$  mV) (see Figure 2) (Gustafson et al., 1986; Sieber et al., 2010). The second step, the oxidation of 3-hydroxybutyryl-CoA to acetoacetyl-CoA ( $E' = -250$  mV), has been shown to be coupled to the reduction of NAD<sup>+</sup> to NADH (Wofford et al., 1986). To continually oxidize butyrate, *S. wolfei* must re-oxidize NADH and ETF<sub>red</sub> by producing hydrogen or formate. For this to happen, the partner microorganism, such as a hydrogenotrophic methanogen, must continually remove hydrogen and formate so that cofactor re-oxidation remains thermodynamically favorable.

### **Figure 2. Reduced Cofactor Generation during Syntrophic Butyrate Oxidation in *S. wolfei*.**

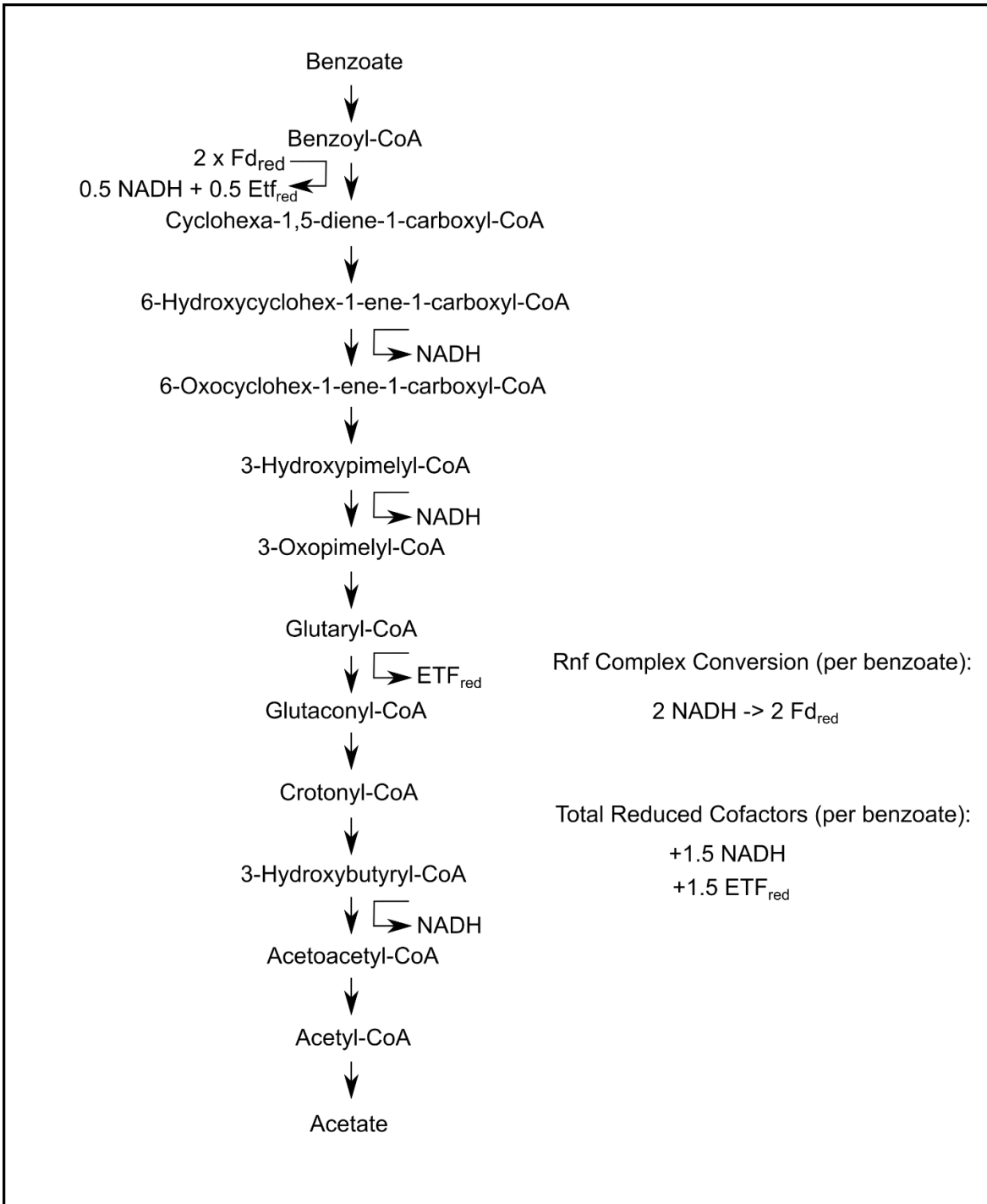
Acyl-CoA oxidation is shown as coupled to Etf reduction and not by an electron-bifurcating mechanism.



In *S. aciditrophicus*, enzymatic analyses suggest that NADH production (see Figure 3) is expected in the following 3-hydroxyacyl-CoA oxidation reactions: 3-hydroxybutyryl-CoA to acetoacetyl-CoA, 3-hydroxypimeyl-CoA oxidation to 3-oxopimeyl-CoA, and 6-hydroxycyclohex-1-ene-1carboxyl-CoA oxidation to 6-oxycyclohex-1-ene-1carboxyl-CoA (Elshahed and McInerney, 2001). The last oxidation step, the oxidation of glutaryl-CoA to glutaconyl-CoA would produce electrons of a similar potential to the butyryl-CoA to crotonyl-CoA oxidation (estimated  $E' = -10$  mV to  $E' = -126$  mV). This oxidation reaction has been suggested to occur by an electron-bifurcating acyl-CoA dehydrogenase (Djurdjevic, 2010) similar to an electron-bifurcating butyryl-CoA dehydrogenase. If the glutaryl-CoA dehydrogenase is electron-bifurcating, a pair of electrons from the low redox potential donor

ferredoxin ( $E' = -410$  mV) and a pair of high redox potential electrons from the oxidation of glutaryl-CoA to glutaconyl-CoA ( $E' = -126$  mV) would be confurcated to an intermediate redox potential to produce two pairs of electrons at the redox potential of NADH ( $E' = -320$  mV). Alternatively, electrons from the oxidation of glutaryl-CoA to glutaconyl-CoA could be transferred to  $Etf_{red}$  and then to a membrane-associated, iron-sulfur oxidoreductase system, which would reduce menaquinone (McInerney et al., 2007). Chemiosmotic energy would be used to lower the redox potential of the electrons in order to produce hydrogen or formate, similar to the mechanism proposed for *S. wolfei* (Crabbe, 2013). As with *S. wolfei*, *S. aciditrophicus* would require continual hydrogen or formate consumption by a partner organism to allow continual cofactor re-oxidation.

**Figure 3. Reduced Cofactors from Syntrophic Benzoate Oxidation in *S. aciditrophicus*.** Note that two NADH molecules are used to make two reduced ferredoxins needed for benzoyl-CoA reduction and have been subtracted from total NADH made during benzoyl-CoA metabolism to acetate and CO<sub>2</sub>. The reduction of benzoyl-CoA is shown with the stoichiometry of an ATP-independent enzyme complex mediating two separate electron-bifurcation reactions as proposed by (Huwiler et al., 2019). Acyl-CoA oxidation is shown as being coupled to Etf reduction and not by an electron-bifurcating mechanism.



Another important step during syntrophic benzoate metabolism in *S. aciditrophicus* is the reduction of benzoyl-CoA (see Figure 3). Evidence suggests that the mechanism is similar to the proposed reaction in *Geobacter metallireducens* involving the low redox potential electron

donor, reduced ferredoxin (Kung et al., 2009). However, a recent publication has shown that the *G. metallireducens* benzoyl-CoA reductase is actually a one megadalton complex and benzoyl-CoA reduction may involve two separate electron bifurcation steps (Huwiler et al., 2019). The overall electron transfer scheme is the oxidation of two pairs of electrons from the low potential donor ferredoxin ( $E' = -410$  mV) with one pair being bifurcated to a lower redox potential ( $E' = -580$  mV) and used to reduce benzoyl-CoA. The second pair of electrons is bifurcated to a higher redox potential ( $E' = -200$  mV). It has been proposed that a second bifurcation reaction bifurcates this higher redox potential electron pair to reduced NADH ( $E' = -320$  mV) and reduced menaquinone (MQ) ( $E' = -70$  mV). However, there is much uncertainty over this second bifurcation reaction. The membrane dependence of the reaction implicates a role for menaquinone but menaquinone involvement has not been demonstrated. If *S. aciditrophicus* utilizes the same enzyme complex for benzoyl-CoA reduction, as genomic analysis suggests (Boll et al., 2014), this would alter the number of predicted reduced cofactors per mole of benzoate oxidized from 2 NADH, 1 Etf<sub>red</sub> to 1.5 NADH and 1.5 Etf<sub>red</sub> as shown in Figure 3.

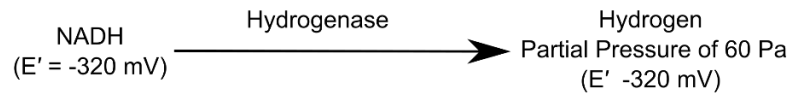
There are two different explanations for how NADH could be re-oxidized to produce hydrogen (or formate) in *S. wolfei* and *S. aciditrophicus*. The first explanation argues that, according to thermodynamic calculations, production of hydrogen using high redox potential electrons from NADH ( $E' = -320$  mV) can occur so long as the hydrogen partial pressure does not exceed 60 pascals (see Figure 4) (Boone et al., 1989; Schink, 1997). As hydrogenotrophic methanogens can maintain hydrogen partial pressures below 60 Pa, the process of producing hydrogen from NADH would continue to function. The observed hydrogen partial pressures in co-cultures of *S. wolfei* and a hydrogenotrophic methanogen (25 Pa) were agreement with this proposal (Boone et al., 1989).

**Figure 4. Alternative Explanations for NADH Re-Oxidation in *S. wolfei* and *S.***

***aciditrophicus*.** A. NADH oxidation by non-electron bifurcating hydrogenase at low hydrogen partial pressures; B. NADH oxidation coupled to reduced ferredoxin oxidation by electron-bifurcating hydrogenases. Reduced ferredoxin could be made from electrons derived from NADH oxidation by the Rnf complex identified in the genome of *S. aciditrophicus* using the chemiosmotic gradient. In *S. wolfei*, FixABCX complex could bifurcate electrons from the high redox potential electron carrier NADH to the even higher potential electron carrier menaquinone to produce reduced ferredoxin. The high redox potential electron carrier menaquinone could be re-oxidized by a putative reverse quinone loop.



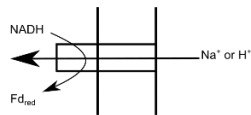
## A. NADH-Dependent Hydrogen Production



## B. Electron Confurcating Hydrogen Production

Step 1. Reduce Ferredoxin with Electrons from NADH using Chemiosmotic Potential

Rnf Complex (*S. aciditrophicus*)

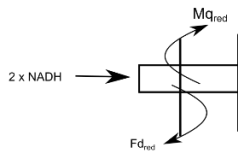


NADH  
(E' -320 mV)

Reverse Electron Transfer  
or Electron-Bifurcation

Ferredoxin  
(E' -410 mV)

FixABCX Complex (*S. wolfei*)



Step 2. Electron Confurcating Hydrogen Production

NADH  
(E' -320 mV)

Confurcated Electrons  
(E' -365 mV)

Ferredoxin  
(E' -410 mV)

Hydrogenase

Hydrogen  
Partial Pressure of up to 1000 Pa  
(E' -365 mV)

However, when the genomes of *S. wolfei* and *S. aciditrophicus* were sequenced, genes were identified that shared high homology to the multimeric [FeFe]-hydrogenase from *T. maritima*. The *T. maritima* [FeFe]-hydrogenase was initially presumed to utilize NADH for hydrogen production, but no production from NADH as a sole donor was observed (Verhagen et al., 1999). Later, it was discovered that the *T. maritima* hydrogenase is electron-bifurcating and required both reduced ferredoxin and NADH in 1:1 ratio to produce hydrogen (Schut and Adams, 2009). Characterization of additional multimeric [FeFe]-hydrogenases showed they were all capable of electron-bifurcation but could not utilize NADH alone. Therefore, the multimeric [FeFe]-hydrogenases in *S. wolfei* and other syntrophic metabolizers were widely assumed to operate only by electron-bifurcation and not capable of utilizing NADH as a sole donor (Stams and Plugge, 2009). However, for an electron-bifurcating [FeFe]-hydrogenase to function in *S. wolfei* there must be a source of reduced ferredoxin. However, the oxidation of fatty acids by *S. wolfei* was only predicted to produce NADH and reduced flavin cofactors. The genes for the Rnf complex capable of making reduced ferredoxin from electrons derived from NADH oxidation were identified in the *S. aciditrophicus* genome (McInerney et al., 2007). However, genes for the Rnf complex were not identified in the *S. wolfei* genome but instead another set of genes encoding proteins for the FixABCX, complex, which could perform a similar function (Sieber et al., 2010; Sieber et al., 2015). Recent studies of the FixABCX complex in *Azotobacter vinelandii* suggest it could provide a source of reduced ferredoxin by bifurcating electrons from NADH to the low potential electron carrier ferredoxin and to the high redox potential electron carrier menaquinone (Ledbetter et al., 2017). Thus, in both syntrophic model organisms, *S. wolfei* and *S. aciditrophicus*, complexes capable of supplying ferredoxin have been proposed. With a source of reduced ferredoxin, electron-bifurcating [FeFe]-hydrogenases could produce hydrogen from

NADH and reduced ferredoxin. From thermodynamic calculations, the redox potential of electrons confurcated from NADH and reduced ferredoxin would be close to  $E' = -360$  mV and capable of producing hydrogen partial pressures of at least 1000 pascals.

The physiological electron acceptors involved in the oxidation of acyl-CoA metabolites in *S. wolfei* and *S. aciditrophicus* have not been demonstrated experimentally. Enzymes that catalyze this reaction in primary fermenters such as *Clostridium kluyveri* have been found to use electron-bifurcation (Li et al., 2008). A glycine residue predicted to be required for binding of the electron-bifurcating flavin cofactor reaction is absent in the EtfB subunits present in the *S. aciditrophicus* and *S. wolfei* genomes (Garcia Costas et al., 2017) (Figure 5).

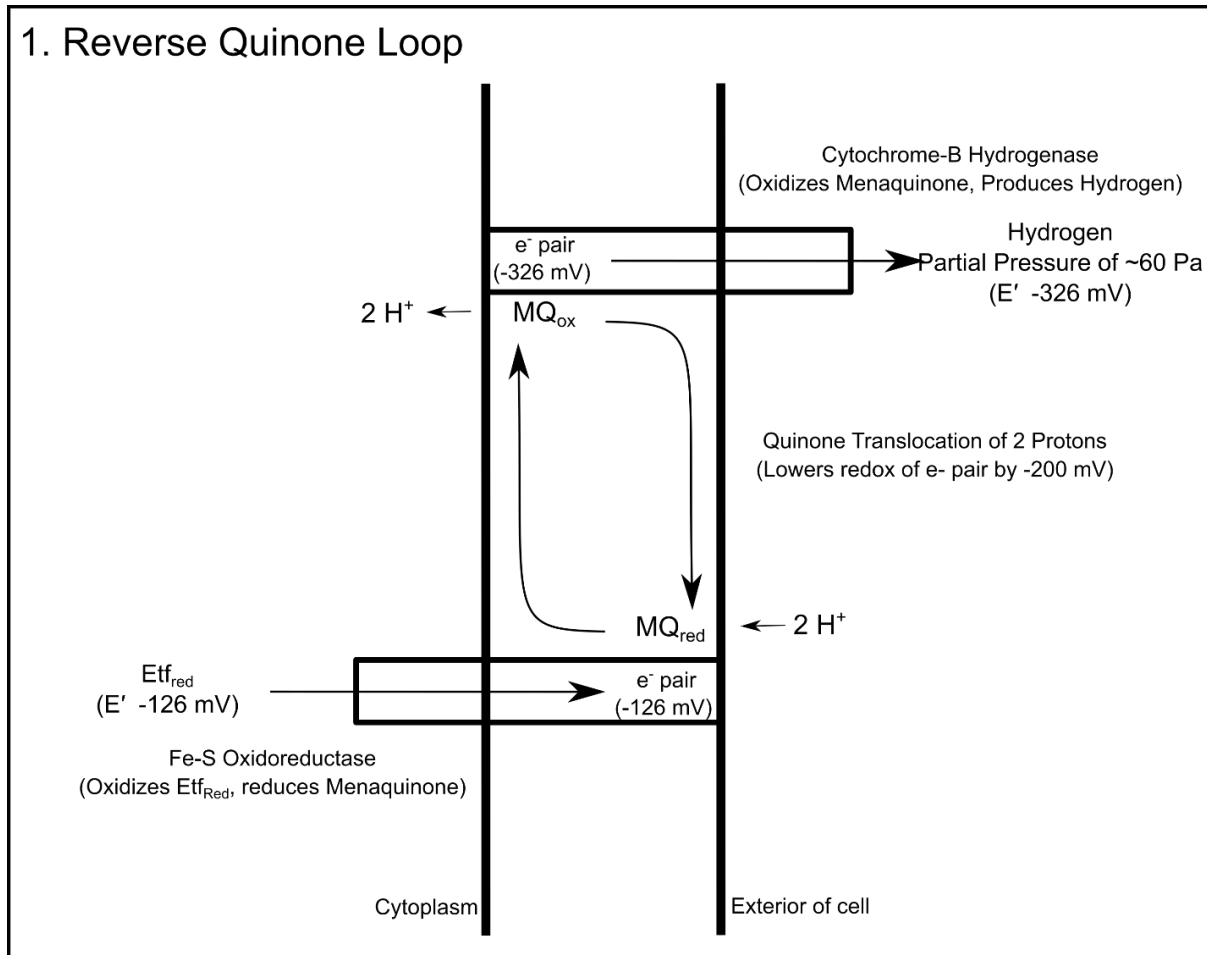
**Figure 5. Alignment *S. wolfei* and *S. aciditrophicus* of EtfB Subunits.** Red indicates residues proposed to be essential to NADH binding in electron-bifurcating EtfB subunits (Garcia Costas et al., 2017) while blue indicates a residue proposed to be required for flavin cofactor binding in electron-bifurcating EtfB subunits. The *Paracoccus nitrificans* EtfB is not predicted to be electron-bifurcating, while the *Acidaminococcus fermentans*, *Acetobacterium woodii*, *Clostridium difficile* and *Clostridium kluyveri* EtfBs are known to perform electron-bifurcation.

	Alignment Position 160	Alignment Position 239
1 <i>A. fermentans</i>	LAVGADEAKLV--SDRA <b>FGGADT</b> LATSAAMANTIKHFGVVDLIL <b>CGRQAIDGDTAQVGP</b> IEAHLGLPQVTAALKVQVKD	
2 <i>A. woodii</i> Copy 1	LAMGADEAYLL--SDRA <b>FGGADT</b> WATSATLAAGIKKVKVDLVL <b>AGRQAIDGDTAQVGSQ</b> IAEQRLKMPVVTVYVEDIKIED	
3 <i>A. woodii</i> Copy 2	FYMGADGCLL--SDRK <b>FGGADV</b> VATSYTLAQGTKRLGDFDLIIC <b>GKQTTDGD</b> T <b>AQVGP</b> EMAEFLGIPHVTNVIKILAAD	
4 <i>C. difficile</i>	LAMGADRGILL--TDRA <b>FGADT</b> WATSSALAGALKNI-DFDII <b>AGRQAIDGDTAQVGP</b> QIAEHLNLPSTIYAEIKTEG	
5 <i>C. kluyveri</i>	LAMGADEAILV--SDRA <b>FGADT</b> QATSYALAGALKNL-EYDLIF <b>AGRQAIDGDTAQVGP</b> QIAEHLNLPSTIYAEIKTEG	
6 <i>S. aciditrophicus</i>	LAMGADKGIHI--DDPA <b>LEGAD</b> AYATATALAAAIKGI-PYDVIF <b>CGRQAID</b> DDSG <b>QVGA</b> ILAEHLGLPQVTAALKVQVKD	
7 <i>S. wolfei</i> Copy 1	LAMGADRGILV--Q <b>QDT</b> -- <b>A</b> DEFARAVALAEAIKGE-NPDIIL <b>AGHVAAD</b> D <b>GSSQV</b> PTRVAEILGLPHVNVITAVEIAG	
8 <i>S. wolfei</i> Copy 2	LAAGADEALLI--IDDE <b>LDK</b> LGS <b>AE</b> TAKILAAAIQRIEKVDLII <b>F</b> GE <b>SGD</b> NY <b>SGQV</b> SRVAEILGLPQVGYASAIELQG	
9 <i>P. nitrificans</i>	LAMGADRAILVVAAD <b>DVQ</b> DI <b>EL</b> AVAKILAAVARAE-GTELI <b>AGKQAID</b> ND <b>MNAT</b> G <b>QML</b> AAIILGWAQATFASKVEIEG	

Therefore, it is unlikely acyl-CoA oxidation during syntrophic metabolism in *S. wolfei* and *S. aciditrophicus* involves electron-bifurcation. Instead an alternative mechanism (see Figure 6) has been proposed in *S. aciditrophicus* (McInerney et al., 2007) and *S. wolfei* involving an iron-sulfur oxidoreductase in conjunction with a membrane-associated [FeFe]-hydrogenase or formate dehydrogenase to form a reverse quinone loop (Sieber et al., 2010; Crable, 2013; Schmidt et al., 2013; Sieber et al., 2015; Crable et al., 2016). The reverse quinone loop would utilize the potential energy from a proton gradient, generated by an ATP synthase to make hydrogen production from the high redox potential electrons generated during acyl-CoA oxidation more favorable (Figure 6).

**Figure 6. Proposed Mechanism of Etf Re-Oxidation in *S. wolfei* and *S. aciditrophicus*.** The proposed redox values are similar to those described by (Schmidt et al., 2013). Redox potential

of  $E_{f_{red}}$  is shown as the same of the butyryl-CoA/crotonyl-CoA redox value (Gustafson et al., 1986). MQ, Menaquinone.



Previously, attempts have been made to investigate formate dehydrogenases and [FeFe]-hydrogenases from syntrophic microorganisms. One investigation of two formate dehydrogenases purified from the syntrophic propionate oxidizer *Syntrophobacter fumaroxidans* described multimeric complexes containing tungstate (de Bok et al., 2003). Both enzymes, FDH-1 and FDH-2, possessed high catalytic activity with the artificial electron acceptor benzyl viologen in both the formate-producing and formate-consuming reactions. However, a

physiological donor could not be identified for either enzyme. FDH-1 consists of three subunits with molecular weights of 89 kDa, 56 kDa, and 19 kDa and resembles the multimeric electron-bifurcating, formate dehydrogenase present in *Clostridium acidurici* (Wang et al., 2013b). Electron-bifurcating formate dehydrogenases require the involvement of both ferredoxin and NADH, which would not have been recognized at the time that the *S. fumaroxidans* formate dehydrogenases were characterized.

A second study described the purification of an enzyme activity with subunits predicted to encode for a multimeric [FeFe]-hydrogenase from *Syntrophomonas wolfei* (Müller et al., 2009). The three subunits for the [FeFe]-hydrogenase co-purified with subunits from a selenocysteine-containing formate dehydrogenase despite the use of various chromatographic steps. The purification was performed under oxic conditions that likely inactivated the catalytic sites of the [FeFe]-hydrogenase and selenocysteine-containing formate dehydrogenase. No hydrogen producing or formate producing activities with physiological electron donors were reported.

I attempted to purify formate dehydrogenases and [FeFe]-hydrogenases from the membrane and soluble fractions of *S. wolfei* without achieving homogeneous preparations. The enrichment of formate dehydrogenase activity from the membrane of *S. wolfei* using gel filtration and hydroxyapatite column chromatography indicated the partial purification of two subunits of predicted molecular weights 96 kDa and 30.8 kDa as identified by peptide mass spectrometry. Both subunits were predicted to be associated with a formate dehydrogenase. However, the predicted encoding genes from the *S. wolfei* genome (Swol\_0798-Swol\_0799) occur in an operon of at least four genes (Swol\_0797-Swol\_0800), suggesting additional subunits were lost during purification. In addition, difficulty was encountered in stabilizing formate dehydrogenase

activity during purification. The ability to identify a physiological electron donor and to place the role of enzyme within the metabolism of *S. wolfei* seemed unlikely and the approach was discontinued. Attempted purification of formate dehydrogenase and hydrogenase activity from the soluble portion of *S. wolfei* indicated that the two activities co-migrated despite the use of several common separation techniques including hydroxyapatite, anion-exchange, and gel-filtration chromatography. The inability to separate the two activities, along with large decrease in the activity during the multi-step purification suggested that another approach would be needed to obtain a pure protein.

The difficulties in purifying formate dehydrogenases and hydrogenases from syntrophic microorganisms were challenging and led to the use of a recombinant DNA approach to clone and express the proteins of interest in *Escherichia coli*. Production and characterization of [FeFe]-hydrogenases by a recombinant DNA approach had been demonstrated before and allowed the rapid purification of large amounts of active enzyme using affinity tag chromatography (Girbal et al., 2005; King et al., 2006). The research for this dissertation describes the properties of two multimeric [FeFe]-hydrogenases from *S. wolfei* and *S. aciditrophicus*. Recombinantly produced, affinity tagged multimeric [FeFe]-hydrogenases from *S. wolfei* and *S. aciditrophicus* were characterized to determine if they required reduced ferredoxin for NADH oxidation. My work shows that both enzymes reoxidize NADH coupled to hydrogen production without ferredoxin involvement so long as the hydrogen partial pressure was low. Thus, continual hydrogen production from NADH by these enzymes would explain the requirement syntrophic organisms have for low hydrogen partial pressures. This in turn explains the obligate requirement for the presence of hydrogen-consuming partner microorganisms during syntrophic fatty and aromatic acid metabolism.

## References

- Angelidaki, I., Karakashev, D., Batstone, D.J., Plugge, C.M., and Stams, A.J.M. (2011). "Chapter sixteen - Biomethanation and Its Potential," in *Methods in Enzymology*, eds. A.C. Rosenzweig & S.W. Ragsdale. Academic Press), 327-351.
- Baymann, F., Schoepp-Cothenet, B., Duval, S., Guiral, M., Brugna, M., Baffert, C., et al. (2018). On the Natural History of Flavin-Based Electron Bifurcation. *Front Microbiol* 9, 1357.
- Beaty, P.S., and McInerney, M.J. (1987). Growth of *Syntrophomonas wolfei* in pure culture on crotonate. *Arch Microbiol* 147(4), 389-393. doi: 10.1007/BF00406138.
- Bertsch, J., Parthasarathy, A., Buckel, W., and Muller, V. (2013). An electron-bifurcating caffeyl-CoA reductase. *J Biol Chem* 288(16), 11304-11311. doi: 10.1074/jbc.M112.444919.
- Biegel, E., and Müller, V. (2010). Bacterial Na<sup>+</sup>/-translocating ferredoxin:NAD<sup>+</sup>/oxidoreductase. *Proc Natl Acad Sci Unit States Am* 107(42), 18138-18142. doi: 10.1073/pnas.1010318107.
- Boll, M., Löffler, C., Morris, B.E.L., and Kung, J.W. (2014). Anaerobic degradation of homocyclic aromatic compounds via arylcarboxyl-coenzyme A esters: organisms, strategies and key enzymes. *Environ Microbiol* 16(3), 612-627. doi: 10.1111/1462-2920.12328.
- Boone, D.R., Johnson, R.L., and Liu, Y. (1989). Diffusion of the Interspecies Electron Carriers H<sub>2</sub> and Formate in Methanogenic Ecosystems and Its Implications in the Measurement of H<sub>2</sub> or Formate Uptake. *Appl Environ Microb* 55(7), 1735.



- Buckel, W., and Thauer, R.K. (2013). Energy conservation via electron bifurcating ferredoxin reduction and proton/Na(+) translocating ferredoxin oxidation. *Biochim Biophys Acta* 1827(2), 94-113. doi: 10.1016/j.bbabi.2012.07.002.
- Buckel, W., and Thauer, R.K. (2018a). Flavin-Based Electron Bifurcation, A New Mechanism of Biological Energy Coupling. *Chem Rev* 118(7), 3862-3886. doi: 10.1021/acs.chemrev.7b00707.
- Buckel, W., and Thauer, R.K. (2018b). Flavin-Based Electron Bifurcation, Ferredoxin, Flavodoxin, and Anaerobic Respiration With Protons (Ech) or NAD+ (Rnf) as Electron Acceptors: A Historical Review. *Front Microbiol* 9, 401.
- Chowdhury, N.P., Mowafy, A.M., Demmer, J.K., Upadhyay, V., Koelzer, S., Jayamani, E., et al. (2014). Studies on the Mechanism of Electron Bifurcation Catalyzed by Electron Transferring Flavoprotein (Etf) and Butyryl-CoA Dehydrogenase (Bcd) of *Acidaminococcus fermentans*. *J Biol Chem* 289(8), 5145-5157. doi: 10.1074/jbc.M113.521013.
- Crable, B. (2013). *Enzyme systems involved in interspecies hydrogen and formate transfer between syntrophic fatty and aromatic acid degraders and Methanospirillum hungatei*. Doctoral Dissertation, University of Oklahoma.
- Crable, B.R., Sieber, J.R., Mao, X., Alvarez-Cohen, L., Gunsalus, R., Ogorzalek Loo, R.R., et al. (2016). Membrane Complexes of *Syntrophomonas wolfei* Involved in Syntrophic Butyrate Degradation and Hydrogen Formation. *Front Microbiol* 7, 1795. doi: 10.3389/fmicb.2016.01795.
- de Bok, F.A.M., Hagedoorn, P.-L., Silva, P.J., Hagen, W.R., Schiltz, E., Fritsche, K., et al. (2003). Two W-containing formate dehydrogenases (CO<sub>2</sub>-reductases) involved in

- syntrophic propionate oxidation by *Syntrophobacter fumaroxidans*. *Eur J Biochem* 270(11), 2476-2485. doi: 10.1046/j.1432-1033.2003.03619.x.
- Djurdjevic, I. (2010). *Production of glutaconic acid in recombinant Escherichia coli*. Doctoral Thesis, Philipps-Universität Marburg.
- Elshahed, M.S., Bhupathiraju, V.K., Wofford, N.Q., Nanny, M.A., and McInerney, M.J. (2001). Metabolism of Benzoate, Cyclohex-1-ene Carboxylate, and Cyclohexane Carboxylate by “*Syntrophus aciditrophicus*” Strain SB in Syntrophic Association with H<sub>2</sub>-Using Microorganisms. *Appl Environ Microb* 67(4), 1728-1738. doi: 10.1128/aem.67.4.1728-1738.2001.
- Elshahed, M.S., and McInerney, M.J. (2001). Benzoate fermentation by the anaerobic bacterium *Syntrophus aciditrophicus* in the absence of hydrogen-using microorganisms. *Appl Environ Microbiol* 67(12), 5520-5525. doi: 10.1128/AEM.67.12.5520-5525.2001.
- Fink, C.W., Stankovich, M.T., and Soltysik, S. (1986). Oxidation-reduction potentials of butyryl-CoA dehydrogenase. *Biochemistry-US* 25(21), 6637-6643.
- Fu, L., Song, T., Zhang, W., Zhang, J., and Lu, Y. (2018). Stimulatory Effect of Magnetite Nanoparticles on a Highly Enriched Butyrate-Oxidizing Consortium. *Front Microbiol* 9(1480). doi: 10.3389/fmicb.2018.01480.
- Garcia Costas, A.M., Poudel, S., Miller, A.F., Schut, G.J., Ledbetter, R.N., Fixen, K.R., et al. (2017). Defining Electron Bifurcation in the Electron-Transferring Flavoprotein Family. *J Bacteriol* 199(21). doi: 10.1128/jb.00440-17.
- Girbal, L., von Abendroth, G., Winkler, M., Benton, P.M.C., Meynial-Salles, I., Croux, C., et al. (2005). Homologous and Heterologous Overexpression in *Clostridium acetobutylicum* and Characterization of Purified Clostridial and Algal Fe-Only Hydrogenases with High

- Specific Activities. *Appl Environ Microb* 71(5), 2777. doi: 10.1128/AEM.71.5.2777-2781.2005.
- Gunsalus, R.P., Cook, L.E., Crable, B., Rohlin, L., McDonald, E., Mouttaki, H., et al. (2016). Complete genome sequence of *Methanospirillum hungatei* type strain JF1. *Stand Genomic Sci* 11, 2. doi: 10.1186/s40793-015-0124-8.
- Gustafson, W.G., Feinberg, B.A., and McFarland, J.T. (1986). Energetics of beta-oxidation. Reduction potentials of general fatty acyl-CoA dehydrogenase, electron transfer flavoprotein, and fatty acyl-CoA substrates. *J Biol Chem* 261(17), 7733-7741.
- Harwood, C.S., Burchhardt, G., Herrmann, H., and Fuchs, G. (1998). Anaerobic metabolism of aromatic compounds via the benzoyl-CoA pathway. *FEMS Microbiol Rev* 22(5), 439-458. doi: [https://doi.org/10.1016/S0168-6445\(98\)00026-6](https://doi.org/10.1016/S0168-6445(98)00026-6).
- Huwiler, S.G., Löffler, C., Anselmann, S.E.L., Stärk, H.-J., von Bergen, M., Flechsler, J., et al. (2019). One-megadalton metalloenzyme complex in *Geobacter metallireducens* involved in benzene ring reduction beyond the biological redox window. *Proc Natl Acad Sci Unit States Am*, 201819636. doi: 10.1073/pnas.1819636116.
- Jackson, B.E., Bhupathiraju, V.K., Tanner, R.S., Woese, C.R., and McInerney, M.J. (1999). *Syntrophus aciditrophicus* sp. nov., a new anaerobic bacterium that degrades fatty acids and benzoate in syntrophic association with hydrogen-using microorganisms. *Arch Microbiol* 171(2), 107-114.
- James, K.L., Kung, J.W., Crable, B.R., Mouttaki, H., Sieber, J.R., Nguyen, H.H., et al. (2019, in preparation). *Syntrophus aciditrophicus* uses the same enzymes in a reversible manner to syntrophically degrade fatty, aromatic and alicyclic acids and to synthesize aromatic and alicyclic acids from crotonate.

- James, K.L., Rios-Hernandez, L.A., Wofford, N.Q., Mouttaki, H., Sieber, J.R., Sheik, C.S., et al. (2016). Pyrophosphate-Dependent ATP Formation from Acetyl Coenzyme A in *Syntrophus aciditrophicus*, a New Twist on ATP Formation. *MBio* 7(4). doi: 10.1128/mBio.01208-16.
- Kaster, A.K., Moll, J., Parey, K., and Thauer, R.K. (2011). Coupling of ferredoxin and heterodisulfide reduction via electron bifurcation in hydrogenotrophic methanogenic archaea. *Proc Natl Acad Sci Unit States Am* 108(7), 2981-2986. doi: 10.1073/pnas.1016761108.
- Kelly, C.L., Pinske, C., Murphy, B.J., Parkin, A., Armstrong, F., Palmer, T., et al. (2015). Integration of an [FeFe]-hydrogenase into the anaerobic metabolism of *Escherichia coli*. *Biotechnol Rep (Amst)* 8, 94-104. doi: <https://doi.org/10.1016/j.btre.2015.10.002>.
- King, P.W., Posewitz, M.C., Ghirardi, M.L., and Seibert, M. (2006). Functional Studies of [FeFe] Hydrogenase Maturation in an *Escherichia coli* Biosynthetic System. *J Bacteriol* 188(6), 2163. doi: 10.1128/JB.188.6.2163-2172.2006.
- Kpebe, A., Benvenuti, M., Guendon, C., Rebai, A., Fernandez, V., Le Laz, S., et al. (2018). A new mechanistic model for an O<sub>2</sub>-protected electron-bifurcating hydrogenase, Hnd from *Desulfovibrio fructosovorans*. *Biochim Biophys Acta Bioenerg* 1859(12), 1302-1312. doi: <https://doi.org/10.1016/j.bbabi.2018.09.364>.
- Kung, J.W., Löffler, C., Dorner, K., Heintz, D., Gallien, S., Van Dorsseleer, A., et al. (2009). Identification and characterization of the tungsten-containing class of benzoyl-coenzyme A reductases. *Proc Natl Acad Sci Unit States Am* 106(42), 17687-17692. doi: 10.1073/pnas.0905073106.

- Ledbetter, R.N., Garcia Costas, A.M., Lubner, C.E., Mulder, D.W., Tokmina-Lukaszewska, M., Artz, J.H., et al. (2017). The Electron Bifurcating FixABCX Protein Complex from *Azotobacter vinelandii*: Generation of Low-Potential Reducing Equivalents for Nitrogenase Catalysis. *Biochemistry* 56(32), 4177-4190. doi: 10.1021/acs.biochem.7b00389.
- Li, B., and Elliott, S.J. (2016). The Catalytic Bias of 2-Oxoacid:ferredoxin Oxidoreductase in CO<sub>2</sub>: evolution and reduction through a ferredoxin-mediated electrocatalytic assay. *Electrochim Acta* 199, 349-356. doi: <https://doi.org/10.1016/j.electacta.2016.02.119>.
- Li, F., Hinderberger, J., Seedorf, H., Zhang, J., Buckel, W., and Thauer, R.K. (2008). Coupled ferredoxin and crotonyl coenzyme A (CoA) reduction with NADH catalyzed by the butyryl-CoA dehydrogenase/Etf complex from *Clostridium kluyveri*. *J Bacteriol* 190(3), 843-850. doi: 10.1128/jb.01417-07.
- Lubner, C.E., Jennings, D.P., Mulder, D.W., Schut, G.J., Zadvornyy, O.A., Hoben, J.P., et al. (2017). Mechanistic insights into energy conservation by flavin-based electron bifurcation. *Nat Chem Biol* 13(6), 655-659. doi: 10.1038/nchembio.2348.
- McInerney, M.J., Bryant, M.P., Hespell, R.B., and Costerton, J.W. (1981). *Syntrophomonas wolfei* gen. nov. sp. nov., an Anaerobic, Syntrophic, Fatty Acid-Oxidizing Bacterium. *Appl Environ Microbiol* 41(4), 1029-1039.
- McInerney, M.J., Rohlin, L., Mouttaki, H., Kim, U., Krupp, R.S., Rios-Hernandez, L., et al. (2007). The genome of *Syntrophus aciditrophicus*: life at the thermodynamic limit of microbial growth. *Proc Natl Acad Sci U S A* 104(18), 7600-7605. doi: 10.1073/pnas.0610456104.

- McInerney, M.J., Sieber, J.R., and Gunsalus, R.P. (2009). Syntrophy in anaerobic global carbon cycles. *Curr Opin Biotechnol* 20(6), 623-632. doi: 10.1016/j.copbio.2009.10.001.
- McInerney, M.J., Struchtemeyer, C.G., Sieber, J., Mouttaki, H., Stams, A.J., Schink, B., et al. (2008). Physiology, ecology, phylogeny, and genomics of microorganisms capable of syntrophic metabolism. *Ann N Y Acad Sci* 1125, 58-72. doi: 10.1196/annals.1419.005.
- Mitchell, P. (1975). The protonmotive Q cycle: a general formulation. *FEBS Lett* 59(2), 137-139.
- Montag, D., and Schink, B. (2018). Formate and Hydrogen as Electron Shuttles in Terminal Fermentations in an Oligotrophic Freshwater Lake Sediment. *Appl Environ Microb* 84(20), e01572-01518. doi: 10.1128/AEM.01572-18.
- Morris, B.E.L., Henneberger, R., Huber, H., and Moissl-Eichinger, C. (2013). Microbial syntrophy: interaction for the common good. *FEMS Microbiol Rev* 37(3), 384-406. doi: 10.1111/1574-6976.12019.
- Mouttaki, H., Nanny, M.A., and McInerney, M.J. (2007). Cyclohexane carboxylate and benzoate formation from crotonate in *Syntrophus aciditrophicus*. *Appl Environ Microbiol* 73(3), 930-938. doi: 10.1128/AEM.02227-06.
- Müller, N., Schleheck, D., and Schink, B. (2009). Involvement of NADH:Acceptor Oxidoreductase and Butyryl Coenzyme A Dehydrogenase in Reversed Electron Transport during Syntrophic Butyrate Oxidation by *Syntrophomonas wolfei*. *J Bacteriol* 191(19), 6167. doi: 10.1128/JB.01605-08.
- Muller, V., Chowdhury, N.P., and Basen, M. (2018). Electron Bifurcation: A Long-Hidden Energy-Coupling Mechanism. *Annu Rev Microbiol* 72, 331-353. doi: 10.1146/annurev-micro-090816-093440.

- Nelson, T.C. (1951). Kinetics of genetic recombination in *Escherichia coli*. *Genetics* 36(2), 162-175.
- Niks, D., and Hille, R. (2019). Molybdenum- and tungsten-containing formate dehydrogenases and formylmethanofuran dehydrogenases: Structure, mechanism, and cofactor insertion. *Protein Sci* 28(1), 111-122. doi: 10.1002/pro.3498.
- Pacheco, A.R., Moel, M., and Segre, D. (2018). Costless metabolic secretions as drivers of interspecies interactions in microbial ecosystems. *bioRxiv*, 300046. doi: 10.1101/300046.
- Peters, J.W., Beratan, D.N., Schut, G.J., and Adams, M.W.W. (2018). On the nature of organic and inorganic centers that bifurcate electrons, coupling exergonic and endergonic oxidation–reduction reactions. *Chem Comm* 54(33), 4091-4099. doi: 10.1039/C8CC01530A.
- Peters, J.W., Lanzilotta, W.N., Lemon, B.J., and Seefeldt, L.C. (1998). X-ray crystal structure of the Fe-only hydrogenase (CpI) from *Clostridium pasteurianum* to 1.8 angstrom resolution. *Science* 282(5395), 1853-1858.
- Peters, J.W., Schut, G.J., Boyd, E.S., Mulder, D.W., Shepard, E.M., Broderick, J.B., et al. (2015). [FeFe]- and [NiFe]-hydrogenase diversity, mechanism, and maturation. *Biochim Biophys Acta Mol Cell Res* 1853(6), 1350-1369. doi: <https://doi.org/10.1016/j.bbamcr.2014.11.021>.
- Plugge, C.M., Henstra, A.M., Worm, P., Swarts, D.C., Paulitsch-Fuchs, A.H., Scholten, J.C.M., et al. (2012). Complete genome sequence of *Syntrophobacter fumaroxidans* strain (MPOB<sup>T</sup>). *Standards in genomic sciences* 7(1), 91-106. doi: 10.4056/sigs.2996379.
- Salvador, A.F., Martins, G., Melle-Franco, M., Serpa, R., Stams, A.J.M., Cavaleiro, A.J., et al. (2017). Carbon nanotubes accelerate methane production in pure cultures of methanogens

- and in a syntrophic coculture. *Environ Microbiol* 19(7), 2727-2739. doi: 10.1111/1462-2920.13774.
- Sato, K., Nishina, Y., Setoyama, C., Miura, R., and Shiga, K. (1999). Unusually High Standard Redox Potential of Acrylyl-CoA/ Propionyl-CoA Couple among Enoyl-CoA/Acyl-CoA Couples: A Reason for the Distinct Metabolic Pathway of Propionyl-CoA from Longer Acyl-CoAs. *J Biochem* 126(4), 668-675. doi: 10.1093/oxfordjournals.jbchem.a022501.
- Schink, B. (1997). Energetics of syntrophic cooperation in methanogenic degradation. *Microbiol Mol Biol Rev* 61(2), 262-280.
- Schink, B., Montag, D., Keller, A., and Müller, N. (2017). Hydrogen or formate: Alternative key players in methanogenic degradation. *Environ Microbiol Rep* 9(3), 189-202. doi: 10.1111/1758-2229.12524.
- Schmehl, M., Jahn, A., Meyer zu Vilsendorf, A., Hennecke, S., Masepohl, B., Schuppler, M., et al. (1993). Identification of a new class of nitrogen fixation genes in *Rhodobacter capsalatus*: a putative membrane complex involved in electron transport to nitrogenase. *Molecular and General Genetics MGG* 241(5), 602-615. doi: 10.1007/BF00279903.
- Schmidt, A., Muller, N., Schink, B., and Schleheck, D. (2013). A proteomic view at the biochemistry of syntrophic butyrate oxidation in *Syntrophomonas wolfei*. *PLoS One* 8(2), e56905. doi: 10.1371/journal.pone.0056905.
- Schuchmann, K., Chowdhury, N.P., and Müller, V. (2018). Complex Multimeric [FeFe] Hydrogenases: Biochemistry, Physiology and New Opportunities for the Hydrogen Economy. *Front Microbiol* 9(2911). doi: 10.3389/fmicb.2018.02911.
- Schuchmann, K., and Muller, V. (2012). A bacterial electron-bifurcating hydrogenase. *J Biol Chem* 287(37), 31165-31171. doi: 10.1074/jbc.M112.395038.



- Schut, G.J., and Adams, M.W.W. (2009). The Iron-Hydrogenase of *Thermotoga maritima* Utilizes Ferredoxin and NADH Synergistically: a New Perspective on Anaerobic Hydrogen Production. *J Bacteriol* 191(13), 4451.
- Sedano-Núñez, V.T., Boeren, S., Stams, A.J.M., and Plugge, C.M. (2018). Comparative proteome analysis of propionate degradation by *Syntrophobacter fumaroxidans* in pure culture and in coculture with methanogens. *Env Microbiol* 20(5), 1842-1856. doi: doi:10.1111/1462-2920.14119.
- Shima, S., Pilak, O., Vogt, S., Schick, M., Stagni, M.S., Meyer-Klaucke, W., et al. (2008). The crystal structure of [Fe]-hydrogenase reveals the geometry of the active site. *Science* 321(5888), 572-575. doi: 10.1126/science.1158978.
- Sieber, J.R., Crable, B.R., Sheik, C.S., Hurst, G.B., Rohlin, L., Gunsalus, R.P., et al. (2015). Proteomic analysis reveals metabolic and regulatory systems involved in the syntrophic and axenic lifestyle of *Syntrophomonas wolfei*. *Front Microbiol* 6, 115. doi: 10.3389/fmicb.2015.00115.
- Sieber, J.R., Le, H.M., and McInerney, M.J. (2014). The importance of hydrogen and formate transfer for syntrophic fatty, aromatic and alicyclic metabolism. *Environ Microbiol* 16(1), 177-188. doi: 10.1111/1462-2920.12269.
- Sieber, J.R., McInerney, M.J., and Gunsalus, R.P. (2012). Genomic Insights into Syntrophy: The Paradigm for Anaerobic Metabolic Cooperation. *Annu Rev Microbiol* 66(1), 429-452. doi: 10.1146/annurev-micro-090110-102844.
- Sieber, J.R., Sims, D.R., Han, C., Kim, E., Lykidis, A., Lapidus, A.L., et al. (2010). The genome of *Syntrophomonas wolfei*: new insights into syntrophic metabolism and biohydrogen

- production. *Environ Microbiol* 12(8), 2289-2301. doi: 10.1111/j.1462-2920.2010.02237.x.
- Soboh, B., Linder, D., and Hedderich, R. (2004). A multisubunit membrane-bound [NiFe] hydrogenase and an NADH-dependent Fe-only hydrogenase in the fermenting bacterium *Thermoanaerobacter tengcongensis*. *Microbiology* 150(Pt 7), 2451-2463. doi: 10.1099/mic.0.27159-0.
- Søndergaard, D., Pedersen, C.N.S., and Greening, C. (2016). HydDB: A web tool for hydrogenase classification and analysis. *Sci Rep* 6, 34212. doi: 10.1038/srep34212 <https://www.nature.com/articles/srep34212#supplementary-information>.
- Stams, A.J., and Plugge, C.M. (2009). Electron transfer in syntrophic communities of anaerobic bacteria and archaea. *Nat Rev Microbiol* 7(8), 568-577. doi: 10.1038/nrmicro2166.
- Stams, A.J.M., and Dong, X. (1995). Role of formate and hydrogen in the degradation of propionate and butyrate by defined suspended cocultures of acetogenic and methanogenic bacteria. *Antonie Leeuwenhoek* 68(4), 281-284. doi: 10.1007/BF00874137.
- Sticht, H., and Rosch, P. (1998). The structure of iron-sulfur proteins. *Prog Biophys Mol Biol* 70(2), 95-136.
- Thamer, W., Cirpus, I., Hans, M., Pierik, A.J., Selmer, T., Bill, E., et al. (2003). A two [4Fe-4S]-cluster-containing ferredoxin as an alternative electron donor for 2-hydroxyglutaryl-CoA dehydratase from *Acidaminococcus fermentans*. *Arch Microbiol* 179(3), 197-204. doi: 10.1007/s00203-003-0517-8.
- Thauer, R.K., Jungermann, K., and Decker, K. (1977). Energy conservation in chemotrophic anaerobic bacteria. *Bacteriol Rev* 41(1), 100-180.

- Thauer, R.K., Kaster, A.-K., Seedorf, H., Buckel, W., and Hedderich, R. (2008). Methanogenic archaea: ecologically relevant differences in energy conservation. *Nat Rev Microbiol* 6, 579. doi: 10.1038/nrmicro1931.
- Verhagen, M.F.J.M., O'Rourke, T., and Adams, M.W.W. (1999). The hyperthermophilic bacterium, *Thermotoga maritima*, contains an unusually complex iron-hydrogenase: amino acid sequence analyses versus biochemical characterization. *Biochim Biophys Acta Bioenerg* 1412(3), 212-229. doi: [https://doi.org/10.1016/S0005-2728\(99\)00062-6](https://doi.org/10.1016/S0005-2728(99)00062-6).
- Vignais, P.M., and Billoud, B. (2007). Occurrence, Classification, and Biological Function of Hydrogenases: An Overview. *Chem Rev* 107(10), 4206-4272. doi: 10.1021/cr050196r.
- Volbeda, A., Charon, M.-H., Piras, C., Hatchikian, E.C., Frey, M., and Fontecilla-Camps, J.C. (1995). Crystal structure of the nickel-iron hydrogenase from *Desulfovibrio gigas*. *Nature* 373, 580. doi: 10.1038/373580a0.
- Walker, D.J.F., Nevin, K.P., Holmes, D.E., Rotaru, A.-E., Ward, J.E., Woodard, T.L., et al. (2018). *Syntrophus* Conductive Pili Demonstrate that Common Hydrogen-Donating Syntrophs can have a Direct Electron Transfer Option. *bioRxiv*, 479683. doi: 10.1101/479683.
- Wang, S., Huang, H., Kahnt, J., Mueller, A.P., Köpke, M., and Thauer, R.K. (2013a). NADP-specific electron-bifurcating [FeFe]-hydrogenase in a functional complex with formate dehydrogenase in *Clostridium autoethanogenum* grown on CO. *J Bacteriol* 195(19), 4373-4386. doi: 10.1128/JB.00678-13.
- Wang, S., Huang, H., Kahnt, J., and Thauer, R.K. (2013b). *Clostridium acidurici* Electron-Bifurcating Formate Dehydrogenase. *Appl Environ Microb* 79(19), 6176.

- Wang, S., Huang, H., Kahnt, J., and Thauer, R.K. (2013c). A Reversible Electron-Bifurcating Ferredoxin- and NAD-Dependent [FeFe]-Hydrogenase (HydABC) in *Moorella thermoacetica*. *J Bacteriol* 195(6), 1267.
- Wang, S., Huang, H., Moll, J., and Thauer, R.K. (2010). NADP<sup>+</sup> reduction with reduced ferredoxin and NADP<sup>+</sup> reduction with NADH are coupled via an electron-bifurcating enzyme complex in *Clostridium kluyveri*. *J Bacteriol* 192(19), 5115-5123. doi: 10.1128/jb.00612-10.
- Weghoff, M.C., Bertsch, J., and Müller, V. (2015). A novel mode of lactate metabolism in strictly anaerobic bacteria. *Environ Microbiol* 17(3), 670-677. doi: 10.1111/1462-2920.12493.
- Wilson, R.M., Tfaily, M.M., Rich, V.I., Keller, J.K., Bridgham, S.D., Zalman, C.M., et al. (2017). Hydrogenation of organic matter as a terminal electron sink sustains high CO<sub>2</sub>:CH<sub>4</sub> production ratios during anaerobic decomposition. *Org Geochem* 112, 22-32. doi: <https://doi.org/10.1016/j.orggeochem.2017.06.011>.
- Wofford, N.Q., Beaty, P.S., and McInerney, M.J. (1986). Preparation of cell-free extracts and the enzymes involved in fatty acid metabolism in *Syntrophomonas wolfei*. *J Bacteriol* 167(1), 179. doi: 10.1128/jb.167.1.179-185.1986.
- Yan, Z., Wang, M., and Ferry, J.G. (2017). A Ferredoxin- and F<sub>420</sub>H<sub>2</sub>-Dependent, Electron-Bifurcating, Heterodisulfide Reductase with Homologs in the Domains Bacteria and Archaea. *mBio* 8(1), e02285-02216. doi: 10.1128/mBio.02285-16.
- Zhao, Z., Li, Y., Yu, Q., and Zhang, Y. (2018). Ferroferric oxide triggered possible direct interspecies electron transfer between *Syntrophomonas* and *Methanosaeta* to enhance

waste activated sludge anaerobic digestion. *Bioresour Technol* 250, 79-85. doi:

<https://doi.org/10.1016/j.biortech.2017.11.003>.

Zheng, Y., Kahnt, J., Kwon, I.H., Mackie, R.I., and Thauer, R.K. (2014). Hydrogen Formation and Its Regulation in *Ruminococcus albus*: Involvement of an Electron-Bifurcating [FeFe]-Hydrogenase, of a Non-Electron-Bifurcating [FeFe]-Hydrogenase, and of a Putative Hydrogen-Sensing [FeFe]-Hydrogenase. *J Bacteriol* 196(22), 3840.

**CHAPTER 2. *Syntrophomonas wolfei* Uses a NADH-Dependent, Ferredoxin-Independent, [FeFe]-Hydrogenase to Reoxidize NADH**

The contents of this chapter were previously published as a manuscript in the journal Applied and Environmental Microbiology in 2017. This chapter represents a pre-print version of that manuscript with modifications to figure numbering, figure placement, and reference style to be consistent with the remainder of this dissertation.

## Abstract

*Syntrophomonas wolfei* Uses a NADH-Dependent, Ferredoxin-Independent, [FeFe]-Hydrogenase to Reoxidize NADH

Nathaniel A. Losey,<sup>a</sup> Florence Mus,<sup>b</sup> John W. Peters,<sup>b</sup> Huynh M. Le,<sup>a†</sup> Michael J. McInerney<sup>a#</sup>

Department of Plant Biology and Microbiology, University of Oklahoma, Norman, Oklahoma, USA<sup>a</sup>; Department of Chemistry and Biochemistry, Institute of Biological Chemistry, Washington State University, Pullman, Washington, USA<sup>b</sup>

Running Head: NADH Reoxidation in *Syntrophomonas wolfei*.

#Address correspondence to Michael J. McInerney, mcinerney@ou.edu.

†Present address: Immuno-Mycologics, Inc. (IMMY), 2701 Corporate Centre Drive, Norman, OK, USA

## Abstract

*Syntrophomonas wolfei* syntrophically oxidizes short-chain fatty acids (four to eight carbon in length) when grown in coculture with a hydrogen- and/or formate-using methanogen. The

oxidation of 3-hydroxybutyryl-CoA, formed during butyrate metabolism, results in the production of NADH. The enzyme systems involved in NADH reoxidation in *S. wolfei* are not well understood. The genome of *S. wolfei* contains a multimeric [FeFe]-hydrogenase that may be a mechanism for NADH reoxidation. The *S. wolfei* genes for the multimeric [FeFe]-hydrogenase (*hyd1ABC*; SWOL\_RS05165, SWOL\_RS05170, SWOL\_RS05175) and [FeFe]-hydrogenase maturation proteins (SWOL\_RS05180, SWOL\_RS05190, SWOL\_RS01625) were co-expressed in *Escherichia coli* and the recombinant Hyd1ABC was purified and characterized. The purified recombinant Hyd1ABC was a heterotrimer with an  $\alpha\beta\gamma$  configuration and a molecular mass of 115 kDa. Hyd1ABC contained  $29.2 \pm 1.49$  mole of Fe and 0.7 mole of FMN per mole enzyme. The purified, recombinant Hyd1ABC reduced  $\text{NAD}^+$  and oxidized NADH without the presence of ferredoxin. The HydB subunit of the *S. wolfei* multimeric [FeFe]-hydrogenase lacks two iron-sulfur centers that are present in known confurcating NADH- and ferredoxin-dependent [FeFe]-hydrogenases. Hyd1ABC is a NADH-dependent hydrogenase that produces hydrogen from NADH without the need of reduced ferredoxin, which differs from confurcating [FeFe]-hydrogenases. Hyd1ABC provides a mechanism by which *S. wolfei* can reoxidize NADH produced during syntrophic butyrate oxidation when low hydrogen partial pressures are maintained by a hydrogen-consuming microorganism.

### **Importance**

Our work provides mechanistic understanding of the obligate metabolic coupling that occurs between hydrogen-producing fatty and aromatic acid-degrading microorganisms and their hydrogen-consuming partners in the process called syntrophy (to feed together). The multimeric [FeFe]-hydrogenase used NADH without the involvement of reduced ferredoxin. The multimeric



[FeFe]-hydrogenase would only produce hydrogen from NADH when hydrogen concentrations are low. Hydrogen production from NADH by *Syntrophomonas wolfei* would likely cease before any detectable amount of cell growth occurred. Thus, continual hydrogen production requires the presence of a hydrogen-consuming partner to keep hydrogen concentrations low and explains, in part, the obligate requirement that *S. wolfei* has for a hydrogen-consuming partner organism during growth on butyrate. We have successfully expressed genes encoding for a multimeric [FeFe]-hydrogenase in *E. coli* demonstrating that such an approach can be advantageous to characterize complex redox proteins from difficult to culture microorganisms.

## **Introduction**

The model syntrophic bacterium, *S. wolfei*, oxidizes butyrate to acetate with the concomitant production of hydrogen and formate (McInerney et al., 1981). During syntrophic butyrate metabolism, the hydrogen- and/or formate-using methanogen maintains low levels of hydrogen and formate so that butyrate oxidation remains thermodynamically favorable (McInerney and Bryant, 1981; Schink, 1997). Butyrate oxidation by *S. wolfei* involves two different oxidation-reduction reactions, generating electrons at two different redox potentials, both of which are used to produce hydrogen or formate (Wofford et al., 1986; Sieber et al., 2010; Schmidt et al., 2013). The first set of electrons is generated during the oxidation of butyryl-CoA to crotonyl-CoA. Due to the high redox potential of this electron pair ( $E^{\circ} = -125$  mV), it has been proposed that membrane complexes utilizing chemiosmotic energy are required for hydrogen or formate production (Sieber et al., 2010; Schmidt et al., 2013; Sieber et al., 2014; Sieber et al., 2015; Crable et al., 2016). The second pair of electrons is generated from the oxidation of 3-hydroxybutyryl-CoA to acetoacetyl-CoA ( $E^{\circ} = -250$  mV) and is used to reduce  $\text{NAD}^+$  to NADH

( $E^{\circ} = -320$  mV). NADH reoxidation must be coupled to hydrogen or formate production during syntrophic butyrate metabolism. Under the low hydrogen partial pressures maintained by hydrogenotrophic methanogens (<10 Pa), the redox potential ( $E'$ ) of hydrogen is about -260 mV, making hydrogen production directly from NADH thermodynamically feasible (Schink, 1997; Sieber et al., 2012).

The analysis of the *S. wolfei* genome identified a multimeric [FeFe]-hydrogenase encoded by the genes (*hydIABC*; SWOL\_RS05165, SWOL\_RS05170, SWOL\_RS05175) that shared similar sequence identity to confurcating [FeFe]-hydrogenases (Schut and Adams, 2009; Sieber et al., 2010; Sieber et al., 2012), a NADPH-linked [FeFe]-hydrogenase (Malki et al., 1995), and NADH-dependent formate dehydrogenases (Hartmann and Leimkuhler, 2013). Most examples of multimeric [FeFe]-hydrogenases have been reported to function in either electron confurcation or the reverse (bifurcating) reaction. Confurcating [FeFe]-hydrogenases couple the unfavorable production of hydrogen from NADH with the favorable production of hydrogen from reduced ferredoxin (Schut and Adams, 2009), utilizing equimolar amounts of NADH and reduced ferredoxin to produce hydrogen, as was first demonstrated in the multimeric [FeFe]-hydrogenase from *Thermotoga maritima* (Schut and Adams, 2009). Additional multimeric [FeFe]-hydrogenases have been studied in *Acetobacterium woodii* (Schuchmann and Muller, 2012), *Moorella thermoacetica* (Wang et al., 2013b), and *Ruminococcus albus* (Zheng et al., 2014).

The beta-oxidation of butyrate by *S. wolfei* does not directly result in the formation of reduced ferredoxin. Thus, *S. wolfei*'s metabolism differs from the metabolism of organisms with reported confurcating/bifurcating [FeFe]-hydrogenases, which have ferredoxin-dependent

oxidoreductases, such as pyruvate:ferredoxin oxidoreductase that produce reduced ferredoxin during substrate degradation (Schut and Adams, 2009; Schuchmann and Muller, 2012; Wang et al., 2013b; Zheng et al., 2014). One potential source of reduced ferredoxin in *S. wolfei* is a putative Fix system, which could produce reduced ferredoxin from the oxidation of NADH (Sieber et al., 2010). However, the use of Fix to produce reduced ferredoxin would place a high energy demand on an organism that uses growth reactions that operate close to thermodynamic equilibrium (Jackson and McInerney, 2002). In the absence of an identifiable source of reduced ferredoxin and with syntrophic growth conditions that would be permissive for hydrogen production from NADH, it is likely that Hyd1ABC functions as a non-branching, NADH-dependent [FeFe]-hydrogenase.

We cloned and expressed the genes of a multimeric [FeFe]-hydrogenase (SWOL\_RS05165, SWOL\_RS05170, SWOL\_RS05175) from *S. wolfei* and characterized the recombinant protein in order to understand the mechanisms by which *S. wolfei* reoxidizes NADH. To obtain an active enzyme, it was also necessary to co-express the genes required for [FeFe]-hydrogenase maturation (SWOL\_RS05180, SWOL\_RS05190, SWOL\_RS01625). This strategy has been used successfully in the past to produce active [FeFe]-hydrogenases using *Escherichia coli* (Girbal et al., 2005; King et al., 2006) and allowed the production of an enzyme with the activity of a NADH-dependent [FeFe]-hydrogenase (Hyd1ABC: SWOL\_RS05165, SWOL\_RS05170, SWOL\_RS05175 gene products).

## Results

**Purification and molecular weight.** The recombinant gene products of SWOL\_RS05165, SWOL\_RS05170, SWOL\_RS05175 were purified to apparent homogeneity using nickel-affinity and anion-exchange chromatography, resulting in an apparent yield of 12.7% (Table 1).

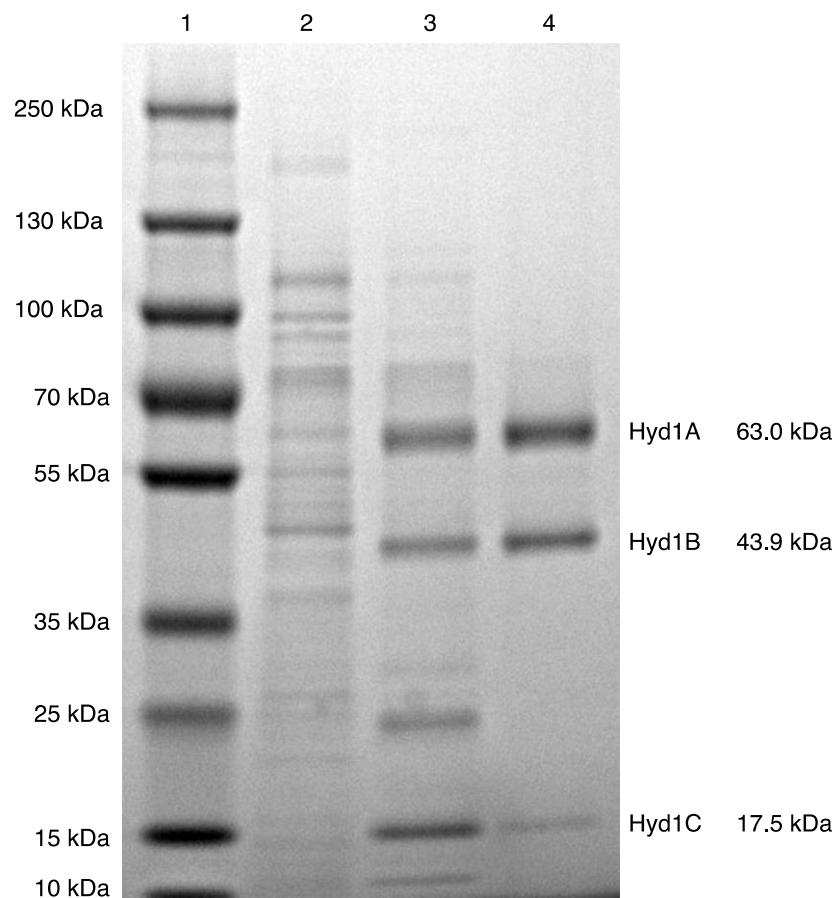
**Table 1. Purification of NADH-dependent [FeFe]-hydrogenase, Hyd1ABC.**

Fraction	Protein (mg)	Specific activity <sup>a</sup> H <sub>2</sub> → MV <sub>ox</sub> (U•mg <sup>-1</sup> )	Total activity <sup>a</sup> H <sub>2</sub> → MV <sub>ox</sub> (U•mg <sup>-1</sup> )	Purification (fold)	Yield (%)
Cell-free extract	670	16.8	11200	1	100
HisTrap HP	4.0	655	2620	38.9	23.4
UNO-Q1	0.43	3340	1430	199	12.7

<sup>a</sup>Activity was determined at 37 °C, pH 7.5; one unit of activity (U) equals 2 μmol of electrons transferred per min.

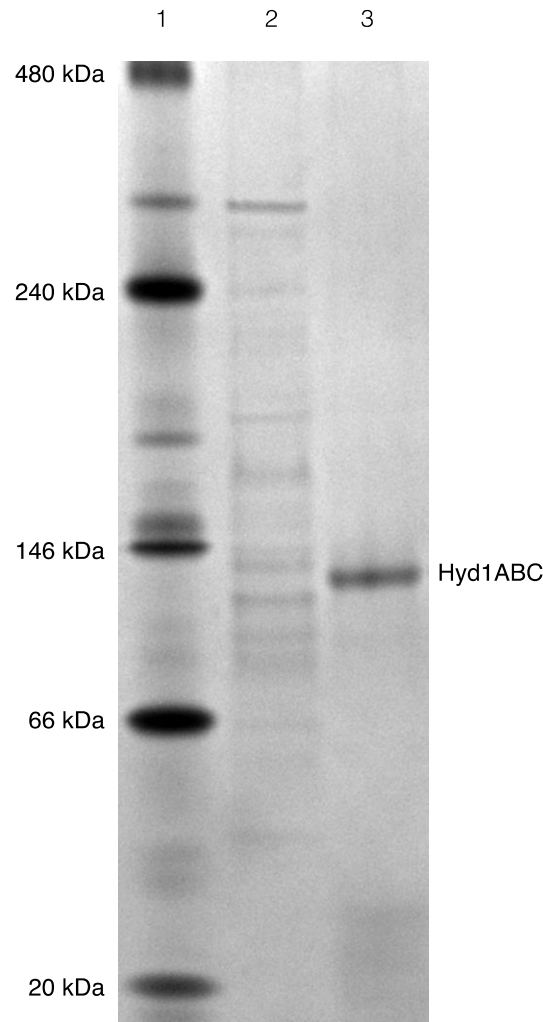
Approximately 0.55 mg of purified recombinant enzyme was obtained from 10.8 g (wet weight) of cells. SDS-PAGE analysis showed that the purified recombinant enzyme consisted of three subunits with molecular weights that were consistent with molecular weights predicted from the sequence of encoding genes; 63 kDa compared to the predicted 63.0 kDa (HydA1), 43 kDa compared to the predicted 43.9 kDa (HydB1), and 13 kDa compared to the predicted 17.6 kDa (HydC1) with the included molecular weight of the His-tag (MGSSHHHHHSQDP, 1.6 kDa) (Figure 7).

**Figure 7. SDS-PAGE of NADH-Dependent [FeFe]-Hydrogenase, Hyd1ABC.** Lane 1, molecular weight markers, Lane 2, *E. coli* cell-free extract, Lane 3, HisTrap HP, Lane 4, UNO-Q1. The displayed molecular masses of Hyd1A-C peptides are predicted from the amino acid sequence.



Native-PAGE gel electrophoresis analysis showed that the purified enzyme migrated as a single band (Figure 8) and size exclusion chromatography gave a molecular weight of 115 kDa.

**Figure 8. Native PAGE of the NADH-Dependent [FeFe]-hydrogenase, Hyd1ABC.** Lane 1: native molecular weight markers, Lane 2: *E. coli* cell-free extract, Lane 3: UNO-Q1 fraction of the purified, Hyd1ABC.



The single visible band from native gel electrophoresis when subjected to peptide analysis showed high coverage scores for the intended peptides (Table S1). Based on the subunit analysis and the native molecular weight, Hyd1ABC is a heterotrimer with an  $\alpha\beta\gamma$  configuration and a molecular mass of 124.5 kDa as predicted by the sequence of the encoding genes. Iron

content was determined to be  $29.2 \pm 1.49$  mole of Fe per mole of enzyme, which matches well with the predicted 30 mole Fe per mole of enzyme from conserved domain analysis, which indicated five [4Fe-4S]-clusters, two [2Fe-2S]-clusters and the six Fe in the [H-Cluster]. The flavin content was 0.7 mole of FMN per mole of enzyme, which agrees with the single flavin-binding site in the HydB subunit, predicted from conserved domain analysis.

**Activity.** The purified recombinant Hyd1ABC had high hydrogen-dependent, methyl viologen-reducing activity and reduced methyl viologen-oxidizing activity (Table 2), typical for many [FeFe]-hydrogenases.

**Table 2. Specific Activities of the Purified, NADH-Dependent [FeFe]-Hydrogenase, Hyd1ABC.**

Reaction	Hydrogenase activity ( $\text{U}\cdot\text{mg}^{-1}$ ) <sup>a</sup>
$\text{H}_2 \rightarrow \text{MV}_{\text{ox}}$	571
$\text{H}_2 \rightarrow \text{NAD}^+$	94.5
$\text{H}_2 \rightarrow \text{NAD}^+ + \text{Fd}_{\text{ox}}$	92.1 <sup>b</sup>
$\text{H}_2 \rightarrow \text{NADP}^+$	<0.01
$\text{H}_2 \rightarrow \text{NADP}^+ + \text{Fd}_{\text{ox}}$	<0.01
$\text{H}_2 \rightarrow \text{Fd}_{\text{ox}}$	<0.01
$\text{MV}_{\text{red}} \rightarrow \text{H}_2$	24.3
$\text{NADH} \rightarrow \text{H}_2$	6.6
$\text{NADH} + \text{Fd}_{\text{red}} \rightarrow \text{H}_2$	6.0

NADPH $\rightarrow$ H <sub>2</sub>	<0.01
NADPH + Fd <sub>red</sub> $\rightarrow$ H <sub>2</sub>	<0.01
Fd <sub>red</sub> $\rightarrow$ H <sub>2</sub>	<0.01

<sup>a</sup>Activity was determined at 37 °C, pH 7.5; one unit of activity (U) equals 2  $\mu$ mol of electrons transferred per min.

<sup>b</sup> Activity is the rate of NAD<sup>+</sup> reduction at 340 nm in the presence of Fd<sub>ox</sub> and not the rate of Fd<sub>ox</sub> reduction (at 430 nm), which was not observed to occur.

The purified recombinant Hyd1ABC also had high NAD<sup>+</sup>-reducing activity with hydrogen as the electron donor (specific activity of 94.5 U•mg<sup>-1</sup> at 37°C) and catalyzed hydrogen production from NADH with a specific activity of 6.6 U•mg<sup>-1</sup> at 37°C (Table 2). The enzyme did not oxidize NADPH nor reduce NADP<sup>+</sup> under any condition tested. Neither the rate of NAD<sup>+</sup> reduction nor the rate of NADH-dependent hydrogen production changed when oxidized or reduced clostridial ferredoxin, respectively, was added (Figure 9 and Figure 10).

**Figure 9. Reduction of NAD<sup>+</sup> by the Purified, NADH-Dependent [FeFe]-Hydrogenase, Hyd1ABC with Hydrogen as the Electron Donor.** Reactions were performed in 1.5 mL, sealed, anaerobic cuvettes containing 0.5 mL of 50 mM potassium phosphate buffer (pH 7.5 at 37°C) 5  $\mu$ M FAD, 5  $\mu$ M FMN, 2 mM DTE, 1 mM NAD<sup>+</sup> and 0.11  $\mu$ g of Hyd1ABC. Clostridial ferredoxin was added at a concentration of 10  $\mu$ M. The change in absorbance ( $\Delta A_{340}$ ) before the addition of hydrogen was 0.129 A•min<sup>-1</sup> and after the addition of oxidized ferredoxin was 0.125 A•min<sup>-1</sup>.



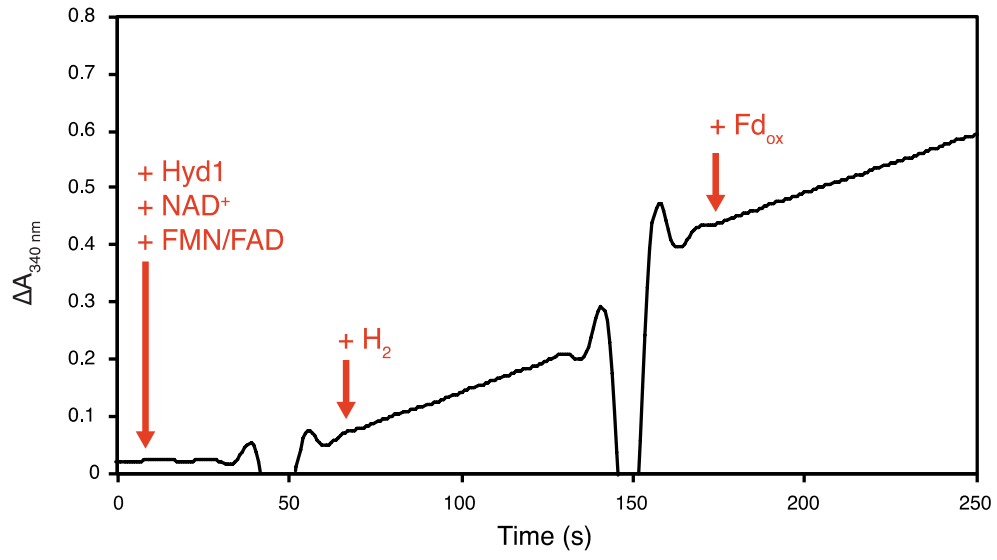
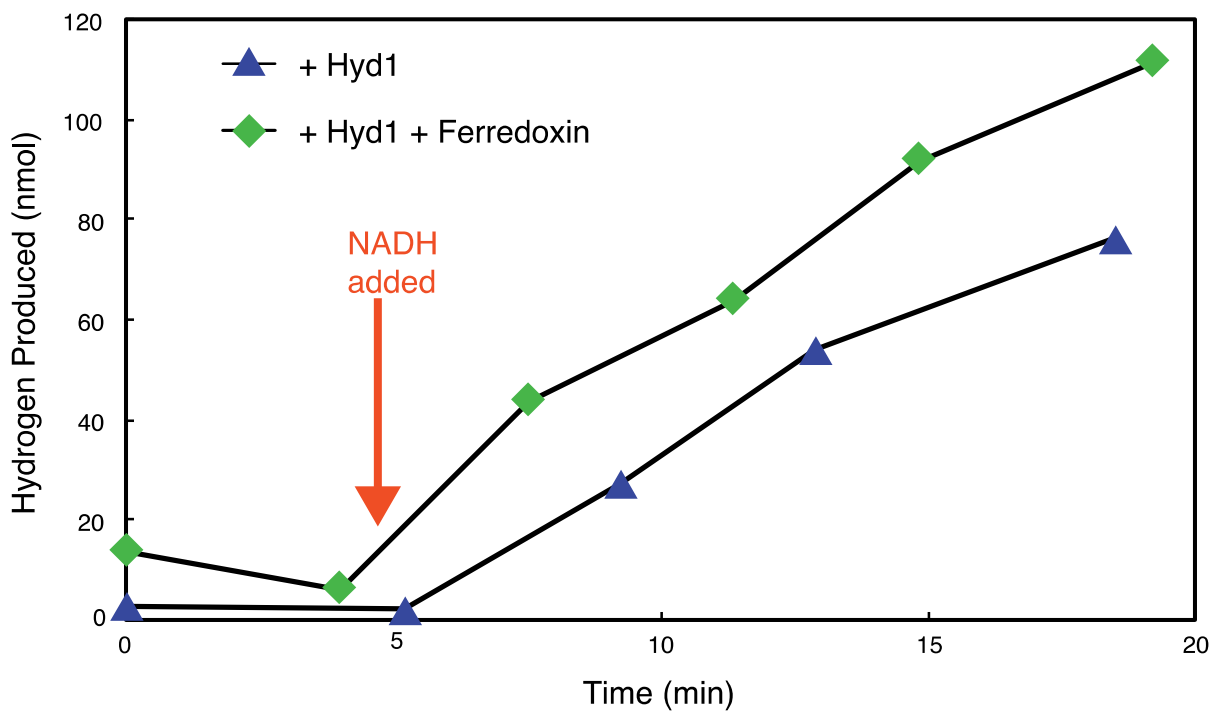


**Figure 10. The Effect of NADH and Reduced Ferredoxin on Hydrogen Production by Hyd1ABC.** Reactions were performed in 6.5 mL serum bottles containing 0.5 mL of 100 mM potassium phosphate buffer (pH 7.5 at 37°C), 5  $\mu$ M FAD, 5  $\mu$ M FMN, 2 mM DTE, 1 mM NADH and 1.3  $\mu$ g of Hyd1ABC. A ferredoxin reduction system as indicated by +Fd consisted of 10 mM pyruvate, 1 mM CoA, 0.1 mM thiamine pyrophosphate, 5  $\mu$ M clostridial ferredoxin and 0.1 U of clostridial pyruvate:ferredoxin oxidoreductase. NADH (1 mM) was added immediately after sampling time points indicated by +NADH.



In addition, the purified recombinant Hyd1ABC did not reduce clostridial ferredoxin either alone or in the presence of NAD<sup>+</sup> with hydrogen as the electron donor. Hyd1ABC did not produce hydrogen from reduced clostridial ferredoxin in the absence of NADH, and the amount of hydrogen produced when both NADH and reduced ferredoxin were present was similar to that

when only NADH was present (Figure 10). The above experiments were repeated with the purified recombinant *S. wolfei* ferredoxin encoded by SWOL\_RS10890 with results similar to those using the clostridial ferredoxin. That is, the recombinant *S. wolfei* ferredoxin did not appear to affect the rate of NAD<sup>+</sup> reduction or NADH oxidation. In addition, Hyd1ABC did not reduce the recombinant *S. wolfei* ferredoxin with hydrogen as the electron donor and did not produce hydrogen with reduced recombinant *S. wolfei* ferredoxin as the electron donor. Kinetics of NAD<sup>+</sup> reduction with hydrogen, where the NAD<sup>+</sup> concentration was varied, indicated a K<sub>m</sub> for NAD<sup>+</sup> of 520 μM, V<sub>max</sub> of 196 U•mg<sup>-1</sup>, and a k<sub>cat</sub> of 406.7 s<sup>-1</sup>, assuming a single catalytic site per a molecular mass of 124.5 kDa. (Figure S1). Hyd1ABC specific activities for methyl viologen and NAD<sup>+</sup> reduction and for NADH oxidation were similar to those reported for other multimeric [FeFe]-hydrogenases; however, the K<sub>m</sub> for reduction of NAD<sup>+</sup> by Hyd1ABC was higher than that of other multimeric [FeFe]-hydrogenases (Table S2).

In the above assays, the purified Hyd1ABC produced hydrogen from NADH under conditions where only a small amount of NADH would be oxidized to NAD<sup>+</sup> during the time course of the assay and thus the ratio of NADH/NAD<sup>+</sup> would remain high. To determine whether Hyd1ABC could produce hydrogen from NADH under more physiological conditions, we varied the ratio of NADH to NAD<sup>+</sup> and pH, but kept the total pyridine nucleotide concentration constant at 5 mM (Table 3).

**Table 3. Equilibrium Hydrogen Partial Pressures Produced by NADH-Dependent [FeFe]-Hydrogenase, Hyd1ABC at Different pH and NADH to NAD<sup>+</sup> ratios. <sup>a</sup>**

Condition	Ratio of NADH/NAD <sup>+</sup>	Hydrogen Partial pressure (Pa) <sup>b</sup>	Hydrogen produced (nmol)
pH 6.5, 2.0 mM NAD <sup>+</sup> , 3.0 mM NADH	1.5	40.0 (6.9)	95.4
pH 6.5, 2.5 mM NAD <sup>+</sup> , 2.5 mM NADH	1.0	21.8 (8.7)	51.8
pH 7.0, 2.0 mM NAD <sup>+</sup> , 3.0 mM NADH	1.5	25.9 (0.8)	61.9
pH 7.0, 2.5 mM NAD <sup>+</sup> , 2.5 mM NADH	1.0	17.0 (11.3)	40.4

<sup>a</sup>Assays were performed in 6.5 mL serum bottles with 0.5 mL of liquid volume containing 0.86 µg of protein and 6 mL of headspace.

<sup>b</sup> Values are the mean and the range (in parentheses) of measured hydrogen values in Pa.

In each case, more hydrogen was produced with a NADH to NAD<sup>+</sup> ratio of 1.5 compared to 1.0. More hydrogen was also produced at pH 6.5 compared to pH 7.0. Hydrogen partial pressures varied from 17.0 Pa with a range of 11.3 Pa to 40.0 Pa with a range of 6.9 Pa with higher partial pressures observed at lower pH values and higher NADH/NAD<sup>+</sup> ratios. Final hydrogen partial pressures detected in these experiments were below that predicted at thermodynamic equilibrium for the given NADH/NAD<sup>+</sup> ratios. With the given liquid and gas

volumes, a NADH/NAD<sup>+</sup> ratio of 1.5 and a pH of 7.0, the redox potential (E') of the NADH/NAD<sup>+</sup> pair should be greater than -320 mV, even with the shift in NADH/NAD<sup>+</sup> ratio as NADH is oxidized. The predicted equilibrium hydrogen partial pressure is in excess of 70 Pa for these conditions; however, the measured hydrogen partial pressure was lower at 25.9 Pa, with a range of 0.8, suggesting that thermodynamic equilibrium was not reached.

**Hydrogen levels in growing coculture.** Hydrogen partial pressures measured during growth of *S. wolfei* in coculture with *M. hungatei* on either butyrate or crotonate were between 4.6 to 18.0 Pa (Figure S2), with the highest concentrations observed at day four and lower concentrations observed during the later stages of growth. Hydrogen partial pressures measured for pure culture *S. wolfei* grown on crotonate were between 27.4 to 40.0 Pa.

## Discussion

The identification of a NADH-dependent [FeFe]-hydrogenase in *S. wolfei* provides an explanation for how electrons derived from 3-hydroxybutyryl-CoA oxidation are used to make hydrogen during syntrophic growth. Stoichiometrically, all electrons derived from the oxidation of butyrate are converted to either hydrogen and formate as *S. wolfei* does not produce any other reduced end products during syntrophic butyrate metabolism (McInerney et al., 1979; Amos and McInerney, 1989). The electrons generated by the oxidation of 3-hydroxybutyryl-CoA to acetoacetyl-CoA are used to reduce NAD<sup>+</sup> to NADH (Wofford et al., 1986). The presence of a multimeric [FeFe]-hydrogenase and NADH-linked formate dehydrogenase genes in the genome of *S. wolfei* (Sieber et al., 2010) suggested that NADH could be reoxidized using these enzyme systems. Hyd1 represents the only hydrogenase encoded within the genome of *S. wolfei*

predicted to catalyze NADH oxidation. Of the two other hydrogenases present within the *S. wolfei* genome, Hyd2, encoded by SWOL\_RS09950, is a membrane-bound [FeFe]-hydrogenase believed to interact with the menaquinone pool (Sieber et al., 2010; Sieber et al., 2015; Crable et al., 2016), while Hyd3, encoded by SWOL\_RS12620, is a monomeric type [FeFe]-hydrogenase (Sieber et al., 2010), which has not been reported to interact with NADH (Poudel et al., 2016). *hyd1A* gene was upregulated under coculture conditions on butyrate compared to coculture conditions on crotonate (Sieber et al., 2014); and Hyd1ABC was confirmed to be present by proteomic techniques (Schmidt et al., 2013; Sieber et al., 2015) during syntrophic coculture growth on butyrate with *M. hungatei*. Thus, Hyd1ABC along with NADH-linked formate dehydrogenases are the likely routes of NADH reoxidation in *S. wolfei*.

The possibility that *S. wolfei* utilizes a NADH-dependent hydrogenase was suggested previously due to the closeness of the redox potentials of 3-hydroxybutyryl-CoA/acetoacetyl-CoA ( $E^{\circ} = -250$  mV), NADH/NAD<sup>+</sup> ( $E^{\circ} = -320$  mV), and H<sub>2</sub>/H<sup>+</sup> at 1 Pa H<sub>2</sub> ( $E^{\circ} = -261$  mV) (Schink, 1997). The amino acid sequence comparisons suggested that Hyd1ABC might be a confurcating hydrogenase (Sieber et al., 2010; Sieber et al., 2012). Confurcating/bifurcating [FeFe]-hydrogenases produce hydrogen from NADH ( $E^{\circ} = -320$  mV) and reduced ferredoxin ( $E^{\circ} = -398$  mV or less) (Schut and Adams, 2009; Schuchmann and Muller, 2014). Coupling the unfavorable hydrogen production from NADH with the favorable hydrogen production from reduced ferredoxin would allow hydrogen production at partial pressures greater than 1000 Pa at equilibrium (equivalent to  $E^{\circ} = -367$  mV). The NADH/NAD<sup>+</sup> midpoint potential ( $E^{\circ} = -320$  mV) would allow for a much lower hydrogen partial pressure of close to 70 Pa at equilibrium. Using fixed NADH/NAD<sup>+</sup> ratios of 1.0 and 1.5, Hyd1ABC produced partial pressures of

hydrogen from 17 to 40 Pa (Table 3). NADH/NAD<sup>+</sup> ratios reported for organisms grown under anaerobic conditions can vary with some values lower than those tested here, for example 0.27 for *Clostridium kluyveri*, 0.29 for *Clostridium welchii* and 0.4 for *E. coli* (Wimpenny and Firth, 1972), while other studies have reported higher ratios of 0.75 for *E. coli* (de Graef et al., 1999) and 1.16 for *Enterococcus faecalis* (Snoep et al., 1991). Thus, the production of hydrogen by Hyd1ABC from NADH/NAD<sup>+</sup> ratios of 1.0 or higher resemble physiological conditions for *S. wolfei* cells, although the actual NADH/NAD<sup>+</sup> ratios during syntrophic growth conditions have not yet been determined.

The partial pressure of hydrogen produced by Hyd1ABC was within the range of the hydrogen partial pressure (25 Pa) produced by cell suspensions of butyrate-grown *S. wolfei* cells when conditions allowed only hydrogen production from NADH (Wallrabenstein and Schink, 1994). Butyrate-oxidizing cocultures of *S. wolfei* and *Methanobacterium formicicum* maintained a partial pressure of hydrogen of 10.6 Pa (Boone et al., 1989), while hydrogen concentrations for cocultures of *S. wolfei* and *M. hungatei* ranged from 4.6 to 18.0 Pa (Figure S2). Measurements of partial pressures of hydrogen from methanogenic butyrate-degrading environments, such as lake sediment and sewage sludge, ranged from 3.7 to 26.9 Pa (Conrad et al., 1986). Hydrogen partial pressures from syntrophic, butyrate-oxidizing biogas reactors ranged from 1 to 4.5 Pa (Montag and Schink, 2016). Methanogenic syntrophic microcosms established from peat soil implicated members of the *Syntrophomonas* genus in butyrate oxidation had hydrogen partial pressures that ranged from 3 to 12.5 Pa (Schmidt et al., 2016). Thus, the hydrogen partial pressure that would allow for reoxidation of NADH during syntrophic butyrate metabolism is considerably less than that achieved by confurcating hydrogenases, but it is within the range of the hydrogen partial

pressures produced by Hyd1ABC from NADH alone (Table 3). Furthermore, such hydrogen partial pressures are observed in coculture, microcosms and environments where members of the *Syntrophomonas* genus would perform syntrophic butyrate oxidation. Thus, the hydrogen partial pressure achieved by Hyd1ABC from NADH would appear to be sufficient to allow syntrophic growth of *S. wolfei* on butyrate in coculture with a hydrogenotrophic methanogen.

Hyd1ABC was capable of both  $\text{NAD}^+$  reduction with hydrogen and the oxidation of NADH to produce hydrogen in the absence of ferredoxin (Figure 9 and 10; Table 2), indicating the lack of a tight coupling that is reported for bifurcating/confurcating [FeFe]-hydrogenases (Schut and Adams, 2009; Schuchmann and Muller, 2012; Wang et al., 2013b). In addition, Hyd1ABC did not reduce ferredoxin even in the presence of  $\text{NAD}^+$ . Thus, if Hyd1ABC is capable of producing hydrogen using electrons from reduced ferredoxin under as yet unidentified conditions, the concomitant reduction of  $\text{NAD}^+$  by hydrogen would result in hydrogen being equilibrated with the redox potential of the  $\text{NADH}/\text{NAD}^+$  pool, preventing higher hydrogen partial pressures that would normally be achievable by confurcating hydrogenases. It is not surprising that Hyd1 does not interact with ferredoxin. Ferredoxin levels are very low in the proteome of *S. wolfei* (Sieber et al., 2015) and we did not detect ferredoxin using the traditional approach to purify ferredoxin (N. Losey and M. J. McInerney, unpublished data), e.g., elution from an ion exchange column after high salt treatment and monitoring of the  $A_{390}/A_{280}$  ratio (Schönheit et al., 1978; Aono et al., 1989). Unlike other organisms known to possess confurcating hydrogenases (Schut and Adams, 2009; Schuchmann and Muller, 2012; Wang et al., 2013b; Zheng et al., 2014), *S. wolfei* does not have a clear mechanism or need to produce reduced ferredoxin in equivalent amounts to the amount of NADH made from butyrate (Sieber et al., 2010; Schmidt et al., 2013).



Microorganisms known to possess confurcating [FeFe]-hydrogenases such as *T. maritima* (Schut and Adams, 2009), *M. thermoacetica* (Wang et al., 2013b) and *R. albus* (Zheng et al., 2014) have fermentative metabolisms with ferredoxin-dependent enzymes such as pyruvate:ferredoxin oxidoreductase, which can produce reduced ferredoxin in amounts needed for the coupled hydrogen production from NADH. However, *S. wolfei* exclusively uses fatty acids as substrates for growth (McInerney et al., 1979; McInerney et al., 1981; Beaty and McInerney, 1987). Beta-oxidation of fatty acids by *S. wolfei* results in the formation of reduced electron transfer flavoprotein and NADH, but not directly in reduced ferredoxin (Wofford et al., 1986).

The presence of both HydB/HydC subunits has been suggested as being more diagnostic for identifying bifurcating [FeFe]-hydrogenases than the composition of the HydA subunit (Poudel et al., 2016). *S. wolfei* Hyd1ABC has two differences in iron-sulfur centers as predicted by NCBI's Conserved Domain Database (Marchler-Bauer et al., 2015) compared to known bifurcating/confurcating [FeFe]-hydrogenases that may relate to its inability to use ferredoxin as an electron donor (Figure 11).

**Figure 11. Comparison of Predicted Conserved Domains Present in Characterized**

**Multimeric [FeFe]-Hydrogenases and Multimeric Formate Dehydrogenases.** The boxes

highlight the heterogeneity in the number of conserved domains in HydB ( $\beta$ ) subunits of

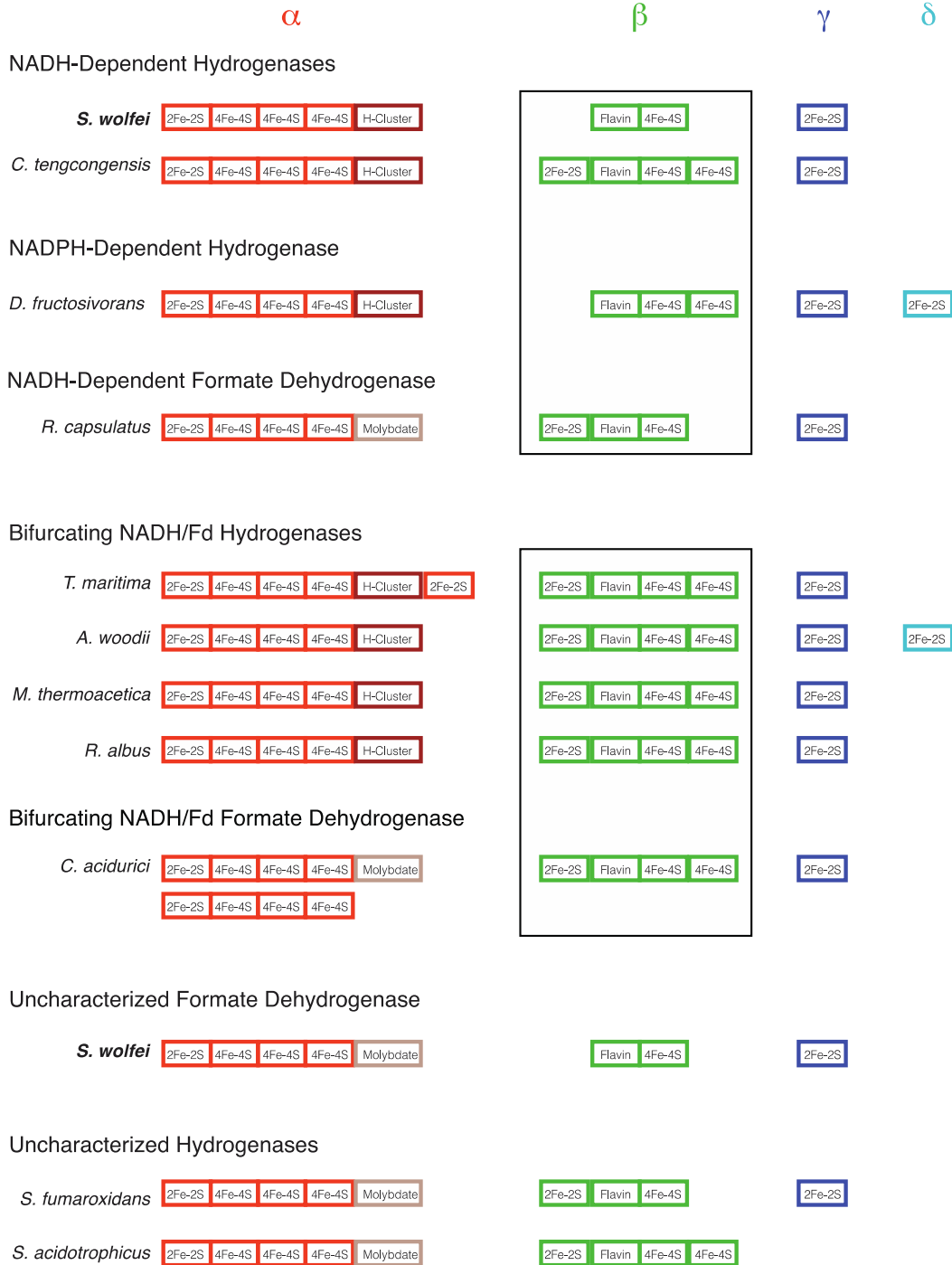
characterized non-bifurcating NADH-dependent [FeFe]-hydrogenases and formate

dehydrogenases compared to the similarity of conserved domains of the HydB ( $\beta$ ) subunits of

characterized bifurcating [FeFe]-hydrogenases and a bifurcating formate dehydrogenase.

Heterogeneity in conserved domains is also present in two unstudied [FeFe]-hydrogenases from

syntrophic metabolizers *S. aciditrophicus* and *S. fumaroxidans* and a formate dehydrogenase from *S. wolfei* previously found to co-purify with Hyd1ABC. The figure is a visual representation of the conserved domains as predicted by NCBI's Conserved Domain Database (40). Greek symbols at the top are the subunit designations. Accession numbers for the sequences of the subunits are given in Table S3. Reported functions of enzymes were obtained from following references: *S. wolfei* hydrogenase, (this publication), *C. tengcongensis* (37), *D. fructosivorans* (12), *R. capsulatus* (13), *T. maritima* (11), *A. woodii* (14), *M. thermoacetica* (15), *R. albus* (16) and *C. acidurici* (36).



The HydB1 subunit lacks a N-terminal [2Fe-2S] cluster and a C-terminal [4Fe-4S] cluster. The difference is reflected in overall peptide length of *S. wolfei* HydB1 of 407 amino

acid residues compared to the approximately 600 residues for HydB subunits of known bifurcating [FeFe]-hydrogenases. The reportedly non-confurcating, NADPH-dependent [FeFe]-hydrogenase from *Desulfovibrio fructosivorans* also lacks a N-terminal [2Fe-2S] cluster in its HydB subunit (Figure 11) (Malki et al., 1995). The number of iron-sulfur centers also seems to match with the ability to bifurcate in multimeric molybdopterin formate dehydrogenases. The multimeric, molybdopterin formate dehydrogenase from *Clostridium acidurici* has been shown to catalyze electron bifurcation and has the same iron-sulfur centers in its HydB and HydC equivalent subunits as known bifurcating [FeFe]-hydrogenases while a non-bifurcating, NADH-dependent formate dehydrogenase from *Rhodobacter capsulatus* lacks a C-terminal [4Fe-4S] cluster in its HydB subunit (Hartmann and Leimkuhler, 2013; Wang et al., 2013a). The NADH-dependent [FeFe]-hydrogenase from *Caldanaerobacter* (formerly *Thermoanaerobacter*) *tengcongensis* may be an example of an enzyme that has an equivalent number of iron-sulfur centers as bifurcating [FeFe]-hydrogenases but with the ability to reduce NAD<sup>+</sup> and oxidize NADH without ferredoxin (Soboh et al., 2004). However, the *C. tengcongensis* [FeFe]-hydrogenase was not tested under bifurcating/confurcating conditions by supplying ferredoxin in the presence of NAD<sup>+</sup> or NADH. While the number of examples of known bifurcating/confurcating and non-bifurcating [FeFe]-hydrogenases and formate dehydrogenases is small, it appears that the type and number of conserved iron-sulfur domains in the HydB/HydC subunits may be important for electron bifurcation activity. Electron bifurcation involves two independent paths of electron flow, either away from the bifurcation site for bifurcating enzymes, or towards the bifurcation site for confurcating enzymes, (Chowdhury et al., 2014; Lubner et al., 2017). A change in the presence of an iron-sulfur cluster or its ability to facilitate the directionality of electron flow due to a change in redox potential or its distance from other redox

centers may affect the bifurcation reaction. It is also possible that the loss of the ability to bifurcate was independent of the change in the number of iron-sulfur clusters and such centers were eliminated overtime as they no longer served a critical function.

Multimeric [FeFe]-hydrogenases with the same number of iron-sulfur centers as *S. wolfei* Hyd1ABC are present in the genomes of other members of the *Syntrophomonadaceae* (see Table S3). This suggests that *Syntrophomonas zehnderi*, *Syntrophothermus lipocalidus*, and *Thermosyntropha lipolytica*, which perform syntrophic oxidation of fatty acids in coculture with hydrogenotrophic methanogens (Svetlitsnyi et al., 1996; Sekiguchi et al., 2000; Sousa et al., 2007), may also utilize non-confurcating, NADH-dependent hydrogen production. Future studies of additional multimeric [FeFe]-hydrogenases may allow the determination of the relationship, if any, between certain iron-sulfur centers in the HydB and HydC subunits and the ability to perform electron bifurcation.

The [FeFe]-hydrogenase in *Syntrophobacter fumaroxidans* lacks a C-terminal [4Fe-4S] domain in the HydB subunit, which differs from reported bifurcating [FeFe]-hydrogenases (Figure 11). However, the metabolism of propionate by the methylmalonyl-CoA pathway by *S. fumaroxidans* leads to pyruvate formation and the ability to produce reduced ferredoxin, which is required as the low potential donor for electron bifurcation (Worm et al., 2014). The [FeFe]-hydrogenase in *Syntrophus aciditrophicus* lacks the HydC subunit, which contains a [2Fe-2S] domain (Figure 11). *S. aciditrophicus* may also have the ability to generate reduced ferredoxin if the acyl-CoA dehydrogenases involved in cyclohex-1-ene-1-carboxylate and cyclohexane-1-carboxylate formation can catalyze electron bifurcation (Kung et al., 2013). The syntrophic metabolism of

ethanol and lactate are believed to generate reduced ferredoxin (Schink, 1997; Sieber et al., 2012; Meyer et al., 2013). The partial pressures observed during syntrophic ethanol oxidation by cocultures of *Pelobacter* species with *M. hungatei* exceeded 1000 Pa (Schmidt et al., 2014), which would not be thermodynamically favorable if NADH was the only electron donor for hydrogen production. Given the higher hydrogen partial pressures and presence of reduced ferredoxin-generating systems, it seems likely that some syntrophic oxidizers may utilize ferredoxin, possibly in a confurcating mechanism, for hydrogen production.

The *S. wolfei* Hyd1ABC was previously found to co-purify with a multimeric, formate dehydrogenase encoded by SWOL\_RS03955, SWOL\_RS03960, SWOL\_RS03965, SWOL\_RS03970 (Muller et al., 2009). The co-purification of Hyd1ABC with an apparent formate dehydrogenase suggested a possible formate dehydrogenase-hydrogenase complex, although an alternative would be that Hyd1 and the multimeric formate dehydrogenase are separate complexes that co-purify, perhaps due to the similar nature of the HydB/HydC subunits (Figure 11). Either as separate complexes or as a single larger complex, Hyd1 and the multimeric formate dehydrogenase could function to convert NADH to hydrogen and formate, respectively, which would mean that both metabolites are linked to the NADH/NAD<sup>+</sup> pool.

The identification of Hyd1ABC as a NADH-dependent hydrogenase suggests NADH-dependent hydrogen production occurs during syntrophic growth on butyrate by *S. wolfei* without the need of reduced ferredoxin. Ferredoxin-independent, hydrogen production from NADH would allow *S. wolfei* to avoid the energetically costly reaction to produce reduced ferredoxin from NADH. Based on the hydrogen partial pressures generated by Hyd1ABC (Table 3), continual NADH-

dependent hydrogen production would require the presence of a hydrogen-consuming organism to maintain a low hydrogen partial pressure. NADH-dependent hydrogen production could explain in part the obligate requirement *S. wolfei* has for a hydrogen-consuming organism such as *M. hungatei* during growth on energetically poor substrates such as butyrate.

## Methods

**Plasmids and Strains.** Genes encoding for a putative multimeric [FeFe]-hydrogenase were amplified by PCR from *S. wolfei* genomic DNA with Phusion High-Fidelity DNA Polymerase (Thermo Fisher Scientific, Waltham, MA) using primers listed in Table 4.

**Table 4. List of Primers Used for Construction of pETDuet-1 SwHydABC, pCDFDuet-1 SwHydEFG and pCDFDuet-1 SwFd.**

Primer <sup>a</sup>	Function
F: CGCGGATCCGATGATGGATTATAAGGAGATAAATGCCAG	Amplify
R: TTGGCGCGCCCTATAAGAATTTTTATTCTTGGCATGG	SWOL_RS05165/SWOL_RS05170/SWOL_RS05175, addition of restriction cut sites for BamHI/AscI
F: TAACCATATGCAGGATACTCCCAAAGCTA	Amplify
R: TAACCTCGAGTTAAAGAATTGCTCGGACCCTG	SWOL_RS01625, addition of restriction cut sites for NdeI/XhoI
F: TTCACCATGGAAGCGATATCAGTTAACC	Amplify
R: ACATGGATCCTTAAACCTGCTTCAAAGG	SWOL_RS05180/SWOL_RS05185/SWOL

F: CTTAGGATCCGATGTCTTACATCATC

R: AGTGATAAGCTTTTAGTCGTC

\_RS05190 addition of

restriction cut sites for

NcoI/BamHI

Amplify

SWOL\_RS010890,

addition of restriction cut

sites for BamHI/HindIII

---

<sup>a</sup>Underlined regions indicates restriction enzyme cut sites.

An amplicon with genes encoding for HydA, HydB, and HydC (SWOL\_RS05165, SWOL\_RS05170, SWOL\_RS05175) with the addition of BamHI and AscI restriction sites was inserted into the first multiple clone site (MCS) of pETDuet-1 (Novagen, Merck KGaA, Darmstadt, Germany) (Figure S3) with the addition of a *N*-terminal (His)<sub>6</sub> residue on HydC to produce pETDuet-1 SwHydABC.

A second plasmid was created to express genes encoding for [FeFe]-hydrogenase maturation proteins. The Hyd maturases, HydE (SWOL\_RS05180) and HydG (SWOL\_RS05190), as well as a 348 base pair open reading frame with no identifiable conserved domains (SWOL\_RS05185) were amplified from *S. wolfei* genomic template with the addition of NcoI and BamHI restriction sites and was inserted into the MCS of pCDFDuet-1 (Novagen, Merck KGaA, Darmstadt, Germany) (Figure S1). In addition, the gene encoding for the Hyd maturase, HydF (SWOL\_RS01625), was amplified with restriction sites for NdeI and XhoI and inserted into the second MCS of pCDFDuet-1 to generate pCDFDuet-1 SwHydEFG.



In addition, a gene encoding for a putative ferredoxin, SWOL\_RS010890, was amplified by PCR with the addition of BamHI and HindIII restriction sites and inserted into the first MCS of pCDFDuet-1 with the addition of a N-terminal (His)<sub>6</sub> residue to generate pCDFDuet-1 SwFd. SWOL\_RS010890 is predicted to encode for a 6-kDa peptide containing a conserved domain for two [4Fe-4S] centers. The SWOL\_RS010890 gene product shares 57% amino acid sequence identity to the ferredoxin from *Clostridium pasteurianum* (GenBank Nucleotide ID: M11214).

Due to changes in the locus tags for *S. wolfei* genes, a table listing the newly assigned locus tags for *S. wolfei* used in this publication, older *S. wolfei* locus tags and GenBank protein accession numbers is included as Table S4.

**Expression Conditions.** *E. coli* BL21(DE3) (Thermo Fisher Scientific, Waltham, MA) cells for expression of the genes for His-tagged hydrogenase and His-tagged ferredoxin were grown in LB medium with 50 mM potassium phosphate (pH 7.5) and 10 g·l<sup>-1</sup> glucose with appropriate antibiotics at 37°C. Cultures were grown aerobically with shaking (200 rpm) to an OD<sub>600</sub> of 0.4 to 0.6 before induction by the addition of 0.5 mM IPTG, followed by the addition of 2 mM ferric ammonium citrate, 10 mM sodium fumarate, and 2 mM cysteine. After induction, the cultures were sealed with rubber stoppers and sparged with nitrogen gas for 6 hours until harvesting. Cells were harvested anaerobically by centrifugation at 6,000 • g for 20 minutes at 4°C, washed by resuspension in 50 mM potassium phosphate (pH 7.5) and then pelleted again by centrifuging at 6,000 • g for 10 minutes at 4°C. The final cell pellets were frozen in liquid N<sub>2</sub> until further use.

**Purification of His-Tagged NADH-Dependent Hydrogenase.** All manipulations, including cell harvesting and protein purification, were performed inside a Coy Chamber with a 95% nitrogen and 1-5% hydrogen atmosphere. All purification buffers were prepared anoxically and contained 2 mM dithioerythritol (DTE) and 5  $\mu$ M of both FAD and FMN. Cell pellets (10.8 g) were thawed, suspended in 20 ml of 50 mM Tris-HCl (pH 7.5) with 0.5 M NaCl, 30 mM imidazole, and the cells broken by passage through a French pressure cell operating at an internal pressure of 140 MPa. Cell debris was removed by centrifugation at 13,000  $\cdot$  g for 20 minutes at 4°C and passage through a 0.22  $\mu$ m filter. Resulting cell lysate was applied to a HisTrap HP 5 ml column (GE Healthcare Life Sciences, Pittsburgh, PA) equilibrated with the buffer used for cell breakage, followed by a wash with 50 mM imidazole in the breakage buffer and His-tagged, NADH-dependent hydrogenase was eluted with 250 mM imidazole in the breakage buffer. Eluted fractions were then concentrated and desalted using an Amicon Ultra 0.5 ml Centrifugal Filters (EMD Millipore) with a 100 kDa nominal molecular weight limit filter. The desalted fractions were applied to a UNO-Q1 (Bio-Rad, Hercules, CA) column equilibrated with 50 mM Tris-HCl (pH 7.5), and eluted with a gradient from 0 to 0.6 M NaCl over a 17-minutes period at a flow rate of 2 ml/min. The purified protein was then aliquoted into several vials and flash frozen in liquid nitrogen until used for further analyses.

His-tagged *S. wolfei* ferredoxin was prepared as described for the His-tagged NADH-dependent hydrogenase, but the purification procedure ended after the HisTrap HP chromatography step.

**Enzymatic Assays.** All assays were performed at 37°C unless noted otherwise. Enzyme activity measurements were determined in triplicate with varying concentrations of protein to ensure

activity was proportional to the amount of protein added. Hydrogenase-oxidizing activity was measured in rubber stopper-sealed, 1.4 ml quartz cuvettes (Nova Biotech, El Cajon, CA) with 600  $\mu$ l of reaction mix and with hydrogen at a pressure of  $1.2 \cdot 10^5$  Pa. The reaction mixture for hydrogen-oxidizing assays consisted of 50 mM Tris-HCl (pH 7.5) or potassium phosphate (pH 7.5), 2 mM DTE, 5  $\mu$ M FAD, and 5  $\mu$ M FMN. NAD(P)<sup>+</sup> reduction was tested with concentration of 1 mM NAD(P)<sup>+</sup> with and without 10  $\mu$ M *C. pasteurianum* ferredoxin. Methyl viologen reduction assays were performed using a concentration of 10 mM methyl viologen. Reactions were initiated by either the addition of enzyme or the addition of  $1.2 \cdot 10^5$  Pa of hydrogen to a 100% nitrogen headspace. The kinetic constants for NAD<sup>+</sup> reduction by hydrogen were determined with varying NAD<sup>+</sup> concentrations (0 to 2.0 mM). Spectrophotometric measurements for the reduction of NAD<sup>+</sup> and NADP<sup>+</sup> were performed at 340 nm ( $\epsilon = 6.2 \text{ mM}^{-1} \text{ cm}^{-1}$ ). Clostridial ferredoxin reduction was measured using 430 nm ( $\epsilon_{\Delta\text{ox-red}} \approx 13.1 \text{ mM}^{-1} \text{ cm}^{-1}$ ) and methyl viologen reduction at 600 nm ( $\epsilon = 10.0 \text{ mM}^{-1} \text{ cm}^{-1}$ ).

Hydrogen-producing activities were measured in serum bottles (6.5 mL) sealed with butyl rubber stoppers with a 0.5 mL reaction mixture and shaken at 200 rpm. The reaction mix consisted of 100 mM potassium phosphate at pH 7.5, unless otherwise indicated, as well as 2 mM DTE, 5  $\mu$ M FAD and 5  $\mu$ M FMN. Reactions for hydrogen production were initiated by either the addition of enzyme or NADH. The headspace was sampled (0.4 mL) every 3.5 minutes and percent hydrogen in the gas phase was determined by a gas chromatograph equipped with a reductive gas analyzer. The concentration of NADH and NADPH was 1 mM. A reduced ferredoxin-generating system was used consisting of 10 mM pyruvate, 1 mM CoA, 0.1 mM thiamine pyrophosphate,

10  $\mu\text{M}$  of clostridial or *S. wolfei* ferredoxin, and 0.1 U of clostridial pyruvate:ferredoxin oxidoreductase.

Assays were set up to determine final hydrogen concentration obtained at different NADH/NAD<sup>+</sup> ratios and pH values. The conditions tested included NADH/NAD<sup>+</sup> ratios of either 1.0 or 1.5 with a total pyridine nucleotide pool size of 5 mM with a buffer of 100 mM potassium phosphate at pH 6.5 or 7.0. The ratios of NADH to NAD<sup>+</sup> used in the above experiments were determined from the measured hydrogen partial pressures of growing *S. wolfei* cultures. Final hydrogen concentrations were determined in duplicate from sealed serum bottles after the reaction mixture was incubated for 24 hours at room temperature.

It has been previously reported that the presence of trace amounts of viologen dyes in cuvettes and stoppers can decouple bifurcating reactions (Kaster et al., 2011). Hydrogen production assays involving NADH were performed using serum bottles and rubber stoppers that were not previously exposed to viologen dyes. Hydrogen-oxidizing assays were performed with stoppers that were not previously exposed to viologen dyes and with extensively washed cuvettes. Methyl viologen reduction assays were done after all other assays were completed.

**Analytical Techniques.** Protein concentration was determined by using the Bradford protein assay with bovine serum albumin as the standard (Thermo Fisher Scientific, Waltham, MA). Sodium dodecyl sulfate-polyacrylamide gel electrophoresis (SDS-PAGE) and native PAGE analysis were performed using precast Novex 8-16% Tris-Glycine (Life Technologies Co., Carlsbad, CA.) according to the manufacturer's instructions. Gels were stained using Coomassie

Brilliant Blue G250 (Thermo Fisher Scientific, Waltham, MA). Bands from the native gel were excised for peptide identification. The protein in the excised band was digested with trypsin and subjected to high performance liquid chromatography-tandem mass spectrometry (HPLC-MS/MS) performed by the Laboratory for Molecular Biology and Cytometry Research at OUHSC (Oklahoma City, OK). Resulting peptide fragments were identified by MASCOT search and compared to the NCBI nr database.

Molecular mass of recombinant Hyd1ABC was determined by size exclusion chromatography. Size exclusion chromatography was performed using a Superdex 200, 10/300 GL (GE Healthcare Life Sciences) calibrated with gel filtration standards (Bio-Rad Laboratories, Hercules, CA) using a buffer of 50 mM potassium phosphate (pH 7.5) with 0.5 M NaCl at a flow rate of 0.45 mL/min.

Iron content of the purified recombinant Hyd1ABC was determined using a ferrozine assay (Riemer et al., 2004). Identification and quantification of bound flavin was performed by high performance liquid chromatography (HPLC). The purified recombinant Hyd1ABC was washed 20-fold by ultrafiltration using flavin free 50 mM Tris-HCl (pH 7.5), boiled for 10 minutes, and denatured protein removed by centrifugation at 13,000 • g for 10 minutes. The supernatant was then analyzed using a Kromasil 100-10-C18 Column (250 × 4.6 mm) using a buffer of 25% methanol in 50 mM ammonium formate similar to a previous HPLC technique (Seedorf et al., 2004) with a UV detector set to 275 nm. Retention times and peak areas were compared to FAD and FMN standards.

Hydrogen concentration was determined by a gas chromatograph (Seiler et al., 1980; Montag and Schink, 2016) equipped with a reductive gas detector Peak Performer RCP-910 (Peak Laboratories, Mountain View, CA.) Hydrogen concentrations were determined by comparing peak areas to standards containing hydrogen concentrations from 0.01% to 1%.

**Biochemicals and Enzymes.** NADH, NAD<sup>+</sup>, FMN, FAD, pyruvate, thiamine pyrophosphate, methyl viologen and coenzyme A were purchased from Sigma-Aldrich (St-Louis, MO).

Clostridial ferredoxin (Schönheit et al., 1978) and pyruvate ferredoxin oxidoreductase (Wahl and Orme-Johnson, 1987) were purified from *Clostridium pasteurianum* (DSM 525).

**Culture Growth Conditions.** Pure cultures of *S. wolfei* (DSM 2245B) and cocultures with *M. hungatei* strain JF-1 (ATCC 27890) were grown anaerobically with resazurin as redox indicator and cysteine sulfide (0.05%) as reducing agent. The culture medium consisted of 10 ml•l<sup>-1</sup> each of mineral, trace metal and vitamin solutions (Tanner, 2007) prepared anaerobically under a N<sub>2</sub>/CO<sub>2</sub> (80:20) atmosphere with 3.5 g•l<sup>-1</sup> NaHCO<sub>3</sub> as buffering agent and either 20 mM butyrate or crotonate as substrate. Cultures were established in triplicate with 160 mL culture medium and 90 mL headspace volumes and incubated at 37°C with shaking (80 rpm). Growth was monitored at OD<sub>600</sub> with measurements for fatty acid, hydrogen and methane concentrations made at four-day intervals. Determination of butyrate, crotonate and methane concentrations were performed by HPLC and GC-FID as described previously (Sieber et al., 2014) while hydrogen concentrations were determined as described for hydrogen production assays.

## Acknowledgements

We thank N. Q. Wofford for technical assistance.

The initial cloning was developed and accomplished as part of the Biological and Electron Transfer and Catalysis (BETCy) EFRC, an Energy Frontier Research Center funded by the US Department of Energy, Office of Science, Basic Energy Sciences under Award # DE-SC0012518 to J.W.P. Additional production and characterization of Hyd1ABC were supported by National Science Foundation grant 1515843 to M.J.M. The funders had no role in study design, data collection and interpretation, or the decision to submit the work for publication.

## References

- Amos, D.A., and McInerney, M.J. (1989). Poly- $\beta$ -hydroxyalkanoate in *Syntrophomonas wolfei*. *Arch Microbiol* 152(2), 172-177. doi: 10.1007/BF00456097.
- Aono, S., Bryant, F.O., and Adams, M.W. (1989). A novel and remarkably thermostable ferredoxin from the hyperthermophilic archaeobacterium *Pyrococcus furiosus*. *J Bacteriol* 171(6), 3433-3439.
- Beatty, P.S., and McInerney, M.J. (1987). Growth of *Syntrophomonas wolfei* in pure culture on crotonate. *Arch Microbiol* 147(4), 389-393. doi: 10.1007/BF00406138.
- Boone, D.R., Johnson, R.L., and Liu, Y. (1989). Diffusion of the Interspecies Electron Carriers H<sub>2</sub> and Formate in Methanogenic Ecosystems and Its Implications in the Measurement of K(m) for H<sub>2</sub> or Formate Uptake. *Appl Environ Microbiol* 55(7), 1735-1741.

- Chowdhury, N.P., Mowafy, A.M., Demmer, J.K., Upadhyay, V., Koelzer, S., Jayamani, E., et al. (2014). Studies on the mechanism of electron bifurcation catalyzed by electron transferring flavoprotein (Etf) and butyryl-CoA dehydrogenase (Bcd) of *Acidaminococcus fermentans*. *J Biol Chem* 289(8), 5145-5157. doi: 10.1074/jbc.M113.521013.
- Conrad, R., Schink, B., and Phelps, T.J. (1986). Thermodynamics of H<sub>2</sub>-consuming and H<sub>2</sub>-producing metabolic reactions in diverse methanogenic environments under in situ conditions. *FEMS Microbiol Lett* 38(6), 353-360. doi: [http://dx.doi.org/10.1016/0378-1097\(86\)90013-3](http://dx.doi.org/10.1016/0378-1097(86)90013-3).
- Crable, B.R., Sieber, J.R., Mao, X., Alvarez-Cohen, L., Gunsalus, R., Ogorzalek Loo, R.R., et al. (2016). Membrane Complexes of *Syntrophomonas wolfei* Involved in Syntrophic Butyrate Degradation and Hydrogen Formation. *Front Microbiol* 7, 1795. doi: 10.3389/fmicb.2016.01795.
- de Graef, M.R., Alexeeva, S., Snoep, J.L., and Teixeira de Mattos, M.J. (1999). The Steady-State Internal Redox State (NADH/NAD) Reflects the External Redox State and Is Correlated with Catabolic Adaptation in *Escherichia coli*. *J Bacteriol* 181(8), 2351-2357.
- Girbal, L., von Abendroth, G., Winkler, M., Benton, P.M., Meynial-Salles, I., Croux, C., et al. (2005). Homologous and heterologous overexpression in *Clostridium acetobutylicum* and characterization of purified clostridial and algal Fe-only hydrogenases with high specific activities. *Appl Environ Microbiol* 71(5), 2777-2781. doi: 10.1128/AEM.71.5.2777-2781.2005.



- Hartmann, T., and Leimkuhler, S. (2013). The oxygen-tolerant and NAD<sup>+</sup>-dependent formate dehydrogenase from *Rhodobacter capsulatus* is able to catalyze the reduction of CO<sub>2</sub> to formate. *FEBS J.* 280(23), 6083-6096. doi: 10.1111/febs.12528.
- Jackson, B.E., and McInerney, M.J. (2002). Anaerobic microbial metabolism can proceed close to thermodynamic limits. *Nature* 415(6870), 454-456.
- Kaster, A.K., Moll, J., Parey, K., and Thauer, R.K. (2011). Coupling of ferredoxin and heterodisulfide reduction via electron bifurcation in hydrogenotrophic methanogenic archaea. *Proc Natl Acad Sci U S A* 108(7), 2981-2986. doi: 10.1073/pnas.1016761108.
- King, P.W., Posewitz, M.C., Ghirardi, M.L., and Seibert, M. (2006). Functional studies of [FeFe] hydrogenase maturation in an *Escherichia coli* biosynthetic system. *J Bacteriol* 188(6), 2163-2172. doi: 10.1128/JB.188.6.2163-2172.2006.
- Kung, J.W., Seifert, J., von Bergen, M., and Boll, M. (2013). Cyclohexanecarboxyl-Coenzyme A (CoA) and Cyclohex-1-ene-1-Carboxyl-CoA Dehydrogenases, Two Enzymes Involved in the Fermentation of Benzoate and Crotonate in *Syntrophus aciditrophicus*. *J. Bacteriol* 195(14), 3193-3200.
- Lubner, C.E., Jennings, D.P., Mulder, D.W., Schut, G.J., Zadvornyy, O.A., Hoben, J.P., et al. (2017). Mechanistic insights into energy conservation by flavin-based electron bifurcation. *Nat Chem Biol* 13(6), 655-659. doi: 10.1038/nchembio.2348.
- Malki, S., Saimmaime, I., De Luca, G., Rousset, M., Dermoun, Z., and Belaich, J.P. (1995). Characterization of an operon encoding an NADP-reducing hydrogenase in *Desulfovibrio fructosovorans*. *J Bacteriol* 177(10), 2628-2636.

- Marchler-Bauer, A., Derbyshire, M.K., Gonzales, N.R., Lu, S., Chitsaz, F., Geer, L.Y., et al. (2015). CDD: NCBI's conserved domain database. *Nucleic Acids Res* 43(Database issue), D222-226. doi: 10.1093/nar/gku1221.
- McInerney, M.J., and Bryant, M.P. (1981). "Basic Principles of Bioconversions in Anaerobic Digestion and Methanogenesis," in *Biomass Conversion Processes for Energy and Fuels*, eds. S.S. Sofer & O.R. Zaborsky. (Boston, MA: Springer US), 277-296.
- McInerney, M.J., Bryant, M.P., Hespell, R.B., and Costerton, J.W. (1981). *Syntrophomonas wolfei* gen. nov. sp. nov., an Anaerobic, Syntrophic, Fatty Acid-Oxidizing Bacterium. *Appl. Environ. Microbiol.* 41(4), 1029-1039.
- McInerney, M.J., Bryant, M.P., and Pfennig, N. (1979). Anaerobic bacterium that degrades fatty acids in syntrophic association with methanogens. *Arch Microbiol* 122(2), 129-135. doi: 10.1007/BF00411351.
- Meyer, B., Kuehl, J., Deutschbauer, A.M., Price, M.N., Arkin, A.P., and Stahl, D.A. (2013). Variation among *Desulfovibrio* Species in Electron Transfer Systems Used for Syntrophic Growth. *J Bacteriol* 195(5), 990-1004.
- Montag, D., and Schink, B. (2016). Biogas process parameters--energetics and kinetics of secondary fermentations in methanogenic biomass degradation. *Appl Microbiol Biotechnol* 100(2), 1019-1026. doi: 10.1007/s00253-015-7069-0.
- Muller, N., Schleheck, D., and Schink, B. (2009). Involvement of NADH:acceptor oxidoreductase and butyryl coenzyme A dehydrogenase in reversed electron transport during syntrophic butyrate oxidation by *Syntrophomonas wolfei*. *J Bacteriol* 191(19), 6167-6177. doi: 10.1128/JB.01605-08.

- Poudel, S., Tokmina-Lukaszewska, M., Colman, D.R., Refai, M., Schut, G.J., King, P.W., et al. (2016). Unification of [FeFe]-hydrogenases into three structural and functional groups. *Biochim. Biophys. Acta.* 1860(9), 1910-1921. doi: 10.1016/j.bbagen.2016.05.034.
- Riemer, J., Hoepken, H.H., Czerwinska, H., Robinson, S.R., and Dringen, R. (2004). Colorimetric ferrozine-based assay for the quantitation of iron in cultured cells. *Anal Biochem* 331(2), 370-375. doi: 10.1016/j.ab.2004.03.049.
- Schink, B. (1997). Energetics of syntrophic cooperation in methanogenic degradation. *Microbiol. Mol Biol Rev* 61(2), 262-280.
- Schmidt, A., Frensch, M., Schleheck, D., Schink, B., and Muller, N. (2014). Degradation of acetaldehyde and its precursors by *Pelobacter carbinolicus* and *P. acetylenicus*. *PLoS One* 9(12), e115902. doi: 10.1371/journal.pone.0115902.
- Schmidt, A., Muller, N., Schink, B., and Schleheck, D. (2013). A proteomic view at the biochemistry of syntrophic butyrate oxidation in *Syntrophomonas wolfei*. *PLoS One* 8(2), e56905. doi: 10.1371/journal.pone.0056905.
- Schmidt, O., Hink, L., Horn, M.A., and Drake, H.L. (2016). Peat: home to novel syntrophic species that feed acetate- and hydrogen-scavenging methanogens. *ISME J* 10(8), 1954-1966. doi: 10.1038/ismej.2015.256.
- Schönheit, P., Wäscher, C., and Thauer, R.K. (1978). A rapid procedure for the purification of ferredoxin from clostridia using polyethyleneimine. *FEBS Lett* 89(2), 219-222. doi: 10.1016/0014-5793(78)80221-X.
- Schuchmann, K., and Muller, V. (2012). A bacterial electron-bifurcating hydrogenase. *J Biol Chem* 287(37), 31165-31171. doi: 10.1074/jbc.M112.395038.

- Schuchmann, K., and Muller, V. (2014). Autotrophy at the thermodynamic limit of life: a model for energy conservation in acetogenic bacteria. *Nature Rev Micro* 12(12), 809-821. doi: 10.1038/nrmicro3365
- <http://www.nature.com/nrmicro/journal/v12/n12/abs/nrmicro3365.html#supplementary-information>.
- Schut, G.J., and Adams, M.W. (2009). The iron-hydrogenase of *Thermotoga maritima* utilizes ferredoxin and NADH synergistically: a new perspective on anaerobic hydrogen production. *J Bacteriol* 191(13), 4451-4457. doi: 10.1128/JB.01582-08.
- Seedorf, H., Dreisbach, A., Hedderich, R., Shima, S., and Thauer, R.K. (2004). F<sub>420</sub>H<sub>2</sub> oxidase (FprA) from *Methanobrevibacter arboriphilus*, a coenzyme F<sub>420</sub>-dependent enzyme involved in O<sub>2</sub> detoxification. *Arch Microbiol* 182(2-3), 126-137. doi: 10.1007/s00203-004-0675-3.
- Seiler, W., Giehl, H., and Roggendorf, P. (1980). Detection of carbon monoxide and hydrogen by conversion of mercury oxide to mercury vapor.
- Sekiguchi, Y., Kamagata, Y., Nakamura, K., Ohashi, A., and Harada, H. (2000). *Syntrophothermus lipocalidus* gen. nov., sp. nov., a novel thermophilic, syntrophic, fatty-acid-oxidizing anaerobe which utilizes isobutyrate. *Int J Syst Evol Microbiol* 50(2), 771-779. doi: doi:10.1099/00207713-50-2-771.
- Sieber, J.R., Crable, B.R., Sheik, C.S., Hurst, G.B., Rohlin, L., Gunsalus, R.P., et al. (2015). Proteomic analysis reveals metabolic and regulatory systems involved in the syntrophic and axenic lifestyle of *Syntrophomonas wolfei*. *Front Microbiol* 6, 115. doi: 10.3389/fmicb.2015.00115.

- Sieber, J.R., Le, H.M., and McInerney, M.J. (2014). The importance of hydrogen and formate transfer for syntrophic fatty, aromatic and alicyclic metabolism. *Environ Microbiol* 16(1), 177-188. doi: 10.1111/1462-2920.12269.
- Sieber, J.R., McInerney, M.J., and Gunsalus, R.P. (2012). Genomic insights into syntrophy: the paradigm for anaerobic metabolic cooperation. *Annu Rev Microbiol* 66, 429-452. doi: 10.1146/annurev-micro-090110-102844.
- Sieber, J.R., Sims, D.R., Han, C., Kim, E., Lykidis, A., Lapidus, A.L., et al. (2010). The genome of *Syntrophomonas wolfei*: new insights into syntrophic metabolism and biohydrogen production. *Environ Microbiol* 12(8), 2289-2301. doi: 10.1111/j.1462-2920.2010.02237.x.
- Snoep, J.L., Joost, M., de Mattos, T., and Neijssel, O.M. (1991). Effect of the energy source on the NADH/NAD ratio and on pyruvate catabolism in anaerobic chemostat cultures of *Enterococcus faecalis* NCTC 775. *FEMS Microbiol Lett* 81(1), 63-66. doi: 10.1111/j.1574-6968.1991.tb04713.x.
- Soboh, B., Linder, D., and Hedderich, R. (2004). A multisubunit membrane-bound [NiFe] hydrogenase and an NADH-dependent Fe-only hydrogenase in the fermenting bacterium *Thermoanaerobacter tengcongensis*. *Microbiology* 150(Pt 7), 2451-2463. doi: 10.1099/mic.0.27159-0.
- Sousa, D.Z., Smidt, H., Alves, M.M., and Stams, A.J.M. (2007). *Syntrophomonas zehnderi* sp. nov., an anaerobe that degrades long-chain fatty acids in co-culture with *Methanobacterium formicicum*. *Int J Syst Evol Microbiol* 57(3), 609-615. doi: 10.1099/ijms.0.64734-0.
- Svetlitsnyi, V., Rainey, F., and W, Juergen. (1996). *Thermosyntropha lipolytica* gen. nov., sp.

- nov., a Lipolytic, Anaerobic, Alkalitolerant, Thermophilic Bacterium Utilizing Short- and Long-Chain Fatty Acids in Syntrophic Coculture with a Methanogenic Archaeum. *Int J of Syst and Evol Microbiol* 46(4), 1131-1137. doi: doi:10.1099/00207713-46-4-1131.
- Tanner, R.S. (2007). "Cultivation of Bacteria and Fungi," in *Manual of Environmental Microbiology, Third Edition*. American Society of Microbiology).
- Wahl, R.C., and Orme-Johnson, W.H. (1987). Clostridial pyruvate oxidoreductase and the pyruvate-oxidizing enzyme specific to nitrogen fixation in *Klebsiella pneumoniae* are similar enzymes. *J Biol Chem* 262(22), 10489-10496.
- Wallrabenstein, C., and Schink, B. (1994). Evidence of reversed electron transport in syntrophic butyrate or benzoate oxidation by *Syntrophomonas wolfei* and *Syntrophus buswellii*. *Arch Microbiol* 162(1), 136-142. doi: 10.1007/BF00264387.
- Wang, S., Huang, H., Kahnt, J., and Thauer, R.K. (2013a). *Clostridium acidurici* electron-bifurcating formate dehydrogenase. *Appl Environ Microbiol* 79(19), 6176-6179. doi: 10.1128/AEM.02015-13.
- Wang, S., Huang, H., Kahnt, J., and Thauer, R.K. (2013b). A reversible electron-bifurcating ferredoxin- and NAD-dependent [FeFe]-hydrogenase (HydABC) in *Moorella thermoacetica*. *J. Bacteriol.* 195(6), 1267-1275. doi: 10.1128/JB.02158-12.
- Wimpenny, J.W.T., and Firth, A. (1972). Levels of Nicotinamide Adenine Dinucleotide and Reduced Nicotinamide Adenine Dinucleotide in Facultative Bacteria and the Effect of Oxygen. *J Bacteriol* 111(1), 24-32.
- Wofford, N.Q., Beaty, P.S., and McInerney, M.J. (1986). Preparation of cell-free extracts and the enzymes involved in fatty acid metabolism in *Syntrophomonas wolfei*. *J Bacteriol* 167(1), 179-185.

- Worm, P., Koehorst, J.J., Visser, M., Sedano-Núñez, V.T., Schaap, P.J., Plugge, C.M., et al. (2014). A genomic view on syntrophic versus non-syntrophic lifestyle in anaerobic fatty acid degrading communities. *BBA Bioenergetics* 1837(12), 2004-2016. doi: <http://dx.doi.org/10.1016/j.bbabio.2014.06.005>.
- Zheng, Y., Kahnt, J., Kwon, I.H., Mackie, R.I., and Thauer, R.K. (2014). Hydrogen formation and its regulation in *Ruminococcus albus*: involvement of an electron-bifurcating [FeFe]-hydrogenase, of a non-electron-bifurcating [FeFe]-hydrogenase, and of a putative hydrogen-sensing [FeFe]-hydrogenase. *J Bacteriol* 196(22), 3840-3852. doi: 10.1128/JB.02070-14.

### Supplemental Figures and Tables

**Table S1. Peptide Matches Obtained from the Excised Band from Native PAGE of the Purified, Expressed Hyd1ABC.**

Old NCBI Locus Tag	New NCBI Gene Locus	Protein Accession Number	Annotation	Matched peptides	Protein sequence coverage
Swol_1 017	SWOL_RS 05165	WP_0116 40436	Hyd1A, iron hydrogenase, small subunit	56	70.6%
Swol_1	SWOL_RS	WP_0116	Hyd1B, NADH	26	71.4%

018	05170	40437	dehydrogenase subunit		
Swol_1	SWOL_RS	WP_0116	Hyd1C, iron-	5	53.4%
019	05175	40438	hydrogenase, gamma subunit		
Swol_2	SWOL_RS	WP_0116	Fe-hydrogenase,	5	5.7%
436	12620	41809	large subunit HymC		
Swol_1	SWOL_RS	WP_0116	NADH	2	4.2%
828	09445	41221	dehydrogenase (Quinone)		

**Table S2. Comparison of Properties of Multimeric [FeFe]-Hydrogenases**

Source organism	Methyl viologen reducing activity (U•mg <sup>-1</sup> ) <sub>a</sub>	NAD <sup>+</sup> reducing activity (U•mg <sup>-1</sup> ) <sub>a</sub>	NADH oxidation activity (U•mg <sup>-1</sup> ) <sub>a</sub>	K <sub>M</sub> for NAD <sup>+</sup> (μM)	Molecular weight (kDa)	Assay temperature (°C)	Ref. No.
<i>S. wolfei</i>	571	94.5	6.6	520	124.5	37	This publication
<i>T. maritima</i>	NR	NR <sup>b</sup>	~1.5 <sup>c</sup>	NR	NR	80	11
<i>A. woodii</i>	711	~3.0 <sup>c</sup>	NR	49	300 <sup>d</sup>	30	14
<i>M.</i>	195	57.5 <sup>c</sup>	4.6 <sup>c</sup>	250	300 <sup>d</sup>	45	15



*thermoacetic*

*a*

*R. albus* NA 60<sup>c</sup> NR NR NR 37 16

*C.* 1671 5 10 90 NR 70 37

*tengcongens*

*is*

<sup>a</sup> One unit of activity (U) equals 2  $\mu$ mol of electrons transferred per min. See the referenced articles for assay conditions.

<sup>b</sup> NR, not reported.

<sup>c</sup> Ferredoxin present.

<sup>d</sup> Reported as a dimer of either  $\alpha\beta\gamma$  heterotrimer or  $\alpha\beta\gamma\delta$  heterotetramer.

**Table S3 Genbank Protein Accession Numbers of Subunits of Multimeric Formate Dehydrogenases and [FeFe]-Hydrogenases.**

Source Organism	Subunit	GenBank Protein Accession Number
<i>Acetobacterium woodii</i>	HydA	AFA49450
<i>Acetobacterium woodii</i>	HydB	AFA49451
<i>Acetobacterium woodii</i>	HydC	AFA49452
<i>Acetobacterium woodii</i>	HydD	AFA49454
<i>Caldanaerobacter tencongensis</i>	HydA	AAM24150
<i>Caldanaerobacter tencongensis</i>	HydB	AAM24149
<i>Caldanaerobacter tencongensis</i>	HydC	AAM24148

<i>Clostridium acidurici</i>	FdhA	AFS79904
<i>Clostridium acidurici</i>	FdhA	AFS79905
<i>Clostridium acidurici</i>	FdhB	AFS79906
<i>Clostridium acidurici</i>	FdhC	AFS79907
<i>Desulfovibrio fructosivorans</i>	HydA	AAA87057
<i>Desulfovibrio fructosivorans</i>	HydB	AAA87056
<i>Desulfovibrio fructosivorans</i>	HydC	AAA87054
<i>Desulfovibrio fructosivorans</i>	HydD	AAA87055
<i>Moorella thermoacetica</i>	HydA	ABC20019
<i>Moorella thermoacetica</i>	HydB	ABC20020
<i>Moorella thermoacetica</i>	HydC	ABC20021
<i>Rhodopsuedomonas capsulatus</i>	FdhA	ADE86759
<i>Rhodopsuedomonas capsulatus</i>	FdhB	ADE86760
<i>Rhodopsuedomonas capsulatus</i>	FdhC	ADE86761
<i>Ruminococcus albus</i>	HydA	ADU23430
<i>Ruminococcus albus</i>	HydB	ADU23431
<i>Ruminococcus albus</i>	HydC	ADU23432
<i>Syntrophobacter fumaroxidans</i>	HydA	ABK16541
<i>Syntrophobacter fumaroxidans</i>	HydB	ABK16542
<i>Syntrophobacter fumaroxidans</i>	HydC	ABK16543
<i>Syntrophomonas wolfei</i>	FdhA	ABI68106/ABI68107
<i>Syntrophomonas wolfei</i>	FdhB	ABI68105

<i>Syntrophomonas wolfei</i>	FdhC	ABI68104
<i>Syntrophomonas wolfei</i>	HydA	ABI68331
<i>Syntrophomonas wolfei</i>	HydB	ABI68332
<i>Syntrophomonas wolfei</i>	HydC	ABI68333
<i>Syntrophomonas zehnderi</i>	HydA	WP_046500146
<i>Syntrophomonas zehnderi</i>	HydB	WP_046500148
<i>Syntrophomonas zehnderi</i>	HydC	WP_046500150
<i>Syntrophothermus lipocalidus</i>	HydA	WP_013174729
<i>Syntrophothermus lipocalidus</i>	HydB	WP_013174328
<i>Syntrophothermus lipocalidus</i>	HydC	WP_013174327
<i>Syntrophus aciditrophicus</i>	HydA	ABC76974
<i>Syntrophus aciditrophicus</i>	HydB	ABC76975
<i>Thermosyntropha lipolytica</i>	HydA	WP_073091114
<i>Thermosyntropha lipolytica</i>	HydB	WP_073091112
<i>Thermosyntropha lipolytica</i>	HydC	WP_073091109
<i>Thermotoga maritima</i>	HydA	AAD36496
<i>Thermotoga maritima</i>	HydB	AAD36495
<i>Thermotoga maritima</i>	HydC	AAD36494

---

**Table S4. Updated Locus Tag Designations of *S. wolfei* Genes.**

Old NCBI Locus Tag	New NCBI Gene Locus	Protein Accession Number	Genome Location
Swol_1017	SWOL_RS05165	WP_011640436	NC_008346 REGION: 1157124.1158848
Swol_1018	SWOL_RS05170	WP_011640437	NC_008346 REGION: 1158873.1160096
Swol_1019	SWOL_RS05175	WP_011640438	NC_008346 REGION: 1160156.1160602
Swol_1020	SWOL_RS05180	WP_041427405	NC_008346 REGION: 1160971.1162029
Swol_1021	SWOL_RS05185	WP_041427406	NC_008346 REGION: 1161998.1162378
Swol_1022	SWOL_RS05190	WP_011640441	NC_008346 REGION: 1162353.1163816
Swol_0318	SWOL_RS01625	WP_011639769	NC_008346 REGION: 384562.385770
Swol_2105	SWOL_RS10890	WP_011641488	NC_008346 REGION: 2424114.2424290
Swol_1925	SWOL_RS09950	WP_011641315	NC_008346 REGION:

2197847.2199010

Swol\_2436 SWOL\_RS12620 WP\_011641809 NC\_008346 REGION:

2765177.2766868

---

**Figure S1. Kinetics of NAD<sup>+</sup> Reduction with Hydrogen by Hyd1ABC.**

Reactions were performed at 37°C in 1.6 ml cuvettes with 800 µl of 50 mM potassium phosphate buffer (pH 7.5), with 5 µM FAD, 5 µM FMN and 86 µg of Hyd1ABC. The data were fit to the reaction curve using non-linear regression with a  $K_m$  of 0.52 mM NAD<sup>+</sup> and a  $V_{max}$  of 196 µmole•min<sup>-1</sup>•mg<sup>-1</sup> of protein. A  $k_{cat}$  of 406.7 s<sup>-1</sup> was determined using a single catalytic site per a molecular mass of 124.5 kDa.

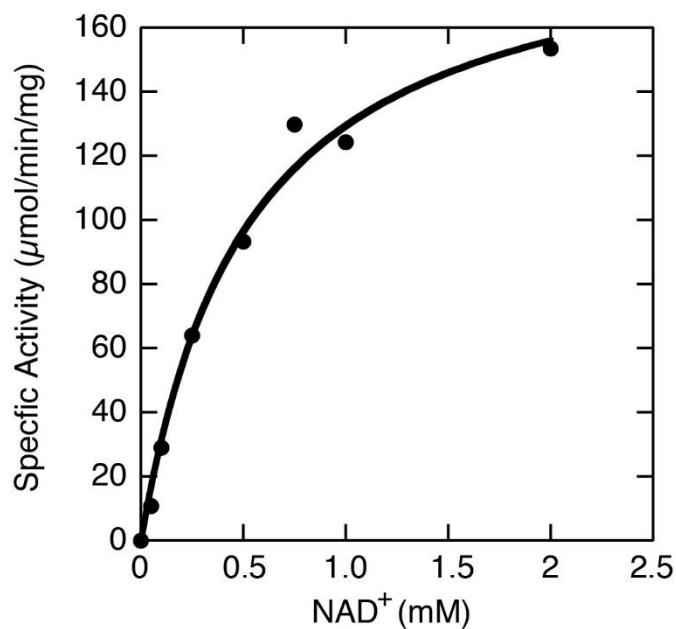


**Figure S2. Hydrogen Partial Pressures During Growth of *S. wolfei* in Pure culture and in Coculture with *M. hungatei*.** (A and B) *S. wolfei* grown in pure culture on crotonate; (C and D) *S. wolfei* grown in coculture with *M. hungatei* on crotonate; (E and F) *S. wolfei* grown in coculture with *M. hungatei* on butyrate. A, C, E, growth (diamonds) and hydrogen (Pa) (triangles); (B, D, F) substrate concentration (crotonate in B and D and butyrate in F) (circles) and methane concentration (squares).

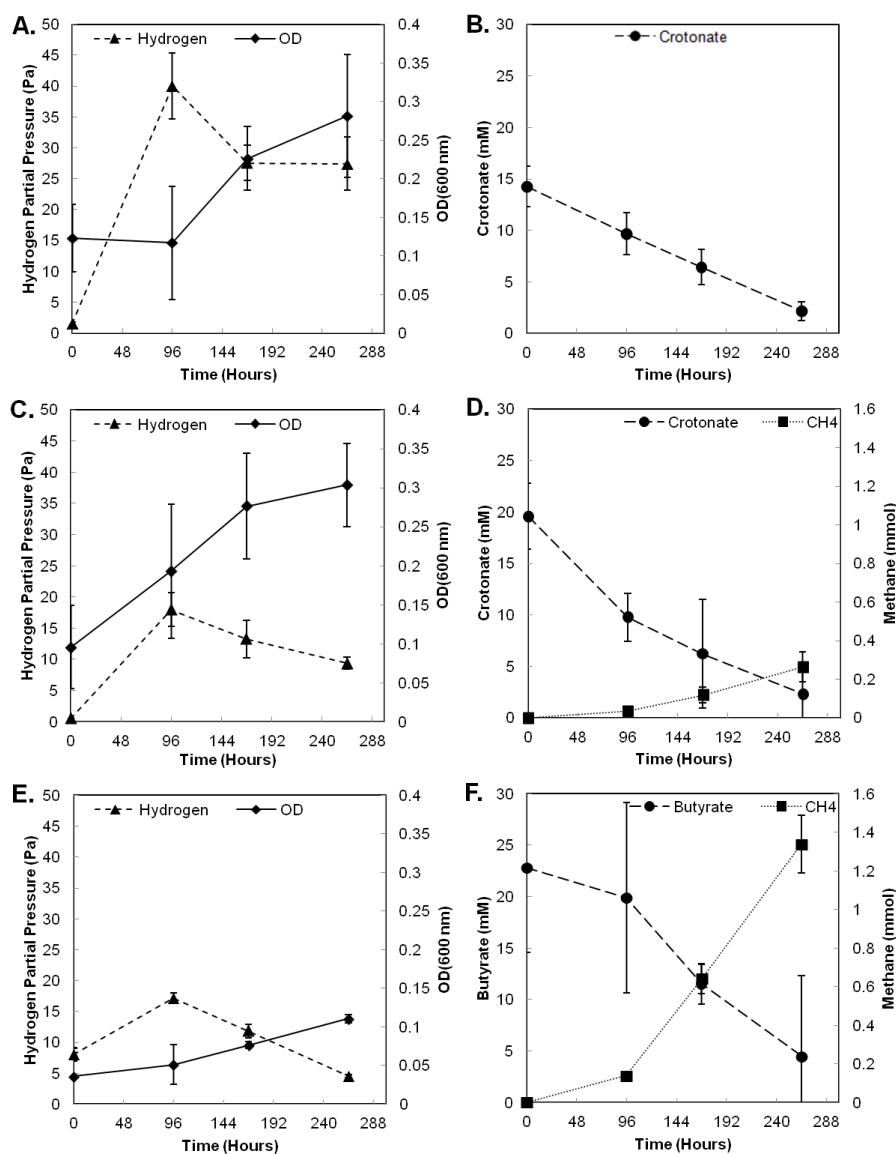
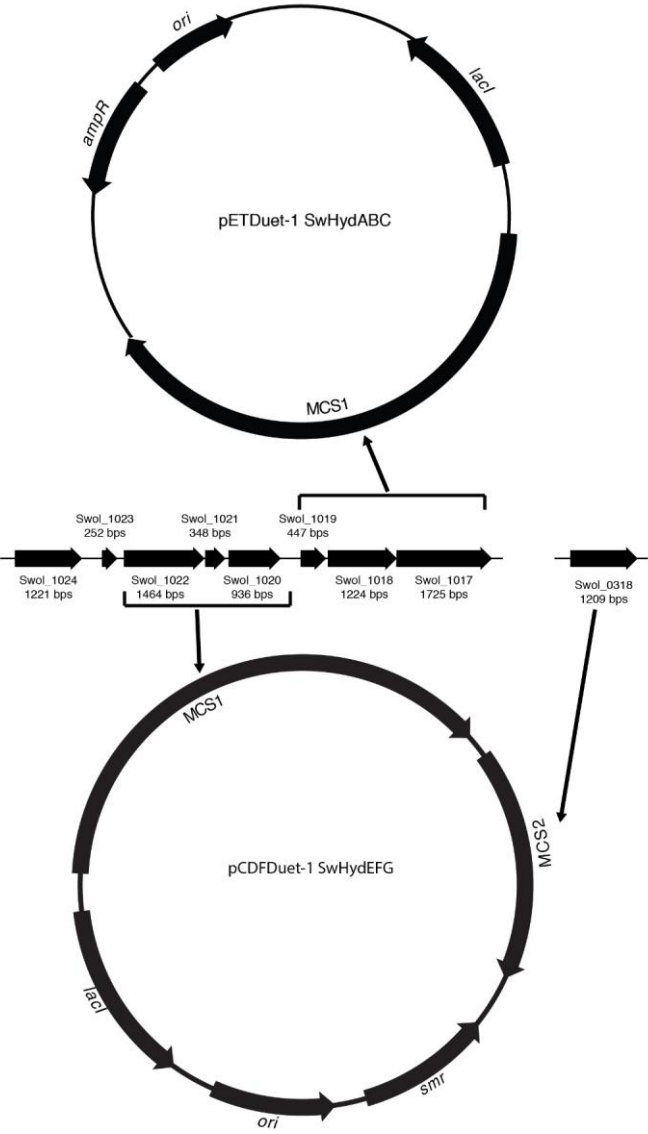


**Figure S3. Construction of Plasmids for Expression of Hyd1ABC and [FeFe]-Hydrogenase Maturation Proteins.**





**CHAPTER 3. A NADH-Dependent, Ferredoxin-Independent [FeFe]-Hydrogenase from**  
*Syntrophus aciditrophicus*

## Abstract

A NADH-dependent, ferredoxin-independent dimeric [FeFe]-hydrogenase (HydAB) from *Syntrophus aciditrophicus* was heterologously expressed in *Escherichia coli*, purified and characterized. The purified recombinant HydAB consisted of two subunits HydA and HydB with molecular weights 68.5 kDa and 66.0 kDa, respectively, as predicted from the encoding DNA sequences. The molecular weight of the HydAB complex as estimated by gel filtration chromatography (287 kDa) and native gel migration (323 kDa) suggested a  $\alpha_2\beta_2$  configuration. The HydAB  $\alpha_2\beta_2$  complex had  $71.7 \pm 15.4$  mole of iron and 1.06 mole of FMN per mole of holoenzyme. HydAB catalyzed NAD<sup>+</sup> reduction coupled to hydrogen oxidation and produced hydrogen from NADH without the involvement of ferredoxin. Pure cultures of *S. aciditrophicus* and cocultures of *S. aciditrophicus* with *Methanospirillum hungatei* generated hydrogen partial pressures of 5.9 to 36.6 Pa with crotonate, benzoate, and cyclohex-1-ene-1-carboxylate as substrates which are the same magnitude as the hydrogen partial pressures (2.2 to 40.2 pascals) produced by the purified recombinant *S. aciditrophicus* HydAB at NADH to NAD<sup>+</sup> ratios of 1 to 5. Thus, the hydrogen partial pressures observed in metabolizing cultures and cocultures of *S. aciditrophicus* can be generated by HydAB if *S. aciditrophicus* maintains NADH to NAD<sup>+</sup> ratios greater than one. These results show that two phylogenetically distinct syntrophic fatty acid-oxidizing bacteria, *S. wolfei* a member of the phylum Firmicutes, and *S. aciditrophicus*, a Deltaproteobacteria, possess functionally similar hydrogenases that produce hydrogen from NADH during syntrophic fatty acid oxidation without the involvement of reduced ferredoxin. Most importantly, the work suggests that hydrogen production from NADH by ferredoxin-independent [FeFe]-hydrogenases may be a core feature of syntrophic fatty acid oxidization. This may be due to energetic advantages where the direct production of hydrogen from NADH

in a ferredoxin-independent mechanism allows the organisms to conserve more energy for growth. In contrast, electron confurcation of NADH and ferredoxin to produce hydrogen would require energy input to generate reduced ferredoxin from NADH. The reliance on a NADH-dependent, ferredoxin-independent [FeFe]-hydrogenase may explain the obligate requirement that syntrophic metabolizers have for a hydrogen-using partner microorganism when grown on fatty, aromatic and alicyclic acids.

## **Introduction**

Benzoate and its activated form, benzoyl-CoA, are key intermediates in the degradation of organic matter in anaerobic environments (Harwood et al., 1998; McInerney et al., 2008; McInerney et al., 2009). In methanogenic environments, benzoate and other aromatic compounds are degraded to acetate, formate, CO<sub>2</sub>, H<sub>2</sub> by syntrophic metabolizers. The degradation of benzoate and other aromatic and fatty acids to acetate, formate, CO<sub>2</sub>, H<sub>2</sub> is thermodynamically unfavorable unless formate and H<sub>2</sub> are kept at low levels by formate- and H<sub>2</sub>-using microorganisms such as methanogens. *Syntrophus aciditrophicus* is a metabolic specialist capable of oxidizing benzoate, alicyclic acids such as cyclohexane-1-carboxylate and fatty acids when paired with a hydrogen- or formate-consuming partner organism such as a methanogen or sulfate reducer (Jackson et al., 1999; Elshahed and McInerney, 2001). *S. aciditrophicus* serves as the model organism to study syntrophic aromatic and alicyclic acid metabolism as its genome has been sequenced (McInerney et al., 2007) and methods have been developed to separate cells of *S. aciditrophicus* from its hydrogen- and formate-using partner (Sieber et al., 2015). Also, it can be grown in pure culture on crotonate (Jackson et al., 1999).

*S. aciditrophicus* syntrophically degrades benzoate and cyclohexane-1-carboxylate to acetate, CO<sub>2</sub>, H<sub>2</sub> and formate via a 6-substituted cyclohex-1-ene-1-carboxyl-CoA intermediate

using a core set of enzymes (James et al., 2019, in preparation). *S. aciditrophicus* uses a unique mechanism for energy generation from acetyl-CoA where an AMP-forming, acetyl-CoA synthetase are used to make acetate, CoA and ATP from acetyl-CoA, AMP and pyrophosphate by an acetyl-CoA synthetase (James et al., 2016). This enzyme requires unusually high pyrophosphate and AMP levels within the cell to make ATP production from acetyl-CoA, AMP and pyrophosphate thermodynamically favorable (James et al., 2016). As part of the metabolism of benzoate or cyclohexane-1-carboxylate, reduced flavins (EtfAB) and NADH are generated (McInerney et al., 2007; McInerney et al., 2009). *S. aciditrophicus* also contains genes for an Rnf complex (McInerney et al., 2007) that can make reduced ferredoxin by oxidizing NADH using energy from a membrane gradient (Schmehl et al., 1993; Biegel and Müller, 2010). The reduced ferredoxin would be required by *S. aciditrophicus* to reduce benzoyl-CoA by an ATP-independent mechanism (Fuchs et al., 2011; Kung et al., 2013). During syntrophic growth, reduced EtfAB and NADH must be re-oxidized by the production of hydrogen or formate (McInerney et al., 2007; McInerney et al., 2009). Hydrogen and formate production from reduced flavin pools (EtfAB) requires energy input from a membrane gradient, a process termed reverse electron transfer (McInerney et al., 2007; McInerney et al., 2009). A membrane-associated iron-sulfur oxidoreductase in conjunction with a reverse quinone loop and membrane-associated formate dehydrogenase may be responsible for EtfAB re-oxidation similar to the mechanism proposed for *Syntrophomonas wolfei* (Schmidt et al., 2013; Sieber et al., 2015; Crable et al., 2016). In *S. aciditrophicus*, the re-oxidation of NADH was previously proposed to involve the use of the Rnf complex to oxidize NADH and produce reduced ferredoxin (McInerney et al., 2007). The reduced ferredoxin would then be used to produce hydrogen or formate (Sieber et al., 2012) by a mechanism referred to as electron bifurcation whereby for

every molecule of NADH oxidized, one molecule of reduced ferredoxin is also oxidized (Schut and Adams, 2009). The favorable production of hydrogen and formate using low potential electrons derived from reduced ferredoxin allows the unfavorable production of hydrogen and formate from the high redox potential electrons from NADH (Schut and Adams, 2009). If *S. aciditrophicus* uses electron-bifurcating hydrogenases and formate dehydrogenases, *S. aciditrophicus* would have to use the Rnf complex to make reduced ferredoxin from electrons derived from NADH oxidation, which consume potential energy from a membrane gradient, leaving less energy to be conserved for growth (Seedorf et al., 2008; Biegel and Müller, 2010).

The genome of *S. aciditrophicus* encodes two predicted hydrogenases, a cytoplasmic [NiFe]-hydrogenase and a dimeric cytoplasmic [FeFe]-hydrogenase (HydAB) (McInerney et al., 2007). The latter is predicted to use NADH as the electron donor. The purpose of the work in this chapter was to determine if the dimeric cytoplasmic [FeFe]-hydrogenase (HydAB) produces hydrogen from NADH and whether this process requires reduced ferredoxin. To produce an active form of HydAB from *S. aciditrophicus*, a recombinant DNA approach was used to express HydAB in *Escherichia coli* and then characterize the purified recombinant HydAB.

## **Results**

### **Purification and characterization of *S. aciditrophicus* hydrogenase, HydAB**

The protein products of SYN\_01369 and SYN\_01370 (HydAB) were recombinantly produced in *E. coli* and purified using nickel-affinity chromatography and molecular weight cut off filters (100 kDa) (Table 5). All further enzymatic assays and properties were determined using this fraction. During purification, hydrogenase activity was followed by methyl viologen reduction with hydrogen as the electron donor. Recombinant HydAB was purified 36-fold with a 62% yield and a final specific activity of 13 U • mg<sup>-1</sup> (Table 5).

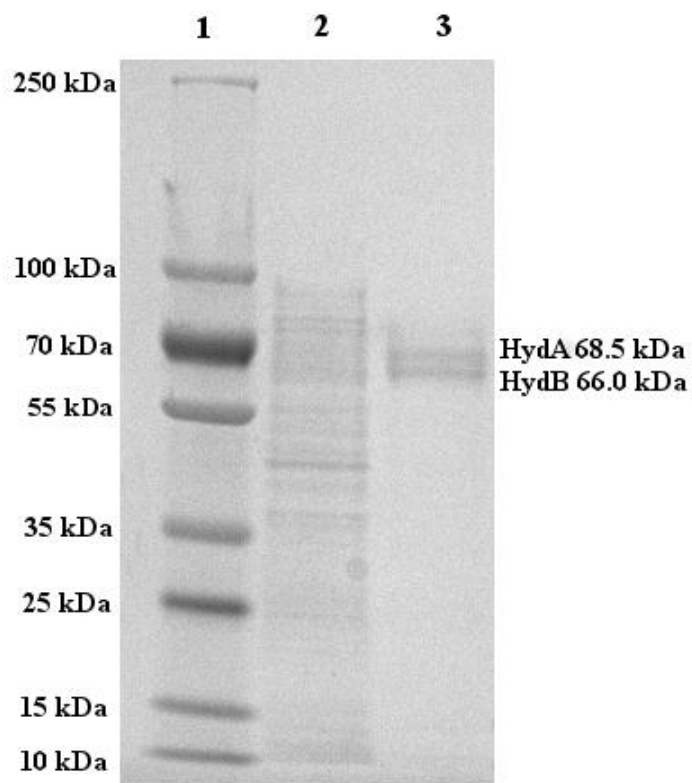
**Table 5. Purification of NADH-Dependent [FeFe]-Hydrogenase, HydAB.**

Fraction	Protein (mg)	Specific Activity* H <sub>2</sub> → MV <sub>ox</sub> (U/mg)	Total Activity* H <sub>2</sub> → MV <sub>ox</sub> (U)	Purification (fold)	Yield (%)
Cell free extract	194	0.36	69.8	1	100
Ni-Affinity	3.3	13.0	42.9	36.1	62

\*HydAB activity was followed by methyl viologen reduction with hydrogen as the electron donor at 37 °C and a pH of 7.5. One unit of activity (U) equals 2 μmoles of electrons transferred per min.

Sodium dodecyl sulfate polyacrylamide gel electrophoresis (SDS-PAGE) and non-denaturing polyacrylamide gel electrophoresis (Native PAGE) analysis indicated that a few contaminants were present in the final purified fractions. SDS-PAGE analysis (Figure 12) showed two bands which by the pattern of gel migration were estimated to be 68 kDa and 64 kDa in size. This compares favorably with the predicted molecular weights of HydA (68.5 kDa) and HydB (66.0 kDa) as estimated from their respective gene sequences. The HydA predicted molecular weight includes the additional N-terminal His tag (2.4 kDa) with the sequence MGSSHHHHHSQDPNSSSARL. Analysis by high performance liquid chromatography coupled to tandem mass spectrometry (HPLC MS-MS analysis) of the peptides present in the purified HydAB fraction showed that many of the peptides that matched HydA and HydB although there were peptides that matched *E. coli* proteins (Table 6).

**Figure 12. SDS PAGE of Recombinant *S. aciditrophicus* HydAB Purified from *E. coli* by Nickel Affinity Chromatography.** Lane 1, molecular weight markers; Lane 2, *E. coli* cell-free extract; Lane 3, fraction after nickel-affinity chromatography. Molecular weights listed on gel image indicate the molecular weight as predicted from the encoding gene sequence.



Further analysis of the purified recombinant HydAB was performed to determine its native molecular weight and cofactor content. Molecular weight determination by size exclusion chromatography indicated a protein of 286.96 kDa that would be consistent with a dimer of the  $\alpha\beta$  heterodimer of the HydAB subunits. Analysis by native PAGE (Figure 13) indicated a band migrating at a molecular weight of 322 kDa, which is consistent with a dimer of the  $\alpha\beta$  heterodimer ( $68.4 \text{ kDa} \cdot 2 + 65.9 \text{ kDa} \cdot 2$ ). The iron content of the purified recombinant HydAB was  $71.7 \pm 15.4$  moles of iron per mole per 287 kDa protein or  $35.9 \pm 7.7$  moles of iron per mole of the single 143.5  $\alpha\beta$  heterodimer. Based on domain analysis, HydAB is predicted to contain five [4Fe-4S]-clusters, two [2Fe-2S]-clusters and six Fe in the [H-Cluster] for an iron content of 30 moles of iron per mole of  $\alpha\beta$  heterodimer, which is lower than the experimentally determined iron content of  $35.9 \pm 7.7$  moles of iron per mole of the 143.5  $\alpha\beta$  heterodimer. The flavin content per dimer of the  $\alpha\beta$  heterodimer was 1.06 mole of flavin mononucleotide (FMN) per mole of 287 kDa or 0.53 FMN per 145.3 kDa  $\alpha\beta$  heterodimer.



**Figure 13. Native PAGE Analysis of Recombinant *S. aciditrophicus* HydAB Purified from *E. coli* by Nickel Affinity Chromatography.** Lane 1, molecular weight markers; Lane 2, *E. coli* cell-free extract; Lane 3, fraction after nickel-affinity chromatography.

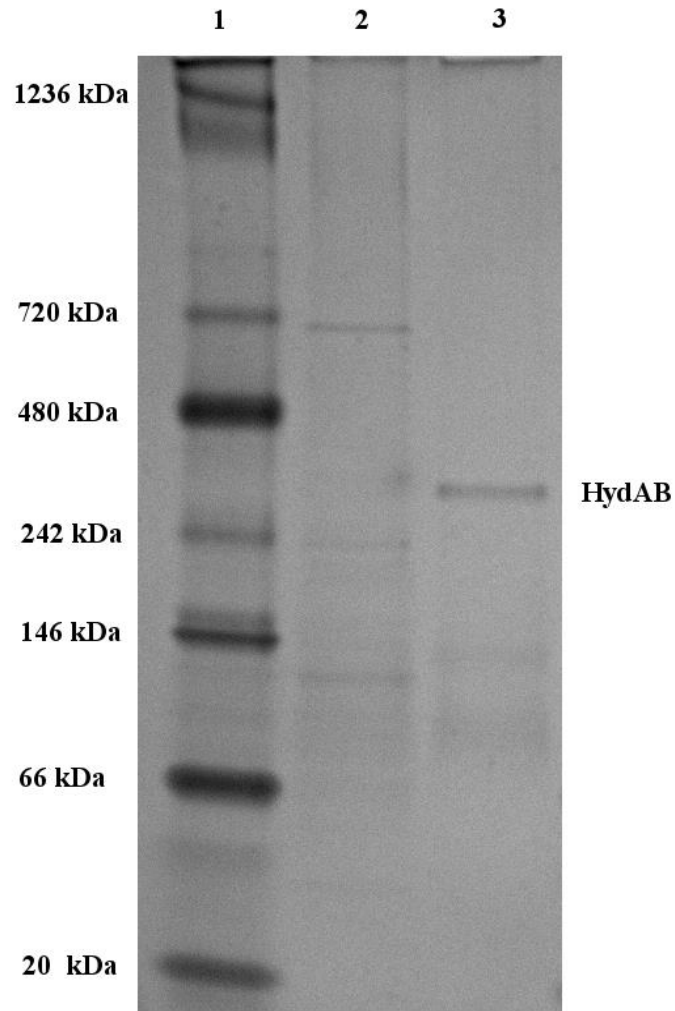


**Table 6. Peptides Detected by HPLC MS-MS Analysis of the Purified Recombinant HydAB****Fraction.**

SwissProt ID	Protein Description	Gene Name	Gene Product	Number of Matches to	Protein Sequence Coverage (%)
Q2LSB7	Iron only hydrogenase large subunit <i>Syntrophus aciditrophicus</i> (strain SB)	SYN_01370		805	81.16
Q2LSB6	NADH-quinone oxidoreductase chain F <i>Syntrophus aciditrophicus</i> (strain SB)	SYN_01369		840	65.07
P0AG44	50S ribosomal protein L17 <i>Escherichia coli</i> (strain K12)	rplQ		83	40.16
P77398	Bifunctional polymyxin resistance protein ArnA <i>Escherichia coli</i> (strain K12)	arnA		195	36.67
P0A9A9	Ferric uptake regulation	fur		56	41.22

	protein <i>Escherichia coli</i> (strain K12)			
P0ACJ8	cAMP-activated global transcriptional regulator CRP <i>Escherichia coli</i> (strain K12)	crp	107	66.67
P17169	Glutamine--fructose-6- phosphate aminotransferase [isomerizing] <i>Escherichia coli</i> (strain K12)	glmS	191	48.77
P0A9K9	FKBP-type peptidyl- prolyl cis-trans isomerase SlyD <i>Escherichia coli</i> (strain K12)	slyD	109	47.96
P0A7S9	30S ribosomal protein S13 <i>Escherichia coli</i> (strain K12)	rpsM	36	49.15
P00393	NADH dehydrogenase <i>Escherichia coli</i> (strain K12)	ndh	89	35.94
Q2LS97	NADH-quinone	SYN_02139	90	12.7

oxidoreductase chain F

*Syntrophus aciditrophicus*

(strain SB)

POCE47	Elongation factor Tu 1	tufA	69	38.83
--------	------------------------	------	----	-------

*Escherichia coli* (strain  
K12)

POCE48	Elongation factor Tu 2	tufB	67	36.04
--------	------------------------	------	----	-------

*Escherichia coli* (strain  
K12)

POA951	Spermidine N(1)-	speG	31	50.54
--------	------------------	------	----	-------

acetyltransferase

*Escherichia coli* (strain  
K12)

POA7V0	30S ribosomal protein S2	rpsB	56	30.71
--------	--------------------------	------	----	-------

*Escherichia coli* (strain  
K12)

---

### **Partial purification of ferredoxin from *S. aciditrophicus* cell-free extracts**

To determine if purified recombinant HydAB is ferredoxin dependent, a protein fraction that contained *S. aciditrophicus* ferredoxin was obtained. After passage of *S. aciditrophicus* cell-free extracts through a DEAE Sepharose column, a dark brown band eluted at a concentration 0.62 M NaCl that contained ferredoxin. The ferredoxin-containing fraction had a 390/280

absorbance ratio of 0.082, which is much lower than the 390/280 absorbance ratio of 0.7 to 0.8 reported for other purified ferredoxins (Schonheit et al., 1978). Characterized ferredoxins have an extinction coefficient of  $30,000 \text{ cm}^{-1} \text{ M}^{-1}$  at 390 nm (Schonheit et al., 1978) suggesting that the concentration of the *S. aciditrophicus* ferredoxin fraction after ion exchange chromatography was  $3.7 \text{ }\mu\text{M}$  with a total protein concentration of  $0.25 \text{ mg}\cdot\text{ml}^{-1}$ . When the *S. aciditrophicus* ferredoxin fraction was subjected to peptide identification by mass spectroscopy, a large number of matches and high sequence coverage to the SYN\_03059 gene product (Table 7) were observed. SYN\_03059 annotates as ferredoxin with two [4Fe-4S] clusters with a predicted 6.01 kDa molecular weight and a pI of 3.63.

**Table 7. HPLC MS-MS Identification Results of Partially Purified *S. aciditrophicus* Ferredoxin Fraction.**

Swissprot ID	Protein Description	Gene Name	Number of Matches to Gene Product	Protein Sequence Coverage (%)
Q2LUB2_SY	Ferridoxin	SYN_03059	24	98.31
NAS	<i>Syntrophus aciditrophicus</i> (strain SB)			

Q2LR25_SY	DNA-binding	SYN_01724	35	27.47
NAS	protein HU			
	<i>Syntrophus</i>			
	<i>aciditrophicus</i>			
	(strain SB)			
ACP_SYNAS	Acyl carrier	acpP	12	11.25
	protein <i>Syntrophus</i>			
	<i>aciditrophicus</i>			
	(strain SB)			
Q2LU87_SY	Hypothetical	SYN_02004	11	13.98
NAS	cytosolic protein			
	<i>Syntrophus</i>			
	<i>aciditrophicus</i>			
	(strain SB)			
Q2LSB7_SY	Iron only	SYN_01370	59	21.32
NAS	hydrogenase large			
	subunit <i>Syntrophus</i>			
	<i>aciditrophicus</i>			
	(strain SB)			
Q2LWS6_SY	Glycine cleavage	gcvH	22	16.28
NAS	system H protein			
	<i>Syntrophus</i>			



	short-chain specific <i>Syntrophus</i> <i>aciditrophicus</i> (strain SB)			
Q2LXH8_SY	ABC-type	SYN_00365	15	10.33
NAS	nitrate/sulfonate/bi carbonate transport systems_ periplasmic components <i>Syntrophus</i> <i>aciditrophicus</i> (strain SB)			
Q2LUY7_SY	Glutaconyl-CoA decarboxylase A subunit <i>Syntrophus</i> <i>aciditrophicus</i> (strain SB)	SYN_00481	15	7.97
Q2LWR8_SY	Acetyl-CoA synthetase <i>Syntrophus</i>	SYN_02635	20	9.91



*aciditrophicus*

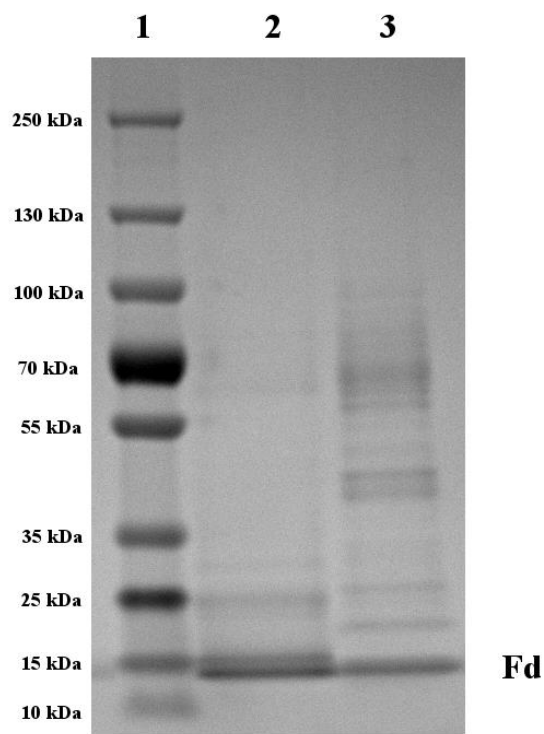
(strain SB)

---

### **Purification of *S. aciditrophicus* ferredoxin recombinantly produced in *E. coli***

The SYN\_03059 gene product was recombinantly produced and purified from *E. coli* cell-free extracts. The protein was eluted with an imidazole concentration of 250 mM during nickel affinity chromatography and had a dark brown color characteristic of iron sulfur proteins. The 390/280 absorbance ratio of the nickel affinity-purified fraction was 0.63 with an estimated ferredoxin concentration of 34  $\mu\text{M}$  based on the extinction coefficient at 390 nm for clostridial ferredoxin of  $30,000 \text{ cm}^{-1} \text{ M}^{-1}$  and a molecular weight of 6,000 daltons (Hong and Rabinowitz 1970). SDS-PAGE analysis of the fractions containing ferredoxin partially purified from *S. aciditrophicus* and ferredoxin recombinantly produced in *E. coli* indicated bands migrating closer to predicted molecular masses of 12 kDa (Figure 14). Negatively charged ferredoxins have been reported to exhibit anomalous migration during SDS-PAGE analysis, which has been proposed to be due to the interactions of the negatively charged peptide and SDS micelles (Darimont and Sterner, 1994; Huang et al., 2016; Kpebe et al., 2018).

**Figure 14. SDS-PAGE of Recombinantly Produced *S. aciditrophicus* Ferredoxin from *E. coli* and Ferredoxin Partially Purified from *S. aciditrophicus*.** Lane 1. molecular weight markers; Lane 2. nickel affinity purified recombinant SYN\_03059 gene product; Lane 3. partially purified ferredoxin fraction from *S. aciditrophicus*.

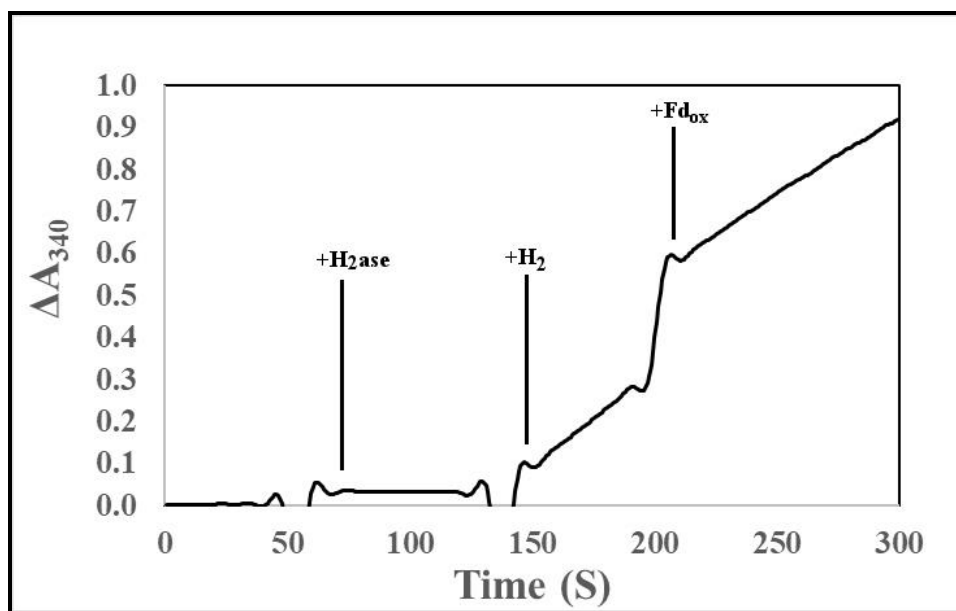


### **Enzyme activities of the purified recombinant *S. aciditrophicus* HydAB**

The purified recombinant HydAB was capable of reducing methyl viologen (specific activity of  $13.0 \text{ U} \cdot \text{mg}^{-1}$  at  $37^\circ\text{C}$ ) and  $\text{NAD}^+$  (specific activity of  $4.75 \text{ U} \cdot \text{mg}^{-1}$  at  $37^\circ\text{C}$ ) with hydrogen as the electron donor (Table 8). Characterized electron-bifurcating hydrogenases

require the addition of oxidized ferredoxin before reduction of  $\text{NAD}^+$  occurs (Schuchmann and Muller, 2012; Wang et al., 2013a). In contrast, the rate of  $\text{NAD}^+$  reduction by purified recombinant *S. aciditrophicus* HydAB was not affected by the presence of oxidized ferredoxin (Figure 15). The change in absorbance ( $\Delta A_{340}$ ) in the absence of ferredoxin was  $0.275 \text{ A} \cdot \text{min}^{-1}$  which was similar to the change in absorbance in the presence of clostridial ferredoxin  $0.23 \text{ A} \cdot \text{min}^{-1}$ . The specific  $\text{NAD}^+$  reduction activity of HydAB was  $4.75 \text{ U} \cdot \text{mg}^{-1}$  of protein in the absence of ferredoxin and was  $3.78 \text{ U} \cdot \text{mg}^{-1}$  of protein in the presence of the clostridial ferredoxin. The reduction of  $\text{NADP}^+$  by purified recombinant HydAB was not observed either in presence or the absence of clostridial ferredoxin. In addition, neither clostridial ferredoxin nor the recombinantly produced *S. aciditrophicus* ferredoxin was reduced by HydAB in either the presence or absence of  $\text{NAD}^+$  (Table 8). The dependence of  $\text{NAD}^+$  reduction on the presence of *S. aciditrophicus* ferredoxin produced recombinantly in *E. coli* was tested only in a single assay and not in triplicate.  $\text{NAD}^+$  reduction before the addition of recombinantly produced *S. aciditrophicus* ferredoxin was  $1.61 \text{ U} \cdot \text{mg}^{-1}$  at  $37^\circ\text{C}$ . After the addition of recombinantly produced *S. aciditrophicus* ferredoxin the rate was  $1.65 \text{ U} \cdot \text{mg}^{-1}$  at  $37^\circ\text{C}$ .

**Figure 15. The Reduction of NAD<sup>+</sup> by HydAB is not Ferredoxin Dependent.** The reaction was performed in 1.5-ml. stopper-sealed cuvettes with 50 mM potassium phosphate (pH 7.5), 5  $\mu$ M FMN, 5  $\mu$ M FAD, 2 mM dithioerythritol, and 1 mM NAD<sup>+</sup> and 8.1  $\mu$ g of purified recombinant HydAB as indicated by +H<sub>2</sub>ase. The reaction was started with the addition of H<sub>2</sub>. Clostridial ferredoxin was added at a concentration of 10  $\mu$ M as indicated by +Fd<sub>ox</sub>. The rate of reduction of NAD ( $\Delta A_{340}$ ) after the addition of hydrogen (0.275  $\Delta A \cdot \text{min}^{-1}$ ) was similar to the change after the addition of clostridial ferredoxin (0.23  $\Delta A \cdot \text{min}^{-1}$ ).



HydAB produced hydrogen from methyl viologen reduced by dithionite (specific activity of 0.42 U $\cdot$ mg<sup>-1</sup> at 37°C) and from NADH (specific activity of 0.027 U $\cdot$ mg<sup>-1</sup>) (Table 8). In contrast to known electron-bifurcating hydrogenases (Schut and Adams, 2009; Schuchmann and Muller, 2012; Wang et al., 2013c), the specific rate of hydrogen production from NADH was not enhanced by the presence of reduced ferredoxin-generating system consisting of clostridial

pyruvate:ferredoxin oxidoreductase, pyruvate, and clostridial ferredoxin (Table 8). The specific hydrogen production rate by HydAB was  $0.014 \text{ U} \cdot \text{mg}^{-1}$  with reduced clostridial ferredoxin generating system compared to  $0.027 \text{ U} \cdot \text{mg}^{-1}$  without the reduced ferredoxin-generating system. The maximum observed hydrogen production rate in the absence of the reduced ferredoxin-generating system was  $1.5 \text{ nanomol} \cdot \text{min}^{-1}$  (Figure 16) compared to a maximum observed hydrogen production rate of  $0.6 \text{ nanomol} \cdot \text{min}^{-1}$  in the presence of the reduced ferredoxin generating system rate (Figure 17). The use of recombinantly produced *S. aciditrophicus* ferredoxin (specific activity of  $0.018 \text{ U} \cdot \text{mg}^{-1}$ ) or ferredoxin partially purified from *S. aciditrophicus* cell-free extracts as part of the reduced ferredoxin generating system did not enhance hydrogen production activity compared to that in the absence of the reduced ferredoxin-generating system (Table 8). Due to the limited yield of *S. aciditrophicus* ferredoxin that was recovered during the partial purification from *S. aciditrophicus* cell-free extracts, only a single hydrogen production assay was performed. In the presence of NADH and reduced ferredoxin partially purified from the *S. aciditrophicus* the maximal hydrogen production was specific activity of  $0.013 \text{ U} \cdot \text{mg}^{-1}$ . The results indicated that regardless of the reduced ferredoxin source (clostridial, recombinantly produced *S. aciditrophicus* ferredoxin or *S. aciditrophicus* ferredoxin partially purified from *S. aciditrophicus* cell-free extracts), no enhancement of hydrogen production rate was observed.

**Table 8. Specific Activities of Purified Recombinant HydAB.** <sup>a</sup> Assays were performed at 37 °C and a pH of 7.5; 1 unit of activity (U) equals 2  $\mu\text{mol}$  of electrons transferred per min.

<sup>b</sup> The activity was measured as the rate of  $\text{NAD}^+$  reduction ( $\Delta 340 \text{ nm}$ ) in the presence of  $\text{Fd}_{\text{ox}}$ , and not the rate of  $\text{Fd}_{\text{ox}}$  reduction ( $\Delta 430 \text{ nm}$ ), which was not observed to occur.

<sup>c</sup>Syntrophus Fd<sub>red</sub> refers to recombinantly produced *S. aciditrophicus* ferredoxin. Clostridial Fd<sub>red</sub> refers to ferredoxin purified from *C. pasteurianum*.

Reaction	Hydrogenase Activity (U/mg) <sup>a</sup>
$H_2 \rightarrow MV_{ox}$	13.0
$H_2 \rightarrow NAD^+$	4.75
$H_2 \rightarrow NAD^+ + \text{Clostridial Fd}_{ox}$	3.78
$H_2 \rightarrow NADP^+$	<0.01
$H_2 \rightarrow NADP^+ + \text{Clostridial Fd}_{ox}$	<0.01
$H_2 \rightarrow \text{Clostridial Fd}_{ox}$	<0.01
$MV_{red} \rightarrow H_2$	0.42
$NADH \rightarrow H_2$	0.027
$NADH + \text{Clostridial Fd}_{red} \rightarrow H_2$	0.014
$NADH + \text{Syntrophus Fd}_{red} \rightarrow H_2$	0.018
$\text{Clostridial Fd}_{red} \rightarrow H_2$	<0.001

**Figure 16. Production of Hydrogen from NADH by HydAB in the Presence of Reduced Ferredoxin Generating System.** Each assay was performed in a 6.5-ml serum bottle containing 1.0 ml of 50 mM Tris (pH 7.5) with 2 mM DTE, 5  $\mu$ M FAD, 5  $\mu$ M FMN, 25.4  $\mu$ g HydAB, and a reduced ferredoxin-generating system consisting of 0.1 unit of pyruvate ferredoxin oxidoreductase, 20  $\mu$ m clostridial ferredoxin, 10 mM pyruvate, 0.1 mM thiamine pyrophosphate, and 1 mM CoA. The reduced ferredoxin-generating system and HydAB were as added as

indicated by +Fd<sub>red</sub> and H<sub>2</sub>ase, respectively. NADH was added to a final concentration of 1 mM as indicated by +NADH. The maximal rate of hydrogen production in the depicted assay was 24.6 nanomoles min<sup>-1</sup>•mg<sup>-1</sup>.

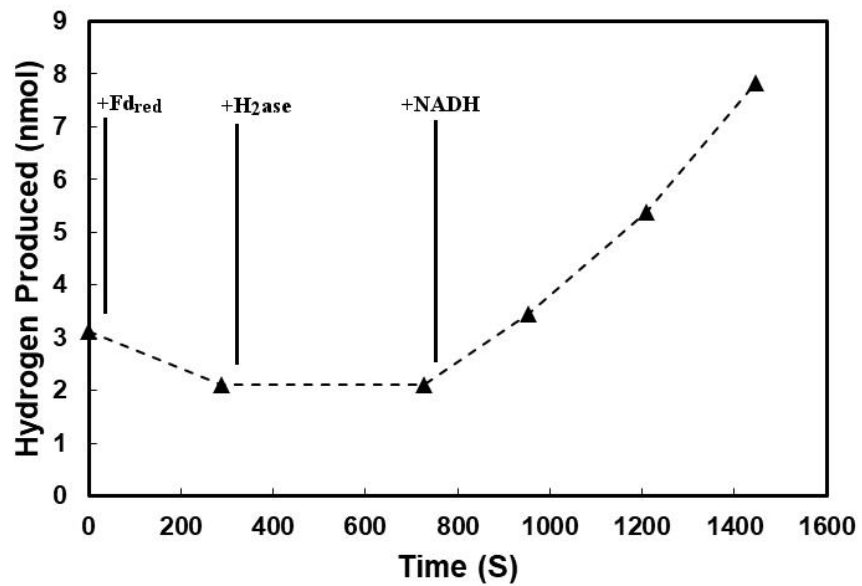
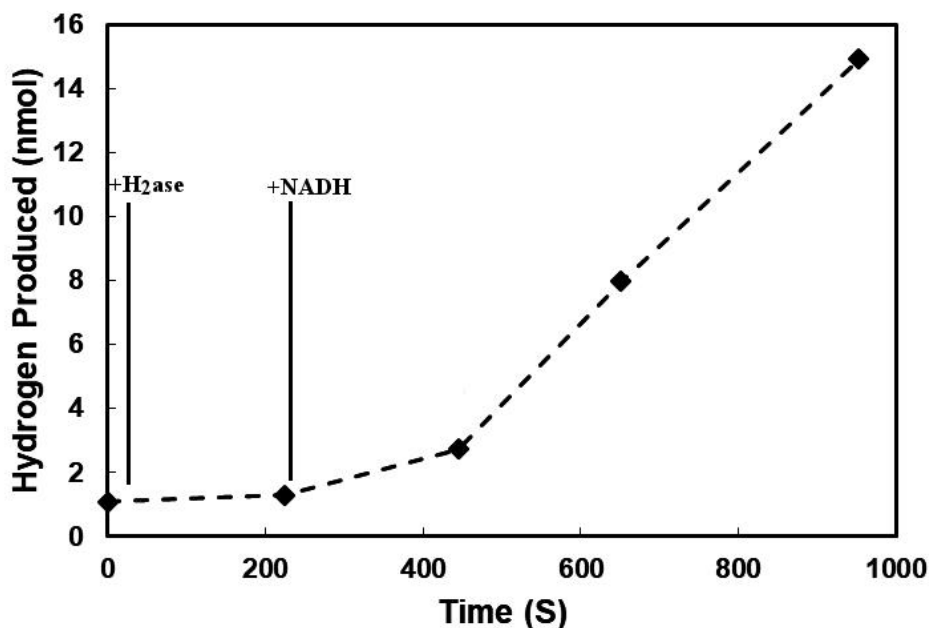


**Figure 17. Production of Hydrogen from NADH by HydAB Independent of Reduced**

**Ferredoxin.** Enzyme assay was performed in a 6.5-ml serum bottle containing 1.0 ml of 50 mM Tris (pH 7.5) with 2 mM DTE, 5  $\mu$ M FAD, 5  $\mu$ M FMN, 50.7  $\mu$ g HydAB (+H<sub>2</sub>ase). NADH was added to a final concentration of 1 mM (+NADH). The maximal rate of hydrogen production in the enzyme assay reaction depicted was 30.1 nanomoles min<sup>-1</sup>•mg<sup>-1</sup>



Equilibrium hydrogen partial pressures produced by HydAB varied with the NADH/NAD<sup>+</sup> ratio (Table 9), ranging from 40.17 ( $\pm$  3.2) pascals with a NADH/NAD<sup>+</sup> ratio of 5.0 to 2.2 ( $\pm$  0.4) pascals at a NADH/NAD<sup>+</sup> ratio of 0.2. These values are much lower than the equilibrium hydrogen partial pressures produced by electron bifurcating hydrogenases of 1,000 Pa at equilibrium (equivalent to E' = -365 mV). Higher hydrogen partial pressures were observed at higher NADH/NAD<sup>+</sup> ratios; however, hydrogen partial pressures never reached the thermodynamically predicted equilibrium pressures for the given NADH/NAD<sup>+</sup> ratio at pH 7.5



(see Table 9). A small amount of hydrogen was observed in the absence of NADH addition, which was likely due to carryover from manipulation of the enzyme inside the anaerobic chamber that contained hydrogen in the atmosphere.

Hydrogen partial pressures observed during the metabolism of crotonate, cyclohex-1-ene-1- carboxylate, and benzoate by pure cultures of *S. aciditrophicus* ranged from 8.3 to 36.6 pascals (Figure 18). Hydrogen partial pressures observed during crotonate, cyclohex-1-ene-1- carboxylate, and benzoate metabolism by cocultures of *S. aciditrophicus* with *M. hungatei* were between 6.6 and 19.1 pascals. Hydrogen partial pressures after 3 days of incubation continued to increase in pure cultures of *S. aciditrophicus* on benzoate and cyclohex-1-ene carboxylate while hydrogen partial pressures decreased after 3 days in cocultures on all three substrates. The hydrogen partial pressures produced by pure cultures and cocultures of *S. aciditrophicus* metabolizing crotonate, cyclohex-1-ene-1- carboxylate, and benzoate (6.6 to 36.6 pascals) could be generated by HydAB operating at NADH/NAD<sup>+</sup> ratios of 1.0 or higher (9.1 to 40.2 pascals).

**Table 9. Equilibrium Hydrogen Concentrations Produced by NADH-Dependent [FeFe]-Hydrogenase, HydAB with Varied NADH/NAD<sup>+</sup> ratios.**

Condition <sup>a</sup>	Ratio of NADH/NAD <sup>+</sup>	Predicted Equilibrium Hydrogen Partial Pressure	Hydrogen Partial Pressure (Pa)	Hydrogen Produced (nanomol)
------------------------	-----------------------------------	--	-----------------------------------	-----------------------------------

		(Pa) <sup>d</sup>		
1.0 mM NAD <sup>+</sup> +	5.0	105.9	40.2 ± 3.2	101.8 ± 8.1
5.0 mM NADH				
3.0 mM NAD <sup>+</sup> +	1.0	21.3	9.1 ± 2.4	23.2 ± 6.0
3.0 mM NADH				
5.0 mM NAD <sup>+</sup> +	0.2	4.24	2.2 ± 0.4	5.4 ± 1.1
1.0 mM NADH				
0.0 mM NAD <sup>+</sup> +	NA <sup>c</sup>	NA	0.4 ± 0.2	1.0 ± 0.6
0.0 mM NADH				

<sup>a</sup> Assays were performed at pH 7.5 in 6.5-mL serum bottles with 1.0 mL of liquid volume containing 69.6 µg of HydAB and 5.5 mL of headspace.

<sup>b</sup> Values are the mean ± the standard deviation of triplicate assays.

<sup>c</sup> NA, not applicable.

<sup>d</sup> The predicted equilibrium concentrations of hydrogen were calculated as described by (Gutekunst and Schulz, 2018). Equation and terms used were:

$$e^{((-0.094 \cdot n \cdot F)/(R \cdot T))} \cdot [\text{NADH}/\text{NAD}^+] \cdot 10^{-(\text{pH} + 7)} = [\text{pH}_2]$$

Faraday's constant =  $F = 96.485 \text{ J} \cdot \text{V}^{-1} \cdot \text{mol}^{-1}$  of electron equivalents

$R = 8.314 \text{ J} \cdot \text{K} \cdot \text{mol}^{-1}$  Gas Constant

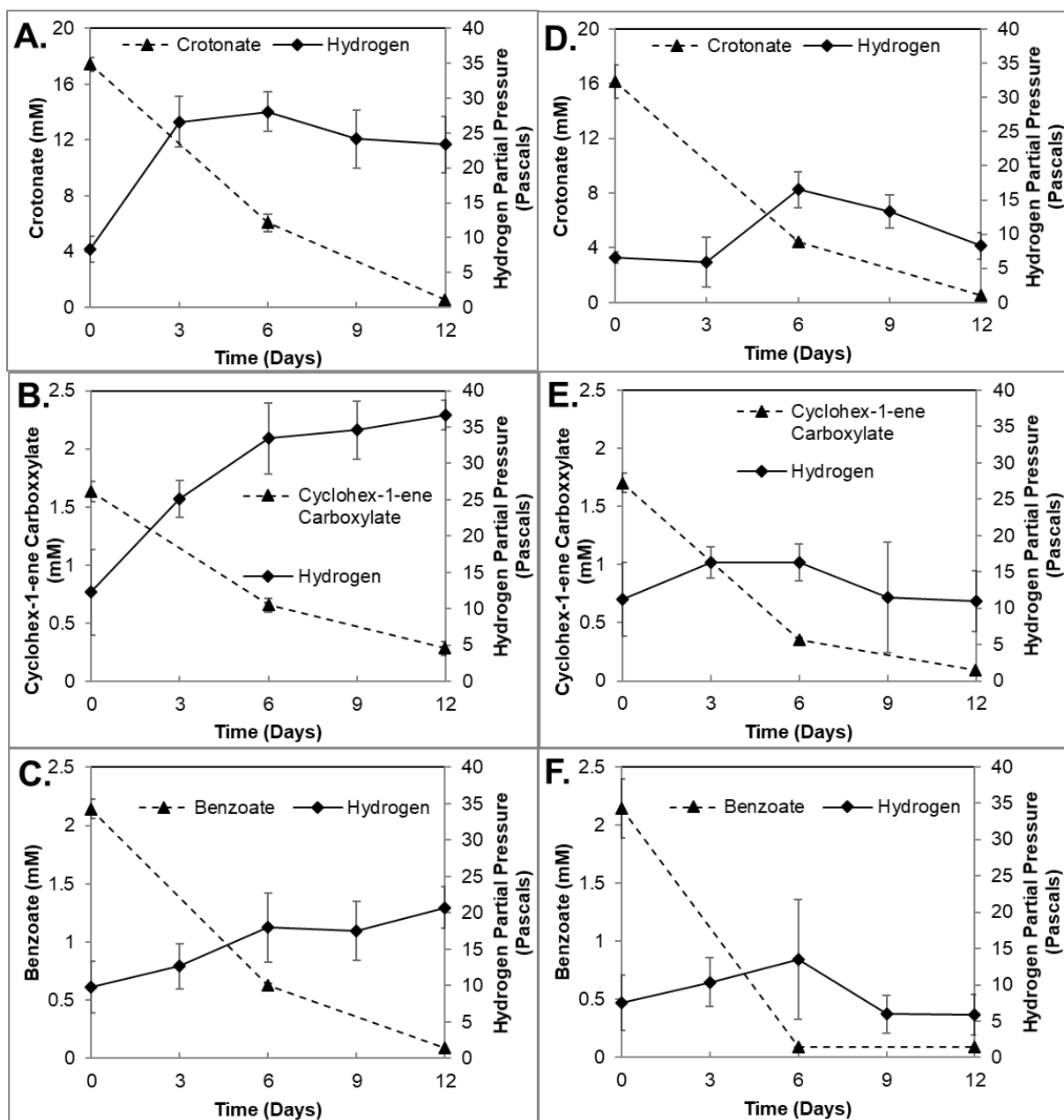
$n = 2$ , number of  $e^-$  in transfer reaction

$T = 298.15$  Kelvin

$[\text{pH}_2]$  = Partial pressure of hydrogen

$-0.094 = \Delta E'$ , difference in standard reduction potentials of  $[H^+/H_2] = -414 \text{ mV}$  and  $[NADH/NAD^+] = -320 \text{ mV}$

**Figure 18. Hydrogen Partial Pressures During the Metabolism of Crotonate, Cyclohex-1-ene-1-carboxylate, and Benzoate by Pure Cultures of *S. aciditrophicus* and Co-cultures of *S. aciditrophicus* with *Methanospirillum hungatei*.** Panels A, B and C: hydrogen and substrate concentrations for metabolism of crotonate (A), cyclohex-1-ene carboxylate (B), and benzoate (C) by pure cultures of *S. aciditrophicus*. Panels D, E, and F: hydrogen and substrate concentrations during the metabolism of crotonate (D), cyclohex-1-ene carboxylate (E), and benzoate (F) by co-cultures of *S. aciditrophicus* with *M. hungatei*.



## Discussion

The results from the enzymatic assays show that HydAB from *S. aciditrophicus* is a NADH-dependent, ferredoxin-independent, dimeric [FeFe]-hydrogenase. HydAB functions in a similar manner as the NADH-dependent ferredoxin-independent [FeFe]-hydrogenase of *S. wolfei*, Hyd1ABC (Losey et al., 2017). Both enzymes function independently of ferredoxin to

produce hydrogen from NADH, as well as the reverse reaction, the reduction of NAD<sup>+</sup> coupled to hydrogen oxidation. The lack of ferredoxin dependence by these enzymes may be the evolutionary outcome unique to syntrophy (i. e., growth at very low hydrogen partial pressures). A NADH-dependent, ferredoxin-independent [FeFe]-hydrogenase provides both organisms with an efficient mechanism for hydrogen production without expending energy from a membrane gradient to generate reduced ferredoxin needed for electron bifurcation. These results are consistent with the known physiological properties of the syntrophic fatty acid oxidizer, *S. wolfei*, which lacks a system capable of generating sufficient amounts of reduced ferredoxin for NADH oxidation and does not have large amounts of ferredoxin (Losey et al., 2017). However, the result is somewhat surprising for *S. aciditrophicus* where ferredoxin (Table 7) and a reduced ferredoxin generating system in the form of the Rnf complex (McInerney et al., 2007) are both present. In addition to genomic evidence for the Rnf complex, experiments with inverted membrane vesicles of *S. aciditrophicus* have demonstrated Rnf activity (reduction of ferredoxin coupled to NADH oxidation dependent on a membrane gradient generated by ATP synthase, M. J. McInerney and N. Q. Wofford, unpublished results). Also, *S. aciditrophicus* has a clostridial like, negatively charged, low molecular weight ferredoxin that can be enriched by anion-exchange chromatography (Figure 14). The *S. aciditrophicus* ferredoxin is predicted to harbor two [4Fe4S]-clusters, as do other ferredoxins that have been used as low potential electron donors for the study of electron-bifurcating hydrogenases (Schut and Adams, 2009; Schuchmann and Muller, 2012; Wang et al., 2013c). It appears that, unlike *S. wolfei*, *S. aciditrophicus* has a mechanism for producing reduced ferredoxin but does not utilize it when producing hydrogen from NADH. This may suggest that ferredoxin-independent, hydrogen production from NADH is a more prevalent strategy than previously thought and may afford some advantage during

syntrophic metabolism. The likely function of the Rnf complex in *S. aciditrophicus* is to provide reduced ferredoxin for benzoyl-CoA reduction and certain biosynthetic reactions (McInerney et al., 2007; Fuchs et al., 2011; Kung et al., 2013).

Pure cultures of *S. aciditrophicus* and co-cultures of *S. aciditrophicus* with *M. hungatei* generated hydrogen partial pressures of 5.9 to 36.6 pascals (Figure 18), which is within the range of the hydrogen partial pressures (2.2 to 40.2 pascals) generated by the purified, recombinant *S. aciditrophicus* HydAB at NADH/NAD<sup>+</sup> ratios of 1 to 5 (Table 9). Thus, ferredoxin-independent, hydrogen production from NADH by HydAB can explain the hydrogen partial pressures observed during the metabolism of crotonate, benzoate, and cyclohex-1-ene by *S. aciditrophicus* but with the requirement of maintaining an intracellular NADH/NAD<sup>+</sup> ratio greater than one. Syntrophic metabolizers are known to require low hydrogen partial pressures for growth and metabolism (Sieber et al., 2012). The use of a ferredoxin-independent, NADH-dependent [FeFe]-hydrogenase would require continual hydrogen use by another microorganism to allow for continual hydrogen production from NADH and could explain, in part, the obligate requirement that *S. aciditrophicus* and *S. wolfei* have for a hydrogen-consuming organism during growth on substrates such as fatty and alicyclic acids. It should be noted that the pure culture metabolism of benzoate is dependent on the transfer of small amounts of crotonate with inoculum (Moultaki et al., 2008), which likely occurred in the cultures used to for these hydrogen measurements.

Despite having similar functions, NADH-dependent ferredoxin-independent hydrogen production, the subunit composition of *S. aciditrophicus* HydAB differs from that of *S. wolfei* Hyd1ABC. The *S. wolfei* Hyd1ABC is a  $\alpha\beta\gamma$  heterotrimeric complex with a molecular weight of ~120 kDa (Losey et al., 2017) while the *S. aciditrophicus* HydAB is a dimer of an  $\alpha\beta$  heterodimer with a molecular weight of ~ 280 kDa (Figure 13). A BLASTP comparison showed

a high homology (37% amino acid sequence identity) between the *S. wolfei* gamma subunit (Hyd1C) and the N-terminal portion (amino acid residues 15 to 152) of the *S. aciditrophicus* beta subunit (HydB). Another BLASTP comparison showed high homology (46% amino acid sequence identity) between the *S. wolfei* beta subunit (Hyd1B) to the C-terminal portion of the *S. aciditrophicus* beta subunit (HydB) (amino acid residues 177 to 585). These data indicate that the *S. aciditrophicus* beta subunit is a fusion of the smaller gamma subunit at the N-terminal portion of the peptide sequence to a beta subunit at the C-terminus (See Figure 19). A similar peptide fusion was reported in a multimeric NADH-dependent formate dehydrogenase (Laukel et al., 2003). A BLASTP comparison indicated that the fused beta subunit from this NADH-dependent formate dehydrogenase shared similarity (32% amino acid sequence identity) to the *S. aciditrophicus* [FeFe]-hydrogenase beta subunit. The differences in the beta subunits of the *S. aciditrophicus* [FeFe]-hydrogenase and *S. wolfei* [FeFe]-hydrogenase demonstrate that there are multiple arrangements of ferredoxin-independent, NADH-dependent [FeFe]-hydrogenases depending on the source organism (see Figure 19).

In addition to the *S. wolfei* and *S. aciditrophicus* [FeFe]-hydrogenases, two additional [FeFe]-hydrogenases were originally described to reduce NAD(P)<sup>+</sup>, in a manner that did not involve electron-bifurcation or require ferredoxin. The first [FeFe]-hydrogenase from *Desulfovibrio fructosovorans* was originally described to reduce NADP<sup>+</sup> using hydrogen (Malki et al., 1995). However, a more recent study where the [FeFe]-hydrogenase was purified and characterized, indicated the enzyme is an electron-bifurcating enzyme, simultaneously reducing both ferredoxin and NADH when oxidizing hydrogen (Kpebe et al., 2018). The other [FeFe]-hydrogenase, from *Caldanaerobacter tencongensis*, was reported to be capable of producing hydrogen from NADH and the reduction of NAD<sup>+</sup> with hydrogen (Soboh et al., 2004). A



subsequent study where the *C. tencongensis* [FeFe]-hydrogenase was expressed heterologously in *E. coli* suggested that the enzyme requires reduced ferredoxin to produce hydrogen (Kelly et al., 2015), which indicates an electron-bifurcating mechanism. Therefore, we note that the only two prior examples of [FeFe]-hydrogenases reducing NAD<sup>+</sup> or NADP<sup>+</sup> in a ferredoxin-independent manner have been found later to be electron-bifurcating, ferredoxin-dependent enzymes. The *S. wolfei* and *S. aciditrophicus* [FeFe]-hydrogenases are the only known examples of NADH-dependent, ferredoxin-independent [FeFe]-hydrogenases. We therefore focused on finding structural features that differentiate the *S. wolfei* and *S. aciditrophicus* NADH-dependent, ferredoxin-independent [FeFe]-hydrogenases from the six known electron-bifurcating, NADH-dependent, ferredoxin-dependent [FeFe]-hydrogenases. As discussed below, we believe that differences in the composition of the beta subunit are key to determining whether the enzyme is or is not electron-bifurcating.

### **Comparison of NADH-dependent, Ferredoxin-Independent Enzymes to Electron Bifurcating, NADH-Dependent, Ferredoxin Dependent [FeFe]-Enzymes**

We compared a group of NADH-dependent, ferredoxin-independent enzymes against a group of the known examples of electron-bifurcating NADH-dependent, ferredoxin-dependent formate dehydrogenases and [FeFe]-hydrogenases. In addition to the *S. wolfei* and *S. aciditrophicus* [FeFe]-hydrogenases, the NADH-dependent, ferredoxin-independent enzymes included NADH-dependent, ferredoxin-independent formate dehydrogenases and NADH:ubiquinone oxidoreductase subunits, Nqo1, Nqo2, and Nqo3. These enzymes share similar properties, the oxidation or reduction of NADH in a ferredoxin-independent manner. The

two groups, ferredoxin-dependent and ferredoxin-independent, were then compared to identify the features that may account for the difference in the requirement for ferredoxin.

### **NADH-Dependent, Ferredoxin-Independent Formate Dehydrogenases**

For this analysis, other ferredoxin-independent enzymes with a composition similar to NADH-dependent, ferredoxin-independent [FeFe]-hydrogenases were needed. One group of enzymes included five formate dehydrogenases that had been previously purified and characterized as NADH-dependent formate dehydrogenases. We suggest that it may be more appropriate that they be referred to as NADH-dependent and ferredoxin-independent formate dehydrogenases. This is to indicate that they are capable of formate oxidation coupled to the reduction of NADH without requiring ferredoxin. The distinction of ferredoxin-independence is important as there is at least one example of an electron-bifurcating formate dehydrogenase (Wang et al., 2013c) that utilizes both NADH and ferredoxin simultaneously. These NADH-dependent, ferredoxin-independent formate dehydrogenases were purified from *Cupriavidus oxalaticus*, (previously *Psuedomonas oxalaticus*) (Ruschig et al., 1976; Muller et al., 1978), *Methylosinus trichosporium* (Jollie and Lipscomb, 1991), *Cupriavidus eutropha*, (previously *Alcaligenes eutropha*) (Friedebold and Bowien, 1993), *Methylobacterium extorquens* (Laukel et al., 2003), and *Rhodobacter capsulatus* (Hartmann and Leimkühler, 2013). With the exception of the *R. capsulatus* formate dehydrogenase, these enzymes were characterized before the first published examples of electron-bifurcating formate dehydrogenases (Wang et al., 2013b) and [FeFe]-hydrogenases (Schut and Adams, 2009), and as such the possibility of electron bifurcation was not recognized or tested. These five NADH-dependent, ferredoxin-independent formate dehydrogenases were reported to be oxygen tolerant and purified from organisms

capable of growth under aerobic conditions. In contrast, all electron-bifurcating formate dehydrogenases and [FeFe]-hydrogenases have been purified from strict anaerobes (Soboh et al., 2004; Schut and Adams, 2009; Schuchmann and Muller, 2012; Wang et al., 2013a; Wang et al., 2013c; b; Zheng et al., 2014; Kpebe et al., 2018). The role of the NADH-dependent, ferredoxin-independent formate dehydrogenases is proposed to be the generation of reduced NADH for aerobic respiration in *C. oxalaticus* (Muller et al., 1978), *C. eutropha* (Friedebold and Bowien, 1993), *M. trichosporium* (Friedebold and Bowien, 1993) and *M. extorquens* (Laukel et al., 2003). It was not stated what the proposed physiological role of the *R. capsulatus* formate dehydrogenase was in the source organism (Hartmann and Leimkühler, 2013), although *R. capsulatus* is capable of aerobic respiration (Zannoni, 1995). In contrast to the proposed role of the NADH-dependent, ferredoxin-independent formate dehydrogenases as a source of reduced NADH, we propose the opposite role for the NADH-dependent, ferredoxin-independent [FeFe]-hydrogenases from *S. wolfei* and *S. aciditrophicus*, where instead the physiological role is NADH oxidation.

The oxygen tolerant nature of the NADH-dependent, ferredoxin-independent formate dehydrogenases is likely due to the use of of cysteine as a ligand to the metallopterin at the active site as opposed to a selenocysteine (Hartmann and Leimkühler, 2013). The replacement of a selenocysteine with a cysteine in the *E. coli* FdhF resulted in a less active enzyme (Axley et al., 1991). However, formate dehydrogenases with a selenocysteine ligand are rapidly inactivated by oxygen as opposed to cysteine-ligand versions (Ferry, 1990). Furthermore, it was observed that, in the presence of oxygen, an electron bifurcating butyryl-CoA dehydrogenase generated superoxide and hydrogen peroxide as byproducts (Chowdhury et al., 2015). This suggests that operation of flavin-dependent electron-bifurcating enzymes in the presence of oxygen can

produce toxic, reactive oxygen compounds (Buckel and Thauer, 2018b). It could be argued that it is unlikely that oxygen-tolerant, NADH-dependent, ferredoxin-independent formate dehydrogenases have an unrecognized electron-bifurcation mechanism, as such a mechanism would produce reactive oxygen compounds that would be toxic to aerobic organisms. However, recent evidence that the FixABCX complex from *Azotobacter vinelandii* performs electron bifurcation under aerobic conditions suggests electron-bifurcating enzymes are not restricted to anaerobes (Ledbetter et al., 2017). Despite incomplete experimental testing of the ability for electron-bifurcation, all current evidence suggests that the oxygen-tolerant, NADH-dependent formate dehydrogenases are ferredoxin-independent. Therefore, these five NADH-dependent, ferredoxin-independent formate dehydrogenases were included in the group of NADH-dependent, ferredoxin-independent enzymes along with the *S. wolfei* and *S. aciditrophicus* [FeFe]-hydrogenases.

### **NADH:Quinone Oxidoreductase Subunits Nqo1, Nqo2, and Nqo3**

Sequence homology between the group of NADH-dependent, ferredoxin-independent formate dehydrogenase and the Nqo1, Nqo2, and Nqo3 (NADH:Quinone oxidoreductase) subunits that comprise the hydrophilic portion of Respiratory Complex I has been discussed extensively (Pilkington et al., 1991; Sazanov and Hinchliffe, 2006; Sieber et al., 2010). This portion of complex I (Nqo1-3) functions to transfer electrons from NADH to the remainder of Respiratory Complex I (Nqo4-15) (Sazanov and Hinchliffe, 2006). Sequence homology suggests that Nqo1, Nqo2, and Nqo3 are analogous to the beta, gamma, and alpha subunits of the NADH-dependent, ferredoxin-independent formate dehydrogenases respectively (Hille et al., 2014). Due to this homology, we included the Nqo1-Nqo3 subunits from *T. thermophilus* and the equivalent

*E. coli* NADH:Ubiquinone oxidoreductase subunits (NuoEFG) as the final members of the group of NADH-dependent, ferredoxin-independent enzymes.

### **Electron-Bifurcating [FeFe]-Hydrogenases and Formate Dehydrogenases**

Electron-bifurcating, NADH- and ferredoxin-dependent enzymes include the [FeFe]-hydrogenases from *Thermotoga martima* (Schut and Adams, 2009), *Acetobacterium woodii* (Schuchmann and Muller, 2012), *Moorella thermoacetica* (Wang et al., 2013c), *Ruminococcus albus* (Zheng et al., 2014), *D. fructosovorans* (Kpebe et al., 2018), and *C. tengcongensis* (Soboh et al., 2004). In addition, there is an electron-bifurcating NADH- and ferredoxin-dependent formate dehydrogenase from *Clostridium acidurici* (Wang et al., 2013b) and a NADPH- and a ferredoxin-dependent [FeFe]-hydrogenase-formate dehydrogenase complex from *Clostridium autoethanogenum* (Wang et al., 2013a). The NADPH- and ferredoxin-dependent [FeFe]-hydrogenase-formate dehydrogenase complex consists of seven subunits; some of these subunits do not appear to have equivalents in any of the other electron-bifurcating enzymes.

**Figure 19. Differences in Cofactor Binding Sites between Electron-Bifurcating, NADH-Dependent and Ferredoxin-Dependent Enzymes and NADH-Dependent, Ferredoxin-Independent Enzymes.** Cofactor binding sites are shown as orientated from the N-terminal to C-terminal portion of the subunits. Dashed boxes indicate subunits that are fused together into a single polypeptide chain. Image depiction is not scaled to accurately reflect number of amino acids in each subunit. Nqo2/NuoE is homologous to the gamma subunits. Nqo1/NuoF is homologous to the beta subunit, and Nqo3/NuoG is homologous to the alpha subunit. Only a small region of 200 residues, predicted to bind a [2Fe-2S] cluster, and two [4Fe-4S], are

homologous between Nqo3, the alpha subunit of the formate dehydrogenases, and the alpha subunit of the [FeFe]-hydrogenases (Pilkington et al., 1991; Vignais et al., 2001; Sazanov and Hinchliffe, 2006) Delta subunits for the *A. woodii*, *C. tengcongensis*, *C. oxalaticus*, and *C. eutropha* are represented by an empty box, indicating that the subunits do not appear to have conserved domains predicted to bind cofactors.

Source Organism(s)	Reported Activity	$\alpha$	$\gamma$	$\beta$	$\delta$
<b>Electron Bifurcating [FeFe]-Hydrogenases/Formate Dehydrogenases</b>					
<i>T. maritima</i>	Bifurcating NADH/Fd Hydrogenase	2Fe-2S 4Fe-4S 4Fe-4S H-Cluster 2Fe-2S	2Fe-2S	2Fe-2S Flavin 4Fe-4S 4Fe-4S	
<i>A. woodii</i>	Bifurcating NADH/Fd Hydrogenase	2Fe-2S 4Fe-4S 4Fe-4S H-Cluster	2Fe-2S	2Fe-2S Flavin 4Fe-4S 4Fe-4S	
<i>M. thermoacetica</i>	Bifurcating NADH/Fd Hydrogenase	2Fe-2S 4Fe-4S 4Fe-4S H-Cluster	2Fe-2S	2Fe-2S Flavin 4Fe-4S 4Fe-4S	
<i>R. albus</i>	Bifurcating NADH/Fd Hydrogenase	2Fe-2S 4Fe-4S 4Fe-4S H-Cluster	2Fe-2S	2Fe-2S Flavin 4Fe-4S 4Fe-4S	
<i>C. tengcongensis</i>	Bifurcating NADH/Fd Hydrogenase*	2Fe-2S 4Fe-4S 4Fe-4S H-Cluster	2Fe-2S	2Fe-2S Flavin 4Fe-4S 4Fe-4S	
<i>C. acidurici</i>	Bifurcating NADH/Fd Formate Dehydrogenase	2Fe-2S 4Fe-4S 4Fe-4S 4Fe-4S Mo	2Fe-2S	2Fe-2S Flavin 4Fe-4S 4Fe-4S	
<i>D. fructosovorans</i>	Bifurcating NADH/Fd Hydrogenase*	2Fe-2S 4Fe-4S 4Fe-4S H-Cluster	2Fe-2S	Flavin 4Fe-4S 4Fe-4S	2Fe-2S
<b>NADH-Dependent, Ferredoxin-Independent Formate Dehydrogenases</b>					
<i>R. capsulatus</i>	NADH-dependent Formate Dehydrogenase	2Fe-2S 4Fe-4S 4Fe-4S 4Fe-4S Mo	2Fe-2S	Flavin 4Fe-4S	
<i>C. oxalaticus</i>	NADH-dependent Formate Dehydrogenase	2Fe-2S 4Fe-4S 4Fe-4S 4Fe-4S Mo	2Fe-2S	Flavin 4Fe-4S	
<i>M. trichosporum</i>	NADH-dependent Formate Dehydrogenase	2Fe-2S 4Fe-4S 4Fe-4S 4Fe-4S W	2Fe-2S	Flavin 4Fe-4S	
<b>NADH-Dependent, Ferredoxin-Independent [FeFe]-Hydrogenases</b>					
<i>S. acidotrophicus</i>	NADH-Dependent Hydrogenase	2Fe-2S 4Fe-4S 4Fe-4S H-Cluster	2Fe-2S	Flavin 4Fe-4S	
<i>S. wolfei</i>	NADH-Dependent Hydrogenase	2Fe-2S 4Fe-4S 4Fe-4S H-Cluster	2Fe-2S	Flavin 4Fe-4S	
<b>NADH-Quinone Oxidoreductase (Nqo1-Nqo3)</b>					
<i>T. thermophilus</i>	NADH-quinone Oxidoreductase	2Fe-2S 4Fe-4S 4Fe-4S	2Fe-2S	Flavin 4Fe-4S	

## Comparison of the Alpha and Gamma Subunits of the Electron-Bifurcating Enzymes to Those from the NADH-Dependent, Ferredoxin-Independent Enzymes

As shown in Figure 19, the alpha subunits of the electron-bifurcating [FeFe]-hydrogenases and the NADH-dependent, ferredoxin-independent *S. wolfei* and *S. aciditrophicus* [FeFe]-hydrogenases share similar predicted cofactor binding sites: a single [2Fe-2S]-cluster, three [4Fe-4S]-clusters and the catalytic [H-cluster]. The *T. maritima* alpha subunit differs from others in containing an additional [2Fe-2S] cluster. The alpha subunits of the NADH-dependent, ferredoxin-independent formate dehydrogenase are similar to the alpha subunit of the electron-bifurcating formate dehydrogenase from *C. aciditrophicus* and are predicted to contain: a single [2Fe-2S] cluster, four [4Fe-4S] clusters and a metallopterin cofactor binding site. The alpha subunits are apparently similar between the electron-bifurcating NADH-dependent, ferredoxin-independent formate dehydrogenases and [FeFe]-hydrogenases and the NADH-dependent, ferredoxin-independent formate dehydrogenase and [FeFe]-hydrogenases.

All of the compared enzymes regardless of ferredoxin dependence possess a similar gamma subunit that has a single [2Fe-2S] cluster (Figure 19). However, in the case of the *S. aciditrophicus* and the *M. extorquens* enzymes, it is proposed that the gamma subunit is fused to the N-terminal portion of the beta subunit. Based on the common presence of a gamma subunit between the ferredoxin-dependent and ferredoxin-independent enzymes, it is unlikely that the gamma subunit determines ferredoxin dependence.

In contrast to the alpha and gamma subunits, there are differences in the beta subunits between the electron-bifurcating NADH-dependent, ferredoxin-dependent [FeFe]-hydrogenases and formate dehydrogenases and the NADH-dependent, ferredoxin-independent formate dehydrogenases, [FeFe]-hydrogenase and the NADH dehydrogenase:ubiquinone oxidoreductase



(Figure 19). All beta subunits from the electron-bifurcating enzymes possess two [4Fe-4S] centers at the C-terminal portion of the protein that are not predicted to occur in any of the NADH-dependent, ferredoxin-independent enzymes. In addition, all of the beta subunits of the electron-bifurcating NADH-dependent, ferredoxin-dependent enzymes with the exception of the *D. fructosovorans* [FeFe]-hydrogenase, contain a N-terminal [2Fe-2S] center. Assuming a fused gamma peptide to the beta subunit for the *M. extorquens* formate dehydrogenase and the *S. aciditrophicus* [FeFe]-hydrogenase, then none of the beta subunits from the NADH-dependent, ferredoxin-independent enzymes possess a N-terminal [2Fe-2S] center. It appears that the N-terminal [2Fe-2S] center and two C-terminal [4Fe-4S] centers are present only in the beta subunits of the electron-bifurcating NADH-dependent, ferredoxin-dependent enzymes and not in the beta subunits of the NADH-dependent, ferredoxin-independent enzymes. Given the readily observable differences in the beta subunits that appeared to correlate with ferredoxin dependence we decided further investigate the beta subunits. This was done by building an alignment of the beta subunits to further investigate the primary amino acid sequences to identify if there were other differences that might differentiate the two groups.

### **Amino Acid Sequence Differences in the Beta Subunits of Electron-Bifurcating and NADH-Dependent, Ferredoxin-Independent Enzymes**

There appears to be strongly conserved regions of amino acids near the predicted NADH binding site, FMN binding site (see Figure 20), and a proposed cofactor binding site (soluble-ligand-binding-beta-grasp or SLBB) that are shared amongst the beta subunits of the electron-bifurcating, NADH-dependent, ferredoxin-dependent enzymes but absent in the NADH-dependent, ferredoxin-independent enzymes. These observations were made by generating an

alignment of the beta subunits from seventeen different enzymes. Included in the alignment were beta subunits from the eight-known electron-bifurcating formate dehydrogenases and [FeFe]-hydrogenases, the five NADH-dependent, ferredoxin-independent formate dehydrogenase, two NADH-dependent, ferredoxin-independent [FeFe]-hydrogenases, the Nqo1 subunit from *T. thermophilus*, and the equivalent NuoF subunit from *E. coli* strain K-12, substrain MG1655. The full alignment can be found in the supplemental figures section of this chapter.

A conserved sequence of DEGDPxxFM was observed in all the beta subunits of the electron-bifurcating, NADH-dependent, ferredoxin-independent enzymes (Figure 20 and 21) that corresponds with a region predicted to be involved in the binding of NADH in the *T. thermophilus* Nqo1 subunit (Walker, 1992; Sazanov and Hinchliffe, 2006). None of beta subunits of the NADH-dependent, ferredoxin-independent enzymes analyzed share a strong consensus sequence over the region. The beta subunits from electron-bifurcating, NADH-dependent, ferredoxin-dependent enzymes contain a methionine residue at the equivalent residue of M<sup>289</sup> in the *T. maritima* HydB sequence (Figure 20). The beta subunits of the NADH-dependent, ferredoxin-independent enzymes have lysine, serine or alanine at this position. The beta subunits from electron-bifurcating enzymes except the sequence from *D. fructosovorans* have alanine at the equivalent position to A<sup>287</sup> of the *T. maritima* HydB sequence while the NADH-dependent, ferredoxin-independent enzymes instead contain a threonine or serine residue. The M<sup>289</sup> as found in the *T. maritima* HydB sequence and the other ferredoxin-dependent enzymes appears to be mutually exclusive to the presence of a serine or threonine residue (located two positions closer towards the N-terminus) which was found in all the ferredoxin-independent enzymes. In *T. thermophilus* Nqo1, the amino groups of Ser<sup>96</sup> and Glu<sup>97</sup> which are in close proximity to the locations of the mutually exclusive methionine or

serine/threonine are proposed to be involved in hydrogen bonding of NADH (Sazanov and Hinchliffe, 2006; Sazanov, 2007). However, the proposed common threonine or serine in the NADH-dependent, ferredoxin-independent enzymes, Ser<sup>100</sup> in the Nqo1 sequence, was not one of the residues suggested to be involved with hydrogen bonding. In summary, in the compared NADH-binding sites, those from the electron-bifurcating enzymes possess a methionine whereas the methionine is absent, and a lysine, serine or alanine is present in the NADH-dependent, ferredoxin-independent enzymes. In addition, in another position two residues closer to the N-terminus, a threonine and serine are present in the NADH-dependent, ferredoxin-independent beta subunits and absent in all electron-bifurcating enzyme beta subunits. It is unclear what roles these residues might play, although the proximity to the NADH binding site would suggest some involvement with the binding and oxidation of NADH.

**Figure 20. Conserved Regions in the NADH and FMN Binding Sites of the Beta Subunits of Electron-Bifurcating [FeFe]-Hydrogenases and Formate Dehydrogenases.** Conserved regions among the beta subunits of the eight electron-bifurcating enzymes are highlighted by dashed box. The solid black box highlights residues that are suggested to be involved in NADH and FMN binding (Walker, 1992; Sazanov and Hinchliffe, 2006). The yellow box highlights amino acid residues where all sequences of the beta subunits of the electron-bifurcating enzymes share a similar pattern and all the NADH-dependent, ferredoxin-independent beta subunits share a different pattern. The electron-bifurcating beta subunits all share a methionine while all the NADH-dependent, ferredoxin-independent beta subunits all lack the methionine but have a lysine, serine or alanine. In the case of the FMN binding site, all electron-bifurcating beta subunits possess a phenylamine while all the NADH-dependent, ferredoxin-independent beta

subunits possess a tyrosine. The alignment of full-length the beta subunits was performed in MEGA7 using the ClustalW algorithm. The alignment was inspected for regions where at least three consecutive amino acid residues were conserved among the sequences of the eight beta subunits of the electron-bifurcating enzymes. NADH-dependent, ferredoxin-independent beta subunit sequences were then inspected to determine if the conserved regions were unique to the electron-bifurcating NADH-dependent, ferredoxin-independent beta subunits.

273 276 278 280 282 284 286 288 290 292 294 296 298 300 302 304 306 308 310 312 314 316 318 320 322 324 326 328 330 333  
 G L K W E F T R K A Q G D - - I K F V V C N G D E G D P G A F M N R T L E R D P H L V L E G M I I A G Y A V G A Q K G Y  
 G V K W E F A Y K Q K E T - - P K Y V V C N A D E G D P G A F M D R S I L E G D P H S V L E A M A I A G Y A I G A N H Q Y  
 G L K W E F A Y R S P G P - - V K Y F V C N A D E G D P G A F M D R S I L E G D P H S V L E A M A I A G Y A I G A S H Q Y  
 G L K W Q F A H D A V S E D G I K Y V A C N A D E G D P G A F M D R S V L E G D P H A V I E A M A I A G Y A V G A S K G Y  
 G R K W M F T K D A P G D - - V K Y V A C N A D E G D P G A F M D R S I L E G D P H A V I E A M T I A S Y A V G A H Q Q Y  
 G L K W E F T A K A T G D - - Q K Y V L C N A D E G D P G A F M D R S I L E G D P H S V I E A M L A G P A I A G Y A I G S D Q G Y  
 G R K W K T A A D I D T S - - P I Y V L C N A D E G D P G A F M D R S I M E G D P H S V I E A M T L C A Y A V G G T N G F  
 G I K W G I A L G N K A D - - Q K Y M V C N A D E G D P G A F M D R A V L E G D P H S V V E A M A I G G Y A I G A T R G T  
 G M K W S F A A G A Q A D - - Q K Y V I C N A D E G E P G T Y K D R L I M E N D P H T L I E G M A I C A Y A I G A T Q Q Y  
 G V K W S F V P K G E M Q - - K Y V I C N A D E G E P G T F K D R V L M E E N P Q Q L I E G M L L C G Y A I G A T L G Y  
 G I K W K T V L G A Q S A - - V K Y I V C N A D E G D S G T F S D R M V M E D D P F M L I E G M T I A A L A V G A E Q Q Y  
 G I K W K T V L G A Q S A - - V K Y I V C N A D E G D S G T F S D R M V M E D D P F M L I E G M T I A G L A V G A E Q Q Y  
 G R K W R S V R G E P G P - - R L M A V N G D E G E P G T F K D Q L Y L N T D P H R F L E G M L I G A H V V E A A D V Y  
 G I K W K T V A D A P A D - - R R Y V V T N A D E G D S G T F A D R M V M E G D P F V L I E G M T I C G Y A I G A S K G F  
 G I K W R T V A A A Q A D - - Q K Y I V C N A D E G D S G S F A D R M L I E G D P F C L V E G M A I A G H A V G A T R G Y  
 G L K W S L M P K D E S M N - I R Y L L C N A D E M E P G T Y K D R L L M E Q L P H L L V E G M L I S A F A L K A Y R G Y  
 G L K W S F M P K D D G K - - Q H Y L L C N A D E S E P G S I F K D R Y I L E D V P H L L I E G M I L A G Y A I R A T V G Y

NADH binding region

- T. maritima HydB
- C. tencongenensis HydB
- M. thermoacetica HydB
- A. woodii HydB
- R. albus HydB
- C. acidurici HydB
- D. autoethanogenum HydB
- D. fructosovorans HydB
- S. wolfei HydB
- S. aciditrophicus HydB
- C. necator FdhB
- C. oxalaticus FdhB
- M. extorquens FdhB
- M. trichosporium FdhB
- R. capsulatus FdhB
- E. coli Nuof
- T. thermophilus Nqo1

352 354 356 358 360 362 364 366 368 370 372 374 376 378 380 382 384 386 388 390 392 394 396 398 400 402 404 406 408 410 412  
 E D A R K L G L G E N I L G T G F S F D L E V K E G A G A I F V C G E E T A L L A S I E G K R G M P R P K P P F P A Q S G  
 Q Q A R E Y G L L G K D I F G T G F D F D I E I R L G A G A F V C G E E T A L L N S I M G K R G E P R P R P P P P A V K G  
 S Q A R E Q G L L G K N L F N S G F D F D I D I R L G A G A F V C G E E T A L L A S I E G R R G E P R P R P P P P A V S G  
 D Q A K E Y G I L G E N I F E T D F S F D I E I R L G A G A F V C G E E T A L M N S I E G R G E P R P R P P P P A N K G  
 D Q A R E Y G L L G K N I L G T G H D F D I E I R L G A G A F V C G E E T A L L T S I E G N R G E P R P R P P P P A V K G  
 D E A K A K G L L G K D I F G T G F N F D M E I R L G A G A F V C G E E T A L I A S I E G Q R G M P R N K P P P P A N K G  
 N K A K D E N L L G N N I L G T D F S F D I Q I V R G G G A F V C G E E T A L M S S I E G M V G E P R A K Y I H T T E K G  
 D D A R E Y G L L G E N I F G S G F D F D I E L K Y I G A G A I F V C G E E T A L I R S M E G K R G E P V T K P P P P A Q S G  
 N Q A K E K G L V K D - - - - F D I E V R S G A G A Y V C G E E T A L I E S I E G K R G E P R F K P P P P S E G  
 D Q A R A K G F L G K I F G S N F D F D I F V K E G G G A Y V C G E E T S L I N S M E G K R G Y P R V R P P P P A A A G  
 G I A N A A G W L G D D I R G S G K R F H L E V R K G A G A Y V C G E E T A L L E S L E G R R G V V R A K P P L P A L Q G  
 A I A H A A G W L G D D L R G S G K R F L E V R K G A G A Y V C G E E T A L L E S L E G K R G V R A K P P L P A L E G  
 A K L P E G G - - - - - T R I H L R R G A G A Y I C G E E S S L I E S L E G K R G L P R H K P P P P F F Q V G  
 E A A R K A G W L G P N V R G S G F A F D I E L R I G A G A Y V C G E E T S L L S L E G K R G I V R A K P P L P A H V G  
 A M A K P F - - - - L A E A G - - F E M E V R V G A G A Y V C G E E T S L L S L E G K R G T V R A K P P L P A L K G  
 A E A T E A G L L G K N I M G T G F D F L F V H T G A G R Y I C G E E T A L I N S L E G R R A N P R S K P P P P A T S G  
 K E A R A R G Y L G K N L F G T D F S F D L H V H R G A G A Y I C G E E T A L M N S L E G L R A N P R L K P P P P A Q S G

FMN binding region

- T. maritima HydB
- C. tencongenensis HydB
- M. thermoacetica HydB
- A. woodii HydB
- R. albus HydB
- C. acidurici HydB
- C. autoethanogenum HydB
- D. fructosovorans HydB
- S. wolfei HydB
- S. aciditrophicus HydB
- C. necator FdhB
- C. oxalaticus FdhB
- M. extorquens FdhB
- M. trichosporium FdhB
- R. capsulatus FdhB
- E. coli Nuof
- T. thermophilus Nqo1

The FMN binding site was a highly conserved region amongst all of the compared beta subunits. The electron-bifurcating NADH-dependent, ferredoxin-independent beta subunits all shared a conserved GxGAFVCGExTAL sequence. The phenylalanine residue present in the electron-bifurcating beta subunits (position 367 of *T. maritima* HydB; position 180 of *T. thermophilus* Nqo1) was replaced with tyrosine in the beta subunits of the NADH-dependent, ferredoxin-independent enzymes (Figure 20). This residue in *T. thermophilus* Nqo1, Tyr<sup>180</sup>, was suggested to play an important role in NADH binding (Sazanov and Hinchliffe, 2006; Burroughs et al., 2007). Simultaneous mutation of the Tyr<sup>180</sup> residue and the Cys<sup>182</sup> residue was associated with a deficiency in mitochondrial complex I by presumably altering FMN or NADH binding (Benit et al., 2001; Sazanov, 2007). In summary, a tyrosine residue previously suggested to play a crucial role in NADH binding is present in the beta subunits of the NADH-dependent, ferredoxin-independent enzymes but is replaced by a phenylalanine residue in the beta subunits all of the electron-bifurcating enzymes.

Several other regions of amino acid residues near a SLBB domain (soluble-ligand-binding-Beta-grasp domain), (*T. thermophilus* Nqo1 positions 254-298, see Figure 21) were conserved in the electron-bifurcating beta subunits and absent in the NADH-dependent, ferredoxin-independent beta subunits. The, SLBB domain is a predicted ligand-binding domain present in Nqo1 (Burroughs et al., 2007). This domain has also been described as ubiquitin like (Sazanov and Hinchliffe, 2006), but it is not known to bind any cofactor in Nqo1. The conserved regions of amino acid residues near the SLBB domain shared among the electron-bifurcating beta subunits are GGPSG (*T. maritima* HydB positions 427-431), GSGG (*T. maritima* HydB positions 456-459) and CMV (*T. maritima* HydB positions 468-470) (Figure 21). There is an

additional group of conserved amino acid residues shared among the electron-bifurcating beta subunits, PNP (*T. maritima* HydB positions 538-540), that is located closer to the C-terminal [4Fe-4S] cluster than the SLBB domain. It is of interest that the electron-bifurcating subunits have conserved residues near the predicted SLBB domain whereas the NADH-dependent, ferredoxin-independent beta subunits do not. This could imply a property exclusively conserved in the electron-bifurcating beta subunits, such as the ability to bind a cofactor responsible for the electron-bifurcation reaction. An additional cofactor, such as FMN, has been proposed to be present in the beta subunit of the *A. woodii* electron-bifurcating [FeFe]-hydrogenase and serve as the site of electron-bifurcation (Buckel and Thauer, 2018). The number of conserved amino acid residues near the proposed SLBB domain in electron-bifurcating beta subunits suggests the domain binds the cofactor acting as the site of electron-bifurcation. As the NADH-dependent, ferredoxin-independent beta subunits do not share these conserved amino acid residues near the proposed SLBB domain, it would be predicted that they would not bind this additional cofactor, consistent with structural studies of Nqo1 that did not detect a cofactor at this location (Sazanov and Hinchliffe, 2006; Sazanov, 2007).

### **Summary of Differences in the Beta Subunits of the Electron-Bifurcating Enzymes**



#### **Compared to the NADH-Dependent, Ferredoxin-Independent Enzymes**

We propose that the ability of the NADH-dependent, ferredoxin-independent [FeFe]-hydrogenases from *S. wolfei* and *S. aciditrophicus* to operate without electron-bifurcation is due to the fact that their beta subunits are more similar to other NADH-dependent, ferredoxin-independent than to the beta subunits of the electron-bifurcating [FeFe]-hydrogenases and formate dehydrogenases. We found several differences that separate the group of beta subunits

from the electron-bifurcating enzymes from the group of beta subunits from the NADH-dependent, ferredoxin-independent subunits. These differences (see Figure 21) include: (1) a N-terminal [2Fe-2S] cluster, (2) a methionine residue exclusive to a threonine or serine (located two residues closer to N-terminus), (3) a phenylalanine as opposed to a tyrosine, (4) conserved glycine rich regions near the SLBB domain, and (5) two C-terminal [4Fe-4S]-clusters. These differences are not a complete list of the differences between these two proposed groups of enzymes as we did not investigate regions that did not have at least three adjacent conserved residues and single site or two consecutive conserved residues could play important roles. In addition, we did not incorporate structural modeling in comparing these two groups that would likely indicate important differences between these two groups. However, we do believe that some of these differences could be responsible for the differing ability to perform electron-bifurcation between the two groups. Given the existing structural information for the Nqo1 structure, which likely encompasses the beta subunits of the other NADH-dependent, ferredoxin-independent enzymes, what is most urgently required is detailed structural information from the electron-bifurcating [FeFe]-hydrogenases and formate dehydrogenases (Buckel and Thauer, 2018).



**Figure 21. Summary of Differences Between the Electron-Bifurcating [FeFe]-Hydrogenases and Formate Dehydrogenases and NADH-Dependent, Ferredoxin-Independent Enzymes**

<p><i>T. maritima</i> HydB Bifurcating Subunit AA Residues 1-626</p>	
<p><i>T. thermophilus</i> Nqo1 Non-Bifurcating Subunit AA Residues 13-438</p>	
<p>Location of Cofactor Binding Sites</p>	<p>[2Fe-2S] TM28-TM125</p> <p>NADH Binding Residues TT64-TT100 TM196-232</p> <p>FMN Binding Residues TT175-220 TM307-TM352</p> <p>SLBB Domain TT254-TT298 TM386-TM432</p> <p>[4Fe-4S] TT354-TT400 TM486-TM531</p> <p>2x [4Fe-4S] TM569-TM676</p>
<p>Location of Conserved Residues Unique to Bifurcating Subunits</p>	<p>TT94-TT102 TM226-TM234 Bifurcating Subunits: DEGDPe<sup>x</sup>FM Non-Bifurcating Subunits: DE<sup>xxx</sup>GS<sup>xx</sup> or DE<sup>xxx</sup>GT<sup>xx</sup></p> <p>TT176-TT188 TM306-TM320 Bifurcating Subunits: GXGA<sup>F</sup>VCGE<sup>x</sup>TAL Non-Bifurcating Subunits: GXGA<sup>F</sup>xxGEE<sup>xx</sup>C</p> <p>TT293-TT296 TM427-TM431 Bifurcating Subunits: GGP<sup>SG</sup> Non-Bifurcating Subunits: G<sup>xxx</sup></p> <p>TT324-TT327 TM456-TM459 Bifurcating Subunits: GSGG Non-Bifurcating Subunits: G<sup>xxx</sup></p> <p>TT335-TT338 TM465-TM470 Bifurcating Subunits: CMV Non-Bifurcating Subunits: xxx</p> <p>TT407-TT409 TM538-TM540 Bifurcating Subunits: PNP Non-Bifurcating Subunits: xxp</p>
<p>Summary of Differences Between Bifurcating Subunits and Non-Bifurcating Subunits</p>	<p>1. N-terminal [2Fe-2S] Cluster Bifurcating: Present (7/8) Non-Bifurcating: Absent (9/9)</p> <p>2. NADH Binding Site Bifurcating: Methionine Residue (8/8) Non-Bifurcating: Threonine or Serine Residue (9/9)</p> <p>3. FMN Binding Site Bifurcating: Phenylalanine Residue (8/8) Non-Bifurcating: Tyrosine Residue (9/9)</p> <p>4. SLBB Domain Bifurcating: GGP<sup>SG</sup> Residues (8/8) Non-Bifurcating: GG<sup>xxx</sup> (9/9)</p> <p>5. Two C-terminal [4Fe-4S] Clusters Bifurcating: Present (8/8) Non-Bifurcating: Absent (9/9)</p>

## **Structural Similarities Between the Alpha Subunit of the NADH-Dependent, Ferredoxin-Independent Enzymes**

A region of roughly 200 amino acid residues at the N-terminal that is responsible for the binding of two [4Fe-4S] centers and a [2Fe-2S] center (Vignais et al., 2001; Sazanov and Hinchliffe, 2006; Hille et al., 2014) is shared between the NADH dehydrogenase subunit Nqo3, the alpha subunits of the NADH-dependent formate dehydrogenases, and monomeric, ferredoxin-dependent [FeFe]-hydrogenases. In addition, there is homology between the FMN, NADH, and [4Fe-4S] cluster binding sites within the beta subunit of the formate dehydrogenases and Nqo1. There is also homology between the [2Fe-2S] cluster containing gamma subunit of the formate dehydrogenases and Nqo3. In short Nqo1, Nqo2, and Nqo3 are directly comparable to the beta, gamma, and alpha subunits of the formate dehydrogenase (Hille et al., 2014). The *S. wolfei* and *S. aciditrophicus* [FeFe]-hydrogenases share this same similarity with the NADH-dependent, ferredoxin-independent formate dehydrogenases and Nqo1, Nqo2, and Nqo3 over a 200 amino acid region of the alpha subunit, over the entire beta subunit, and the entire gamma subunit. This similarity can be used to predict how electron flow may occur within the *S. wolfei* and *S. aciditrophicus* NADH-dependent, ferredoxin-independent [FeFe]-hydrogenases.

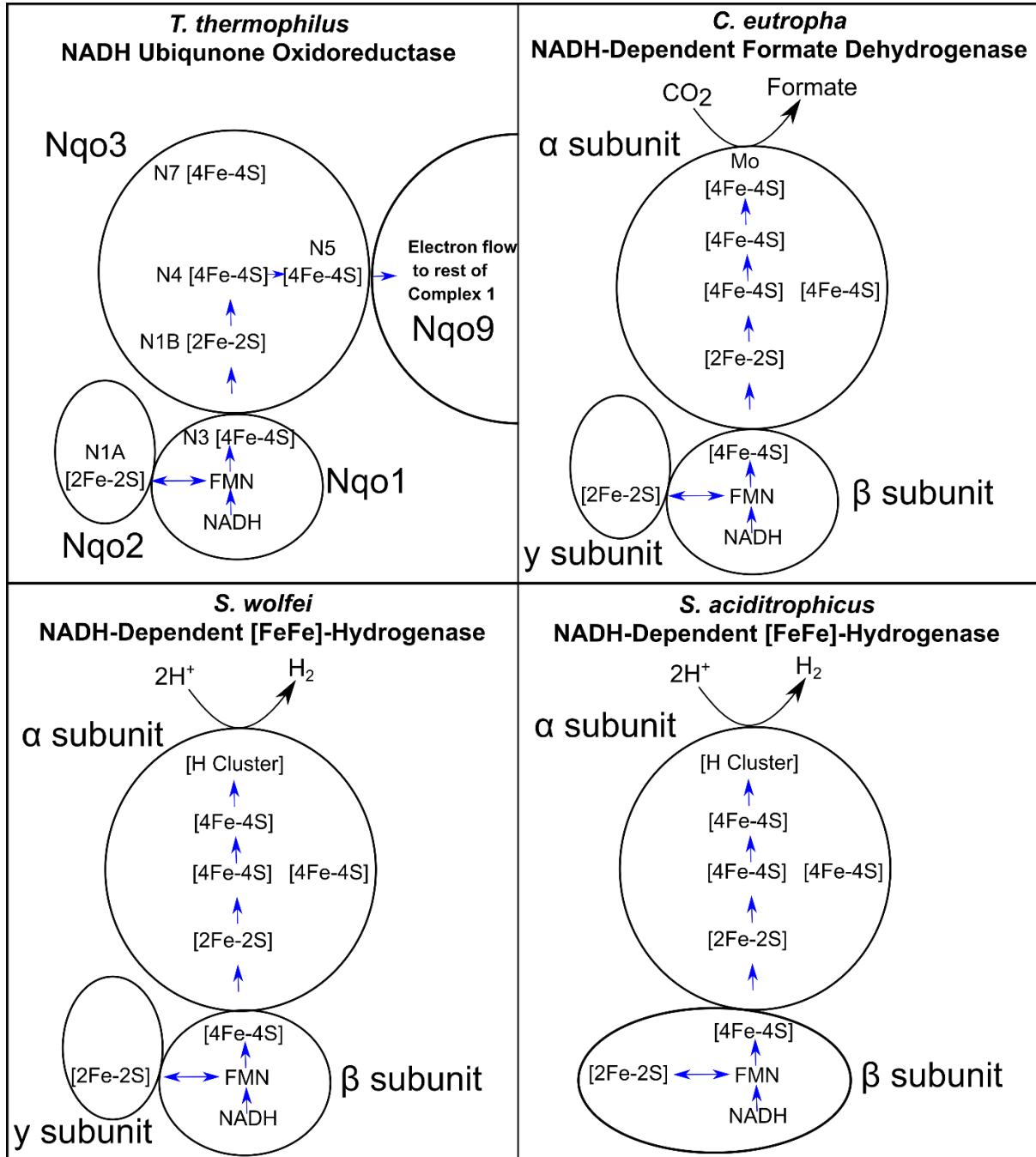
Strong similarities exist between the NADH-dependent, ferredoxin-independent formate dehydrogenases and the NADH:ubiquinone oxidoreductase complex (Sazanov and Hinchliffe, 2006; Hille et al., 2014). These similarities allowed for homology modeling of the proposed structural model of the *Cupriavidus necator* (formerly *Ralstonia eutropha*) NADH-dependent, ferredoxin-independent formate dehydrogenase (Hille et al., 2014). The model was built using models of the *T. thermophilus* Nqo1, Nqo2 and Nqo3 subunits and *E. coli* FdhF and included a

proposed electron flow path from the NADH binding site in the beta subunit to the catalytic site in the alpha subunit. A V-shaped fork (see Figure 22) differentiates the proposed electron flow path in Nqo3 and the alpha subunit of the *C. necator* formate dehydrogenase (Hille et al., 2014). In Nqo3, electrons are proposed to first move from the N4 [4Fe-4S] cluster to the N5 [4Fe-4S] cluster and then to the N6A [4Fe-4S] cluster in the Nqo9 subunit cluster in a path away from the vestigial molybpterin cofactor binding site near the N7 [4Fe-4S] cluster (Sazanov and Hinchliffe, 2006). However, in the *C. necator* formate dehydrogenase, the electron flow path differs after the N4 equivalent [4Fe-4S] cluster. Instead of moving to the N5 cluster as occurs in Nqo3, electrons are proposed to move to a [4Fe-4S] cluster present in the *C. necator* formate dehydrogenase alpha subunit that has been lost in Nqo3. This [4Fe-4S] cluster allows further electron transfer to the N7 [4Fe-4S] cluster and the active site with the molybdopterin cofactor. There is shared homology and a similar predicted cofactor binding sites between this formate dehydrogenase and the NADH-dependent, ferredoxin-independent [FeFe]-hydrogenases. Therefore, it can be proposed that similar electron flow path occurs in both types of enzymes as diagrammed in Figure 22. Most of the electron flow path from the beta subunit to alpha subunit would be identical between these enzymes and would not involve electron-bifurcation mechanism. The electron transfer from the NADH binding site in the beta subunit to the N4 equivalent [4Fe-4S] center in the alpha subunit would be the same, but different after this point. This is because the peptide sequences for the regions of the catalytic [H]-cluster and the closest [4Fe-4S] cluster in the *S. acidotrophicus* and *S. wolfei* [FeFe]-hydrogenases have little similarity to the molybdopterin cofactor binding site and the two closest [4Fe-4S] clusters in the *C. necator* formate dehydrogenase. Presumably, this additional [4Fe-4S] center allows electron flow from the N4 equivalent [4Fe-4S] center to the [H]-cluster. The N5 equivalent [4Fe-4S] center would

not be used for electron flow from NADH to the [H]-cluster in the NADH-dependent, ferredoxin-independent [FeFe]-hydrogenases similar to the electron flow path of the *C. necator* formate dehydrogenase.

The structural similarities in the alpha, beta and gamma subunits of the *S. wolfei* and *S. aciditrophicus* NADH-dependent, ferredoxin-independent [FeFe]-hydrogenases to the alpha, beta and gamma subunits of the NADH-dependent, ferredoxin-independent formate dehydrogenases and Nqo1, Nqo2, and Nqo3 argue that electron flow paths are similar. This electron flow path allows passage of electrons from the NADH binding site to the [H]-cluster catalytic site without electron input from another path as expected for electron bifurcation. Also, it argues against the [H]-cluster as the site of electron bifurcation as the alpha subunits of electron-bifurcating, ferredoxin-dependent [FeFe]-hydrogenases and NADH-dependent, ferredoxin-independent [FeFe]-hydrogenases are similar in cofactor arrangement and conserved amino acid regions (Figure 19). Presumably, the proposed electron flow paths for the *S. wolfei* and *S. aciditrophicus* NADH-dependent, ferredoxin-independent [FeFe]-hydrogenases does not occur in the electron-bifurcating [FeFe]-hydrogenases and formate dehydrogenases as these enzymes cannot reduce  $\text{NAD}^+$  without also reducing ferredoxin.

**Figure 22. Proposed Electron Flow in NADH-Dependent, Ferredoxin-Independent [FeFe]-Hydrogenases.** Electron flow depicted for *T. thermophilus* Nqo1-Nqo and, *C. eutropha* formate dehydrogenase as illustrated by Hille et al. 2014. Blue arrows indicate electron flow.



### **Additional Example of a NADH-Dependent, Ferredoxin-Independent, [FeFe]-Hydrogenase**

Previously, a [FeFe]-hydrogenase from the hydrogenosome of the anaerobic ciliate *Nyctotherus ovalis* was proposed to be a NADH-dependent, ferredoxin-independent [FeFe]-hydrogenase (Boxma et al., 2007). This is unusual in that hydrogenosomes in many other anaerobic ciliates produce hydrogen from reduced ferredoxin and not from NADH (de Graaf et al., 2011). This is because anaerobic ciliates other than *N. ovalis* have the enzyme, pyruvate:ferredoxin oxidoreductase, which makes reduced ferredoxin, which is then used by a monomeric [FeFe] hydrogenase to make hydrogen (Peters et al. 1998). However, genes for pyruvate:ferredoxin oxidoreductase are absent in the *N. ovalis* genome (de Graaf et al., 2011). Instead, *N. ovalis* has the genes for pyruvate dehydrogenase, which produces NADH. The *N. ovalis* pyruvate-metabolizing enzyme has not been purified or enzymatically characterized, but is presumed to be NADH-dependent, ferredoxin-independent based on genomic analyses (Boxma et al., 2007). The *N. ovalis* [FeFe]-hydrogenase has the same conserved domains as both the *S. wolfei* and *S. aciditrophicus* NADH-dependent, ferredoxin-independent [FeFe]-hydrogenases but consists of a fused peptide where the alpha, beta, and gamma subunits as found in the *S. wolfei* [FeFe]-hydrogenase are fused into a single peptide. This is in contrast to the *S. aciditrophicus* [FeFe]-hydrogenase where only the gamma and beta subunits are fused together. In addition, the *N. ovalis* hydrogenase (Genbank Protein Accession ID: AAU14235) possesses the features that we propose can be used to differentiate the NADH-dependent, ferredoxin-independent [FeFe]-hydrogenases from the electron-bifurcating [FeFe]-hydrogenases (see Figure 21). Furthermore, as the production of hydrogen from NADH requires low hydrogen partial pressures to operate, the hydrogenosome would need to be in close proximity to a hydrogen-consuming organism to maintain low hydrogen partial pressures to allow continual NADH re-oxidation. A

hydrogenotrophic methanogen, presumably *Methanobrevibacter*, was found as an endosymbiont of *N. ovalis* and in close association to the hydrogenosome organelle (Gijzen et al., 1991). This fulfills the requirement that a hydrogen-consuming partner organism, in this case a methanogen, be present for hydrogen production from NADH. This [FeFe]-hydrogenase, despite being an apparent fusion of the equivalent *S. wolfei* [FeFe]-hydrogenase alpha, beta and gamma subunits into a single peptide, still shares key features that we propose distinguish NADH-dependent, ferredoxin-independent [FeFe]-hydrogenases from the electron-bifurcating, ferredoxin-dependent [FeFe]-hydrogenases.

## **Conclusion**

The results obtained from studying the recombinantly produced *S. aciditrophicus* HydAB indicate that it functions as a ferredoxin-independent, NADH-dependent [FeFe]-hydrogenase. In combination with the previous example of a ferredoxin-independent, NADH-dependent [FeFe]-hydrogenase, Hyd1ABC from *S. wolfei*, it appears that hydrogen production from NADH is a key feature of syntrophic fatty acid-oxidizing bacteria. Any organism producing hydrogen from NADH in a ferredoxin-independent manner could be viewed as a syntrophic metabolizer, as the process matches with the original definition of syntrophy in that a hydrogen or formate consuming microorganism is needed. Hydrogen production from NADH cannot be used to produce any useful amount of hydrogen under fermentative conditions in pure culture and only serves a function when used in combination with a hydrogen-consuming organism, such as a hydrogenotrophic methanogen or sulfate reducer. It remains to be fully demonstrated if the system for oxidizing reduced flavin cofactors (EtfAB) during syntrophic fatty acid metabolism also requires a low hydrogen partial pressure (<60 Pascals). While the concept of syntrophic



fatty, aromatic and alicyclic acid metabolism involves the use NADH-dependent, ferredoxin independent hydrogenases and formate dehydrogenase is based on only two examples, it does provide a biochemical explanation for syntrophy. The conclusion that a microorganism uses electron-bifurcating or non-electron bifurcating hydrogenases or formate dehydrogenases should be made only after careful consideration of the organism's physiology and after appropriate enzymatic analysis. It would be prudent when attempting to classify multimeric [FeFe]-hydrogenases to make the comparisons described here to determine if the beta subunit more closely resembles that of a NADH-dependent, ferredoxin-independent enzyme or electron bifurcating [FeFe]- hydrogenases.

NADH-dependent, ferredoxin-independent [FeFe]-hydrogenases present in *S. wolfei* and *S. aciditrophicus* can be used to re-oxidize NADH without energy input needed to make reduced ferredoxin. This would allow more energy to be used for growth rather than NADH re-oxidation. Adaptations such as these that maximize energy conservation by utilizing high redox potential electrons to produce hydrogen or formate may be responsible for the defining requirement of syntrophic organisms, partners that maintain low hydrogen partial pressures.

## **Methods**

### **Plasmid Design**

A DNA sequence encoding for the genes for the *S. aciditrophicus* dimeric [FeFe]-hydrogenase (SYN\_01369 and SYN\_01370) (HydAB) was ordered from Integrated DNA Technologies (Coralville, Iowa, USA) and delivered in a suitable plasmid for recombinant protein expression, including a T7 promoter region for protein expression. This plasmid was designated as pIDTKan-SbHyd. An additional amino acid sequence including six histidine

residues (MGSSHHHHHSQDPNSSSARL) was added to the N-terminal region of SYN\_01370 to allow for nickel affinity purification of the protein product. A homology search of the *Syntrophus acidotrophicus* genome using the *Clostridium pasteurianum* ferredoxin (GenBank Nucleotide ID: M11214) identified SYN\_03059 as the most similar match. A DNA sequence encoding for SYN\_03059 was also ordered from Integrated DNA Technologies for recombinant protein expression and the plasmid is referred to as pIDTAmp-SbFd.

**Table 10. List of Plasmids Used for the Expression of the *S. aciditrophicus* HydAB and Ferredoxin.**

Plasmid	Function	Source
pCDFDuet-1 SwHydEFG	Production of <i>S. wolfei</i> HydEFG	See (Losey et al., 2017)
pIDTKan-SbHyd	Production <i>S. aciditrophicus</i> HydAB	This work
pIDTAmp-SbFd	Production of <i>S. aciditrophicus</i> ferredoxin	This work

<sup>a</sup> Underlined regions indicate restriction enzyme cut sites.

### Expression of HydAB in *E. coli*

*E. coli* BL21(DE3) cells were co-transformed with pIDTKan-SBHydAB and pCDFDuet-1 SwHydEFG and used for expression (See Table 10). The latter plasmid contains maturation genes needed for the expression of a functional HydAB protein. The cells were grown at pH 7.5 in LB medium containing 50 mM potassium phosphate, 10 g · l<sup>-1</sup> glucose, and the appropriate selective antibiotics. Expression conditions were similar to those used previously for expression

of the trimeric *S. wolfei* hydrogenase (see Chapter 2) although lower iron and cysteine concentrations were used. Briefly, cultures were incubated aerobically to an O.D. of 0.4-0.6 followed by induction by the addition of 0.5 mM IPTG. After induction, 10 mM sodium fumarate, 0.5 mM cysteine, and 0.5 mM ferric ammonium citrate were added. Cultures were then purged with nitrogen overnight to create anaerobic conditions and harvested by centrifugation (6,000 • g for 20 minutes at 4°C). Cell pellets were stored in liquid nitrogen until used. After induction, all additional manipulations of cell pellets and protein fractions were performed under anaerobic conditions inside a Coy anaerobic chamber operated with a 95% nitrogen and 1-5% hydrogen atmosphere.

### **Purification of recombinant HydAB**

BL21(DE3) cells (3.05 g) induced for HydAB expression were resuspended in 30 mL of lysis buffer (50 mM potassium phosphate (pH 7.5), 0.5 M NaCl, 2 mM dithioerythritol 5 µM FAD, 5 µM FMN, 20 mM imidazole, 0.5 mg lysozyme, and 0.1% Triton X-100). The cells were passed through a French press cell operating at 140 MPa (Megapascals) and the resulting fluid was clarified by centrifugation at 13,000 • g for 10 minutes. The cell-free extract was then loaded onto a HisTrap Hp 5 ml column (GE Healthcare Life Sciences, Pittsburgh, PA) with an imidazole concentration of 20 mM, washed with 50 mM imidazole, and eluted with 250 mM imidazole. The fraction eluted with 250 mM was concentrated using an Amicon Ultra 0.5 ml centrifugal filter with a 100 kDa molecular weight cut-off (MWCO) filter and stored in liquid nitrogen until used for further analyses.

### **Partial purification of ferredoxin from *S. acidotrophicus***

Approximately 5 grams of wet cell mass of *S. aciditrophicus* were disrupted by passage through a French pressure cell operating at 140 MPa. The lysis buffer consisted of 25 mM potassium phosphate (pH 6.5) with 2 mM DTE, 5 mg·l<sup>-1</sup> lysozyme, 0.125 mg·l<sup>-1</sup> DNase and 0.5% Triton X-100. The resulting extract was clarified by centrifugation at 12,000 • g for 10 minutes and loaded onto a DEAE-Sepharose anion exchange column and eluted with a gradient from 0 to 1.0 M NaCl. The last dark brown fraction to elute was collected and passed first through a 100 kDa MWCO filter to remove high molecular weight proteins and then concentrated and desalted using a 10 kDa MWCO filter.

### **Production and purification of recombinantly produced *Syntrophus* ferredoxin**

*E. coli* BL21(DE3) cells (4.5 grams) transformed with pIDTAmp-SbFd were grown and induced using the same conditions as those used for production of *S. aciditrophicus* HydAB. The cells were lysed using a French pressure cell and the protein purified using nickel affinity chromatography as described for HydAB.

### **Enzymatic assays**

Hydrogen-oxidizing assays were performed in 1.4 ml quartz cuvettes (Nova Biotech, El Cajon, CA) with gas tight rubber stoppers. The assays were performed in 1 ml volumes at 37°C using an assay buffer (50 mM Tris pH 7.5, 2 mM dithioerythritol, 5 µM FMN, and 5 µM FAD). NAD(P)<sup>+</sup> reduction was tested using a concentration of 1 mM NAD<sup>+</sup> or 1 mM NADP<sup>+</sup> with and without 10 µM clostridial ferredoxin in cuvettes that were never exposed to viologen dyes. Hydrogen-dependent clostridial ferredoxin reduction was tested using 30 µM clostridial ferredoxin. Hydrogen-dependent reduction of methyl viologen was monitored using 10 mM methyl viologen as electron acceptor. Hydrogen-oxidizing assays were initiated with the addition of hydrogen at a pressure of 1.2 X 10<sup>5</sup> Pa to a 100 % nitrogen headspace. NAD<sup>+</sup> and NADP<sup>+</sup>

reduction was followed at 340 nm ( $\epsilon_{340} = 6.2 \text{ mM}^{-1} \text{ cm}^{-1}$ ); ferredoxin reduction was followed at 430 nm ( $\epsilon_{430} = 13.1 \text{ mM}^{-1} \text{ cm}^{-1}$ ); and methyl viologen reduction was followed at 600 nm ( $\epsilon_{600} = 10.0 \text{ mM}^{-1} \text{ cm}^{-1}$ ).

Hydrogen production assays were conducted using 6.5-ml serum bottles with a 1.0 ml liquid assay volume with shaking (200 rpm) at 37°C. The reaction buffer contained 50 mM Tris (pH 7.5), 2 mM DTE, 5  $\mu\text{M}$  FMN, and 5  $\mu\text{M}$  FAD. Hydrogen production was tested with either 1 mM NADH or a reduced ferredoxin generating system consisting of 0.1 U pyruvate ferredoxin oxidoreductase, 10 mM pyruvate, 0.1 mM thiamine pyrophosphate, 1 mM CoA and either 0.5  $\mu\text{M}$  ferredoxin partially purified from *S. aciditrophicus*, 5.0  $\mu\text{M}$  of recombinantly ferredoxin produced *S. aciditrophicus* ferredoxin, or 20  $\mu\text{M}$  clostridial ferredoxin.

Hydrogen production assays to determine equilibrium hydrogen concentration at different NADH/NAD<sup>+</sup> ratios were performed using 6.5 ml serum bottles with a 1.0 ml liquid assay volume. Reaction buffer consisted of 10 mM Tris (pH 7.5), 2 mM dithioerythritol, 5  $\mu\text{M}$  FMN, and 5  $\mu\text{M}$  FAD. The total concentration of NADH and NAD<sup>+</sup> was held constant at 6 mM with variable NADH/NAD<sup>+</sup> ratios of 5.0, 1.0, and 0.2. Hydrogen production assay bottles were incubated for 24 h at room temperature before measurement.

### **Growth Conditions of Cultures for Hydrogen Partial Pressure Measurements**

Hydrogen concentrations were measured from triplicate cultures of either pure cultures of *S. aciditrophicus* or cocultures of *S. aciditrophicus* with *M. hungatei* grown on the following substrates: 20 mM crotonate, 2.5 mM sodium benzoate, or 2.5 mM cyclohex-1-ene-1-carboxylate. The basal medium consisted of a mineral solution (10 ml  $\cdot$  l<sup>-1</sup>), a trace metal solution (5 ml  $\cdot$  l<sup>-1</sup>), and a vitamin solution (10 ml  $\cdot$  l<sup>-1</sup>) (Tanner, 2007). The medium was prepared anaerobically under a N<sub>2</sub>/CO<sub>2</sub> (80:20) atmosphere with 3.5 g  $\cdot$  liter<sup>-1</sup> sodium

bicarbonate as buffering agent. Each culture consisted of 20 ml medium in a 159-ml serum bottle. Cysteine sulfide (0.05%) was used a reductant and resazurin was used a redox indicator. The inoculum was a 10 to 15% (v/v) transfer of *S. aciditrophicus* grown in pure culture on 20 mM crotonate with the aforementioned basal medium (culture O.D.= 0.54). Cocultures were created by addition of 2.0 to 2.5% (volume to volume) of a *M. hungatei* culture grown on H<sub>2</sub>/CO<sub>2</sub> (80:20), 0.05% sodium acetate (culture O.D.= 0.41) in the basal medium. Cultures were grown at 37°C but allowed to equilibrate to room temperature before hydrogen measurements were taken.

Crotonate, benzoate and cyclohex-1-ene-1-carboxylate concentrations were determined by high performance liquid chromatography (HPLC) analysis while methane measurements were made gas chromatography-flame ionization detector as previously described (Sieber et al., 2014). Hydrogen measurements were determined with a gas detector (Seiler et al., 1980) (Peak Performer RCP-910, Peak Laboratories, Mountain View, CA). Crotonate, benzoate and cyclohex-1-ene-1-carboxylate concentrations were determined every six days while hydrogen and methane concentrations were determined every 3 days.

### **Analytical Techniques**

SDS-PAGE and native PAGE analysis were performed using precast 8-16% Tris-Glycine gels (Life Technologies Co., Carlsbad, CA) according to manufacturer's instruction and stained using Coomassie Brilliant Blue G-250. The Bradford protein assay (Life Technologies Co., Carlsbad, CA) was used to determine protein concentrations with bovine serum album as the standard. Protein fractions of purified HydAB and ferredoxin partially purified from *S. aciditrophicus* were sent to for peptide identification. Peptide identification was performed at the Laboratory for Molecular Biology and Cytometry Research at OUHSC (Oklahoma City, OK).

Peptides were digested by trypsin followed by high-performance, liquid chromatography-tandem mass spectrometry (HPLC-MS/MS). Peptides were identified by Mascot search of the NCBI nonredundant (nr) database.

The iron content, flavin content, and molecular mass of HydAB was determined as described previously for Hyd1AB from *S. wolfei* (Losey et al., 2017). Iron content determination was performed using the ferrozine assay (Riemer et al., 2004), flavin content was determined by HPLC analysis using a UV detector (Seedorf et al., 2004), and the molecular mass was determined by size-exclusion chromatography using a Superdex 200 10/300 GL (GE Healthcare Life Sciences) calibrated with gel filtration standards (Bio-Rad Laboratories, Hercules, CA).

Hydrogen concentrations were determined by comparison against hydrogen standards (0.01%-1.0%) using a reductive trace gas analyzer RCP-910 (Peak Laboratories, Mountain View, CA).

### **Reagents and chemicals**

Biochemicals (NADH, NAD<sup>+</sup>, FMN, FAD, pyruvate, thiamine pyrophosphate, methyl viologen, and coenzyme A) were purchased from Sigma-Aldrich (St. Louis, MO).

### **References**

Benit, P., Chretien, D., Kadhom, N., de Lonlay-Debeney, P., Cormier-Daire, V., Cabral, A., et al. (2001). Large-scale deletion and point mutations of the nuclear NDUFV1 and NDUFS1

- genes in mitochondrial complex I deficiency. *Am J Hum Genet* 68(6), 1344-1352. doi: 10.1086/320603.
- Biegel, E., and Müller, V. (2010). Bacterial Na<sup>+</sup>/-translocating ferredoxin:NAD<sup>+</sup>/oxidoreductase. *Proc Natl Acad Sci Unit States Am* 107(42), 18138-18142. doi: 10.1073/pnas.1010318107.
- Boxma, B., Ricard, G., van Hoek, A.H., Severing, E., Moon-van der Staay, S.-Y., van der Staay, G.W., et al. (2007). The [FeFe] hydrogenase of *Nyctotherus ovalis* has a chimeric origin. *BMC Evol Biol* 7(1), 230. doi: 10.1186/1471-2148-7-230.
- Buckel, W., and Thauer, R.K. (2018). Flavin-Based Electron Bifurcation, A New Mechanism of Biological Energy Coupling. *Chem Rev* 118(7), 3862-3886. doi: 10.1021/acs.chemrev.7b00707.
- Burroughs, A.M., Balaji, S., Iyer, L.M., and Aravind, L. (2007). A novel superfamily containing the beta-grasp fold involved in binding diverse soluble ligands. *Biol Direct* 2, 4. doi: 10.1186/1745-6150-2-4.
- Crable, B.R., Sieber, J.R., Mao, X., Alvarez-Cohen, L., Gunsalus, R., Ogorzalek Loo, R.R., et al. (2016). Membrane Complexes of *Syntrophomonas wolfei* Involved in Syntrophic Butyrate Degradation and Hydrogen Formation. *Front Microbiol* 7, 1795. doi: 10.3389/fmicb.2016.01795.
- Darimont, B., and Sterner, R. (1994). Sequence, assembly and evolution of a primordial ferredoxin from *Thermotoga maritima*. *EMBO J* 13(8), 1772-1781.
- de Graaf, R.M., Ricard, G., van Alen, T.A., Duarte, I., Dutilh, B.E., Burgdorf, C., et al. (2011). The organellar genome and metabolic potential of the hydrogen-producing



- mitochondrion of *Nyctotherus ovalis*. *Mol Biol Evol* 28(8), 2379-2391. doi: 10.1093/molbev/msr059.
- Elshahed, M.S., and McInerney, M.J. (2001). Benzoate fermentation by the anaerobic bacterium *Syntrophus aciditrophicus* in the absence of hydrogen-using microorganisms. *Appl Environ Microbiol* 67(12), 5520-5525. doi: 10.1128/AEM.67.12.5520-5525.2001.
- Friedebold, J., and Bowien, B. (1993). Physiological and biochemical characterization of the soluble formate dehydrogenase, a molybdoenzyme from *Alcaligenes eutrophus*. *J Bacteriol* 175(15), 4719-4728.
- Fuchs, G., Boll, M., and Heider, J. (2011). Microbial degradation of aromatic compounds — from one strategy to four. *Nat Rev Microbiol* 9, 803. doi: 10.1038/nrmicro2652.
- Gijzen, H.J., Broers, C.A., Barughare, M., and Stumm, C.K. (1991). Methanogenic bacteria as endosymbionts of the ciliate *Nyctotherus ovalis* in the cockroach hindgut. *Appl Environ Microbiol* 57(6), 1630-1634.
- Gutekunst, K., and Schulz, R. (2018). "CHAPTER 4 The Physiology of the Bidirectional NiFe-hydrogenase in Cyanobacteria and the Role of Hydrogen Throughout the Evolution of Life," in *Microalgal Hydrogen Production: Achievements and Perspectives*. The Royal Society of Chemistry), 107-138.
- Hartmann, T., and Leimkühler, S. (2013). The oxygen-tolerant and NAD<sup>+</sup>-dependent formate dehydrogenase from *Rhodobacter capsulatus* is able to catalyze the reduction of CO<sub>2</sub> to formate. *FEBS J* 280(23), 6083-6096. doi: 10.1111/febs.12528.
- Harwood, C.S., Burchhardt, G., Herrmann, H., and Fuchs, G. (1998). Anaerobic metabolism of aromatic compounds via the benzoyl-CoA pathway. *FEMS Microbiol Rev* 22(5), 439-458. doi: [https://doi.org/10.1016/S0168-6445\(98\)00026-6](https://doi.org/10.1016/S0168-6445(98)00026-6).

- Hille, R., Hall, J., and Basu, P. (2014). The Mononuclear Molybdenum Enzymes. *Chem Rev* 114(7), 3963-4038. doi: 10.1021/cr400443z.
- Huang, H., Hu, L., Yu, W., Li, H., Tao, F., Xie, H., et al. (2016). Heterologous overproduction of 2[4Fe4S]- and [2Fe2S]-type clostridial ferredoxins and [2Fe2S]-type agrobacterial ferredoxin. *Protein Expr Purif* 121, 1-8. doi: 10.1016/j.pep.2015.12.019.
- Jackson, B.E., Bhupathiraju, V.K., Tanner, R.S., Woese, C.R., and McInerney, M.J. (1999). *Syntrophus aciditrophicus* sp. nov., a new anaerobic bacterium that degrades fatty acids and benzoate in syntrophic association with hydrogen-using microorganisms. *Arch Microbiol* 171(2), 107-114.
- James, K.L., Kung, J.W., Crable, B.R., Mouttaki, H., Sieber, J.R., Nguyen, H.H., et al. (2019, in preparation). *Syntrophus aciditrophicus* uses the same enzymes in a reversible manner to syntrophically degrade fatty, aromatic and alicyclic acids and to synthesize aromatic and alicyclic acids from crotonate.
- James, K.L., Rios-Hernandez, L.A., Wofford, N.Q., Mouttaki, H., Sieber, J.R., Sheik, C.S., et al. (2016). Pyrophosphate-Dependent ATP Formation from Acetyl Coenzyme A in *Syntrophus aciditrophicus*, a New Twist on ATP Formation. *MBio* 7(4). doi: 10.1128/mBio.01208-16.
- Kelly, C.L., Pinske, C., Murphy, B.J., Parkin, A., Armstrong, F., Palmer, T., et al. (2015). Integration of an [FeFe]-hydrogenase into the anaerobic metabolism of *Escherichia coli*. *Biotechnol Rep (Amst)* 8, 94-104. doi: <https://doi.org/10.1016/j.btre.2015.10.002>.
- Kpebe, A., Benvenuti, M., Guendon, C., Rebai, A., Fernandez, V., Le Laz, S., et al. (2018). A new mechanistic model for an O<sub>2</sub>-protected electron-bifurcating hydrogenase, Hnd from

- Desulfovibrio fructosovorans*. *Biochim Biophys Acta Bioenerg* 1859(12), 1302-1312. doi: <https://doi.org/10.1016/j.bbabi.2018.09.364>.
- Kung, J.W., Seifert, J., von Bergen, M., and Boll, M. (2013). Cyclohexanecarboxyl-Coenzyme A (CoA) and Cyclohex-1-ene-1-Carboxyl-CoA Dehydrogenases, Two Enzymes Involved in the Fermentation of Benzoate and Crotonate in *Syntrophus aciditrophicus*. *J Bacteriol* 195(14), 3193. doi: 10.1128/JB.00322-13.
- Laukel, M., Chistoserdova, L., Lidstrom, M.E., and Vorholt, J.A. (2003). The tungsten-containing formate dehydrogenase from *Methylobacterium extorquens* AM1: purification and properties. *Eur J Biochem* 270(2), 325-333.
- Ledbetter, R.N., Garcia Costas, A.M., Lubner, C.E., Mulder, D.W., Tokmina-Lukaszewska, M., Artz, J.H., et al. (2017). The Electron Bifurcating FixABCX Protein Complex from *Azotobacter vinelandii*: Generation of Low-Potential Reducing Equivalents for Nitrogenase Catalysis. *Biochemistry* 56(32), 4177-4190. doi: 10.1021/acs.biochem.7b00389.
- Losey, N.A., Mus, F., Peters, J.W., Le, H.M., and McInerney, M.J. (2017). *Syntrophomonas wolfei* Uses an NADH-Dependent, Ferredoxin-Independent [FeFe]-Hydrogenase To Reoxidize NADH. *Appl Environ Microb* 83(20), e01335-01317. doi: 10.1128/AEM.01335-17.
- Malki, S., Saimmaime, I., De Luca, G., Rousset, M., Dermoun, Z., and Belaich, J.P. (1995). Characterization of an operon encoding an NADP-reducing hydrogenase in *Desulfovibrio fructosovorans*. *J Bacteriol* 177(10), 2628-2636.
- McInerney, M.J., Rohlin, L., Mouttaki, H., Kim, U., Krupp, R.S., Rios-Hernandez, L., et al. (2007). The genome of *Syntrophus aciditrophicus*: life at the thermodynamic limit of

- microbial growth. *Proc Natl Acad Sci U S A* 104(18), 7600-7605. doi:  
10.1073/pnas.0610456104.
- McInerney, M.J., Sieber, J.R., and Gunsalus, R.P. (2009). Syntrophy in anaerobic global carbon cycles. *Curr Opin Biotechnol* 20(6), 623-632. doi: 10.1016/j.copbio.2009.10.001.
- McInerney, M.J., Struchtemeyer, C.G., Sieber, J., Mouttaki, H., Stams, A.J., Schink, B., et al. (2008). Physiology, ecology, phylogeny, and genomics of microorganisms capable of syntrophic metabolism. *Ann N Y Acad Sci* 1125, 58-72. doi: 10.1196/annals.1419.005.
- Mouttaki, H., Nanny, M.A., and McInerney, M.J. (2008). Use of benzoate as an electron acceptor by *Syntrophus aciditrophicus* grown in pure culture with crotonate. *Environ Microbiol* 10(12), 3265-3274. doi: 10.1111/j.1462-2920.2008.01716.x.
- Muller, U., Willnow, P., Ruschig, U., and Hopner, T. (1978). Formate dehydrogenase from *Pseudomonas oxalaticus*. *Eur J Biochem* 83(2), 485-498.
- Riemer, J., Hoepken, H.H., Czerwinska, H., Robinson, S.R., and Dringen, R. (2004). Colorimetric ferrozine-based assay for the quantitation of iron in cultured cells. *Anal Biochem* 331(2), 370-375. doi: 10.1016/j.ab.2004.03.049.
- Sazanov, L.A. (2007). Respiratory complex I: mechanistic and structural insights provided by the crystal structure of the hydrophilic domain. *Biochemistry* 46(9), 2275-2288. doi:  
10.1021/bi602508x.
- Sazanov, L.A., and Hinchliffe, P. (2006). Structure of the hydrophilic domain of respiratory complex I from *Thermus thermophilus*. *Science* 311(5766), 1430-1436. doi:  
10.1126/science.1123809.
- Schmehl, M., Jahn, A., Meyer zu Vilsendorf, A., Hennecke, S., Masepohl, B., Schuppler, M., et al. (1993). Identification of a new class of nitrogen fixation genes in *Rhodobacter*

- capsalatus*: a putative membrane complex involved in electron transport to nitrogenase. *Molecular and General Genetics MGG* 241(5), 602-615. doi: 10.1007/BF00279903.
- Schmidt, A., Muller, N., Schink, B., and Schleheck, D. (2013). A proteomic view at the biochemistry of syntrophic butyrate oxidation in *Syntrophomonas wolfei*. *PLoS One* 8(2), e56905. doi: 10.1371/journal.pone.0056905.
- Schonheit, P., Wascher, C., and Thauer, R.K. (1978). A rapid procedure for the purification of ferredoxin from Clostridia using polyethyleneimine. *FEBS Lett* 89(2), 219-222.
- Schuchmann, K., and Muller, V. (2012). A bacterial electron-bifurcating hydrogenase. *J Biol Chem* 287(37), 31165-31171. doi: 10.1074/jbc.M112.395038.
- Schut, G.J., and Adams, M.W.W. (2009). The Iron-Hydrogenase of *Thermotoga maritima* Utilizes Ferredoxin and NADH Synergistically: a New Perspective on Anaerobic Hydrogen Production. *J Bacteriol* 191(13), 4451.
- Seedorf, H., Dreisbach, A., Hedderich, R., Shima, S., and Thauer, R.K. (2004). F<sub>420</sub>H<sub>2</sub> oxidase (FprA) from *Methanobrevibacter arboriphilus*, a coenzyme F<sub>420</sub>-dependent enzyme involved in O<sub>2</sub> detoxification. *Arch Microbiol* 182(2-3), 126-137. doi: 10.1007/s00203-004-0675-3.
- Seedorf, H., Fricke, W.F., Veith, B., Brüggemann, H., Liesegang, H., Strittmatter, A., et al. (2008). The genome of *Clostridium kluyveri*, a strict anaerobe with unique metabolic features. *Proc Natl Acad Sci Unit States Am* 105(6), 2128.
- Seiler, W., Giehl, H., and Roggendorf, P. (1980). Detection of carbon monoxide and hydrogen by conversion of mercury oxide to mercury vapor.
- Sieber, J.R., Crable, B.R., Sheik, C.S., Hurst, G.B., Rohlin, L., Gunsalus, R.P., et al. (2015). Proteomic analysis reveals metabolic and regulatory systems involved in the syntrophic

- and axenic lifestyle of *Syntrophomonas wolfei*. *Front Microbiol* 6, 115. doi: 10.3389/fmicb.2015.00115.
- Sieber, J.R., Le, H.M., and McInerney, M.J. (2014). The importance of hydrogen and formate transfer for syntrophic fatty, aromatic and alicyclic metabolism. *Environ Microbiol* 16(1), 177-188. doi: 10.1111/1462-2920.12269.
- Sieber, J.R., McInerney, M.J., and Gunsalus, R.P. (2012). Genomic Insights into Syntrophy: The Paradigm for Anaerobic Metabolic Cooperation. *Annu Rev Microbiol* 66(1), 429-452. doi: 10.1146/annurev-micro-090110-102844.
- Soboh, B., Linder, D., and Hedderich, R. (2004). A multisubunit membrane-bound [NiFe] hydrogenase and an NADH-dependent Fe-only hydrogenase in the fermenting bacterium *Thermoanaerobacter tengcongensis*. *Microbiology* 150(Pt 7), 2451-2463. doi: 10.1099/mic.0.27159-0.
- Tanner, R.S. (2007). "Cultivation of Bacteria and Fungi," in *Manual of Environmental Microbiology, Third Edition*. American Society of Microbiology).
- Vignais, P.M., Billoud, B., and Meyer, J. (2001). Classification and phylogeny of hydrogenases. *FEMS Microbiol Rev* 25(4), 455-501.
- Walker, J.E. (1992). The NADH:ubiquinone oxidoreductase (complex I) of respiratory chains. *Q Rev Biophys* 25(3), 253-324.
- Wang, S., Huang, H., Kahnt, J., Mueller, A.P., Köpke, M., and Thauer, R.K. (2013a). NADP-specific electron-bifurcating [FeFe]-hydrogenase in a functional complex with formate dehydrogenase in *Clostridium autoethanogenum* grown on CO. *J Bacteriol* 195(19), 4373-4386. doi: 10.1128/JB.00678-13.

- Wang, S., Huang, H., Kahnt, J., and Thauer, R.K. (2013b). *Clostridium acidurici* Electron-Bifurcating Formate Dehydrogenase. *Appl Environ Microb* 79(19), 6176.
- Wang, S., Huang, H., Kahnt, J., and Thauer, R.K. (2013c). A Reversible Electron-Bifurcating Ferredoxin- and NAD-Dependent [FeFe]-Hydrogenase (HydABC) in *Moorella thermoacetica*. *J Bacteriol* 195(6), 1267.
- Zannoni, D. (1995). "Aerobic and Anaerobic Electron Transport Chains in Anoxygenic Phototrophic Bacteria," in *Anoxygenic Photosynthetic Bacteria*, eds. R.E. Blankenship, M.T. Madigan & C.E. Bauer. (Dordrecht: Springer Netherlands), 949-971.
- Zheng, Y., Kahnt, J., Kwon, I.H., Mackie, R.I., and Thauer, R.K. (2014). Hydrogen Formation and Its Regulation in *Ruminococcus albus*: Involvement of an Electron-Bifurcating [FeFe]-Hydrogenase, of a Non-Electron-Bifurcating [FeFe]-Hydrogenase, and of a Putative Hydrogen-Sensing [FeFe]-Hydrogenase. *J Bacteriol* 196(22), 3840.

## Supplemental Figures and Tables

**Supplemental Figure S3.1 Full Alignment of Beta Subunits from NADH-Dependent, Ferredoxin-Independent [FeFe]-Hydrogenases and Formate Dehydrogenases, Electron-Bifurcating, NADH-Dependent, Ferredoxin-Dependent [FeFe]-Hydrogenases and Formate Dehydrogenases, and NADH:Quinone Oxidoreductases.** Residues highlighted in yellow correspond to residues that appeared to be differentially conserved solely amongst the electron-bifurcating NADH-dependent, ferredoxin-dependent [FeFe]-Hydrogenases and Formate Dehydrogenases. The alignment of full-length the beta subunits was performed in MEGA7 using the ClustalW algorithm.



*T. maritima*\_HydB -----MFKNAKEFVQYAN 50  
*C. tencongenensis*\_HydB ----- 50  
*M. thermoacetica*\_HydB -----MIKSMEELQKFESQL 50  
*A. woodii*\_HydB ----- 50  
*R. albus*\_HydB -----MTIEELNKIKAAKA 50  
*C. acidurici*\_HylB -----MITINDLKIKKEETL 50  
*C. autoethanogenum*\_HytB ----- 50  
*D. fructosovorans*\_HydB ----- 50  
*S. wolfei*\_HydB ----- 50  
*S. aciditrophicus*\_HydB MITVQDIENVIAARGNAREHLMAILRDLENLSGRNVLDVSVLNTLAMKMD 50  
*C. necator*\_FdhB ----- 50  
*C. oxalaticus*\_FdhB ----- 50  
*M. extorquens*\_FdhB -----MSEASGTVRSFA 50  
*M. trichosporium*\_FdhB ----- 50  
*R. capsulatus*\_FdhB ----- 50  
*E. coli*\_NuoF ----- 50  
*T. thermophilus*\_Nqo1 ----- 50

*T. maritima*\_HydB KLKTLRE-----KKLNGVSIYVCGGTGCTAKGALKVYSAFEEL 100  
*C. tencongenensis*\_HydB -----MLYRSHVMVCGGTGCTSSGSDEVAERFIEEI 100  
*M. thermoacetica*\_HydB EAMQSQ-----EAGAKAKIVVGMGTCCGIAAGAREVMNAILDEV 100  
*A. woodii*\_HydB -----MAYKRSQILICGGTCTSSGSMLVVKELKKEEL 100  
*R. albus*\_HydB DIVKVRTIIAEEGEKLAKETGYRKQVLVCGGTGQSSSHSMDVLKALKEEL 100  
*C. acidurici*\_HylB PKVSLRGDIEG-GEK--IESTYRKQILLCRGTGCTSSKSDKIEERFQELL 100  
*C. autoethanogenum*\_HytB -----MSDKKTVNICCGTGCLAKGSMEVYEEEMKAQI 100  
*D. fructosovorans*\_HydB ----- 100  
*S. wolfei*\_HydB ----- 100  
*S. aciditrophicus*\_HydB LPQSAISGFTSFYTMFSTEPRAKFIIRVCKSGPCHVMGARTIFDVIENHL 100  
*C. necator*\_FdhB -----MITITTFVPRDSTALALGADVARAIAREA 100  
*C. oxalaticus*\_FdhB -----MSAAVNSTVNTIFVPRDSTALALGADEVARAIAREA 100  
*M. extorquens*\_FdhB HPGRGRNVARAVPKGRQVDPHAKVEIEELLGTRPRQRDLLIEHLHLIQDT 100  
*M. trichosporium*\_FdhB -----MTKVYVPRDMAALAVGAKRVLAATIEKEA 100  
*R. capsulatus*\_FdhB -----MKIWLPCDAAAKACGAEAVLAALRLEA 100  
*E. coli*\_NuoF ----- 100  
*T. thermophilus*\_Nqo1 ----- 100

*T. maritima*\_HydB KKRNLGQVTLEKIDDDKVTLNRTGCCGRSSGPLVKIMPYR----- 150  
*C. tencongenensis*\_HydB KKAGLDKEILVV-----RTGCFGLCELGPVVVYPEG----- 150  
*M. thermoacetica*\_HydB AKR-QLTGVTVS-----QTSICIGLCAQEPLVDVILPGQP----- 150  
*A. woodii*\_HydB VKHDILDEVEVV-----TTGCFGLCELGPVIVYPEG----- 150  
*R. albus*\_HydB AAKGIADEVLVV-----RTGCFGLCSLGPVIVYPEG----- 150  
*C. acidurici*\_HylB KEKGIQDEVNVV-----RTGCFGLCEAGPIVVVYPPG----- 150  
*C. autoethanogenum*\_HytB AKLGANAENVVK-----LKATGCDGLCEKGPVLKIYPDD----- 150  
*D. fructosovorans*\_HydB ----- 150  
*S. wolfei*\_HydB ----- 150  
*S. aciditrophicus*\_HydB GIRAGETTADGLFH-----LEECECLGLCSAAPAMMVNYDMH----- 150  
*C. necator*\_FdhB AARNEHVRIVRN-----GSRGMFWLEPLVEVQTGAG----- 150  
*C. oxalaticus*\_FdhB ARRGEAVRIVRN-----GSRGMFWLEPLVEVQTEAG----- 150  
*M. extorquens*\_FdhB YGQISADHLAALADEMSLAFAEVFEATATFYAHFDVVKEGEADIPRLTIRV 150  
*M. trichosporium*\_FdhB AARGEAIQIVRN-----GSRGLLWLEPLVEVETPEG----- 150  
*R. capsulatus*\_FdhB EKRGGALDIARN-----GSRGMIWLEPLLEVETPAG----- 150  
*E. coli*\_NuoF ----- 150  
*T. thermophilus*\_Nqo1 -----MTGPILSG----- 150

*T. maritima*\_HydB ---FFYSNVAPEDVPEIVDRTVLKGEP IERFLTDPLTGE-KVPRIEDTT 200  
*C. tencongensis*\_HydB ---VFYSRVKPEYVPEIVEEHLKGRPVRYIYGESLEEK-AIKPLEETP 200  
*M. thermoacetica*\_HydB --KVTYGVDAARAREIVGRHVVDGHI VTEWVVRQGDVAV---RPTYTELP 200  
*A. woodii*\_HydB ---TFYSRVEAADIPEMVEEHLVKGRPLDRLIYNEKGDGH-HPLSINELG 200  
*R. albus*\_HydB ---AFYAQATPEGIKRIVDEHLVNGEICKDILLYQETVHEDGSIISLYETN 200  
*C. acidurici*\_HylB ---TFYSHIKVEDVDQIVEEDLNNVVIKELLYKGSIDGD-KIKAISEVA 200  
*C. autoethanogenum*\_HytB ---IAYFKVKVEDVVDVVKKTLMNGEIIEKLLYFETATKQ-RLRNHKESE 200  
*D. fructosovorans*\_HydB -----MAATTE----- 200  
*S. wolfei*\_HydB ----- 200  
*S. aciditrophicus*\_HydB -----GNLSENIKEILDSYSAREPAPKA EYGP-----IEGRAVII 200  
*C. necator*\_FdhB --RVAYGPVSAADVPGLFDAGLLQGG EHALSQ-----VTEEIP 200  
*C. oxalaticus*\_FdhB --RVAYGPVSAEDVPALFDAGLLQGG AHALAHG-----LTEEIP 200  
*M. extorquens*\_FdhB CDSITCAMFGABELLETLQRELASDAVRVVRAPCVGLCDHAPAVEVGHFN 200  
*M. trichosporium*\_FdhB --RIGYGNVKPSDVP SLFDAGFLRGG AHPLSIG-----KVEEHP 200  
*R. capsulatus*\_FdhB --RIGFGPMTPADVPALFDA--LES--HPKALG-----LVEEIP 200  
*E. coli*\_NuoF ----- 200  
*T. thermophilus*\_Nqo1 ----- 200

*T. maritima*\_HydB LFKNQDFYIMEAIGESE-----DSIEDYIARSGYESLVKALTS-MTP 250  
*C. tencongensis*\_HydB FFRKQRRIALRNCVGINP-----EDIREAIAFDG YKALAKVLTE-MTP 250  
*M. thermoacetica*\_HydB FFKHQVRIALRNCGLIDP-----ESIG EYIAHDGYQALS KVLTT-MKP 250  
*A. woodii*\_HydB FFKQRRIALANCGVINP-----ENIDEYIGFDG YLALKEVLLT-MSP 250  
*R. albus*\_HydB FYRKQKRIALRNCVIDP-----EDIEEYIATDGY QALYKALTS-MTP 250  
*C. acidurici*\_HylB FYAKQKRVS LKNCGLINP-----ECIDEYI SHDGYFALHKALTE-MKP 250  
*C. autoethanogenum*\_HytB FCKRQYKIALRNVGEIDP-----ISLEDYVERGGY KALKKAISS-MKP 250  
*D. fructosovorans*\_HydB --KKQLRIATRNCGFIDP-----ESIDDIYALRG YEGLAKVLT--MTP 250  
*S. wolfei*\_HydB -MAEEMRIVLRNYGKIDP-----LKIDDYLAQGGY K SLEKARA--MNT 250  
*S. aciditrophicus*\_HydB NNSQQTRRLLENVGVKIDP-----ASIESYLQNGG YEAAARKAF AE--YSP 250  
*C. necator*\_FdhB FLKQQRERTFARVGITDP-----LSLDDYRAHEG FAGLERALA--MQP 250  
*C. oxalaticus*\_FdhB FLKQQRERTFARIGITDP-----LSLDDYRAHEG F AALERALS--MAP 250  
*M. extorquens*\_FdhB LHRADLASVRAAEVAEDTHAHIPTYVDYDAYRAGG GYATLERLRSGELPV 250  
*M. trichosporium*\_FdhB YWAKQTRVTFERVGVIDP-----VNLDDYVAHG GQGLAKAFE--IGP 250  
*R. capsulatus*\_FdhB FFKRQTRTLTFARCGRIEP-----LSLAQFAAAE GWAGLRKALK--MTP 250  
*E. coli*\_NuoF RTPETHPLTWRLRDKQP-----VWLDEYRSKNGY EGARKALTG--LSP 250  
*T. thermophilus*\_Nqo1 LDPRFERTLYAHVKGEGS-----WTLDYLLRHGGY ETAKRVLKE-KTP 250

\* :

*T. maritima*\_HydB EEI IETVKASGLRGRGGGFPTGLKWEFTRKAQGD--IKFVVCNGDEGDP 300  
*C. tencongensis*\_HydB EQVIEEVKKSGLRGRGGGFPTGVKWEFAYKQKET--PKYVVCNADEGDP 300  
*M. thermoacetica*\_HydB YEVIETIKKSGLRGRGGGFPTGLKWEFAYRSPGP--VKYFVCNADEGDP 300  
*A. woodii*\_HydB VDVINEVKASGLRGRGGGFPTGLKWQFAHDAVSE DGIKYVACNADEGDP 300  
*R. albus*\_HydB DEVVKEVLDSGIRGRGGAGFPTGRKWMFTK DAPGD--VKYVACNADEGDP 300  
*C. acidurici*\_HylB EDVIETMKKSGLKGRGGGFPTGLKWEFTAKATGD--QKYVLCNADEGDP 300  
*C. autoethanogenum*\_HytB EDVLEEITKSGLRGRGGAGFPTGRKWKTAADIDTS--PIYVVCNGDEGDP 300  
*D. fructosovorans*\_HydB AEVVDLVKRSGLRGRGGAGFPTGIKWGIALGNKAD--QKYMVCNADEGDP 300  
*S. wolfei*\_HydB ADLIAEVKKS NLRGRGGAGFNCGMKWSFAAGA QAD--QKYVICNADEGEP 300  
*S. aciditrophicus*\_HydB EQVIGIVKDSGLRGRGGAGFPVGVKWSFV PKGEMQ---KYVICNADEGEP 300  
*C. necator*\_FdhB AEIVQEVTD SGLRGGAAFPTGIKWKTVLGAQSA--VKYIVCNADEGDS 300  
*C. oxalaticus*\_FdhB AEIVQEVTD SGLRGGAAFPTGIKWKTVLGAQSA--VKYIVCNADEGDS 300  
*M. extorquens*\_FdhB DDVLKVLDDGGLRGLGGAGFPTGRKWSRVRGEPGP---RLMAVNGDEGEP 300  
*M. trichosporium*\_FdhB AKVIEEVTKSGLRGRGGAGFPAGIKWKTVADAPAD--RRYVVTNADEGDS 300  
*R. capsulatus*\_FdhB AEVVEEVLASGLRGRGGAGFPTGIKWRVAAAQAD--QKYIVCNVDEGDS 300  
*E. coli*\_NuoF DEIVNQVKDAGLKGRGGAGFSTGLKWSLMPKDESMN-IRYLLCNADEMEP 300  
*T. thermophilus*\_Nqo1 DEVIEEVKRSGLRGRGGAGFPTGLKWSFMPKDDGK--QHYLICNADESEP 300

.:: : .::\* \*\*.\* \* \*\* . \* \*\* .:

T. maritima\_HydB GAFMNR... 350  
C. tencongenensis\_HydB GAFM... 350  
M. thermoacetica\_HydB GAFM... 350  
A. woodii\_HydB GAFM... 350  
R. albus\_HydB GAFM... 350  
C. acidurici\_HylB GAFM... 350  
C. autoethanogenum\_HytB GAFM... 350  
D. fructosovorans\_HydB -EFM... 350  
S. wolfei\_HydB GTYK... 350  
S. aciditrophicus\_HydB GTFK... 350  
C. necator\_FdhB GTF... 350  
C. oxalaticus\_FdhB GTF... 350  
M. extorquens\_FdhB GTF... 350  
R. trichosporium\_FdhB GTF... 350  
M. capsulatus\_FdhB GSF... 350  
E. coli\_NuoF GTYK... 350  
T. thermophilus\_Nqo1 GSF... 350

T. maritima\_HydB IEDARK... 400  
C. tencongenensis\_HydB IQQARE... 400  
M. thermoacetica\_HydB ISQARE... 400  
A. woodii\_HydB IDQAKEY... 400  
R. albus\_HydB LDQARE... 400  
C. acidurici\_HylB IDEAKAK... 400  
C. autoethanogenum\_HytB INKAKD... 400  
D. fructosovorans\_HydB IDDARE... 400  
S. wolfei\_HydB INQAKEY... 400  
S. aciditrophicus\_HydB IDQARAK... 400  
C. necator\_FdhB IGIANA... 400  
C. oxalaticus\_FdhB IAIAHA... 400  
M. extorquens\_FdhB IAKLPE... 400  
M. trichosporium\_FdhB LEAARK... 400  
R. capsulatus\_FdhB IAMAKP... 400  
E. coli\_NuoF IAEATE... 400  
T. thermophilus\_Nqo1 IKEARAR... 400

T. maritima\_HydB PRPKPP... 450  
C. tencongenensis\_HydB PRPRPP... 450  
M. thermoacetica\_HydB PRPRPP... 450  
A. woodii\_HydB PRPRPP... 450  
R. albus\_HydB PRPRPP... 450  
C. acidurici\_HylB PRNKPP... 450  
C. autoethanogenum\_HytB PRAKYI... 450  
D. fructosovorans\_HydB PVTKPP... 450  
S. wolfei\_HydB PRFKPP... 450  
S. aciditrophicus\_HydB PRVRPP... 450  
C. necator\_FdhB VRAKPP... 450  
C. oxalaticus\_FdhB VRAKPP... 450  
M. extorquens\_FdhB PRHKPP... 450  
M. trichosporium\_FdhB VRAKPP... 450  
R. capsulatus\_FdhB VRAKPP... 450  
E. coli\_NuoF PRSKPP... 450  
T. thermophilus\_Nqo1 PRLKPP... 450

T. maritima\_HydB GTKMFS... 500  
C. tencongenensis\_HydB GTKVFAL... 500  
M. thermoacetica\_HydB GTKVFAL... 500  
A. woodii\_HydB GTKVFAL... 500  
R. albus\_HydB GTKVFAL... 500  
C. acidurici\_HylB GTKVFAL... 500  
C. autoethanogenum\_HytB GTKVFS... 500  
D. fructosovorans\_HydB GTKVFAL... 500  
S. wolfei\_HydB GTKVFT... 500  
S. aciditrophicus\_HydB GTKLYC... 500  
C. necator\_FdhB GTLFFQ... 500  
C. oxalaticus\_FdhB GTLFFQ... 500  
M. extorquens\_FdhB GLRSYS... 500  
M. trichosporium\_FdhB GTMPLQ... 500

*T. maritima*\_HydB SGACLS--EDFIDMPLDYDTLKKADAMVSGGGIVVITKKT~~CMV~~EVARFFL 550  
*C. tencongenesi*s\_HydB SGGCIP--AELLDTPIDYDSLTSAGAMMGGGGLVVMDEDT~~CMV~~NVAKFFL 550  
*M. thermoacetica*\_HydB SGGCIP--AEHLDAPIDYENLTALGTIMGSGGLIIMDEDT~~CMV~~DVAKFFM 550  
*A. woodii*\_HydB SGGCLP--ESLLDTEIDYDNLIAAGSMMSGGGLIVMDEDN~~CMV~~DVARFFL 550  
*R. albus*\_HydB SGGCIP--AQHIDTPIDYESLAALGSMMGGGGLIVMDEDN~~CMV~~DVSKFYL 550  
*C. acidurici*\_HylB SGGCIT--ADYIDTEIDFATLNLGLSMMGGGGMIVMDEDT~~CMV~~DIARFFL 550  
*C. autoethanogenum*\_HytB SGGCLP--AEYLDLPVDYDTLVKADSMMSGGGMIVMDDRT~~CMV~~DVTRYL 550  
*D. fructosovorans*\_HydB SGGALA--NKDLLVAIDYESLAACKSIMGGGGMVVMDEDD~~CMV~~SVAKFFL 550  
*S. wolfei*\_HydB SGAFIP--DALLDTVPVAFDSMSAIGATLGSATFVIDESRDIVDVATRIA 550  
*S. aciditrophicus*\_HydB AGGILG--ADLMDLPLDIDSTIKAGVTLGSGVVLVCDQETCAVDLFLNLV 550  
*C. necator*\_FdhB LGAYLP--ESRFDVPLDYEAAYAAGGGVGHGGIVVFDDETVDMAKQARYAM 550  
*C. oxalaticus*\_FdhB LGAYLP--ESRFDVPLDYEAAYAAGGGVGHGGIVVFDDETVDMAKQARYAM 550  
*M. extorquens*\_FdhB SGGILP--ASMNDIPLDFGTLEKYGCFIGSAAVVILSDQDDVRGAALNLM 550  
*M. trichosporium*\_FdhB LGAYVP--PSLFDTPFDYEAFAQHDSLIGHGGVLFVFDDETVDMAQMARFGM 550  
*R. capsulatus*\_FdhB LGAYHP--VSDYHLPCYEQFAGQGGLVGHAGLVVHDDTADMLKLARFAM 550  
*E. coli*\_NuoF GTDFLT--EAHLDPMEFESIGKAGSRLGTALAMAVDHEINMVSLVRNLE 550  
*T. thermophilus*\_Nqo1 STPPLPFTTEVLDTPMSYEHLQAKGSMGLTGGVILIPERVSMVDAMWNLT 550

. . . : \* . . .

*T. maritima*\_HydB DFTKRESCGKCVPCREGTM-QAYNILEKFTHGKATYEDLKTLEHLSKTIK 600  
*C. tencongenesi*s\_HydB EFTVDESCGKCPCPRIGTK-RMLELLDKITSGKGEEDIEKLEELAKTIK 600  
*M. thermoacetica*\_HydB DFVKDESCGKCTPCRIGTT-RMLEILNRITRGGQEEKDLDDLVELARQIK 600  
*A. woodii*\_HydB DFTQDESCGKCPPCRIGTK-RMLEILERICDGGKVEGDIERLEELAVGIK 600  
*R. albus*\_HydB NFTVDESCGKCTPCRIGTR-KLLQLLEKITDGGKEMEDLEKIQLDATHMK 600  
*C. acidurici*\_HylB DFTVEESCGKCTPCRIGTK-RMLELLEKITDGGKEMEDLDRLES LAETIK 600  
*C. autoethanogenum*\_HytB SFLAEESCGKCVPCREGVK-RMLEILTDICNGDGKEGDI EELLEICSMTS 600  
*D. fructosovorans*\_HydB DFTMDETCGKCTPCRIGSK-RLYEILDRTKGGKTRADLDRKLSLSEIK 600  
*S. wolfei*\_HydB GFFEHEESCGKCAPREGTA-RTAELMEKINEGRGSNKDVALLEKLGTVMS 600  
*S. aciditrophicus*\_HydB NFFEHEESCGQICPKLGTS-QLHYVAQKFAMREAEKDIQLMIDTAKMMK 600  
*C. necator*\_FdhB EFCAIESCGKCTPCRIGST-RGVEVMDRIIAGEQPVKHVALVRDLCDTML 600  
*C. oxalaticus*\_FdhB EFCAIESCGKCTPCRIGST-RGVEVMDRIIAGEQPVKHVKLVDRDLCDTML 600  
*M. extorquens*\_FdhB KFFEDEESCGQCTPCRSGTQ-----KARMLMENGVDTDLLGELAQCMR 600  
*M. trichosporium*\_FdhB EFCAIESCGKCTPCRIGST-RGVETIDRIVEGVDVEANI ELLSDLCHTMK 600  
*R. capsulatus*\_FdhB EFCAIESCGTCTPCRIGAV-RGVEVIDRIAAGD--ASAMPLDLDLCQTMK 600  
*E. coli*\_NuoF EFFARESCGWCTPCRDLGP-WSVKILRALEREGEQPGDIETLEQLCRFLG 600  
*T. thermophilus*\_Nqo1 RFYAHESCGKCTPCRREGVAGFMVNLFAKIGTGQGEKDVENLEALLPLIE 600

\* \* : \*\* \* \*\* : \*

*T. maritima*\_HydB TA-SLCGLGKTA~~PNP~~ILSTLKLFREEYIAHIEG-ECPSGMCTAFKKYVIN 650  
*C. tencongenesi*s\_HydB AT-ALCGLGQTA~~PNP~~VLSTLRYFRHEYEAHIKEKRCPAGVCTALLSFVID 650  
*M. thermoacetica*\_HydB DT-ALCGLGQTA~~PNP~~VLSTITYFRDEYLAHIRDHRCPAHVQC ELLSYVID 650  
*A. woodii*\_HydB SS-ALCGLGQTA~~PNP~~VLSTIRFRDEYEAHIRDKKCPAGVCKHLLDFKIN 650  
*R. albus*\_HydB SS-SLCALGQSA~~PNP~~VLSTLQYFGDEYLAHIKEKKCPAGVCKNLLQYEII 650  
*C. acidurici*\_HylB SS-SLCGLGQTA~~PNP~~VLSTLKYFRDEYEAHVVDKDKCPAGACQSLEFYIT 650  
*C. autoethanogenum*\_HytB KA-SLCSLGKSA~~PNP~~VIASIRYFRDEFEEHIKNKRCRAGVCKLTTFGID 650  
*D. fructosovorans*\_HydB DT-ALCGLGQTM~~PNP~~ILSTMDTFANEYEAHVDDKDKCPAHVCTALLTYTID 650  
*S. wolfei*\_HydB YS-CLCGLGQAAPAVLTTIKHFADYEAKFV----- 650  
*S. aciditrophicus*\_HydB LA-SLCALGQSPILPIETMIRNFRFEFVKHCDPDYECPCDASLQAYYL 650  
*C. necator*\_FdhB NG-SLCAMGGMTPYPVLSALNEFPEDFGLASNPAKAA----- 650  
*C. oxalaticus*\_FdhB YG-SLCAMGGMTPYPVLSALNEFPEDFGLAPNPAHAAKAA----- 650  
*M. extorquens*\_FdhB DA-SICGLGQAASNVPSTVIKYFPDLFPEPRAVAEE----- 650  
*M. trichosporium*\_FdhB FG-SLCALGGFAPYPVESALRHYPEDFRKATLPAAAE----- 650  
*R. capsulatus*\_FdhB LG-SLCALGGFTYPVQSAIRHFPADFP CAREAAE----- 650  
*E. coli*\_NuoF PGKTFCAHAPGAVEPLQSAIKYFREEFEAGIKQFFSNTHLINGIQPNLLK 650  
*T. thermophilus*\_Nqo1 GR-SFCPLADAAVWPVKGLSRHFKDQYLALAREKRPVPRPSLWR----- 650

:\* . . \* : : : :

```

T. maritima_HydB      PDICKGCGLCARSCPQNAITGERGKPYTIDQEKCVKCGLCASKCPFFKAIE 700
C. tencongenensis_HydB PEKCKACGICAKNCPVGAISGKPKTPYVIDQEKCIKCGTCIDKCPFGAIY 700
M. thermoacetica_HydB AGKCTGCGACSRVCPVGAISGGKKEAHQIDPAACIKCGSCYEKCRFGAIT 700
A. woodii_HydB       ADTCKGCGICAKKCPADAISGEKKKPYNIDTSKCIKCGACIEACPFPGSIS 700
R. albus_HydB        ADKCKGCTLCARNCPANAITGTVKNPHVIDTTRKCIKCGVCMNNCKFGAII 700
C. acidurici_HylB    -DKCIGCTKCARQCPASCIDGKVKERHVINTSACVKCGACADVCPVNAVI 700
C. autoethanogenum_HytB EDKCKGCDMCKKNCPADCITGEIKKPHTIDADRCLRCNCMNICKFDPAVK 700
D. fructosovorans_HydB PARCTGCGGLCTRVCPEECISGTRKQPHTIDTTRKCIKCGACYDKCKFDSII 700
S. wolfei_HydB      ----- 700
S. aciditrophicus_HydB ----- 700
C. necator_FdhB     ----- 700
C. oxalaticus_FdhB  ----- 700
M. extorquens_FdhB  ----- 700
M. trichosporium_FdhB ----- 700
R. capsulatus_FdhB  ----- 700
E. coli_NuoF        ERW----- 700
T. thermophilus_Nqo1 ----- 700

```

```

T. maritima_HydB      LV- 703
C. tencongenensis_HydB KK* 703
M. thermoacetica_HydB RE- 703
A. woodii_HydB       KA- 703
R. albus_HydB        KK- 703
C. acidurici_HylB    KR- 703
C. autoethanogenum_HytB VL- 703
D. fructosovorans_HydB KQ- 703
S. wolfei_HydB      --- 703
S. aciditrophicus_HydB --- 703
C. necator_FdhB     --- 703
C. oxalaticus_FdhB  --- 703
M. extorquens_FdhB  --- 703
M. trichosporium_FdhB --- 703
R. capsulatus_FdhB  --- 703
E. coli_NuoF        --- 703
T. thermophilus_Nqo1 --- 703

```

### Supplemental Table S3.1 Genbank Accession Numbers for Protein Sequences in Chapter 3.

Source Organism	Subunit	GenBank Protein Accession Number
<i>Acetobacterium woodii</i>	HydA	AFA49450
<i>Acetobacterium woodii</i>	HydB	AFA49451
<i>Acetobacterium woodii</i>	HydC	AFA49452
<i>Acetobacterium woodii</i>	HydD	AFA49454
<i>Caldanaerobacter tencongenensis</i>	HydA	AAM24150
<i>Caldanaerobacter tencongenensis</i>	HydB	AAM24149
<i>Caldanaerobacter tencongenensis</i>	HydC	AAM24148
<i>Clostridium acidurici</i>	FdhA	AFS79904

<i>Clostridium acidurici</i>	FdhA	AFS79905
<i>Clostridium acidurici</i>	FdhB	AFS79906
<i>Clostridium acidurici</i>	FdhC	AFS79907
<i>Clostridium autoethanogenum</i>	HytA	AGT29713
<i>Clostridium autoethanogenum</i>	HytB	AGT29710
<i>Clostridium autoethanogenum</i>	HytC	AGT29709
<i>Clostridium autoethanogenum</i>	HytD	AGT29711
<i>Clostridium autoethanogenum</i>	HytE1	AGT29712
<i>Clostridium autoethanogenum</i>	HytE2	AGT29714
<i>Clostridium autoethanogenum</i>	FdhA	AGT29705
<i>Cupriavidus necator</i>	FdhA	WP_011614623
<i>Cupriavidus necator</i>	FdhB	WP_011614622
<i>Cupriavidus necator</i>	FdhC	WP_011614621
<i>Cupriavidus necator</i>	FdhD	WP_010811246
<i>Cupriavidus oxalaticus</i>	FdhA	WP_063236918
<i>Cupriavidus oxalaticus</i>	FdhB	WP_063236917
<i>Cupriavidus oxalaticus</i>	FdhC	WP_063236916
<i>Cupriavidus oxalaticus</i>	FdhD	WP_063236919
<i>Desulfovibrio fructosivorans</i>	HydA	AAA87057
<i>Desulfovibrio fructosivorans</i>	HydB	AAA87056
<i>Desulfovibrio fructosivorans</i>	HydC	AAA87054
<i>Desulfovibrio fructosivorans</i>	HydD	AAA87055

<i>Escherichia coli str. K-12</i>	NuoE	NP_416788
<i>Escherichia coli str. K-12</i>	NuoF	NP_416787
<i>Escherichia coli str. K-12</i>	NuoG	NP_416786
<i>Methylobacterium extorquens</i>	FdhA	ACS42636
<i>Methylobacterium extorquens</i>	FdhB	ACS42635
<i>Methylobacterium trichosporium</i>	FdhA	WP_003614381
<i>Methylobacterium trichosporium</i>	FdhB	WP_003614380
<i>Methylobacterium trichosporium</i>	FdhC	WP_003614379
<i>Methylobacterium trichosporium</i>	FdhD	WP_003613007
<i>Moorella thermoacetica</i>	HydA	ABC20019
<i>Moorella thermoacetica</i>	HydB	ABC20020
<i>Moorella thermoacetica</i>	HydC	ABC20021
<i>Rhodospirillum rubrum</i>	FdhA	ADE86759
<i>Rhodospirillum rubrum</i>	FdhB	ADE86760
<i>Rhodospirillum rubrum</i>	FdhC	ADE86761
<i>Ruminococcus albus</i>	HydA	ADU23430
<i>Ruminococcus albus</i>	HydB	ADU23431
<i>Ruminococcus albus</i>	HydC	ADU23432
<i>Syntrophomonas fumaroxidans</i>	HydA	ABK16541
<i>Syntrophomonas fumaroxidans</i>	HydB	ABK16542
<i>Syntrophomonas fumaroxidans</i>	HydC	ABK16543
<i>Syntrophomonas wolfei</i>	FdhA	ABI68106/ABI68107

(Swol_0783-Swol_0786)		
<i>Syntrophomonas wolfei</i>	FdhB	ABI68105
(Swol_0783-Swol_0786)		
<i>Syntrophomonas wolfei</i>	FdhC	ABI68104
(Swol_0783-Swol_0786)		
<i>Syntrophomonas wolfei</i>	FdhA	ABI68342/ ABI68343
(Swol_1024/Swol_1025 Swol_1028/Swol_1029)		
<i>Syntrophomonas wolfei</i>	FdhB	ABI68338
(Swol_1024/Swol_1025 Swol_1028/Swol_1029)		
<i>Syntrophomonas wolfei</i>	FdhC	ABI68339
(Swol_1024/Swol_1025 Swol_1028/Swol_1029)		
<i>Syntrophomonas wolfei</i>	FdhA	ABI69128/ ABI68343
(Swol_1828-Swol_1831)		
<i>Syntrophomonas wolfei</i>	FdhB	ABI69126
(Swol_1828-Swol_1831)		
<i>Syntrophomonas wolfei</i>	FdhC	ABI69127
(Swol_1828-Swol_1831)		
<i>Syntrophomonas wolfei</i>	HydA	ABI68331
<i>Syntrophomonas wolfei</i>	HydB	ABI68332



<i>Syntrophomonas wolfei</i>	HydC	ABI68333
<i>Syntrophomonas zehnderi</i>	HydA	WP_046500146
<i>Syntrophomonas zehnderi</i>	HydB	WP_046500148
<i>Syntrophomonas zehnderi</i>	HydC	WP_046500150
<i>Syntrophothermus lipocalidus</i>	HydA	WP_013174729
<i>Syntrophothermus lipocalidus</i>	HydB	WP_013174328
<i>Syntrophothermus lipocalidus</i>	HydC	WP_013174327
<i>Syntrophus aciditrophicus</i> (Syn_00629-Syn_00631)	FdhA	ABC76020/ABC76021
<i>Syntrophus aciditrophicus</i> (Syn_00629-Syn_00631)	FdhB	ABC76022
<i>Syntrophus aciditrophicus</i> (Syn_02137-Syn_02139)	FdhA	ABC76957/ABC76958
<i>Syntrophus aciditrophicus</i> (Syn_02137-Syn_02139)	FdhB	ABC76959
<i>Syntrophus aciditrophicus</i>	HydA	ABC76974
<i>Syntrophus aciditrophicus</i>	HydB	ABC76975
<i>Thermosyntropha lipolytica</i>	HydA	WP_073091114
<i>Thermosyntropha lipolytica</i>	HydB	WP_073091112
<i>Thermosyntropha lipolytica</i>	HydC	WP_073091109
<i>Thermotoga maritima</i>	HydA	AAD36496
<i>Thermotoga maritima</i>	HydB	AAD36495

<i>Thermotoga maritima</i>	HydC	AAD36494
<i>Thermus thermophilus</i>	Nqo1	AAA97943
<i>Thermus thermophilus</i>	Nqo2	AAA97942
<i>Thermus thermophilus</i>	Nqo3	AAA97944

---

**CHAPTER 4: NADH-Dependent, Ferredoxin-Independent Hydrogen Production as a  
Detailed Example of Syntrophic Metabolism**

## **Characteristics of Proposed NADH-Dependent, Ferredoxin-Independent Hydrogen and Formate Production by *S. wolfei* and *S. aciditrophicus***

In Chapter 3, I argued that the differences between the beta subunits of electron-bifurcating NADH-dependent, ferredoxin-dependent [FeFe]-hydrogenases and those of two NADH-dependent, ferredoxin-independent [FeFe]-hydrogenases from *S. wolfei* and *S. aciditrophicus* could explain the observed ferredoxin dependence. The basis for this differentiation included a number of features found in ferredoxin-dependent [FeFe]-hydrogenases but not in ferredoxin-independent [FeFe]-hydrogenases such as: the presence of an additional N-terminal [2Fe-2S] center, two C-terminal [4Fe-4S] centers, specific residues near the predicted NADH and FMN binding sites, and a glycine-rich region that is proposed to be a SLBB domain. Glycine-rich regions are characteristic of some flavin and NADPH binding sites, as proposed for the *E. coli* NADPH:flavin oxidoreductase (Ingelman et al., 1999) and NADH:ubiquinone oxidoreductase (Nqo1) (Sazanov, 2007; Berrisford and Sazanov, 2009), which suggests that the glycine-rich region may be a flavin binding site. The above listed features present only in the electron-bifurcating [FeFe]-hydrogenases could facilitate an alternative electron flow path in the beta subunit that mediates the electron-confurcating reaction from NADH and reduced ferredoxin.

During syntrophic metabolism in *S. wolfei* and *S. aciditrophicus*, the re-oxidation of NADH can also be coupled to the production of formate. The *S. wolfei* genome is predicted to encode three multimeric, cytoplasmic formate dehydrogenases (Sieber et al., 2010) while the *S. aciditrophicus* genome is predicted to contain two formate dehydrogenases (McInerney et al., 2007; Sieber et al., 2012). As subunit and domain composition and other features of the beta subunits of these formate dehydrogenases are similar to those of the NADH-dependent,

ferredoxin-independent [FeFe]-hydrogenases, I propose that the formate dehydrogenases in *S. wolfei* and *S. aciditrophicus* are also NADH-dependent, ferredoxin-independent (see Figure 23, see alignment in supplemental figures).

**Figure 23. Conserved Domains in Predicted Cytoplasmic *S. wolfei* and *S. aciditrophicus***

**Formate Dehydrogenases Suggest Function as NADH-Dependent, Ferredoxin-Independent.**

Source Locus Tags  $\alpha$   $\beta$   
 Organism(s) Of Encoding Genes

*S. wolfei* NADH-Dependent, Ferredoxin-Independent [FeFe]-Hydrogenases and Formate Dehydrogenases

<i>S. wolfei</i>	Swol_1017, Swol_1018 Swol_1019	2Fe-2S	4Fe-4S	4Fe-4S	H-Cluster	2Fe-2S	Flavin	4Fe-4S
<i>S. wolfei</i>	Swol_0783, Swol_0784 Swol_0785, Swol_0786	2Fe-2S	4Fe-4S	4Fe-4S	Mo or W	2Fe-2S	Flavin	4Fe-4S
<i>S. wolfei</i>	Swol_1024, Swol_1025 Swol_1028, Swol_1029	2Fe-2S	4Fe-4S	4Fe-4S	Mo or W	2Fe-2S	Flavin	4Fe-4S
<i>S. wolfei</i>	Swol_1828, Swol_1829 Swol_1830, Swol_1831	2Fe-2S	4Fe-4S	4Fe-4S	Mo or W	2Fe-2S	Flavin	4Fe-4S

*S. aciditrophicus* NADH-Dependent, Ferredoxin-Independent [FeFe]-Hydrogenases and Formate Dehydrogenases

<i>S. aciditrophicus</i>	Syn_01369, Syn_01370	2Fe-2S	4Fe-4S	4Fe-4S	H-Cluster	2Fe-2S	Flavin	4Fe-4S
<i>S. aciditrophicus</i>	Syn_00629-Syn_00630 Syn_00631	2Fe-2S	4Fe-4S	4Fe-4S	Mo or W	2Fe-2S	Flavin	4Fe-4S
<i>S. aciditrophicus</i>	Syn_02137-Syn_02138 Syn_02139	2Fe-2S	4Fe-4S	4Fe-4S	Mo or W	2Fe-2S	Flavin	4Fe-4S

Beta Subunit Properties

1. N-terminal [2Fe-2S]: Absent 7/7
2. NADH Binding Site (Serine/Threonine): 7/7
3. FMN (Tyrosine): 7/7
4. SLBB Domain (residues GGPSG): Absent 7/7
5. C-terminal 2 x [4Fe-4S]: Absent 7/7

These enzymes could allow both organisms to produce formate from NADH without requiring ferredoxin, similar to how both organisms produce hydrogen from NADH without ferredoxin. It is impossible to discern which observed differences between the NADH-dependent, ferredoxin-independent [FeFe]-hydrogenases/formate dehydrogenases and the electron bifurcating NADH-dependent, ferredoxin-dependent [FeFe]-hydrogenases/formate dehydrogenases are ultimately responsible for the difference in ferredoxin-dependence. However, as all of the proposed differences for ferredoxin-independence were present in the *S. wolfei* and *S. aciditrophicus* formate dehydrogenases, it seems reasonable to conclude that they are likely NADH-dependent and ferredoxin-independent.

As detailed by the research presented in Chapters 2 and 3, *S. wolfei* and *S. aciditrophicus* both possess cytoplasmic [FeFe]-hydrogenases capable of producing hydrogen from NADH independently of ferredoxin. While less favorable for hydrogen production, NADH-dependent, ferredoxin-independent hydrogen production allows *S. wolfei* and *S. aciditrophicus* to re-oxidize NADH without having to convert NADH to reduced ferredoxin. This avoids the energy costly step of reverse electron transfer needed to make reduced ferredoxin from NADH, which could occur by either a Rnf Complex or FixABCX complex. By avoiding the reverse electron transfer from NADH to ferredoxin, more energy can be conserved for growth as exemplified in the following discussion (Figures 24 and 25).

**Figure 24. Butyrate Oxidation by *S. wolfei* with NADH-Dependent, Ferredoxin-Independent Hydrogen Production.** Values shown with the assumption that hydrolysis of one ATP to ADP is equivalent to translocation of 3.35 protons. The actual ATP to proton ratio is dependent on the number of ion binding sites within the *c* ring of the ATP synthase (Müller and Hess, 2017) and has not been specifically determined for *S. wolfei*.

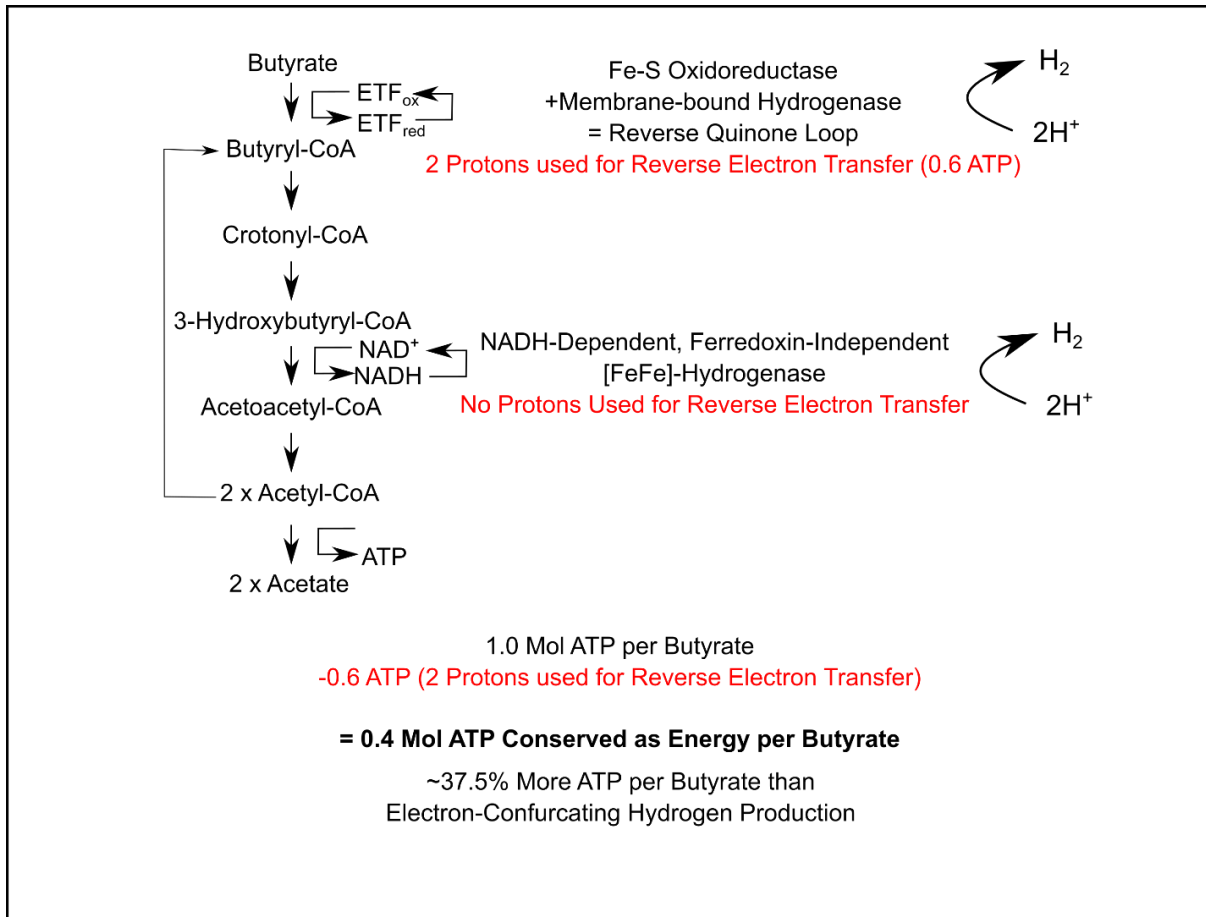
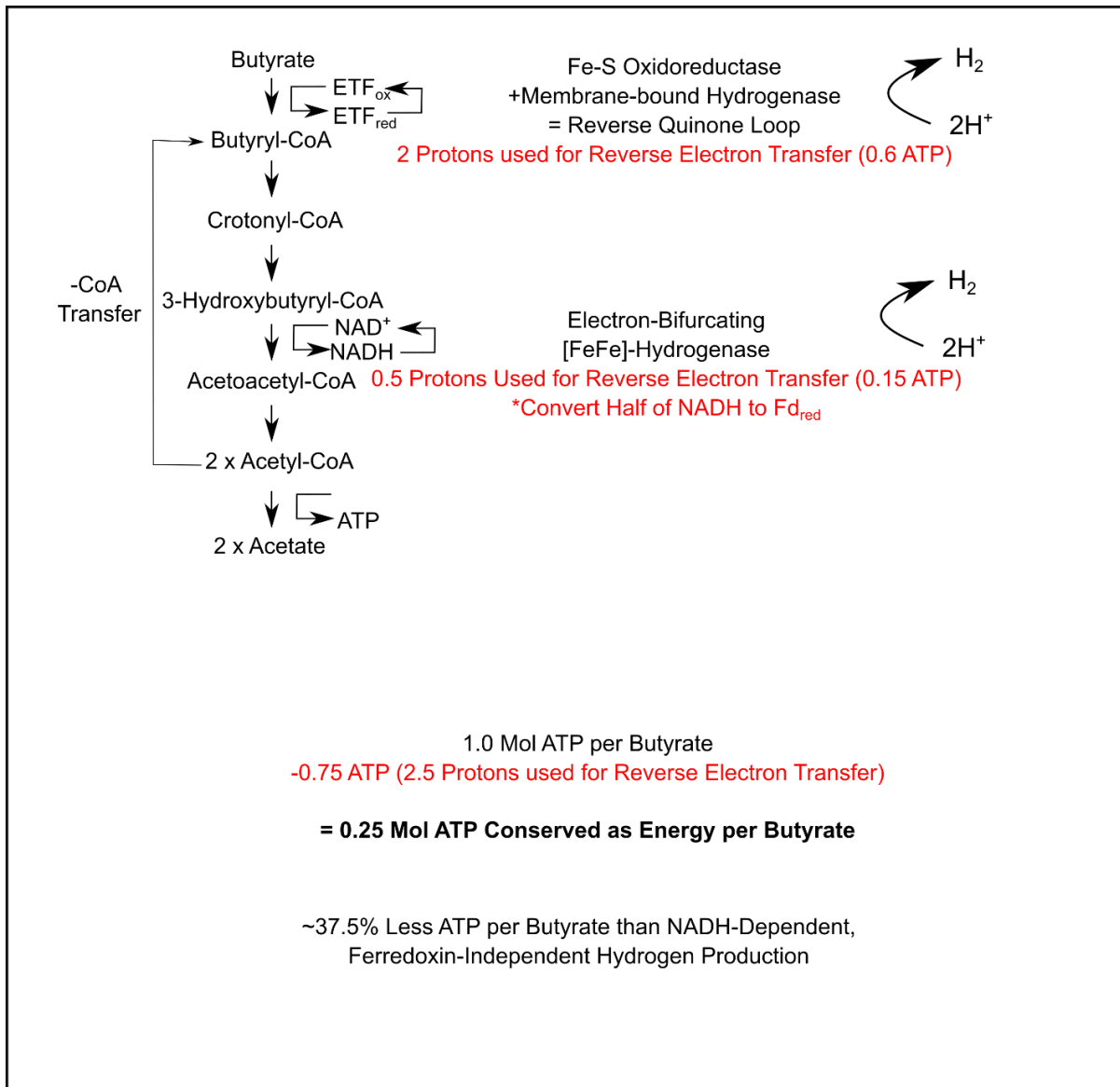




**Figure 25. Butyrate Oxidation by *S. wolfei* with NADH-Dependent, Ferredoxin-Dependent, Electron-Confurcating Hydrogen Production.** Values shown with the assumption that hydrolysis of one ATP to ADP is equivalent to translocation of 3.35 protons. Also assumes that one proton is used to convert one pair of electrons from NADH to reduced ferredoxin.

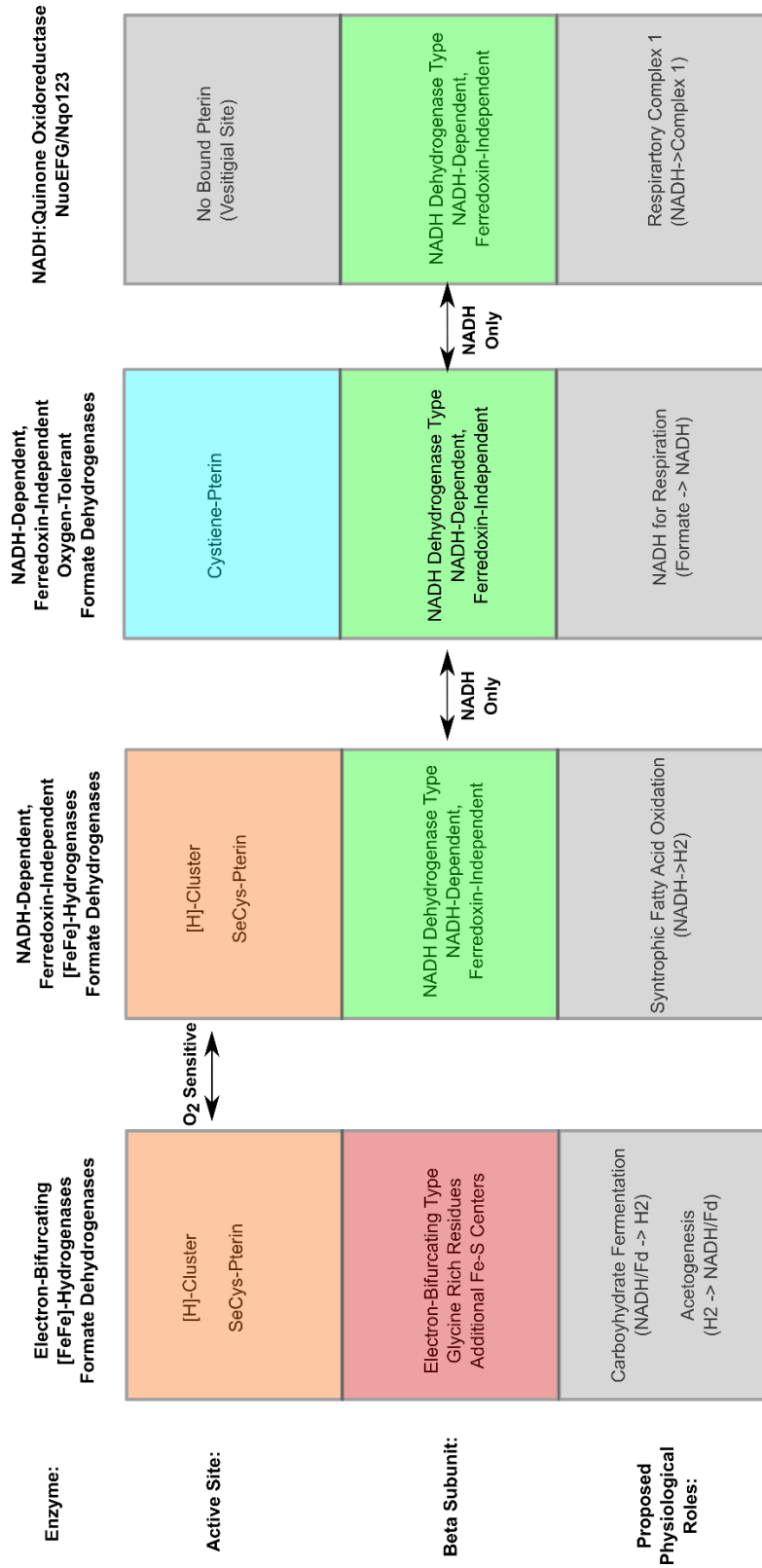


Syntrophic butyrate metabolism by *S. wolfei* when modeled using NADH dependent hydrogen production is predicted to produce 0.4 moles of ATP per mol of butyrate (Figure 24). In contrast, if half of the NADH is converted to ferredoxin as needed for electron bifurcation, the predicted ATP yield from butyrate is 0.25 moles of ATP per butyrate, which is 37.5% less than when a non-electron bifurcating hydrogenase is used (Figure 25). Thus, NADH-dependent, ferredoxin-independent hydrogen production allows more energy to be conserved per mole of butyrate.

It is unclear if NADH-dependent, ferredoxin-dependent, electron-confurcating hydrogen production would provide any advantage for a butyrate oxidizer like *S. wolfei*. This determination is based on the manner in which the  $\text{Etf}_{\text{red}}$  cofactors are re-oxidized. The current model for  $\text{Etf}_{\text{red}}$  reoxidation involves the use of a reverse quinone loop where the predicted redox potential of the electrons ( $E' = -326 \text{ mV}$ ) used to produce hydrogen or formate from  $\text{Etf}_{\text{red}}$  would be similar to NADH ( $E' = -320 \text{ mV}$ ). Thus, the higher hydrogen partial pressures generated from confurcated electrons from NADH and ferredoxin ( $E' = -365 \text{ mV}$ ) by an electron-confurcating hydrogenase may inhibit  $\text{Etf}_{\text{red}}$  re-oxidation. In order for  $\text{Etf}_{\text{red}}$  re-oxidation to occur, hydrogen consumption by a hydrogen-consuming partner would have to lower the hydrogen partial pressure from  $\sim 1000$  pascals ( $E' = -365 \text{ mV}$ ) to closer to 60 pascals ( $E' = -326 \text{ mV}$ ) that is currently predicted for the redox potential of the reverse quinone loop model. However, it should be noted that redox potential of electrons from the reverse quinone loop have not yet been determined. Regardless of what the redox potential of the quinone pool is, this example illustrates that the utilization of NADH-dependent, ferredoxin-independent [FeFe]-hydrogenases and formate dehydrogenases as the primary means of NADH re-oxidation provides an energetic advantage during close association with hydrogenotrophic methanogens.

This dissertation argues that similarities in the beta subunit may explain why *S. wolfei* and *S. aciditrophicus* [FeFe]-hydrogenases and formate dehydrogenases utilize NADH to produce formate and hydrogen without requiring ferredoxin. However, it should be noted that several aspects of the alpha subunits from the *S. wolfei* and *S. aciditrophicus* [FeFe]-hydrogenases and formate dehydrogenases are shared with the electron-bifurcating formate dehydrogenases and [FeFe]-hydrogenases (Figure 26). More specifically, the nature of the catalytic sites for hydrogen and formate reduction are shared. The Nqo1 subunit has a vestigial metallopterin binding site (Sazanov and Hinchliffe, 2006). The oxygen-tolerant, NADH-dependent, ferredoxin-independent formate dehydrogenases ligand the metallopterin cofactor with a cysteine (Muller et al., 1978; Jollie and Lipscomb, 1991; Laukel et al., 2003; Niks and Hille, 2019). However, the *S. wolfei* and *S. aciditrophicus* are predicted to use selenocysteine to ligand the metallopterin cofactor and such selenocysteine-containing formate dehydrogenases are known to be highly oxygen sensitive (Ferry, 1990). The *S. wolfei* and *S. aciditrophicus* NADH-dependent, ferredoxin-independent [FeFe]-hydrogenases have the same [H]-cluster as the electron-bifurcating [FeFe]-hydrogenases (Figure 26). The H-cluster is also known to be highly oxygen sensitive and rapidly inactivated in the presence of oxygen (Peters et al., 2015). Thus, the alpha subunits of *S. wolfei* and *S. aciditrophicus* formate dehydrogenases and [FeFe]-hydrogenases share catalytic site properties with alpha subunit of the electron-bifurcating formate dehydrogenases and [FeFe]-hydrogenases that render them oxygen sensitive but differ in the type of beta subunit (see Figure 26).

**Figure 26. Features of *S. wolfei* and *S. aciditrophicus* [FeFe]-Hydrogenases and Formate Dehydrogenases Match Proposed Physiological Role, Hydrogen Production from NADH.**



[FeFe]-hydrogenases and selenocysteine-ligand formate dehydrogenases allow faster hydrogen and formate production rates than cysteine-ligand formate dehydrogenases and NADH-dependent group 3 [NiFe]-hydrogenases. The trade-off of, inactivation by oxygen, may not be detrimental as the required partner, in this case a methanogen, is also obligately anaerobic. Group 3 [NiFe]-hydrogenases are notably more tolerant of oxygen and can catalyze the production of hydrogen coupled to oxidation of NADH (Peters et al., 2015). The group 3 [NiFe]-hydrogenases have recently been suggested to be capable of electron-bifurcation (Gutekunst and Schulz, 2018; Preissler et al., 2018), and do not appear to be as specific for which reduced cofactors are used as physiological electron donors (Peters et al., 2015; Gutekunst and Schulz, 2018; Preissler et al., 2018). Group 3 [NiFe]-hydrogenases also have different subunit compositions that the NADH-dependent [FeFe]-hydrogenases (Peters et al., 2015; Peters et al., 2018). It is interesting to note that the specific activity for hydrogen production from NADH by the *S. wolfei* Hyd1ABC [FeFe]-hydrogenase ( $6.6 \text{ U} \cdot \text{mg}^{-1}$  at  $37 \text{ }^\circ\text{C}$ ) was higher than that of any NADH-dependent [NiFe]-hydrogenases (Preissler et al., 2018), with the highest specific activity for hydrogen production from being  $2.81 \text{ U} \cdot \text{mg}^{-1}$  at  $60 \text{ }^\circ\text{C}$  with the HoxHYFUE from *Synechocystis* sp. PCC 6803 (Schmitz et al., 2002). The *S. wolfei* and *S. aciditrophicus* [FeFe]-hydrogenases and formate dehydrogenases possess combinations of oxygen sensitive active sites with superior catalysis rates for hydrogen and formate production that are combined with beta subunits that allow the oxidation of NADH without requiring reduced ferredoxin. This combination would be ideal for their proposed physiological role, the rapid re-oxidation of NADH to produce only low partial pressures of hydrogen and formate during syntrophic fatty acid oxidation.

A recent bioinformatic classification of over 714 [FeFe]-hydrogenase amino acid sequences did not identify NADH-dependent, ferredoxin-independent [FeFe]-hydrogenases as a group separate from NADH-dependent, ferredoxin-dependent electron-bifurcating [FeFe]-hydrogenases, possibly due to the criteria used in the classification scheme (Poudel et al., 2016). Classifications schemes commonly used for [FeFe]-hydrogenases, classify the NADH-dependent, ferredoxin-independent [FeFe]-hydrogenases with the Group 3A electron-bifurcating [FeFe]-hydrogenases due to the presence of subunits homologous to NuoE and NuoF (Peters et al., 2015; Poudel et al., 2016; Søndergaard et al., 2016). However, we suggest that more in-depth examination of the beta subunit, the NuoF homolog, may determine ferredoxin dependence.

The only NADH-dependent, ferredoxin-independent [FeFe]-hydrogenases that we have identified are from the *Syntrophomonadaceae* (See Chapter 2), *S. aciditrophicus* (See Chapter 3), and *N. ovalis* (see Chapter 3). It is possible that NADH-dependent, ferredoxin-independent [FeFe]-hydrogenases are relatively rare in comparison to NADH-dependent, ferredoxin-dependent electron-bifurcating [FeFe]-hydrogenases as they may only be useful under syntrophic conditions and less useful when performing primary fermentation which provides both NADH and reduced ferredoxin or under oxic conditions where their oxygen lability would favor [NiFe]-hydrogenases.

An unanswered question is if the NADH-dependent, ferredoxin-independent [FeFe]-hydrogenases from *S. wolfei*, *S. aciditrophicus*, and *N. ovalis* share a common origin where they separate from the NADH-dependent, ferredoxin-dependent electron-bifurcating [FeFe]-hydrogenases or if the transition from electron bifurcating, ferredoxin-dependent to ferredoxin-independent occurred multiple times as a form of convergent evolution. The selective pressure could possibly be close association with hydrogenotrophic methanogens. The distribution of

NADH-dependent, ferredoxin-independent [FeFe]-hydrogenases in different syntrophic organisms is currently unknown but their proposed energetic advantages over electron-bifurcating, NADH-dependent, ferredoxin-independent [FeFe]-hydrogenases suggests they may be present in other syntrophic metabolisms.

### **Unanswered Questions: Acyl-CoA Oxidation Mechanisms in *S. wolfei* and *S.***

#### ***aciditrophicus*: and Intracellular NADH/NAD<sup>+</sup> Ratios**

While we have provided details on how NADH is re-oxidized in *S. wolfei* and *S. aciditrophicus*, the manner in which Etf<sub>red</sub> is re-oxidized, presumably a reverse quinone loop, remains undemonstrated by biochemical methods. Quinone loops have been proposed in additional syntrophic metabolisms such as syntrophic lactate oxidation by members of the genus *Desulfovibrio* (Li et al., 2011; Meyer et al., 2013) and syntrophic propionate oxidation by *Syntrophobacter fumaroxidans* (Müller et al., 2010; Plugge et al., 2012). The high redox potential of menaquinone,  $E' = -94$  mV, when combined with a reverse quinone loop which involves the translocation of two protons (which lowers the redox potential by approximately -200 mV) would indicate high redox potential electrons are still used for hydrogen or formate production.

As we can explain hydrogen production from NADH during syntrophic metabolism, the question turns to how to explain hydrogen production from Etf<sub>red</sub>. *S. wolfei* appears to be capable of dissipating differences between the redox potentials of hydrogen and formate (Boone et al., 1989) and it presumably produces both NADH-dependent, ferredoxin-independent [FeFe]-hydrogenase and NADH-dependent, ferredoxin-independent formate dehydrogenases simultaneously (Sieber et al., 2014; Sieber et al., 2015). Therefore, it seems unlikely that re-

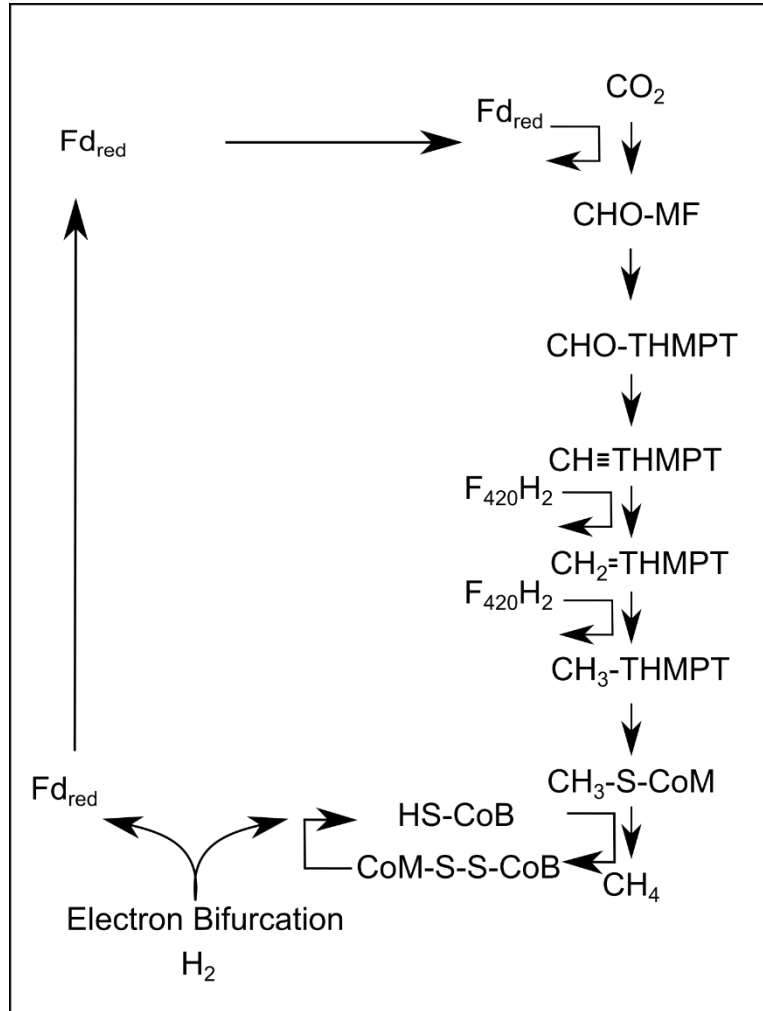


oxidation of NADH and Etf<sub>red</sub> can be explained by one process using hydrogen production and the other process using formate production. Thus, either simultaneous hydrogen production from NADH and Etf<sub>red</sub> occurs or simultaneous production of formate from NADH and Etf<sub>red</sub> occurs. Either scenario would produce a situation where either hydrogen or formate production from NADH is equilibrated with hydrogen or formate production from the proposed reverse quinone loop. It is possible that for all intents and purposes, the redox potentials of the electrons from NADH and those involved in the reverse quinone loop are near equilibrium. This raises the question of how interactions between multiple cofactor re-oxidation processes simultaneously occur and are managed during syntrophic metabolism. This aspect of syntrophy cannot be addressed until a thorough understanding of the proposed reverse quinone loop is available.

Thermodynamic calculations for NADH-dependent, ferredoxin-independent hydrogen production by *S. wolfei* and *S. aciditrophicus* suggest both organisms need to maintain high NADH/NAD<sup>+</sup> ratios to generate the hydrogen partial pressures that were observed for both pure culture and co-culture growth. The other piece of the puzzle is the hydrogenotrophic methanogen partner, which in these experiments was *M. hungatei* which has a strongly contrasting situation in terms of intracellular cofactor pools. During the eight-electron reduction of CO<sub>2</sub> to methane, four pairs of electrons are consumed.

**Figure 27. Redox Reactions in Cytochrome-Free Hydrogenotrophic Methanogens such as *Methanosprillum hungatei*.** MF:methanofuran, THMPT:tetrahydromethanopterin,

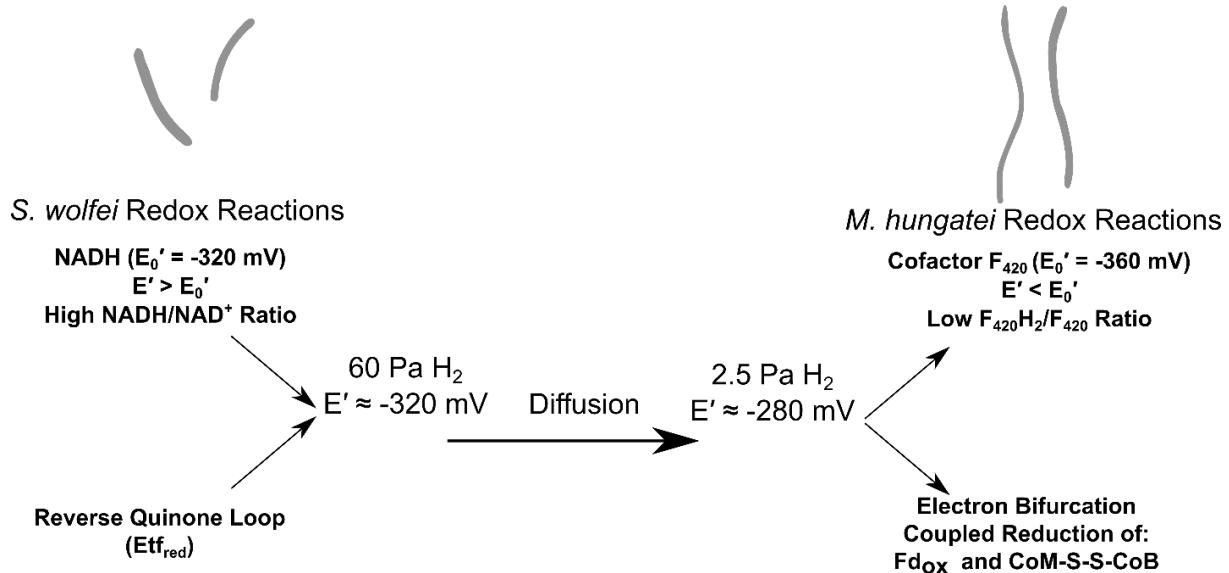
HS-CoB:coenzyme B, HS-CoM:coenzyme M, Fd:ferredoxin, F<sub>420</sub>:Cofactor F<sub>420</sub>.



Two pairs of electrons come from reduced cofactor F<sub>420</sub>, one pair from the low potential redox carrier ferredoxin, and one pair of electrons is from the oxidation of hydrogen coupled to the reduction of the disulfide bond between coenzyme B and coenzyme M (Figure 27). The low potential carrier, ferredoxin, is difficult to reduce by hydrogen at low hydrogen partial pressures and is regenerated by an electron-bifurcation mechanism involving CoM-S-S-CoB heterodisulfide reductase (Buckel and Thauer, 2013). The redox potential of NADH under standard conditions is

$E_0' = -320$  mV while the redox potential of the methanogenic cofactor  $F_{420}$  under standard conditions is  $E_0' = -360$  mV. For *S. wolfei* and *S. aciditrophicus* to produce the hydrogen at the partial pressures that, were observed, the NADH/NAD<sup>+</sup> ratio would have to be high, which would result in a redox potential of at least  $E' = -320$  mV if not lower. In contrast, the cofactor  $F_{420}$  reduced to oxidized (the  $F_{420}H_2/F_{420}$ ) ratio in hydrogenotrophic methanogens would have to be low, below one, when hydrogen partial pressures are low. A fluorescence-based technique to measure the cofactor  $F_{420}$  reduced to oxidized (the  $F_{420}H_2/F_{420}$ ) ratio showed that it was below 1.0 in the hydrogenotrophic methanogen *Methanobacterium thermautotrophicus* when grown with hydrogen partial pressures below 200 pascals (de Poorter et al., 2005).

**Figure 28. Syntroph NADH/NAD<sup>+</sup> Ratio Compared to Methanogen  $F_{420}H_2/F_{420}$  Ratio.**



The reduced nature of the NADH/NAD<sup>+</sup> pool (where  $E' > E_0'$ ) indicates that the syntrophic metabolizer is pushing the limits of this thermodynamically unfavorable process of producing hydrogen from NADH. This is stark contrast to cofactor  $F_{420}$  pool, which is kept highly oxidized (where  $E_0' > E'$ ). The apparent difference in the hydrogen redox potential (and

concentration) at the syntrophic metabolizer cell and the hydrogenotrophic methanogen cell may be important to the process of hydrogen diffusion, as the larger the difference between the concentration of hydrogen at the syntrophic metabolizer (the source) compared to the hydrogen concentration by the hydrogenotrophic methanogen (the sink), the faster the diffusion rate will be as predicted by Fick's law of diffusion (Schink and Thauer, 1988). This expected difference in hydrogen concentrations was observed when an ethanol-oxidizing, hydrogen-producing bacterium was separated by dialysis tubing from a hydrogen-consuming homoacetogen (Schink and Stieb, 1987). Separating the organisms resulted in a hydrogen concentration ten times higher in the compartment with the hydrogen-producing organism than when the organisms were grown in the same compartment. The observed hydrogen partial pressures measured in the *S. wolfei* and *M. hungatei* co-culture experiments are therefore likely intermediate between the hydrogen concentrations at each organism. The hydrogen concentrations at each organism should be reflected in the NADH/NAD<sup>+</sup> ratio of *S. wolfei* and the F<sub>420</sub>H<sub>2</sub>/F<sub>420</sub> ratio of *M. hungatei* and would offer an alternative mechanistic view on the syntrophic, hydrogen-based relationship.

**Summary: NADH-Dependent, Ferredoxin-Independent Hydrogen Production, Exemplifies the Intimate Nature of Syntrophic Metabolism in Co-Culture Between Syntrophic Metabolizers and Methanogenic Partners**

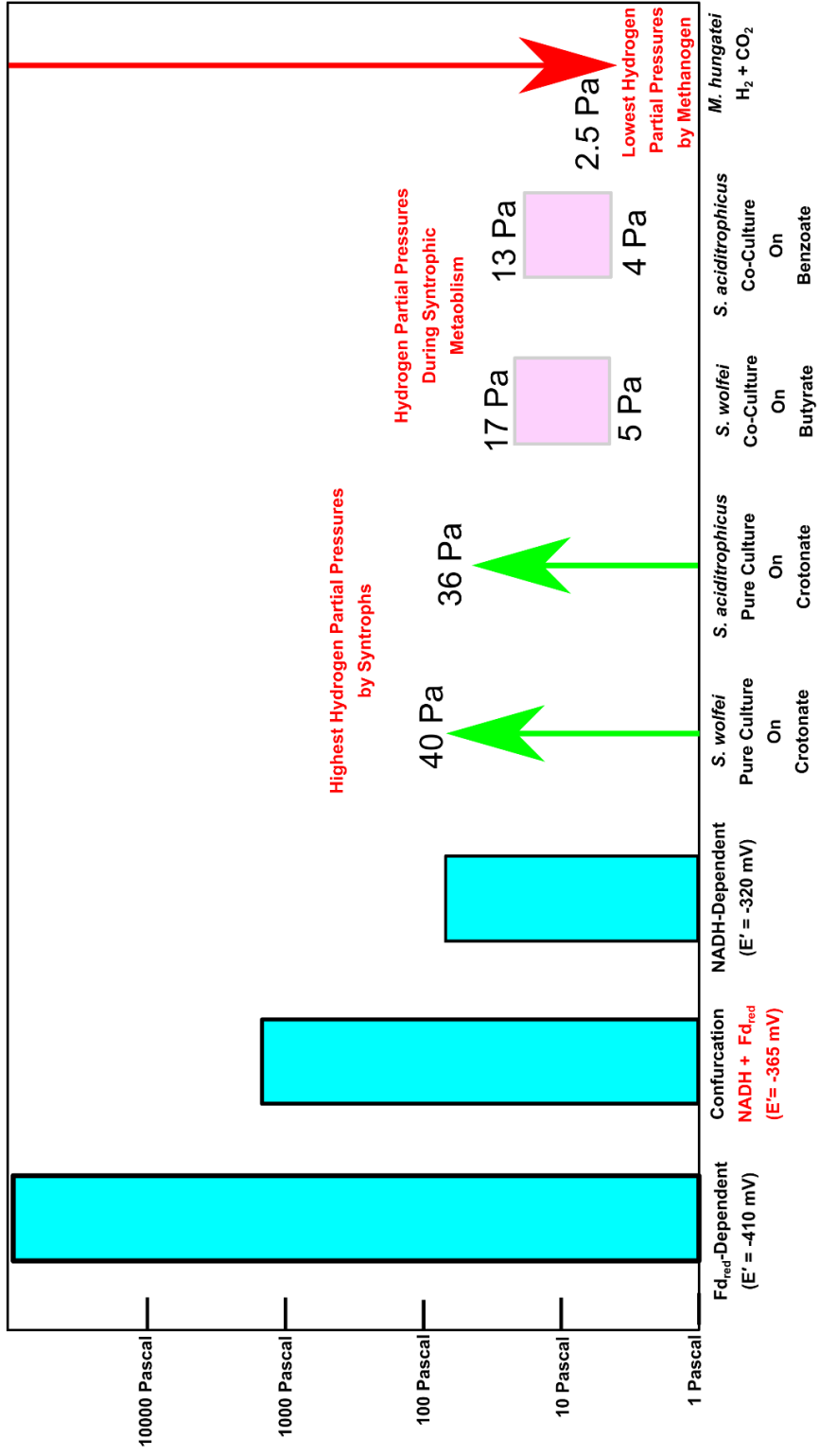
Syntropy was originally proposed to be dependent on low hydrogen and formate concentrations as explained by thermodynamics (McInerney et al., 1979; McInerney et al., 1981). This dependence in *S. wolfei* and *S. aciditrophicus* has been extensively detailed by physiological studies of co-cultures employing a wide range of culture-based (Wofford et al., 1986; Elshahed et al., 2001; Elshahed and McInerney, 2001), proteomic (Sieber et al., 2015;

James et al., 2019, in preparation), and transcriptional techniques (Sieber et al., 2014; James et al., 2019, in preparation). This dissertation suggests that from the perspective of the syntrophic metabolizer, syntrophy is the result of a dependence on cofactor re-oxidation mechanisms that utilize specifically high redox potential electrons to produce hydrogen or formate. NADH-dependent, ferredoxin-independent hydrogen production mechanisms in the syntrophic model organisms *S. wolfei* and *S. aciditrophicus* demonstrate how high redox potential electrons ( $E' = -320$  mV) from fatty acid oxidation (NADH) are used to produce hydrogen as had been predicted for *S. wolfei* nearly 30 years ago (Boone et al., 1989). The original observation that syntrophic metabolism is dependent on low hydrogen concentrations may be viewed alternatively as result of an obligate dependence on cofactor re-oxidation mechanisms that utilize high redox potential electrons. This argument is a rephrasing of the original thermodynamic argument, but with an additional emphasis on the physiological electron donors utilized by hydrogenases. The proposed cofactor re-oxidation mechanisms appear to agree with the original predicted thermodynamic constraints by allowing cofactor re-oxidation while maximizing the meager amount of energy that can be conserved for growth.

Butyrate oxidation and benzoate oxidation by *S. wolfei* and *S. aciditrophicus* are among the most difficult syntrophic metabolisms as predicted by thermodynamic modelling and the organisms appear to require lower hydrogen and formate concentrations than many other proposed syntrophic interactions. For example, syntrophic ethanol oxidation by the genus *Pelobacter* (Schmidt et al., 2014) or the altered fermentation profile of *Ruminococcus albus* (Zheng et al., 2014) are dependent on a hydrogen-consuming organism but utilize electron-confurcating hydrogenases. However, NADH-dependent hydrogen production as occurs in *S. wolfei* and *S. aciditrophicus* is clearly much closer to the limits that a hydrogenotrophic

methanogen can accommodate than the hydrogen partial pressure that would be produced by electron-confurcation from NADH and reduced ferredoxin (Figure 29).

**Figure 29. Narrow Hydrogen Partial Pressure Overlap Between Syntrophic Metabolizers and Methanogenic Partner.** Hydrogen partial pressures from *S. wolfei* and *S. aciditrophicus* cultures are from Chapters 2 and 3. The 2.5 pascal value was reported by (Cord-Ruwisch et al., 1988).



This exemplifies the degree to which these organisms as syntrophic specialists have adapted to an obligate dependence on hydrogenotrophic methanogenic partners. Other syntrophic metabolisms such as syntrophic acetate oxidation and propionate oxidation may involve similar high redox potential electron-donating, hydrogen-producing reactions such as NADH-dependent, ferredoxin-independent hydrogen production or the proposed reverse quinone loop. The work in this dissertation, demonstrates NADH-dependent, ferredoxin-independent hydrogen production in two obligately syntrophic model organisms and provides mechanistic understanding of the thermodynamic constraints placed on syntrophy. This suggests other high redox potential electron donor reactions should be expected for hydrogen production or other means of interspecies electron transfer in obligately syntrophic metabolizers.

## References

- Berrisford, J.M., and Sazanov, L.A. (2009). Structural Basis for the Mechanism of Respiratory Complex I. *J Biol Chem* 284(43), 29773-29783. doi: 10.1074/jbc.M109.032144.
- Boone, D.R., Johnson, R.L., and Liu, Y. (1989). Diffusion of the Interspecies Electron Carriers H<sub>2</sub> and Formate in Methanogenic Ecosystems and Its Implications in the Measurement of H<sub>2</sub> or Formate Uptake. *Appl Environ Microb* 55(7), 1735.
- Buckel, W., and Thauer, R.K. (2013). Energy conservation via electron bifurcating ferredoxin reduction and proton/Na(+) translocating ferredoxin oxidation. *Biochim Biophys Acta* 1827(2), 94-113. doi: 10.1016/j.bbabi.2012.07.002.
- Cord-Ruwisch, R., Seitz, H.-J., and Conrad, R. (1988). The capacity of hydrogenotrophic anaerobic bacteria to compete for traces of hydrogen depends on the redox potential of



- the terminal electron acceptor. *Arch Microbiol* 149(4), 350-357. doi: 10.1007/bf00411655.
- de Poorter, L.M., Geerts, W.J., and Keltjens, J.T. (2005). Hydrogen concentrations in methane-forming cells probed by the ratios of reduced and oxidized coenzyme F<sub>420</sub>. *Microbiology* 151(Pt 5), 1697-1705. doi: 10.1099/mic.0.27679-0.
- Elshahed, M.S., Bhupathiraju, V.K., Wofford, N.Q., Nanny, M.A., and McInerney, M.J. (2001). Metabolism of Benzoate, Cyclohex-1-ene Carboxylate, and Cyclohexane Carboxylate by “*Syntrophus aciditrophicus*” Strain SB in Syntrophic Association with H<sub>2</sub>-Using Microorganisms. *Appl Environ Microb* 67(4), 1728-1738. doi: 10.1128/aem.67.4.1728-1738.2001.
- Elshahed, M.S., and McInerney, M.J. (2001). Benzoate fermentation by the anaerobic bacterium *Syntrophus aciditrophicus* in the absence of hydrogen-using microorganisms. *Appl Environ Microbiol* 67(12), 5520-5525. doi: 10.1128/AEM.67.12.5520-5525.2001.
- Ferry, J.G. (1990). Formate dehydrogenase. *FEMS Microbiol Ecol* 7(3-4), 377-382. doi: 10.1111/j.1574-6968.1990.tb04940.x.
- Gutekunst, K., and Schulz, R. (2018). "CHAPTER 4 The Physiology of the Bidirectional NiFe-hydrogenase in Cyanobacteria and the Role of Hydrogen Throughout the Evolution of Life," in *Microalgal Hydrogen Production: Achievements and Perspectives*. The Royal Society of Chemistry), 107-138.
- Ingelman, M., Ramaswamy, S., Nivière, V., Fontecave, M., and Eklund, H. (1999). Crystal Structure of NAD(P)H:Flavin Oxidoreductase from *Escherichia coli*. *Biochemistry* 38(22), 7040-7049. doi: 10.1021/bi982849m.

- James, K.L., Kung, J.W., Crable, B.R., Mouttaki, H., Sieber, J.R., Nguyen, H.H., et al. (2019, in preparation). *Syntrophus aciditrophicus* uses the same enzymes in a reversible manner to syntrophically degrade fatty, aromatic and alicyclic acids and to synthesize aromatic and alicyclic acids from crotonate.
- Jollie, D.R., and Lipscomb, J.D. (1991). Formate dehydrogenase from *Methylosinus trichosporium* OB3b. Purification and spectroscopic characterization of the cofactors. *J Biol Chem* 266(32), 21853-21863.
- Laukel, M., Chistoserdova, L., Lidstrom, M.E., and Vorholt, J.A. (2003). The tungsten-containing formate dehydrogenase from *Methylobacterium extorquens* AM1: purification and properties. *Eur J Biochem* 270(2), 325-333.
- Li, X., McInerney, M.J., Stahl, D.A., and Krumholz, L.R. (2011). Metabolism of H<sub>2</sub> by *Desulfovibrio alaskensis* G20 during syntrophic growth on lactate. *Microbiology* 157(Pt 10), 2912-2921. doi: 10.1099/mic.0.051284-0.
- McInerney, M.J., Bryant, M.P., Hespell, R.B., and Costerton, J.W. (1981). *Syntrophomonas wolfei* gen. nov. sp. nov., an Anaerobic, Syntrophic, Fatty Acid-Oxidizing Bacterium. *Appl Environ Microbiol* 41(4), 1029-1039.
- McInerney, M.J., Bryant, M.P., and Pfennig, N. (1979). Anaerobic bacterium that degrades fatty acids in syntrophic association with methanogens. *Arch Microbiol* 122(2), 129-135. doi: 10.1007/bf00411351.
- McInerney, M.J., Rohlin, L., Mouttaki, H., Kim, U., Krupp, R.S., Rios-Hernandez, L., et al. (2007). The genome of *Syntrophus aciditrophicus*: life at the thermodynamic limit of microbial growth. *Proc Natl Acad Sci U S A* 104(18), 7600-7605. doi: 10.1073/pnas.0610456104.

- Meyer, B., Kuehl, J., Deutschbauer, A.M., Price, M.N., Arkin, A.P., and Stahl, D.A. (2013). Variation among *Desulfovibrio* Species in Electron Transfer Systems Used for Syntrophic Growth. *J Bacteriol* 195(5), 990. doi: 10.1128/JB.01959-12.
- Müller, N., Worm, P., Schink, B., Stams, A.J.M., and Plugge, C.M. (2010). Syntrophic butyrate and propionate oxidation processes: from genomes to reaction mechanisms. *Environ Microbiol Rep* 2(4), 489-499. doi: doi:10.1111/j.1758-2229.2010.00147.x.
- Muller, U., Willnow, P., Ruschig, U., and Hopner, T. (1978). Formate dehydrogenase from *Pseudomonas oxalaticus*. *Eur J Biochem* 83(2), 485-498.
- Müller, V., and Hess, V. (2017). The Minimum Biological Energy Quantum. *Front Microbiol* 8(2019). doi: 10.3389/fmicb.2017.02019.
- Niks, D., and Hille, R. (2019). Molybdenum- and tungsten-containing formate dehydrogenases and formylmethanofuran dehydrogenases: Structure, mechanism, and cofactor insertion. *Protein Sci* 28(1), 111-122. doi: 10.1002/pro.3498.
- Peters, J.W., Beratan, D.N., Schut, G.J., and Adams, M.W.W. (2018). On the nature of organic and inorganic centers that bifurcate electrons, coupling exergonic and endergonic oxidation–reduction reactions. *Chem Comm* 54(33), 4091-4099. doi: 10.1039/C8CC01530A.
- Peters, J.W., Schut, G.J., Boyd, E.S., Mulder, D.W., Shepard, E.M., Broderick, J.B., et al. (2015). [FeFe]- and [NiFe]-hydrogenase diversity, mechanism, and maturation. *Biochim Biophys Acta Mol Cell Res* 1853(6), 1350-1369. doi: <https://doi.org/10.1016/j.bbamcr.2014.11.021>.

- Plugge, C.M., Henstra, A.M., Worm, P., Swarts, D.C., Paulitsch-Fuchs, A.H., Scholten, J.C.M., et al. (2012). Complete genome sequence of *Syntrophobacter fumaroxidans* strain (MPOB<sup>T</sup>). *Stand Genomic Sci* 7(1), 91-106. doi: 10.4056/sigs.2996379.
- Poudel, S., Tokmina-Lukaszewska, M., Colman, D.R., Refai, M., Schut, G.J., King, P.W., et al. (2016). Unification of [FeFe]-hydrogenases into three structural and functional groups. *Biochim Biophys Acta Gen Subj* 1860(9), 1910-1921. doi: <https://doi.org/10.1016/j.bbagen.2016.05.034>.
- Preissler, J., Wahlefeld, S., Lorent, C., Teutloff, C., Horch, M., Lauterbach, L., et al. (2018). Enzymatic and spectroscopic properties of a thermostable [NiFe]-hydrogenase performing H<sub>2</sub>-driven NAD<sup>+</sup>-reduction in the presence of O<sub>2</sub>. *Biochim Biophys Acta Bioenerg* 1859(1), 8-18. doi: <https://doi.org/10.1016/j.bbabbio.2017.09.006>.
- Sazanov, L.A. (2007). Respiratory complex I: mechanistic and structural insights provided by the crystal structure of the hydrophilic domain. *Biochemistry* 46(9), 2275-2288. doi: 10.1021/bi602508x.
- Sazanov, L.A., and Hinchliffe, P. (2006). Structure of the hydrophilic domain of respiratory complex I from *Thermus thermophilus*. *Science* 311(5766), 1430-1436. doi: 10.1126/science.1123809.
- Schink, B., and Stieb, M. (1987). Cultivation of syntrophic anaerobic bacteria in membrane-separated culture devices. *FEMS Microbiol Ecol* 3(2), 71-76. doi: 10.1111/j.1574-6968.1987.tb02341.x.
- Schink, B., and Thauer, R. (1988). Energetics of syntrophic methane formation and the influence of aggregation. *Granular anaerobic sludge*, 5-17.

- Schmidt, A., Frensch, M., Schleheck, D., Schink, B., and Muller, N. (2014). Degradation of acetaldehyde and its precursors by *Pelobacter carbinolicus* and *P-acetylenicus*. *PLoS ONE* 9. doi: 10.1371/journal.pone.0115902.
- Schmitz, O., Boison, G., Salzmann, H., Bothe, H., Schütz, K., Wang, S.-h., et al. (2002). HoxE—a subunit specific for the pentameric bidirectional hydrogenase complex (HoxEFUYH) of cyanobacteria. *Biochim Biophys Acta Bioenerg* 1554(1), 66-74. doi: [https://doi.org/10.1016/S0005-2728\(02\)00214-1](https://doi.org/10.1016/S0005-2728(02)00214-1).
- Sieber, J.R., Crable, B.R., Sheik, C.S., Hurst, G.B., Rohlin, L., Gunsalus, R.P., et al. (2015). Proteomic analysis reveals metabolic and regulatory systems involved in the syntrophic and axenic lifestyle of *Syntrophomonas wolfei*. *Front Microbiol* 6, 115. doi: 10.3389/fmicb.2015.00115.
- Sieber, J.R., Le, H.M., and McInerney, M.J. (2014). The importance of hydrogen and formate transfer for syntrophic fatty, aromatic and alicyclic metabolism. *Environ Microbiol* 16(1), 177-188. doi: 10.1111/1462-2920.12269.
- Sieber, J.R., McInerney, M.J., and Gunsalus, R.P. (2012). Genomic Insights into Syntrophy: The Paradigm for Anaerobic Metabolic Cooperation. *Annu Rev Microbiol* 66(1), 429-452. doi: 10.1146/annurev-micro-090110-102844.
- Sieber, J.R., Sims, D.R., Han, C., Kim, E., Lykidis, A., Lapidus, A.L., et al. (2010). The genome of *Syntrophomonas wolfei*: new insights into syntrophic metabolism and biohydrogen production. *Environ Microbiol* 12(8), 2289-2301. doi: 10.1111/j.1462-2920.2010.02237.x.
- Søndergaard, D., Pedersen, C.N.S., and Greening, C. (2016). HydDB: A web tool for hydrogenase classification and analysis. *Sci Rep* 6, 34212. doi: 10.1038/srep34212

<https://www.nature.com/articles/srep34212#supplementary-information>.

Wofford, N.Q., Beaty, P.S., and McInerney, M.J. (1986). Preparation of cell-free extracts and the enzymes involved in fatty acid metabolism in *Syntrophomonas wolfei*. *J Bacteriol* 167(1), 179. doi: 10.1128/jb.167.1.179-185.1986.

Zheng, Y., Kahnt, J., Kwon, I.H., Mackie, R.I., and Thauer, R.K. (2014). Hydrogen Formation and Its Regulation in *Ruminococcus albus*: Involvement of an Electron-Bifurcating [FeFe]-Hydrogenase, of a Non-Electron-Bifurcating [FeFe]-Hydrogenase, and of a Putative Hydrogen-Sensing [FeFe]-Hydrogenase. *J Bacteriol* 196(22), 3840.

## Supplemental Figures

**Supplemental Figure 4.1 Full Alignment of Beta Subunits from NADH-Dependent, Ferredoxin-Independent [FeFe]-Hydrogenases and Formate Dehydrogenases, Electron-Bifurcating, NADH-Dependent, Ferredoxin-Dependent [FeFe]-Hydrogenases and Formate Dehydrogenases, and NADH:Quinone Oxidoreductases Including Specifically Proposed NADH-Dependent, Ferredoxin-Independent Formate Dehydrogenases from *S.***

*aciditrophicus* and *S. wolfei*. Residues highlighted in yellow correspond to residues that appeared to be differentially conserved solely amongst the electron-bifurcating NADH-dependent, ferredoxin-dependent [FeFe]-Hydrogenases and Formate Dehydrogenases. The alignment of full-length the beta subunits was performed in MEGA7 using the ClustalW algorithm.

<i>T. maritima</i> HydB	-----	50
<i>C. tencongenesis</i> HydB	-----	50
<i>M. thermoacetica</i> HydB	-----	50
<i>A. woodii</i> HydB	-----	50
<i>R. albus</i> HydB	-----	50
<i>C. acidurici</i> HylB	-----	50
<i>C. autoethanogenum</i> HytB	-----	50
<i>D. fructosovorans</i> HydB	-----	50
<i>C. necator</i> FdhB	-----	50
<i>C. oxalaticus</i> FdhB	-----	50
<i>M. extorquens</i> FdhB	-----MSE	50
<i>M. trichosporium</i> FdhB	-----	50
<i>R. capsulatus</i> FdhB	-----	50
<i>E. coli</i> NuoF	-----	50
<i>T. thermophilus</i> Nqo1	-----	50
<i>S. wolfei</i> HydB	-----	50
Swol_0784	-----	50
Swol_1024	-----	50
Swol_1828	-----	50
Syn_02139	MTRWIRSARSPNIRSVLAKSKKFTCKEGIAMITTENIQEVINNRGKAREH	50
Syn_00631	-----MITEQLKNDIHRLGGRYPEK	50
<i>S. aciditrophicus</i> HydB	-----MITVQDIENVIARGNAREH	50
<i>T. maritima</i> HydB	-----MFKNAKEFVQYANKLKTLR-----	100
<i>C. tencongenesis</i> HydB	-----	100
<i>M. thermoacetica</i> HydB	-----MIKSMEELQKFESQLEAMQSQ-----	100
<i>A. woodii</i> HydB	-----	100
<i>R. albus</i> HydB	-----MTIEELNKKIAAKADIVKVRTIIAEEGEKLA	100
<i>C. acidurici</i> HylB	-----MITINDLKKIKEETLPKVSLRGDIEG-GEK--	100
<i>C. autoethanogenum</i> HytB	-----	100
<i>D. fructosovorans</i> HydB	-----	100
<i>C. necator</i> FdhB	-----	100
<i>C. oxalaticus</i> FdhB	-----MSA	100
<i>M. extorquens</i> FdhB	ASGTVRSFAHPGRGRNVARAVPKGRQVDPHAKVEIEELGTRPRQRDLI	100
<i>M. trichosporium</i> FdhB	-----	100
<i>R. capsulatus</i> FdhB	-----	100
<i>E. coli</i> NuoF	-----	100
<i>T. thermophilus</i> Nqo1	-----	100
<i>S. wolfei</i> HydB	-----	100
Swol_0784	-----	100
Swol_1024	-----	100
Swol_1828	-----	100
Syn_02139	LMAILRDLENLSGNQQ--LSPETLNAVAEAMNLPQSTVAGFVGFYTMFST	100
Syn_00631	QSALMPALMLAQKENANRLDQDDIRTVAELVDVDFGKAYGLATYYSMYNV	100
<i>S. aciditrophicus</i> HydB	LMAILRDLENLSGRNV--LDVSVLNTLAMKMDLPQSAISGFTSFYTMFST	100

*T. maritima* HydB EKKLNGVSIYVCGVTGCTAKGALKVYSAFEELKKNLLGQVTLEKIDDD 150  
*C. tencongenesis* HydB --MLYRSHVMVCGGTGCTSSGSDEVAERFIEEIKKAGLDKEILVVR---- 150  
*M. thermoacetica* HydB -EAGAKAKIVVGMGTGCGIAAGAREVMNAILDVAKR-QLTGVTVSQ---- 150  
*A. woodii* HydB -MAYKRSQILICGGTGC TSSGSMVLVKELKELVKHDILDEVEVVT---- 150  
*R. albus* HydB KETGYRKQVLVCGGTGCQSSHSMDVLKALKEELAAGKIADEVLVVR---- 150  
*C. acidurici* HylB IESTYRKQILLCRGTGCTSSKSKIEERFQELLKEKGIQDEVNVVR--- 150  
*C. autoethanogenum* HytB --MSDKKTVNICCGTGC LAKGSMEVYEMKAQIAKLGANAEVNVKLLKA-- 150  
*D. fructosovorans* HydB ----- 150  
*C. necator* FdhB --MITITTFVPRDSTALALGADDVARAIAAREAAARNEHVRIVRNG---- 150  
*C. oxalaticus* FdhB AVNSTVNTIFVPRDSTALALGADEVARAIEREAAARGEAVRIVRNG---- 150  
*M. extorquens* FdhB EHLHLIQDTYQGISADHLAALADEMSLAFAEVFETATFYAHFDVVKEGE- 150  
*M. trichosporium* FdhB -----MTKVYVPRDMAALAVGAKRVLAAIEKEAAARGEAIQIVRNG--- 150  
*R. capsulatus* FdhB -----MKIWLPCDAAAKACGAEAVLAAALRLEAEKRGALDIARNG---- 150  
*E. coli* NuoF ----- 150  
*T. thermophilus* Nqo1 ----- 150  
*S. wolfei* HydB ----- 150  
Swol\_0784 ----- 150  
Swol\_1024 ----- 150  
Swol\_1828 ----- 150  
Syn\_02139 R-PRAKFLIRVCKSGPCHVMGARTIFDYVEKHLGISPGQTTADGLFH--- 150  
Syn\_00631 EKPVGRYHLQVDTNIPATLMGAGEILDHLEKTLNIRAGETTPDGLFT--- 150  
*S. aciditrophicus* HydB E-PRAKFLIRVCKSGPCHVMGARTIFDVIENHLGIRAGETTTADGLFH--- 150

*T. maritima* HydB KVTILNRTGCCGRCSSGPLVKIMPYR---FFYSNVAPEDVPEIVDRTVLKG 200  
*C. tencongenesis* HydB -----TGCFGLCELGPVVVVYPEG---VFYSRVKPEYVPEIVEEHLKLG 200  
*M. thermoacetica* HydB -----TSCIGLCAQEPLVDVILPGQPKVTYGVKVDAAKAREIVGRHVVDG 200  
*A. woodii* HydB -----TGCFGLCELGPVVIVYPEG---TFYSRVEAADIPEMVEEHLVKG 200  
*R. albus* HydB -----TGCFGLCSLGPVIVIVYPEG---AFYAQATPEGIKRIVDEHLVNG 200  
*C. acidurici* HylB -----TGCFGLCEAGPIVVVYPPG---TFYSHIKVEDVDQIVEEDLINN 200  
*C. autoethanogenum* HytB -----TGDGLCEKGPVLKIYPDD---IAYFKVKVEDVEDVVKKTLMNG 200  
*D. fructosovorans* HydB -----MAATTE----- 200  
*C. necator* FdhB -----SRGMFWLEPLVEVQTEGAG-RVAYGPVSAADVPGLFDAGLLQG 200  
*C. oxalaticus* FdhB -----SRGMFWLEPLVEVQTEAG-RVAYGPVSAEDVPALFDAGLLQG 200  
*M. extorquens* FdhB --ADIPRLTIRVCDISITCAMFGADELLETQLRELASDAVRVVRAPCVGLC 200  
*M. trichosporium* FdhB -----SRGLLWLEPLVEVETPEG-RIGYGNVKPSDVPPLFDAGFLRG 200  
*R. capsulatus* FdhB -----SRGMIWLEPLLEVETPAG-RIGFGPMTPADVPALFDA--LES 200  
*E. coli* NuoF ----- 200  
*T. thermophilus* Nqo1 -----MTGPILSG----- 200  
*S. wolfei* HydB ----- 200  
Swol\_0784 ----- 200  
Swol\_1024 ----- 200  
Swol\_1828 ----- 200  
Syn\_02139 ---LEACECLGICSVAPAMMIN-----YDLHGNTTEER IATILDGYSRE 200  
Syn\_00631 ---LSEVECLASCGTCPVIQVN-----DVYYENMTREKVDSDLDSLR--- 200  
*S. aciditrophicus* HydB ---LEECECLGLCSAAPAMMVN-----YDMHGNTSESNIKEILDSYSARE 200



<i>T. maritima</i> HydB	EPIERLFLTDPLTGE-KVPRIEDTTLFKNQDFYIMEAIGESECDSDIEDYI	250
<i>C. tencongenesis</i> HydB	RPVRKYIYGESLEEK-AIKPLEETPFRRKQRRIALRNCGVINPEDIREAI	250
<i>M. thermoacetica</i> HydB	HIVTEWVNRQGDVAV---RPYTELPPFFKHQVRIALRNCLIDPESIGEYI	250
<i>A. woodii</i> HydB	RPLDRLIYNEKGDGH-HPLSINELGFFKKQRRIALANCGVINPENIDEYI	250
<i>R. albus</i> HydB	EICKDLLYQETVHEDGSIISLYETNFYRKQKRIALRNCGVIDPEDIIEYI	250
<i>C. acidurici</i> HylB	NVIKELLYKGSIDGD-KIKAISEVAFYAKQKRVSLLKNCGLINPECIDEYI	250
<i>C. autoethanogenum</i> HytB	EIIEKLLYFETATKQ-RLRNHKESEFCRQYKIALRNVEGIDPISLEDYV	250
<i>D. fructosovorans</i> HydB	-----KKQLRIATRNCGFIDPESIDYI	250
<i>C. necator</i> FdhB	GEHALSQG-----VTEEIPFLKQERLTFARVGITDPLSLDDYR	250
<i>C. oxalaticus</i> FdhB	GAHALAHG-----LTEEIPFLKQERLTFARIGITDPLSLDDYR	250
<i>M. extorquens</i> FdhB	DHAPAVEVGHNFLLHR-----ADLASVRAAVEAEDTHAHIPTVVDYDAYR	250
<i>M. trichosporium</i> FdhB	GAHPLSIG-----KVEEHYPYAKQTRVTFERVGVIDPVNLLDYV	250
<i>R. capsulatus</i> FdhB	--HPKALG-----LVEEIPFFKRQTRLTFARCGRIEPLSLAQFA	250
<i>E. coli</i> Nuof	-----MKNIIRTPETHPLTWRLRDDKQPVWLDEYR	250
<i>T. thermophilus</i> Nqol	-----LDPRFERTLYAHVKGEGSWTLDYYL	250
<i>S. wolfei</i> HydB	-----MAEEMRIVLRNYGKIDPLKIDYI	250
Swol_0784	-----MAEEIRILLAHADQIDPAQAEDYI	250
Swol_1024	-----MAEEMRIVLRNYGKIDPLKIDYI	250
Swol_1828	-----MAEEMRIVLRNYGKVDPLNIDSYT	250
Syn_02139	PPFGGACGPEVEGRV-----CMLDEPGQTQRLTEKIGSIDPLSVDSYL	250
Syn_00631	----KGMPPESE-----TIYSFGSVCNVLLKNRQVGDATALAVAK	250
<i>S. aciditrophicus</i> HydB	PAFKAAYGPGIEGRA-----VIINNSQOTRRLLENVGVDPASIESYL	250
<i>T. maritima</i> HydB	ARSGYESLVKALTS-MTPEEIIETVKASGLRGRGGGGFPTGLKWEFTRKA	300
<i>C. tencongenesis</i> HydB	AFDGYKALAKVLTE-MTPEQVIEEVKKSGLRGRGGGGFPTGVKWEFAYKQ	300
<i>M. thermoacetica</i> HydB	AHDGYQALSQVLLT-MKPYEVIEETIKKSGLRGRGGGGFPTGLKWEFAYRS	300
<i>A. woodii</i> HydB	GFDGYLALAKVLLT-MSPVDVINEVKASGLRGRGGGGFPTGLKWFQFAHDA	300
<i>R. albus</i> HydB	ATDGYQALYKALTS-MTPDEVVKEVLDLSDGIRGRGGAGFPTGRKWMFTKDA	300
<i>C. acidurici</i> HylB	SHDGYFALHKALTE-MKPEDVIETMKSGLKGRGGGGFPTGLKWEFTAKA	300
<i>C. autoethanogenum</i> HytB	ERGGYKALKKAISS-MKPEDVLEEITKSGLRGRGGAGFPTGRKWKTAADI	300
<i>D. fructosovorans</i> HydB	ALRGYEGLAKVLT--MTPAEVVDLVKRSGLRGRGGAGFPTGIKWGIALGN	300
<i>C. necator</i> FdhB	AHEGFAGLERALA--MQPAEIVQEVTDLSDGIRGRGGAAFFPTGIKWKTVLGA	300
<i>C. oxalaticus</i> FdhB	AHEGFAALERALS--MAPAEIVQEVTDLSDGIRGRGGAAFFPTGIKWKTVLGA	300
<i>M. extorquens</i> FdhB	AGGGYATLERLRSGELPVDVLDVLDGGLRGLGGAGFPTGRKWRVSRGE	300
<i>M. trichosporium</i> FdhB	AHGGGQGLAKAFE--IGPAKVIEEVTKSGLRGRGGAGFPAGIKWKTVADA	300
<i>R. capsulatus</i> FdhB	AAEGWAGLRKALK--MTPAEVVEEVLASGLRGRGGAGFPTGIKWRVAAA	300
<i>E. coli</i> Nuof	SKNGYEGARKALTG-LSPDEIVNQVKDAGLKGRRGGAGFSTGLKWSLMPKD	300
<i>T. thermophilus</i> Nqol	RHGGYETAKRVLKE-KTPDEVIEEVKRSGLRGRGGAGFPTGLKWSFMPKD	300
<i>S. wolfei</i> HydB	AQGGYKSLEKARA--MNTADLIAEVKKSNLRGRGGAGFNCGMKWSFAAGA	300
Swol_0784	KVGGFKGLEKARG--MTSKDLIEEVKKSGLRGRGGAGFNAGMKWSFVP--	300
Swol_1024	AAGGYKSLEKARS--MKQTEVIEEVKKSNLRGRGGAGFNAGMKWNFSYQV	300
Swol_1828	QVGGYQALAKAKS--MSQTDLIEEVKKSGLRGRGGAGFNTGMKWSFSYGV	300
Syn_02139	EKGGYAAIKKALAE-YQPDVIAIVKDSGLRGRGGAGFPAGVKWSFLPKG	300
Syn_00631	GNGAYQALAKAGTM-K-PEEILEEVKKANLRGRGGAGFPAGVKWGFIPKD	300
<i>S. aciditrophicus</i> HydB	QNGGYEAARKAFAE-YSPEQVIGVKDSGLRGRGGAGFPVGVKWSFVPKG	300
	. : .:: : .:::* **.* * **	

*T. maritima* HydB QGD--IKFVVCNGDEGDPGAFMNRLLERDPHLVLEGMIIAGYAVGAQKG 350  
*C. tencongenesis* HydB KET--PKYVVCNADEGDPGAFMDRSILEGDPHVSLEAMAIAGYAIGANHG 350  
*M. thermoacetica* HydB PGP--VKYFVCNADEGDPGAFMDRSILEGDPHAVLEGMAIGAYAIGASQG 350  
*A. woodii* HydB VSEDGIKYVACNADEGDPGAFMDRSVLEGDPHAVIEAMAIAGYAVGASKG 350  
*R. albus* HydB PGD--VKYVACNADEGDPGAFMDRSILEGDPHVEIAMTIASAVGAHQG 350  
*C. acidurici* HylB TGD--QKYVLCNADEGDPGAFMDRSILEGDPHVSIEAMALAGYAIGSDQG 350  
*C. autoethanogenum* HytB DTS--PIYVVCNGDEGDPGAFMDRSIMEGDPNSVIEGMTLCAYAVGGTNG 350  
*D. fructosovorans* HydB KAD--QKYMVCNADEGDP-**EFM**DRAVLEGDPHVSVEAMAIGGYAIGATRG 350  
*C. necator* FdhB QSA--VKYIVCNADEGDSGT**FS**DRVMEDDPFLIEGMTIAALAVGAEQG 350  
*C. oxalaticus* FdhB QSA--VKYIVCNADEGDSGT**FS**DRVMEDDPFLIEGMTIAGLAVGAEQG 350  
*M. extorquens* FdhB PGP---RLMAVNGDEGEPGT**TFK**DQLYLNTDPHRFLEGMLIGAHVVEAADV 350  
*M. trichosporium* FdhB PAD---RRYVVTNADEGDSGT**FA**DRVMMEGDPFVFLIEGMTICGYAIGASKG 350  
*R. capsulatus* FdhB QAD--QKYIVCNVDEGDSGS**FA**DRMLIEGDPFCLVEGMAIAGHAVGATRG 350  
*E. coli* Nuof ESMN-IRYLLCNADMEMEPGT**TYK**DRLLMQLPHLLVEGMLISAFALKAYRG 350  
*T. thermophilus* Nqol DGK--QHLYLCNADESEPG**SFK**DRYILEDPHLLIEGMILAGYAIRATVG 350  
*S. wolfei* HydB QAD--QKYVICNADEGEPGT**TYK**DRILIMENDPHTLIEGMAICAYAIGATQG 350  
Swol\_0784 PAE--VKYVVCNLDEGEPGT**TYK**DRICEKNAQALIEGMAICGVAINAKQG 350  
Swol\_1024 QSE--EKYVVCNADEGEPGT**TYK**DRIMENDPQSVIEGMAICGYAIGSKKG 350  
Swol\_1828 KAD--QKYVICNADEGEPGT**TYK**DRIMENDPQSVLEGMAICGYAIGANKG 350  
Syn\_02139 -DMQ--KYVICNADEGEPGT**TYK**DRILMEENPHGLLEGMLCGYATGATVG 350  
Syn\_00631 TDKP--VYLICNADEGEPGT**TYK**DRQIMEYDPHLLIEGMAIAARAIGARQA 350  
*S. aciditrophicus* HydB -EMQ--KYVICNADEGEPGT**TFK**DRVLMEEENPQQLIEGMLCGYAIGATLG 350

. \* \* \* . . : : : . . : \* . \* : . . .

*T. maritima* HydB YAYIRAEYFFAVKMFKKAIEDARKLGLLGENILGTGFSFDLEVKEGAGAF 400  
*C. tencongenesis* HydB YIYVRAEYPLAVKRLKIAIQQAREYGLLGKDIFGTGFDFDIEIRLGAGAF 400  
*M. thermoacetica* HydB YIYVRAEYPVAVQRLKLAISQAREQGLLGKLNLFNSGFDFDIDIRLGAGAF 400  
*A. woodii* HydB YVYVRAEYPIAVNRLQIAIDQAKEYGILGENIFETDFSFDEIRLGAGAF 400  
*R. albus* HydB YVYVRAEYPVAVNRLQIALDQAREYGLLGKNIILGTGHDFDIEIRLGAGAF 400  
*C. acidurici* HylB YVYVRAEYPIAVKRLQIAIDEAKAKGLLGKDIFGTGFNFDMIEIRLGAGAF 400  
*C. autoethanogenum* HytB FAYIRDEYGLAVENMQAKINKAKDENLLGNILGTDFSFDIQIVRGGGAF 400  
*D. fructosovorans* HydB TVYIRAEYPLAIKRLKKAIDDAREYGLLGENIFGSGFDFDIELKYGAGAF 400  
*C. necator* FdhB YIYCRSEYPHAIIVLESIAIGIANAAGWLGDDIRGSGKRFHLEVRKAGAY 400  
*C. oxalaticus* FdhB YIYCRSEYPHAIIVLESIAIAHAAGWLGDDLRSKGRFRLEVRKAGAY 400  
*M. extorquens* FdhB YIYLRDEYPIISREILAREIAKLPEGG-----TRIHRRGAGAY 400  
*M. trichosporium* FdhB FIYLRAEYQCAEVLTEALEAARKAGWLGPNVRGSGFAFDIELRIGAGAY 400  
*R. capsulatus* FdhB YVYIRSEYPDIAIVMRAAIAMAKPF-----LAEAG--FEMEVRVAGAY 400  
*E. coli* Nuof YIFLRGEYIEAAVNLRRAIAEATEAGLLGKNIMGTGFDFELFVHTGAGRY 400  
*T. thermophilus* Nqol YIYVRGEYRRAADRLEQAIKEARARGYLGNLFGTDFSFDLHVHRGAGAY 400  
*S. wolfei* HydB YIYLRGEY PFLVSTLNTAINQAKEKGLVK-----DFDIEVRSAGAY 400  
Swol\_0784 YIYCRGEY PFFVDDLKAIQSAKDVGALG-----EFDIEVRMGAGAY 400  
Swol\_1024 YIYCRGEY PYYVDILNQAIAQAKAGVLG-----DFDVEVRMGAGAY 400  
Swol\_1828 YIYCRGEY PYYVEILNKAIAQASEKGLLG-----DFNIEVRMGAGAY 400  
Syn\_02139 YIYIRGEYRRSIERLQRAIDQAREKGLGDNI FGSFRFDIFIKEGGGAY 400  
Syn\_00631 FIYIRGEFAWIADILEKAI GEAKADGQLS-----ELDIIVHRGAGAY 400  
*S. aciditrophicus* HydB YIYVRGEYRRSIERLQSAIDQARAKGFLGKKIFGSNFDIFVKEGGGAY 400

: \* \* : : : : : \* . \* :

<i>T. maritima</i> HydB	VCGEETALLASIEGKRGMPRPKPPFFPAQSGLWGKPTLINNVETYANI PRI	450
<i>C. tencongenesis</i> HydB	VCGEETALLNSIMGKRGEPRPRPPFFPAVKGVWGKPTI INNVETFANIPPI	450
<i>M. thermoacetica</i> HydB	VCGEETALLASIEGRRGEPRPRPPFFPAVSGLWGKPTVINNVETLANIPTI	450
<i>A. woodii</i> HydB	VCGEETALMNSIEGKRGEPRPRPPFPANKGLFGKPTVLNNVETYANIPKI	450
<i>R. albus</i> HydB	VCGEETALLTSIEGNRGEPRPRPPFFPAVKGLFGKPTLINNVETYANIAQI	450
<i>C. acidurici</i> HylB	VCGEETALIASIEGQRGMFPRNKPPFPANKGLWDKPTLINNVETYANVPQI	450
<i>C. autoethanogenum</i> HytB	VCGESTALMSSIEGMVGEPRAKYIHTTEKGLWGQPTVLNNVETWANVPPI	450
<i>D. fructosovorans</i> HydB	VCGEETALIRSMGKRGEFVTKPPFFPAQSGYWEKPTIVNNVETFANIPAI	450
<i>C. necator</i> FdhB	VCGEETALLESLEGRGVVRAKPPALQGLFGKPTVINNVISLATVPVI	450
<i>C. oxalaticus</i> FdhB	VCGEETALLESLEGKRGVVRAKPPALQGLFGKPTVINNVISLATVPVI	450
<i>M. extorquens</i> FdhB	ICGEESLLESLEGKRGVPRKPPFFQVGLFNRPTLINNIETLFWVRDI	450
<i>M. trichosporium</i> FdhB	VCGEETSLLSLEGKRGIVRAKPPPAHVGFMSRPTVNNVLTATAPAI	450
<i>R. capsulatus</i> FdhB	VCGEETSLLNSLEGKRGTVRAKPPALQGLFGKPTVNNLLSLAAVPWI	450
<i>E. coli</i> Nuof	ICGEETALINSLEGRANPRSKPPFPATSGAWGKPTCVNNVETLCNVPAI	450
<i>T. thermophilus</i> Nqol	ICGEETALMNSLEGLRANPRLKPPFFPAQSGLWGKPTI INNVETLASVPI	450
<i>S. wolfei</i> HydB	VCGEETALIESIEGKRGEPRFKPPYPPSEGLWGWKPTIVNNVETFANIPVI	450
Swol_0784	VCGEETALIESIEGHRGEPRFKPPFPVAGLWGVPTVNNVETFACLPII	450
Swol_1024	VCGEESALIESIEGHRGEPRFKPPFPVIGLWGWKPTIVNNVETFANIPPI	450
Swol_1828	VCGEESALIESIEGHRGEPRFKPPFPVIGLWGWKPTIVNNVETFANIPAI	450
Syn_02139	VCGEESLMSMEGKRGYPRFRPPFPAGAGFLAKPSNVNNVETYASVPMI	450
Syn_00631	VCGEETALIESIEGKRGQPRIRPPFPVAVGLGCPTIVNNVETLASVPFI	450
<i>S. aciditrophicus</i> HydB	VCGEETSLLNSMEGKRGYPRVRPPFPAAAGFMGMPNSVNNVETLSSIPMI	450
	:***.:*: *: * . : . * *: :***: :	
<i>T. maritima</i> HydB	LRDGVENYRKRGTGTE-NSPGTKMFSVAGPLKATGIIIEVEFGTTLRDIINYI	500
<i>C. tencongenesis</i> HydB	ILNGGEWFASIGTE-KSKGTKVFALTKGVNNTGLIEVPMGTTLREIIEYI	500
<i>M. thermoacetica</i> HydB	IRQGWEIFAGIGTE-KSKGTKVFALAGKINNNGLVEIPMGTSRQVIYI	500
<i>A. woodii</i> HydB	ILNGAEWFASVGTGTE-KSKGTKVFALGGKINNTGLLEIPMGTTLREIIEYI	500
<i>R. albus</i> HydB	IRKGAAWYSAMGTGTE-KSKGTKVFALGGKITNVGLVEIPMGTTLREIIEEI	500
<i>C. acidurici</i> HylB	ILKGADWFTSFGTK-DSPGTKVFALGGKINNTGLVEIPMGTTLREVIYDV	500
<i>C. autoethanogenum</i> HytB	IEKGGDWYHAIGTMEKSKGTKVFSLVGKVKNTGLVEVPMGTTLREIYDI	500
<i>D. fructosovorans</i> HydB	IINGADWFSIGTA-TSKGTKVFALAGKI QNVGLIEVPMGISLREVIYDI	500
<i>C. necator</i> FdhB	LARGAQYRDYGMG-RSRGTLFPQLAGNIKQGGGLVEKAFGVTLRELLVDY	500
<i>C. oxalaticus</i> FdhB	LARGAQYRDYGMG-RSRGTLFPQLAGNIRQGGGLVEKAFGVTLRELLVDY	500
<i>M. extorquens</i> FdhB	IERGAEWKSHGRN-GRVGLRSYSVSGRVKEPGVKLAPAGLTIQELIDEY	500
<i>M. trichosporium</i> FdhB	LAKGGEYYASLVG-RSRGTMLQIAGNVKFGGLYETPFGLTLGEIVNDI	500
<i>R. capsulatus</i> FdhB	IAHGAKAYESFGMD-RSRGTIPLQIGGNVKKRGLFETGFGITLGEIVEDI	500
<i>E. coli</i> Nuof	LANGVIEWYQNISS-KDAGTKLMGFSGRVKNPGLWELPFGTTAREIILEDY	500
<i>T. thermophilus</i> Nqol	MERGADWFAQMGTE-QSKGMKLYQISGPVKRPGVYELPMGTTFRELIYEW	500
<i>S. wolfei</i> HydB	IEKGADWYASIGNP-AYPGTKVFTLTGDINNRTFFEVPTNTTIREIVFQF	500
Swol_0784	LTNGADWFASIGAP-KYPGTKVLTLTGDVNNPTYFEVPTNYILSDVIYKL	500
Swol_1024	IEKGGDWYKAIGAP-NYPGTKVLTLTGDVNNRTFFEVPTNTTIREVIFGL	500
Swol_1828	VDKGADWYKIGAAA-GYPGTKVMTLTGDIVNRTVIEVPTNTTIRQVLDDF	500
Syn_02139	IEKGAAWYKSVGLE-TCTGTKLYCLSGKLNRTGLVEMPMGTTLREIIEYI	500
Syn_00631	IEKGAEAFKQWGFENNYGFKLFGISGCVNKPGVYIPLGVSFNELMEAA	500
<i>S. aciditrophicus</i> HydB	VARGADWFKSVGTA-TCAGTKLYCLSGKVNQTLGVELPMGATLRQIMDTF	500
	: * : . * . * : . :::	

*T. maritima* HydB CGGFVEGEEFKAVQIGGPSGACLS--EDFIDMPLDYDTLKKADAMVGGGG 550  
*C. tencongenesis* HydB GGGIPGGKFKFKAQVIGGPSGGCIP--AELLDTPIDYDSLTSAGAMVGGGG 550  
*M. thermoacetica* HydB GGGIPGGKFKFKAQVIGGPSGGCIP--AEHLDAPIDYENLTALGTIMGGGG 550  
*A. woodii* HydB GGGIPNGKAFKAAQTGGPSGGCLP--ESLLDTEIDYDNLIAAGSMMGGGG 550  
*R. albus* HydB GGGIPDGKAFKAAQTGGPSGGCIP--AQHIDTEIDYESLAALGSMMGGGG 550  
*C. acidurici* HylB GGGIPDGKQFKAVQTGGPSGGCIT--ADYIDTEIDFATLNLGSMMGGGG 550  
*C. autoethanogenum* HytB GGGVLNDRKFKAVQIGGPSGGCLP--AEYLDLPVDYDTLVKADSMMGGGG 550  
*D. fructosovorans* HydB GGGCPDGKAFKAVQTGGPSGGALA--NKDLDAIDYESLAACKSIMGGGG 550  
*C. necator* FdhB GGGTRSGRAIRAVQVGGPLGAYLP--ESRFDVPLDYEAYAAFVGGVGHGG 550  
*C. oxalaticus* FdhB GGGTRSGRAIRAVQVGGPLGAYLP--ESRFDVPLDYEAYAAFVGGVGHGG 550  
*M. extorquens* FdhB GGGISDGHSAAYLPGGASGGILP--ASMNDIPLDFGTLEKYGCFIGSAA 550  
*M. trichosporium* FdhB GGGSLSGRPFVRAVQCGGPLGAYVP--PSLFDTPFDYEAQKHDSLIGHGG 550  
*R. capsulatus* FdhB CGGTASGRPVKAVQVGGPLGAYHP--VSDYHLPCFYEQFAGQGGVLGHAG 550  
*E. coli* Nuof AGGMRDGLKFKAWQPPGGAGTDFLT--EAHLDLPEFESIGKAGSRLGTAL 550  
*T. thermophilus* Nqol AGG--PLEPIQAIIPGGSSTPPLPFTEEVLDTPMSYEHQAKGSMLGTGG 550  
*S. wolfei* HydB GGGVPGDKKFKAVQIGGTSAGFIP--DALLDTPVAFDMSAIGATLGSAA 550  
Swol\_0784 GGGIKNGRKFKAQVGGTSGAFIP--EQNLNTSIDFDSMSAIGAALGSGA 550  
Swol\_1024 GGGVAGGKFKFKAQVIGGTSGGFIP--ESNLDTPIDFDSMNSIGAVLGSAA 550  
Swol\_1828 GGGITGGKFKFKAQVIGGTSGGFIP--ESLLDTPIDFDSMSAIGATLGSAA 550  
Syn\_02139 GKGIKNGKTFKFAQVGGASAGIILG--PELMDLPLDIDSTIKAGVTLGSAA 550  
Syn\_00631 G-GVKG--KLKAAIVGGLSVAILKA-EELQDLTMDYDSCAKHGTGLGSGG 550  
*S. aciditrophicus* HydB GGGMKSAGSFFKAQVGGAAAGGILG--ADLMDLPLDIDSTIKAGVTLGSAA 550

\* . \*\* . . :\*

*T. maritima* HydB IVVITKKT~~CMV~~EVARFFLDFTKRESCGKCVPCREGTM-QAYNILEKFTHG 600  
*C. tencongenesis* HydB LVVMEDED~~CMV~~NVAKFFLEFVDES CGKCAPCRIGTK-RMLELLDKITSG 600  
*M. thermoacetica* HydB LIIMDEDT~~CMV~~DVAKFFMDFVKDES CGKCTPCRIGTT-RMLEILNRITRG 600  
*A. woodii* HydB LIVMEDED~~CMV~~DVARFFLDFTQDES CGKCPPCRIGTK-RMLEILERICDG 600  
*R. albus* HydB LIVMEDED~~CMV~~DVSKFYLNFTVDES CGKCTPCRVGTR-KLLQLEKIDTG 600  
*C. acidurici* HylB MIVMEDED~~CMV~~DIARFFLDFTVEES CGKCTPCREGTK-RMLELLEKIDTG 600  
*C. autoethanogenum* HytB MIVMDDRT~~CMV~~DVTRYLLSFLAEES CGKCVPCREGVK-RMLEILTDICNG 600  
*D. fructosovorans* HydB MVVMEDED~~CMV~~SVAKFFLDFTMDET CGKCTPCRIGSK-RLYEILDRITKG 600  
*C. necator* FdhB IVVFEDETVDMAKQARYAMEFCAIES CGKCTPCRIGST-RGVEVMDRIAG 600  
*C. oxalaticus* FdhB IVVFEDETVDMAKQARYAMEFCAIES CGKCTPCRIGST-RGVEVMDRIAG 600  
*M. extorquens* FdhB VVILSDQDDVRGAALNLMKFFFEDES CGQCTPCRSQTQ-----KARMLM 600  
*M. trichosporium* FdhB LVVFDDETVDMAQMARFGMEFCAIES CGKCTPCRIGST-RGVETIDRIVEG 600  
*R. capsulatus* FdhB LVVHDDTADMLKLARFAMEFCAIES CGTCTPCRIGAV-RGVEVIDRIAAG 600  
*E. coli* Nuof AMAVDHEINMVSLVRNLEEFFARESCGWCTPCRDGLP-WSVKILRALERG 600  
*T. thermophilus* Nqol VILIPERVSMVDAMNLTFRFYAHES CGKCTPCREGVAGFMVNLFAKIGTG 600  
*S. wolfei* HydB TFVIDESRDIVDVATRIAGFFEHES CGKCAPREGTA-RTAELMEKINEG 600  
Swol\_0784 VLVMDETRDIVDIVTRISKFFEHES CGKCNPCREGTF-RCREIMEKINSG 600  
Swol\_1024 VFVMEDES RDIVNVVARIAKFFEHES CGKCSPCREGTK-RMHMMERLNAG 600  
Swol\_1828 FFVMEDETRDIVVIDRISKFFAHES CGKCTPCREGTQ-RMHMLHRVKNG 600  
Syn\_02139 VLVCDEDTCVDFLLDVLNFFEHES CGQCVPCRVTGR-QLHHLARKFATG 600  
Syn\_00631 IMVISEDFSIPELALRTIKFYAHES CGKCVPCREGSY-TLVKILHKLKLSG 600  
*S. aciditrophicus* HydB VLVCDETCVAVDFLLNVLNFFEHES CGQCPCKLGTG-QLHYVAQKFAMR 600

. . \* : \*\* \* \* : \*

*T. maritima* HydB KATYEDLKTLEHLSKTIKTA-SLCGLGKTAPNPILSTLKLFREEYIAHIE 650  
*C. tencongenesis* HydB KGEEDIEKLEELAKTIKAT-ALCGLGQTAPNPVLSTLRYFRHEYEAHIK 650  
*M. thermoacetica* HydB QGEEKDLLLVELARQIKDT-ALCGLGQTAPNPVLSTITYFRDEYLAHIR 650  
*A. woodii* HydB KGVEGDIERLEELAVGIKSS-ALCGLGQTAPNPVLSTIRFFRDEYEAHIR 650  
*R. albus* HydB KGEMEDLEKIQLDLATHMKSS-SLCALGQSAPNPVLSTLQYFGDEYLAHIK 650  
*C. acidurici* HylB KGEMEDLDRLES LAETIKSS-SLCGLGQTAPNPVLSTLKYFRDEYEAHVK 650  
*C. autoethanogenum* HytB DGKEGDIEELLECSMTSKA-SLCSLGKSAPNPVIASIRYFRDEFEEHIK 650  
*D. fructosovorans* HydB KGTRADLDRKLSLSEIIKDT-ALCGLGQTMPNPILSTMDTFANEYEAHVD 650  
*C. necator* FdhB EQPVKHVALVRDLCDTMLNG-SLCAMGGMTPYPVLSALNEFPEDFGLASN 650  
*C. oxalaticus* FdhB EQPVKHVKLVRDLCDTMLYG-SLCAMGGMTPYPVLSALNEFPEDFGLAPN 650  
*M. extorquens* FdhB ENGVWDTDLLGELAQCMRDA-SICGLGQAASNVPSTVIKYFPDLFPEPRA 650  
*M. trichosporium* FdhB VDVEANIELLSLDCHTMKFG-SLCALGGFAPYPVESALRHYPEDFRKATL 650  
*R. capsulatus* FdhB D--ASAMPLDDLCQTMKLG-SLCALGGFTPYPVQSAIRHFPAADFPCARE 650  
*E. coli* NuoF EGQPGDIETLEQLCRFLGPGKTFCAHAPGAVEPLQSAIKYFREEFEAGIK 650  
*T. thermophilus* Nqo1 QGEEKDVENLEALLPLIEGR-SFCPLADAAVWPVKGSLRHFKDQYLALAR 650  
*S. wolfei* HydB RGSNKDVALLEKLGTVMSYS-CLCGLGQAAPAPVLTITIKHFKADYEAKFV 650  
Swol\_0784 RATEADIDNLLLARVMKRA-ALCGLGQAAPVPIITSTIEHFGHEYRRKLL 650  
Swol\_1024 EGNAEDVELLGRLGKVMVA-CLCGLGQAAPAPVLTITIKNFNADYQAKFN 650  
Swol\_1828 GAVAGDLDYMERLGSVMSKA-CLCGLGQAAPAPVLTITLKHFRNDYAKFN 650  
Syn\_02139 TAVPGDLDLMVEKAKLMKN--SLCGLGQSPILPITTMLKYFREDFLRHCD 650  
Syn\_00631 QGEAADIEKILGICNTVRGL-TLCPTGEAFVPIQAMVEKFRSEFDALIK 650  
*S. aciditrophicus* HydB EAEEKDIQLMIDTAKMMKLA-SLCALGQSPILPIETMIRNFREEFVKHCD 650

: \* . \*: : :

*T. maritima* HydB G-ECPSGMCTAFKKYVINPDIKGGGLCARSQPQNAITGERGKPYTIDQE 700  
*C. tencongenesis* HydB EKRCPAGVCTALLSFVIDPEKCKACGICAKNCPVGAISGKPKTPYVIDQE 700  
*M. thermoacetica* HydB DHRCPAHVQCQELLSYVIDAGKCTGGACSRVCPVGAISGGKKEAHQIDPA 700  
*A. woodii* HydB DKKCPAGVCKHLLDFKINADTKGCGICAKKCPADAISGEKKKPYNIDTS 700  
*R. albus* HydB EKKCPAGVCKNLLQYEIADKCKGCTLCARNCPANAITGTVKNPHVIDTT 700  
*C. acidurici* HylB DKKCPAGACQSLLIFYIT-DKICGCTKCARQCPASCIDGKVKERHVINTS 700  
*C. autoethanogenum* HytB NKRCRAGVCKKLTTFGIDEDKCKGCDMCKKNCPADCITGEIKKPHITDAD 700  
*D. fructosovorans* HydB DKKCPAHVCTALLTYTIDPAKCTGCGLCTRVCPVECISGTKKQPHTIDTT 700  
*C. necator* FdhB PAKAA----- 700  
*C. oxalaticus* FdhB PAHAAKAA----- 700  
*M. extorquens* FdhB VAAE----- 700  
*M. trichosporium* FdhB PAAAE----- 700  
*R. capsulatus* FdhB AAE----- 700  
*E. coli* NuoF QPFSNTHLINGIQPNLLKERW----- 700  
*T. thermophilus* Nqo1 EKRPVPRPSLWR----- 700  
*S. wolfei* HydB ----- 700  
Swol\_0784 QYA----- 700  
Swol\_1024 ----- 700  
Swol\_1828 ----- 700  
Syn\_02139 PSLCCPECANSLAHYYRGH----- 700  
Syn\_00631 K----- 700  
*S. aciditrophicus* HydB PDYECPCDASLQAYYL----- 700

<i>T. maritima</i> HydB	G-ECPSGMCTAFKKYVINPDI	CKGCGLCARS	CPQNAITGERGKPYTIDQE	700
<i>C. tencongenesis</i> HydB	EKRCPAGVCTALLSFVIDPEK	CKACGICAKNC	PVGAIISGKPKTPYVIDQE	700
<i>M. thermoacetica</i> HydB	DHRCPAHVCQELLSYVIDAGK	CTGCGACSRVC	PVGAIISGGKKEAHQIDPA	700
<i>A. woodii</i> HydB	DKKCPAGVCKHLLDFKINADT	CKGCGICAKKC	PADAISGEKKKPYNIDTS	700
<i>R. albus</i> HydB	EKKCPAGVCKNLLQYEIIADK	CKGCTLCARNC	PANAITGTVKNPVIDTT	700
<i>C. acidurici</i> HylB	DKKCPAGACQSLLLEFYIT-	DKCIGCTKCARQC	PASCIDGKVKERHVINTS	700
<i>C. autoethanogenum</i> HytB	NKRCRAGVCKKLTTFGIDEDK	CKGCDMCKKNC	PADCITGEIKKPHTIDAD	700
<i>D. fructosovorans</i> HydB	DKKCPAHVCTALLTYTIDPAK	CTGCGLCTRVC	PVECISGTTKQPHTIDTT	700
<i>C. necator</i> FdhB	PAKAA-----			700
<i>C. oxalaticus</i> FdhB	PAHAAKAA-----			700
<i>M. extorquens</i> FdhB	VAAE-----			700
<i>M. trichosporium</i> FdhB	PAAAE-----			700
<i>R. capsulatus</i> FdhB	AAE-----			700
<i>E. coli</i> NuoF	QPFSNTHLINGIQPNLLKERW			700
<i>T. thermophilus</i> Nqo1	EKRFPVPRPSLWR-----			700
<i>S. wolfei</i> HydB	-----			700
Swol_0784	QYA-----			700
Swol_1024	-----			700
Swol_1828	-----			700
Syn_02139	PSLCCPECANSLAHYYRGH			700
Syn_00631	K-----			700
<i>S. aciditrophicus</i> HydB	PDYECPCDASLQAYYL-----			700

<i>T. maritima</i> HydB	KCVKCGLC	ASKC	PFKAIELV-	721
<i>C. tencongenesis</i> HydB	KCIKCGTC	CIDK	CPFGAIYKK*	721
<i>M. thermoacetica</i> HydB	ACIKCGSC	YEKCR	FRFGAITRE-	721
<i>A. woodii</i> HydB	KCIKCGAC	IEACP	FGSISKA-	721
<i>R. albus</i> HydB	KCIKCGV	CMNNCK	FGAIIKK-	721
<i>C. acidurici</i> HylB	ACVKCGAC	ADVCP	VNAVIKR-	721
<i>C. autoethanogenum</i> HytB	KCLRCGN	CMNIC	KFDVAVKL-	721
<i>D. fructosovorans</i> HydB	RCIKCGAC	YDKCK	FDSIIKQ-	721
<i>C. necator</i> FdhB	-----			721
<i>C. oxalaticus</i> FdhB	-----			721
<i>M. extorquens</i> FdhB	-----			721
<i>M. trichosporium</i> FdhB	-----			721
<i>R. capsulatus</i> FdhB	-----			721
<i>E. coli</i> NuoF	-----			721
<i>T. thermophilus</i> Nqo1	-----			721
<i>S. wolfei</i> HydB	-----			721
Swol_0784	-----			721
Swol_1024	-----			721
Swol_1828	-----			721
Syn_02139	-----			721
Syn_00631	-----			721
<i>S. aciditrophicus</i> HydB	-----			721